

**Developing peptide-based inhibitors  
of amylin aggregation as a novel  
treatment for type 2 diabetes**

**By**

**Idira Christopher Obasse**

**Submitted in total fulfilment of the requirements of**

**The degree of Doctor of Philosophy**

**In Biomedical and Life Sciences**

**Lancaster University**

**November 2017**

## Abstract

Human islet amyloid polypeptide (hIAPP), also known as amylin, is the main constituent of the amyloid deposits present in approximately 95% of people with type 2 diabetes. Amylin aggregates into oligo-/polymeric  $\beta$  sheet structures which are considered to be cytotoxic to pancreatic  $\beta$ -cells. Inhibiting the early stages of amylin aggregation could provide a potential therapeutic strategy for the treatment of type 2 diabetes. In this study, overlapping peptides were designed to target the binding region (RLANFLVHSS, residues 11-20) of human amylin and their effects on amylin fibril formation were studied. The first generation of peptides, IO1, IO2, IO3, IO4, IO5, IO6 and IO7, showed less than 50% inhibition of amylin aggregation as observed using a Thioflavin T (Th-T) fluorescence assay. The next generation of peptides, IO8 and RI-IO8, were assessed using Th-T, Congo red and transmission electron microscopy (TEM) techniques. IO8 ( $\text{H}_2\text{N-RGANFLVHGR-NH}_2$ ) showed strong inhibitory effects on amylin aggregation, up to 71% inhibition, with TEM studies revealing a total inhibition of amylin fibril formation at a 1:1 molar ratio of peptide to amylin. MTS and LDH cytotoxicity studies revealed that IO8 protected human pancreatic islet  $\beta$  PANC-1 insulin producing cells from the toxic effects of human amylin. IO8 proved to be a significantly more potent inhibitor than the NMeG24 NMeI26 peptide reported in literature. In fact, contrary to reports in the literature, NMeG24 NMeI26 significantly enhanced amylin fibril formation. In addition, a homoarginine version of IO8, designed by replacing the arginine residues in IO8 ( $\text{H}_2\text{N-RGANFLVHGR-NH}_2$ ) with homoarginine ( $\text{H}_2\text{N-HarGANFLVHGHAr-NH}_2$ ) also significantly impeded amylin fibril formation as

observed by Th-T assay. To completely stabilise IO8 from proteolytic degradation, we designed RI-IO8 (Ac-rGhvlfnaGr-NH<sub>2</sub>), a retro-inverso peptide with L-replaced by D-amino acids. RI-IO8, however, significantly enhanced amylin fibril formation. Th-T experiments, Congo red assay and TEM revealed that two N-methylated versions of IO8, N1-IO8 (H<sub>2</sub>N-RGAmNFmLVmHGR-NH<sub>2</sub>) and N2-IO8 (H<sub>2</sub>N-RGANmFLmVHmR-NH<sub>2</sub>) significantly inhibited amylin aggregation by up to 85% and 87%, respectively, as observed by Th-T assay. TEM images revealed complete inhibition of fibril formation by N1-IO8 at a 1:1 molar ratio of peptide to amylin, and by N2-IO8 even at a 1:5 molar ratio of peptide to amylin. N1-IO8 and N2-IO8 were found to be stable against proteolytic enzymes, and in plasma, unlike IO8, and also protected human pancreatic islet  $\beta$  PANC-1 cells from the toxic effects of human amylin, and were themselves non-toxic to cells. These studies show that these N-methylated peptides, N1-IO8 and N2-IO8, are potent inhibitors of amylin aggregation and could be developed as a novel treatment for type 2 diabetes.

## **Declaration**

This thesis is my own work and has not been submitted in a significantly similar form for the award of a higher degree elsewhere.

Idira Obasse

November, 2017

Lancaster University

## **Acknowledgements**

My sincere appreciation goes to my supervisor, Professor David Allsop, without whom this project would not be a success. Special thanks to Dr. Mark Taylor and Dr. Craig Delury for their great assistance in the laboratory; Dr. Fuyuki Kametani (Tokyo, Japan) for the peptide HPLC-MS analysis. Special thanks to Dr. Nigel Fullwood for his immense help with the transmission electron microscope. Special thanks to Dr. Elizabeth Shaw for her great help with the confocal microscopy. Many thanks Dr. Edward Parkin and all the Faculty of Health and Medicine staff who gave me assistance in the laboratory. Further thanks to the Faculty of Health and Medicine Lancaster University, for offering me a scholarship for the last 2 years of my PhD. My very special appreciation goes to my beloved husband, for his constant love and support. Finally, and by no means the least, special appreciation goes to my lovely parents who sponsored my PhD, and for their continued support and encouragement.

## Table of Contents

<b>Abstract</b> .....	<b>i</b>
<b>Declaration</b> .....	<b>iii</b>
<b>Acknowledgement</b> .....	<b>iv</b>
<b>Table of Contents</b> .....	<b>v</b>
<b>List of Tables</b> .....	<b>ix</b>
<b>List of Figures</b> .....	<b>x</b>
<b>List of abbreviated terms</b> .....	<b>xiii</b>
<b>Chapter 1: Introduction</b> .....	<b>1</b>
1.1 Amyloid Protein Misfolding and Disease .....	1
1.2 Diabetes .....	2
1.2.1 Diabetes prevalence .....	2
1.2.2 Diabetes Risk Factors .....	6
1.2.3 Secondary Complications of Diabetes .....	8
1.2.4 Current Methods for Diagnosis of Diabetes .....	8
1.2.5 Current Methods for Treatment of Diabetes .....	9
1.2.5.1 Stem Cell Treatment for Diabetes .....	11
1.2.6 Animal models of Diabetes .....	13
1.3 Structure of Amylin .....	17
1.4 Expression of Amylin .....	20
1.5 Effects of Amylin .....	27
1.5.1 General Effects of Amylin .....	27
1.5.2 Anorectic Effects of Amylin .....	27
1.5.3 Effects of Amylin on Pancreatic Islet Cells .....	28
1.5.4 Other Effects of Amylin .....	29
1.6 Amylin and Oxidative Stress .....	30
1.7 Amylin Toxicity .....	31
1.8 Amylin and Type 2 Diabetes .....	37
1.9 Purpose of Study .....	39
1.9.1 Objectives of Study .....	44

<b>Chapter 2: Materials and Methods</b> .....	<b>45</b>
2.1 Suppliers and Equipment .....	45
2.2 Peptides .....	46
2.3 Solutions and Buffers .....	51
2.3.1 10 mM Phosphate buffer, pH 7.4, containing 150 mM NaCl (PBS) .....	51
2.3.2 10 mM Phosphate buffer, pH 7.4, containing 300 mM NaCl (PB 2.S) .....	51
2.3.3 10 mM Phosphate buffer, pH 7.4 (PB) .....	52
2.3.4 15 mM Thioflavin T (Th-T) solution .....	52
2.3.5 2% Phosphotungstic acid (solution) .....	52
2.4 Peptide Preparation .....	53
2.4.1 Deseeding Human Amylin .....	53
2.4.2 Preparation of Peptide Inhibitors .....	54
2.5 Thioflavin T (Th-T) Assays .....	55
2.5.1 Mechanism of Th-T Assay .....	55
2.5.2 Th-T Assay Protocol .....	56
2.6 Cell Culture .....	56
2.6.1 Cell Maintenance .....	56
2.6.2 The CellTiter 96 Aqueous One Solution Cell Proliferation (MTS) Assay .....	57
2.6.3 Cell toxicity protocol for MTS assay .....	58
2.6.4 The CytoTox-ONE Homogeneous Membrane Integrity (LDH) Assay .....	59
2.6.5 Cell Toxicity Protocol for LDH Assay .....	60
2.6.6 Cell Penetration Assay .....	61
2.6.7 Cell Penetration Protocol .....	62
2.7 Congo Red Assay .....	63
2.7.1 Protocol for Procedures for Congo Red spectroscopic assay .....	63
2.8 Stability Assay using High Performance Liquid Chromatography .....	65
2.9 Transmission Electron Microscopy .....	67
2.9.1 Statistical Analysis .....	68
<b>Chapter 3: Quantitative analysis of peptide-based inhibitors on amylin aggregation</b> .....	<b>69</b>
3.1 Thioflavin-T Assay .....	69
3.1.1 Peptide based inhibitors show inhibitory effects on amylin aggregation .....	70

3.1.2	Effect of amylin derived peptide inhibitors (IO8 and RI-IO8) peptide inhibitors on amylin aggregation .....	74
3.1.3	Effect of IO8, NMeG24 NMeI26 and ANFLVH on amylin aggregation .....	76
3.1.4	Effect of H <sub>2</sub> N-RGNFGAILSGR-NH <sub>2</sub> on amylin aggregation .....	78
3.1.5	Effect of HIO8 on amylin aggregation .....	80
3.1.6	Effect of N1-IO8 and N2-IO8 on amylin aggregation .....	82
3.2	Quantifying amylin aggregation using the Congo Red Spectrophotometric Assay .....	84
3.2.1	Congo red binding studies of amylin aggregation in the presence of IO8 inhibitor .....	85
3.2.2	Congo red binding studies of amylin aggregation in the presence of RI-IO8.....	87
3.2.3	Congo red binding studies of amylin aggregation in the presence of N1-IO8 inhibitor .....	89
3.2.4	Congo red binding studies of amylin aggregation in the presence of N2-IO8 inhibitor .....	91
3.3	Discussion .....	93
3.3.1	Conclusion .....	103

#### **Chapter 4: Qualitative analysis of the effects of peptide-based inhibitors on amylin**

<b>aggregation .....</b>	<b>104</b>	
4.1	IO8 inhibits amylin aggregation .....	105
4.2	RI-IO8 stimulates amylin aggregation .....	107
4.3	N1-IO8 inhibits amylin aggregation .....	109
4.4	N2-IO8 inhibits amylin aggregation .....	111
4.5	Disaggregation of pre-formed amyloid fibrils .....	113
4.6	Discussion .....	119
4.7	Conclusion .....	124

#### **Chapter 5: Peptide Stability Studies .....**

5.1	The stability of IO8 in the presence of proteolytic enzymes .....	128
5.2	The stability of N1-IO8 in the presence of proteolytic enzymes .....	138
5.3	The stability of N2-IO8 in the presence of proteolytic enzymes .....	148
5.4	The stability of peptide inhibitors in plasma .....	158
5.5	Discussion .....	163
5.6	Conclusion .....	167

#### **Chapter 6: Cell Based Studies .....**

6.1	Effect of IO8 on amylin-induced toxicity in PANC-1 human pancreatic cells .....	170
6.2	Effect of N1-IO8 on amylin-induced toxicity in PANC-1 human pancreatic cells .....	172
6.3	Effect of N2- IO8 on amylin-induced toxicity in PANC-1 human pancreatic cells .....	174
6.4	LDH analysis of IO8 on amylin-induced toxicity PANC-1 human pancreatic cells .....	176
6.5	LDH analysis of N1-IO8 on amylin-induced toxicity PANC-1 human pancreatic cells ...	178
6.6	LDH analysis of N2-IO8 on amylin-induced toxicity PANC-1 human pancreatic cells ...	180
6.7	Peptide Cell Uptake Experiment .....	182
6.8	Discussion .....	184
6.9	Conclusion .....	190
<b>Chapter 7: General Discussion and Conclusion .....</b>		<b>192</b>
7.0	Discussion .....	192
7.1	Conclusion .....	206
7.2	Limitations of Study and Future Experimental Plans .....	208
7.2.1	Limitations of Study .....	208
7.2.2	Future Research .....	209
<b>References .....</b>		<b>211</b>
<b>APPENDICES .....</b>		<b>242</b>
APPENDIX A:	Reversed-Phase High-Performance Liquid Chromatography of IO8, N1-IO8 and N2-IO8 .....	242
APPENDIX B:	Reversed-Phase High-Performance Liquid Chromatography of RIO8 and HIO8 ...	270
APPENDIX C:	HPLC-MS data for China made peptides .....	275
APPENDIX D:	Th-T data of peptides alone in the absence of amylin .....	284
APPENDIX E:	List of publications .....	285
APPENDIX F:	List of trainings/courses attended with dates.....	286

## LIST OF TABLES

Table 1.1	The primary amino acid sequences of human CGRP and amylin of different species .....	19
Table 2.1	List of suppliers used and location .....	45
Table 2.2	List of equipment used .....	46
Table 2.3	Peptide inhibitors of amylin aggregation and their sequence (IO1-IO7) .....	48
Table 2.4	IO8 and RI-IO8 inhibitors .....	49
Table 2.5	Peptide inhibitors reported in literature to inhibit amylin aggregation .....	49
Table 2.6	N-methylated peptide inhibitors. ....	51
Table 2.7	Preparation of 1 mM of each of the peptide inhibitors .....	54
Table 2.8	List of proteolytic enzymes used .....	67
Table 5.1	Susceptibility of IO8 to individual proteases .....	129
Table 5.2	N1- IO8 susceptibility to individual proteases .....	139
Table 5.3	N2-IO8 susceptibility to individual proteases .....	149
Table 5.4	Peptide stability in plasma .....	159

## LIST OF FIGURES

Figure 1.1	The regulatory pathways of glucose, controlled by the pancreas .....	5
Figure 1.2	Processing of human PreProAmylin to form mature Amylin .....	21
Figure 1.3	Structural model of the amylin fibril derived from steric zipper studies .....	26
Figure 1.4	Schematic representation of the amyloid forming phases .....	32
Figure 1.5	General representation of fibril formation from natively unfolded monomers ....	38
Figure 1.6	Design of peptide inhibitors .....	42
Figure 2.1	Structure of L-homoarginine .....	50
Figure 2.2	The structure of Th-T .....	55
Figure 3.1.1	Examples of Th-T fluorescence of fibrillar human amylin in the presence of inhibitors .....	72
Figure 3.1.1.1	Effect of IO1, IO2, IO3, IO4, IO5, IO6 and IO7 peptides on amylin aggregation .....	73
Figure 3.1.2	Percentage aggregation of amylin in the presence of IO8 and RI-IO8 peptides ..	75
Figure 3.1.3	Effect of IO8 and NMeG24 NMeI26 peptides on amylin aggregation .....	77
Figure 3.1.4	Effect of IO8 and NFGAILS peptides on amylin aggregation .....	79
Figure 3.1.5	Effect of IO8 and HIO8 peptides on amylin aggregation .....	81
Figure 3.1.6	Effect of N1-IO8 and N2-IO8 peptides on amylin aggregation .....	83
Figure 3.2.1	Effect of IO8 on human amylin fibril as monitored by Congo Red Assay .....	86
Figure 3.2.2	Effect of RI-IO8 on human amylin fibril as monitored by Congo Red Assay .....	88
Figure 3.2.3	Effect of N1-IO8 on human amylin fibril as monitored by Congo Red Assay ....	90
Figure 3.2.4	Effect of N2-IO8 on human amylin fibril as monitored by Congo Red Assay ....	92
Figure 4.1	TEM examination of the effect of IO8 on amylin fibril formation .....	106
Figure 4.2	TEM examination of the effect of RI-IO8 on amylin fibril formation .....	108
Figure 4.3	TEM examination of the effect of N1-IO8 on amylin fibril formation .....	110
Figure 4.4	TEM examination of the effect of N2-IO8 on amylin fibril formation .....	112
Figure 4.5.1	Experiment to monitor possible disaggregation of pre-formed amylin fibrils by IO8 .....	115
Figure 4.5.2	Experiment to monitor possible disaggregation of pre-formed amylin fibrils by RI-IO8 .....	116

Figure 4.5.3	Experiment to monitor possible disaggregation of pre-formed amylin fibrils by N1-IO8 .....	117
Figure 4.5.4	Experiment to monitor possible disaggregation of pre-formed amylin fibrils by N2-IO8 .....	118
Figure 5.1.1	RP-HPLC profile of 100 $\mu$ M IO8 and effects of proteolysis by Trypsin .....	130
Figure 5.1.2	RP-HPLC profile of 100 $\mu$ M IO8 and effects of proteolysis by Chymotrypsin .	131
Figure 5.1.3	RP-HPLC profile of 100 $\mu$ M IO8 to proteolysis by Cathepsin G .....	132
Figure 5.1.4	RP-HPLC profile of 100 $\mu$ M IO8 to proteolysis by Elastase .....	133
Figure 5.1.5	RP-HPLC profile of 100 $\mu$ M IO8 to proteolysis by Thrombin .....	134
Figure 5.1.6	RP-HPLC profile of 100 $\mu$ M IO8 to proteolysis by Kallikrein .....	135
Figure 5.1.7	RP-HPLC profile of 100 $\mu$ M IO8 to proteolysis by Plasmin .....	136
Figure 5.1.8	RP-HPLC profile of 100 $\mu$ M IO8 to proteolysis by Factor X .....	137
Figure 5.2.1	RP-HPLC profile of 100 $\mu$ M N1-IO8 to proteolysis by Trypsin .....	140
Figure 5.2.2	RP-HPLC profile of 100 $\mu$ M N1-IO8 to proteolysis by Chymotrypsin .....	141
Figure 5.2.3	RP-HPLC profile of 100 $\mu$ M N1-IO8 to proteolysis by Cathepsin G .....	142
Figure 5.2.4	RP-HPLC profile of 100 $\mu$ M N1-IO8 to proteolysis by Elastase .....	143
Figure 5.2.5	RP-HPLC profile of 100 $\mu$ M N1-IO8 to proteolysis by Thrombin .....	144
Figure 5.2.6	RP-HPLC profile of 100 $\mu$ M N1-IO8 to proteolysis by Kallikrein .....	145
Figure 5.2.7	RP-HPLC profile of 100 $\mu$ M N1-IO8 to proteolysis by Plasmin .....	146
Figure 5.2.8	RP-HPLC profile of 100 $\mu$ M N1-IO8 to proteolysis by Factor X .....	147
Figure 5.3.1	RP-HPLC profile of 100 $\mu$ M N2-IO8 to proteolysis by Trypsin .....	150
Figure 5.3.2	RP-HPLC profile of 100 $\mu$ M N2-IO8 to proteolysis by Chymotrypsin .....	151
Figure 5.3.3	RP-HPLC profile of 100 $\mu$ M N2-IO8 to proteolysis by Cathepsin G .....	152
Figure 5.3.4	RP-HPLC profile of 100 $\mu$ M N2-IO8 to proteolysis by Elastase .....	153
Figure 5.3.5	RP-HPLC profile of 100 $\mu$ M N2-IO8 to proteolysis by Thrombin .....	154
Figure 5.3.6	RP-HPLC profile of 100 $\mu$ M N2-IO8 to proteolysis by Kallikrein .....	155
Figure 5.3.7	RP-HPLC profile of 100 $\mu$ M N2-IO8 to proteolysis by Plasmin .....	156
Figure 5.3.8	RP-HPLC profile of 100 $\mu$ M N2-IO8 to proteolysis by Factor X .....	157
Figure 5.4.1	RP-HPLC profile of 100 $\mu$ M IO8 in plasma .....	160
Figure 5.4.2	RP-HPLC profile of 100 $\mu$ M N1-IO8 in plasma .....	161
Figure 5.4.3	RP-HPLC profile of 100 $\mu$ M N2-IO8 in plasma .....	162

Figure 6.1	Cytotoxic effect of amylin in the presence or absence of IO8 peptide on PANC-1 cells .....	171
Figure 6.2	Cytotoxic effect of amylin in the presence or absence of N1-IO8 peptide on PANC-1 cells .....	173
Figure 6.3	Cytotoxic effect of amylin in the presence or absence of N2-IO8 peptide on PANC-1 cells .....	175
Figure 6.4	IO8 inhibits the toxic effects of human amylin on pancreatic islet $\beta$ cells, as measured by LDH assay .....	177
Figure 6.5	N1-IO8 inhibits the toxic effects of human amylin on pancreatic islet $\beta$ cells, as measured by LDH assay .....	179
Figure 6.6	N2-IO8 inhibits the toxic effects of human amylin on pancreatic islet $\beta$ cells, as measured by LDH assay .....	181
Figure 6.7	Confocal microscope image of PANC-1 cells exposed to fluorescently tagged peptides. ....	183

## List of abbreviated terms

Amputee Statistical Database	ASD
Amyloid <i>beta</i>	A $\beta$
Atomic force microscopy	AFM
Calcitonin, calcitonin gene-related peptide	CGRP
Carboxypeptidase E	CPE
Cell-Penetrating Peptides	CPPs
CellTiter 96 aqueous one solution	MTS
Circular dichroism	CD
Congo Red	CR
Cross-Polarization Magic-angle Spinning	CP-MAS
CytoTox-ONE homogeneous membrane integrity	LDH
Deionized water	dH <sub>2</sub> O
Dynamic Light Scattering	DLS
Embryonic Stem Cell	ESC
Endoplasmic reticulum	ER
Glucagon-like Peptides	GLP
1,1,1,3,3,3-hexafluoro-2-propanol	HFIP
High performance liquid chromatography	HPLC
Human Islet amyloid polypeptide	hIAPP
International Diabetic Federation	IDF
Juvenile Diabetes Research Foundation	JDRF
National Institute of Diabetes and Digestive and Kidney Disease	NIDDK
National Service Framework	NSF

Nuclear magnetic resonance	NMR
Nucleobindin 1	NUCB1
Pancreatic and duodenal homeobox 1	PDX1
Phosphotungstic Acid	PTA
Prion protein	PrP
Prohormone convertase	PC
Reactive Oxygen Species	ROS
Relative Centrifugal Force	RCF
Royal College of Paediatric and Child Health	RCPCH
Scanning Transmission Electron Microscopy	STEM
Streptozotocin	STZ
Surface Plasmon Resonance	SPR
Thioflavin-T	Th-T
Transmission electron microscopy	TEM
Transcription factor 7-like 2	TCF7L2
Trifluoroacetic acid	TFA
Type 2 diabetes mellitus	T2DM
World Health Organisation	WHO

# Chapter 1

## Introduction

### 1.1 Amyloid Protein Misfolding and Disease

Amyloid is a generic term for abnormal protein fibrils that accumulate when protein molecules in a predominantly  $\beta$ -pleated sheet conformation bind to each other, mainly, but not exclusively, by hydrogen bonds (Dobson, 1999; Rochet and Lansbury, 2000). More than 30 proteins are known to form amyloid fibrils in a variety of different diseases in humans (Westermarck *et al.*, 2007; Westermarck, 2005), including Alzheimer's disease (Humpel 2011; Marchesi, 2011), Huntington's disease (Lee *et al.*, 2011), Parkinson's disease (Dillin and Cohen, 2011), prion disease (Brown and Mastrianni, 2010) and type 2 diabetes mellitus (T2DM) (Ahmad *et al.*, 2011; Kapurniotu, 2001; Westermarck, 2011). The misfolded proteins in these diseases are amyloid *beta* ( $A\beta$ ) and Tau, huntingtin,  $\alpha$ -synuclein, prion protein (PrP) and amylin, respectively. The presence of amyloid deposits, which are predominantly made up of islet amyloid polypeptide (IAPP), also known as amylin, is a major pathological feature of T2DM. These deposits are found in about 90% of people with T2DM (Kahn, 2003a; Zraika *et al.*, 2010). Amylin aggregation is strongly linked with the development of  $\beta$  cell failure in this disease (Hull *et al.*, 2004), and the protein has other regulatory functions in normal physiology (Kahn *et al.*, 1999). This review aims to provide an in-depth overview of diabetes and the molecular mechanism of amylin aggregation, as well as amylin-mediated toxicity. This

study aims to develop peptide-based inhibitors that are designed to prevent amylin aggregation.

## **1.2 Diabetes**

The World Health Organisation (WHO) defines diabetes as a chronic disease, resulting from insufficient insulin production by pancreatic  $\beta$  cells, and/or failure of the body to utilize the insulin being produced, leading to an increased blood glucose level, a condition referred to as hyperglycaemia (WHO, 2016). This can lead to secondary defects in many body systems, such as blood vessels and nerves (Spellman, 2010). Insulin is a hormone that helps cells to take up glucose from the blood, for energy production. There are two major types of diabetes; type 1 and type 2 diabetes. The symptoms of diabetes include excessive urination (polyuria), fatigue, persistent hunger, thirst (polydipsia), weight loss and vision impairment. These symptoms appear suddenly in type 1 diabetes, but are less marked in T2DM, and the latter disease is often diagnosed many years after onset, following the appearance of secondary complications (Taniguchi *et al.*, 2006).

### **1.2.1 Diabetes Prevalence**

The prevalence of diabetes is constantly growing. Currently, approximately 425 million people globally have diabetes and this figure is expected to rise to 642 million by 2040 (Diabetes UK, 2015). About 4.8 million people worldwide died of diabetes in 2012, and approximately 4.7 billion US dollars was spent on diabetes in the same year (IDF, 2012). Total deaths from diabetes have been

predicted to increase by 50% in the next 10 years (WHO, 2014). Approximately 3.5 million people are currently living with diabetes in the UK, and this number has been estimated to increase to 5 million by 2025 (Diabetes UK, 2015). Approximately 1 in 2 adults with diabetes worldwide are undiagnosed (IDF, 2015), and in the UK, about 549,000 people are estimated to have undiagnosed diabetes (Diabetes UK, 2015). Diabetes is predicted to be the 7<sup>th</sup> leading cause of death in the world by 2030 (WHO, 2014).

Type 1 diabetes is also known as insulin dependent diabetes and is a chronic disease in which insulin-producing  $\beta$  cells are destroyed so that the pancreas is unable to produce sufficient insulin (Abreu and Roep, 2013). The initial cause of the  $\beta$  cells destruction in type 1 diabetes is not fully understood. It is thought that genetic and environment factors like viruses may trigger the development of type 1 diabetes (Knip *et al.*, 2005). Insulin injections are often used in these patients to control blood glucose levels, but many of them cannot maintain stable blood sugar levels (Coppeters *et al.*, 2012) and so they often experience hypo- and hyperglycaemic states, which progress into long term complications. Type 1 diabetes accounts for around 10% of all people with diabetes (Diabetes UK, 2016).

T2DM is the most common form of diabetes and accounts for approximately 90% of the diabetic population (Diabetes UK, 2016). The pathogenesis of T2DM is multifaceted and is a topic that has been studied intensely (DeFronzo, 2004; Taniguchi *et al.*, 2006). Two major factors, each based on varying mechanisms, play a role in the pathogenesis of this disease (Kahn, 2003a; Kahn

*et al.*, 2009). The first is insulin resistance, resulting in the reduced effectiveness of, and a high demand for insulin (figure 1.1). The second major factor is the failure of pancreatic  $\beta$  cells to produce enough insulin, due to a decrease in both  $\beta$  cell mass (Clark *et al.*, 1998; Kaye *et al.*, 2009) and  $\beta$  cell function (Kahn, 2000).

Type 1 diabetes typically appears before the age of 40, and T2DM occurs majorly in middle aged and older adults from about age 40 onwards. However, in recent times, T2DM has also been reported among children. In the UK, 8 overweight girls of Arabic, Indian and Pakistani origin between the ages of 9 to 16 were diagnosed with T2DM (Ehtisham *et al.*, 2000). It is estimated that about 31,500 children and young people currently have diabetes in the UK (Diabetes UK, 2015). Out of this number, 95.1% have type 1 diabetes, while 1.9% have T2DM, and the remaining 3% have other rarer conditions, such as diabetes related to cystic fibrosis.

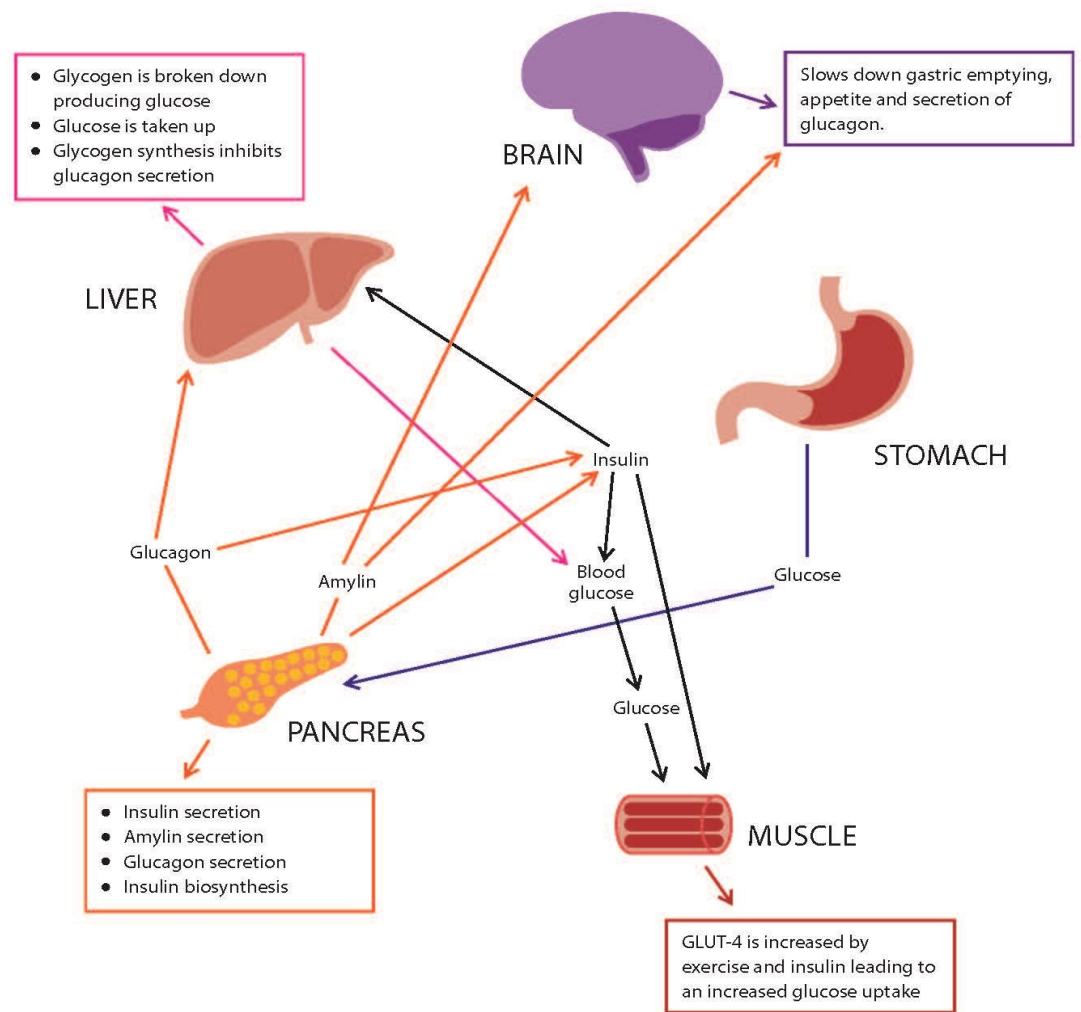


**Figure 1.1:** The regulatory pathways of glucose, controlled by the pancreas. After insulin secretion from the  $\beta$  cells of the pancreas a number of activities take place including, glucose uptake, gluconeogenesis by the liver, up-regulation of the GLUT-4 glucose transporter in muscle, and attenuation of glucagon secretion from the islets. Glucagon secreted by the  $\alpha$  cells triggers the breakdown of glycogen by the liver, thereby releasing glucose when required. Somatostatin secreted from the  $\delta$  cells decreases the secretion of insulin and glucagon. Amylin secreted by  $\beta$  cells delays gastric emptying, reduces appetite, and suppresses the secretion of glucagon after a meal. Islet cells are in close proximity to one another.

## 1.2.2 Diabetes Risk Factors

Several risk factors have been associated with diabetes. Genes, lifestyle and environmental factors all influence the risk of developing T2DM (Diabetes UK, 2015). Obesity is a major risk factor, constituting 80-85% of the overall risk (Hauner, 2010). Approximately 2 in every 3 persons in the UK are obese (WHO, 2016). The increasing prevalence of T2DM may be due to the increasing aging population and the increasing number of overweight and obese people. Additionally, some women develop diabetes during pregnancy; this condition is called gestational diabetes. About 5% of all pregnant women develop gestational diabetes (Inkster *et al.*, 2006), and women who have gestational diabetes are more likely to develop T2DM in their later life.

People who have a family history of diabetes are 2 to 6 times more likely to develop the disease than those without a family history (Vaxillaire and Froguel, 2010). With regards to ethnicity, South Asian individuals are 6 times more likely to have diabetes, while individuals of African and Caribbean origin are 3 times more likely to have diabetes than people from other populations (NSF, 2013). In 2015, it was estimated that approximately 14.2 million people in Africa had diabetes, with 75% of this estimate being undiagnosed (IDF, 2015).

A number of genes have been found to play key roles in susceptibility to diabetes. Of particular importance is the gene for transcription factor 7-like 2 (*TCF7L2*), which was first regarded as a diabetes susceptibility gene following a strong signal that mapped to chromosome 10q in a Mexican-American population. Fine mapping of this region was carried out in Danish and United States cohorts with the risk locus being located to intron 3 of the *TCF7L2* gene

(Ali, 2013). *TCF7L2* variants have been linked with T2DM in various ethnic groups (Scott *et al.*, 2006; Cauchi *et al.*, 2006; Sale *et al.*, 2007). *TCF7L2* is a transcription factor that plays a key role in the Wnt signaling pathway and in the development of various cell lineages (Klaus and Birchmeier, 2008). Its role in  $\beta$  cell survival, pancreatic islet development, insulin secretory granule function, adipogenesis and myogenesis, all reflect its impact on diabetes (Shu *et al.*, 2008; da Silva *et al.*, 2009). It is also a key component in the transcriptional regulation of the genes for proglucagon and the glucagon-like peptides GLP-1 and GLP-2, which are major players in postprandial insulin secretion (Doria *et al.*, 2008). *TCF7L2* polymorphisms have been linked with glucose tolerance and impaired insulin secretion by direct impact on pancreatic islet  $\beta$  cells (Lyssenko *et al.*, 2007; Schafer *et al.*, 2007). Moreover, studies have shown that elevated levels of gastric inhibitory peptide and glycated hemoglobin (HbA1c), decreased processing of proinsulin, and dysregulation of glucose metabolism, have all been seen in normoglycemic individuals with particular *TCF7L2* polymorphisms prior to the development of T2DM (Gjesing *et al.*, 2011; Gautier *et al.*, 2011). In addition, studies have shown that genetic tests for *TCF7L2* are useful in predicting the incidence of this disease (Silbernagel *et al.*, 2011). These studies suggest that detection of *TCF7L2* variants could be a good strategy for the early detection, intervention and prevention of T2DM (Florez *et al.*, 2006). However, there is currently no clinically approved role for routine screening for these variants in potential diabetics.

### **1.2.3 Secondary Complications of Diabetes**

Diabetes leads to a number of secondary complications including blindness, heart disease, kidney failure and stroke (WHO, 2015), and people with diabetes have a two times higher risk of developing cardiovascular disease than healthy individuals (Sarwar *et al.*, 2010). Diabetes is a common cause for lower limb amputations (ASD, 2007) and 70% of people die within 5 years of amputation due to diabetes (Schofield *et al.*, 2006). Nephropathy occurs in approximately 50% of individuals with diabetes (Diabetes UK, 2015). A healthy diet, weight management, keeping active, and using medication including insulin therapy, are necessary for managing diabetes and its complications (Colhoun *et al.*, 2004; Morrish *et al.*, 2001) as there is currently no cure for the disease.

### **1.2.4 Current Methods for Diagnosis of Diabetes**

The diagnosis of diabetes can be carried out in various ways. T2DM is usually diagnosed by symptoms, including polyuria (excessive urination) and polydipsia (excessive thirst). Screening tests used in diagnosing diabetes and pre-diabetes include the Fasting Plasma Glucose Test, Oral Glucose Tolerance Test, Glycated Hemoglobin test (HbA1c Test) which shows the average plasma glucose concentration, and Random Blood Glucose Test (Diabetes UK, 2016). The Fasting Plasma Glucose Test is the most prevalent of these tests because it is more convenient and cheaper to administer than the Oral Glucose Tolerance Test. To measure blood glucose levels using this test, a person must have fasted for at least 8 hours, and the most accurate results are obtained when the test is taken in the morning. A fasting glucose level of 100 to 125 mg/dL indicates

impaired fasting glucose or prediabetes, whereas a level of 126 mg/dL or above indicates diabetes if confirmed by a second test (NIDDK, 2014). However, the Oral Glucose Tolerance Test has a higher sensitivity than the Fasting Plasma Glucose Test, even though it is less convenient to administer. Blood glucose level is measured by the Oral Glucose Tolerance Test after a person fasts for at least 8 hours and 2 hours after the person drinks a liquid containing 75 grams of glucose dissolved in water. A person with a 2-hour blood glucose level between 140 and 199 mg/dL is considered pre-diabetic (NIDDK, 2014). A level of at least 200 mg/dL indicates that a person is diabetic, if confirmed by a second test. The HbA1c test is also an effective way of detecting T2DM and pre-diabetes. A level below 42 mmol/mol indicates that the individual is non-diabetic. A level between 42 and 47 mmol/mol indicates impaired fasting glucose (prediabetic), whereas a level of 48 mmol/mol and above indicates diabetes (Diabetes UK, 2016). The Random Plasma Glucose Test is used to detect diabetes during routine health checkup. A level of 200 mg/dL or above in addition to the presence of diabetes symptoms is a pointer for the diagnosis of diabetes. Other diagnostic tests used to differentiate between type 1 and T2DM include ketone tests, Glutamic Acid Decarboxylase autoantibody tests, and C-peptide tests.

### **1.2.5 Current Methods for Treatment of Diabetes**

In addition to life style changes such as diet and exercise, a number of treatment options are available for the management of diabetes. Insulin injections are usually administered to compensate for the non-production of insulin in type 1 diabetes (NHS UK, 2015). Patients with T2DM are eventually treated with

insulin as their insulin production levels decrease with disease progression (Diabetes UK, 2016). There are three main types of insulin; animal insulin, human insulin (produced synthetically) and insulin analogues where the chemical structure of human insulin is altered to provide a more rapid or long lasting effect. Other treatments for T2DM include biguanide, sulphonylureas, prandial glucose regulators, alpha glucosidase inhibitor, DPP-4 inhibitors (gliptins), thiazolidinediones (glitazones), incretin mimetics and SGLT2 inhibitors (Diabetes UK, 2016). These treatment options are only able to manage diabetes but do not prevent secondary complications. As there is currently no cure for diabetes, there is a need for more research to develop treatment options that more effectively manage and potentially cure diabetes (Diabetes UK, 2016). Recent animal and human studies showed that berberine, an isoquinoline alkaloid extract, is a promising hypoglycemic agent (Chang *et al.*, 2015). Interestingly, recent studies have shown that drugs used to treat T2DM may be useful for Alzheimer's disease (Holscher, 2014). Lixisenatide, a diabetes drug, shows neuroprotective effects in mouse models of Alzheimer's disease (McClellan and Holscher, 2014). Further studies have also reported that diabetic individuals with very poor blood sugar control experience a high risk of developing dementia and Alzheimer disease (Luchsinger *et al.*, 2004; Gella and Durany, 2009). These data strongly suggest a relationship between T2DM and Alzheimer's disease. Both diabetes and Alzheimer's disease are characterised by accumulation of advanced glycation end products and oxidative damage (Ott *et al.*, 1999), further suggesting mechanistic links between these two apparently different diseases. Although this correlation is not fully understood, the above

data suggest that a cure for diabetes could be an indicator for finding a cure for other amyloid related diseases.

### **1.2.5.1 Stem Cell Treatment for Diabetes**

Approaches that stimulate replication and regeneration of  $\beta$  cells may lead to increased amounts of  $\beta$  cells available for the regulation of blood glucose. Stem cell therapy and organ transplantation holds huge possibilities for the treatment of diabetes through the isolation and transplantation of  $\beta$  cells or an entire pancreas from a donor to a patient (EuroStemCell, 2016). Whole pancreas transplants have been used to help the body re-attain its ability to regulate blood sugar levels. Islet transplantation is however more prevalent as whole pancreas transplant is associated with a high surgical risk. Despite the huge potential pancreas transplantation holds for diabetes treatment, it involves a number of risk, for example, the immune system has to be suppressed with immune suppressing drugs during transplantation, so the foreign organ is not rejected. However, suppressing the immune system exposes the recipient to infection and may also produce adverse effects (EuroStemCell, 2016). The immune suppressing drugs are ultimately destroyed by the immune system and another transplant would invariable be required. Thus, most organ transplants are rejected. On the other hand cells transplantation hold huge potential for replacement tissues *in vitro* as well as autologous cells specifically from the patients. Hanna *et al.*, 2007, showed that hematopoietic progenitors were successfully used to treat sickle cell in an anemia mouse. This is supported by a previous study which showed that engrafting embryonic stem cell (ESC)-

derived cardiomyocytes into injured heart muscle effectively impeded arrhythmias (Shiba *et al.*, 2012). Furthermore, a study on rats with spinal cord injuries showed that ESC-derived oligodendrocyte progenitor cells re-instated their mobility (Keirstead *et al.*, 2005).  $\beta$  cells also holds an attractive potential for cell replacement strategy as replacement is required for only a single cell type, thus replacement can be carried out in non-endogenous sites which alleviates the risk of invasive surgeries.  $\beta$  cell transplantation into a non-endogenous site using immunoprotective devices also protects the cells from autoimmune attack (CFRI, 2016; JDRF, 2016; HSCI, 2016). This is supported by previous studies where  $\beta$  cell transplantation into the hepatic porta vein showed to be very effective in diabetes treatment (Shapiro *et al.*, 2000; Bellin *et al.*, 2012; Shapiro *et al.*, 2006).

A major challenge with islet transplantation is the fact that there are very few good quality islets from donors compared to the demand for transplantation. Thus, producing  $\beta$  cells from alternative sources in the laboratory could significantly help with generating a reliable and unlimited source of islets, given that most patients require more than a single donor. Research has shown new approaches for making  $\beta$  cells for therapeutic purposes (Lumelsky *et al.*, 2001). Studies have shown the transplantation of mature pluripotent stem cells namely embryonic and induced pluripotent stem cells, into pancreatic  $\beta$  cells (Hori *et al.*, 2002). Pluripotent stem cells can make any cell type in the body and have shown to be very beneficial in cell replacement approaches as it is highly available, has high expansion and differentiation capabilities and have phenotypically established hallmarks (Soria *et al.*, 2000). Mature  $\beta$  cells have

also been made from other cell types. For example, acinar cells of the pancreas have been shown to form new  $\beta$  cells, Zhou *et al.*, 2007 showed that acinar cells differentiate into  $\beta$  cells following overexpression of major transcription factors including MafA, Ngn3 and Pdx1 (D'Amour *et al.*, 2006). Also, more  $\beta$  cells can be endogenously produced through induction replication of existing  $\beta$  cells. Although tissues such as blood and skin regenerate through differentiation of tissue specific stem cell, new pancreatic  $\beta$ -cells are often generated from the replication of existing  $\beta$ -cells (Dor and Melton, 2004). In spite of the huge potential this holds, the main risk associated with this replication induction approach is the spontaneous stimulation of tumorigenesis. Inducing acinar tissue to proliferate with  $\beta$  cells imposes cancer risk. However, this risk can be averted if the agent used in replication has a high specificity for  $\beta$ -cells comparable to other cell types. Stem cell treatment offers a huge potential for the treatment of diabetes, however, the likelihood of success for stem cell treatment in diabetes mellitus is very narrow, and this procedure is very expensive and requires specialist intervention, and given the large population of people suffering from diabetes, a more convenient, easily assessable and less expensive approach is required.

### **1.2.6 Animal Models of Diabetes**

A number of animal models of type 1 and T2DM are available for pharmacological testing, the study of disease mechanisms, and for genetic studies. These animal models have varying degrees of physiological relevance,

with some of them depicting the actual human disease condition more accurately than others.

Streptozotocin (STZ) is a chemical broadly used for the induction of experimental diabetes in rodents (Szkudelski, 2001; Lenzen, 2008). Ever since the discovery of its diabetogenic properties (Rakieten *et al.*, 1963), STZ has been used, alone or in combination with other chemicals, for inducing type 1 or T2DM. A single STZ injection induces type 1 diabetes (Junod *et al.*, 1969; Yin *et al.*, 2006), while T2DM is induced through a number of techniques including STZ injection during the neonatal period (Patil *et al.*, 2014; Portha *et al.*, 1989), after nicotinamide administration (Wu *et al.*, 2008; Szkudelski, 2012), or low-dose STZ injection after a high fat diet (Skovs, 2014). These STZ diabetic models have been very advantageous in studying the pathogenesis of diabetes and for screening of pharmacological agents which can potentially lower blood glucose levels (Srinivasan *et al.*, 2005; Kumar *et al.*, 2012). Following intraperitoneal or intravenous administration, STZ penetrates into pancreatic  $\beta$  cells by means of the Glut-2 transporter, resulting in DNA alkylation (Szkudelski, 2001) and eventual inhibition of insulin production (Sandler and Swenne, 1983). STZ also produces free radicals, which play a role in DNA damage and eventually cell death. Intraperitoneal injections of STZ are eliminated within 48 hours of administration (Karunanyake *et al.*, 1974) but  $\beta$  cell function still progressively declines even when STZ is no longer detected (Rerup, 1970), indicating that acute STZ toxicity induces a sustained hyperglycaemic state which facilitates long-term  $\beta$  cell destruction (Matsuda *et al.*, 2002). Although STZ induction is a widely accepted and well known system for studying the pathogenesis and complications of diabetes, induction of

diabetes through STZ is by no means identical to the human disease state. STZ does not produce the pathophysiological insulin resistance observed in human state diabetic conditions (Wu and Yan, 2015). Additionally, there are no standard protocols for STZ administration and the diabetic state is influenced by many factors including the specie, sex, body weight and age of animals used (Deeds *et al.*, 2011).

Models of type 1 and T2DM have also been created using transgenic mice, including humanized mice with aspects of the human immune system, hIAPP mice that express human amylin, and mice that permit conditional ablation of  $\beta$  cells (Hara *et al.*, 2003). Knock-out and transgenic mice are key players in studying the impact of particular genes in glucose metabolism and diabetes pathogenesis, including an understanding of insulin signaling pathways (Kahn, 2003b; Wang and Jin, 2009) and elucidation of the transcription factors involved in pancreatic development (Habener *et al.*, 2005). The diabetogenic effects of human amylin have been studied by using transgenic mice overexpressing biologically active amylin in their pancreatic islet  $\beta$  cells (Höppener *et al.*, 1993; Ahrén *et al.*, 1998). Here, it is important to note that endogenous rodent amylin does not form islet amyloid (Höppener *et al.*, 1993; Ahrén *et al.*, 1998). Studies have shown that overexpressing human amylin alone does not stimulate hyperinsulinemia, hyperglycemia or obesity in mice (Höppener *et al.*, 1993). However, substantial islet amyloid formation with compounding diabetes is observed upon cross breeding of amylin transgenic mice with leptin-deficient and insulin-resistant ob/ob (ob = obese) mice (Höppener *et al.*, 1999). Studies

have also shown that a long-term, high-fat diet stimulates hyperinsulinemia, hyperglycemia and obesity in amylin transgenic mice (Surwit *et al.*, 1998; Ahrén *et al.*, 1997; Höppener *et al.*, 2008). In addition, a high-fat diet has been shown to enhance islet amyloid formation in amylin transgenic mice (Verchere *et al.*, 1996).

When evaluating drug interventions on diabetic animal models, a common measurement is determination of blood glucose levels. The presence of glucose in urine is also indicative of diabetes. It is, however, important to note that different species have different blood glucose levels compared to humans, and the diabetic state in humans would not necessarily be regarded as diabetic in animals. For example, mice naturally have a higher blood glucose level than humans (Leiter, 2009). Also, since diabetes is multifaceted, other measures need to be taken into consideration, depending on the drug mechanism and animal model used. For example, in studies of type 1 diabetes, it is necessary that the animals used are weighed to make certain that any fall in blood glucose levels is not linked with weight loss, which could indicate a toxic effect of the treatment, or simple loss of appetite. On the other hand, in models of T2DM weight loss may be an impact of the glucose lowering effects of the drug (Knudsen, 2010). The stages of disease progression should also be considered, depending on the purpose of the study, as the disease stage may influence the measurement criteria. Because the onset of T2DM appears later in life, it may be necessary to use older mice when carrying out studies on this disease.

In addition, when choosing an animal model, it is important to consider variations between species, and between animal strains, as this will have a

bearing on their predisposition to diabetes treatment (Brosius III *et al.*, 2009). For example, some species and strains of animals do not develop diabetic complications, and so other suitable models may be required for studies focused on diabetic complications (Breyer *et al.*, 2005; Sullivan *et al.*, 2007).

### **1.3 Structure of Amylin**

Amylin is a 37 amino acid residue peptide belonging to the calcitonin family, which also contains adrenomedullin, calcitonin, calcitonin gene-related peptide (CGRP) and intermedin (Roh *et al.*, 2004; Wimalawansa, 1997). Members of the calcitonin family, including amylin, have a disulphide bridge between Cys residues 2 and 7, as well as an amidated carboxyl terminus, which are posttranslational modifications necessary for biological activity (Wimalawansa, 1997). Amylin has sequence homology of 43% and 49% with human CGRP-1 (hCGRP-1) and hCGRP-2 respectively (Cooper, 1994). Amylin is thought to have a random coil structure (Kayed *et al.*, 1999). On the other hand, circular dichroism (CD) (Knight *et al.*, 2006) and nuclear magnetic resonance (NMR) (Nanga *et al.*, 2009; Patil *et al.*, 2009) spectroscopy studies have suggested that the peptide forms a temporary amphipathic  $\alpha$ -helix in the amino terminal segment (Abedini and Raleigh, 2009), separate from the very end of the amino terminal region, giving rise to the disulphide bridge at residues 2 and 7. The helix extends from residues 5-23 in solution (Knight *et al.*, 2006). The carboxyl terminal region of the molecule is undefined (Nanga *et al.*, 2009), and the helical region is thought to play a key role in its pathological change to amyloid fibrils.

Amylin is a polypeptide hormone that is conserved throughout evolution and has been characterised in birds, mammals and teleostean fishes (Johnson *et al.*, 1990; Martínez-Álvarez *et al.*, 2008; Miyazato *et al.*, 1992; Westermark *et al.*, 2002), where mainly the amino and carboxyl terminal segments are conserved (figure 1.3). Amylin deposits are found in the pancreatic islets of humans and other mammals and probably lead to pathological symptoms in these organisms. Previous difficulty in accepting the role of amylin-derived amyloid in the pathogenesis of T2DM may have emerged from the fact that islet amyloid is not present in most mammalian species used for diabetic research, such as rats and mice (Westermark *et al.*, 1992). Although the amylin molecule is conserved throughout evolution, there are interspecies modifications at key amino acid residues. The variations at amylin 20-29 region are most apparent, and account for five out of six variations between human and rat amylin (table 1). The rat/mouse amylin has three proline residues in this region which are known to be  $\beta$  sheet breakers. While synthetic human, non-human primate and cat amylin are very fibrillogenic, rat/mouse and several other rodent forms of amylin are not (Westermark *et al.*, 1990; Betsholtz *et al.*, 1990., Betsholtz *et al.*, 1989b), and this can be attributed to these variations in primary structure. Further studies suggest that while the amylin 20-29 region is vital in amyloid formation, other regions of the molecule also play key roles in fibrillogenesis (Abedini and Raleigh, 2006; Goldsbury *et al.*, 2000; Koo and Miranker, 2005; Nilsson and Raleigh, 1999). The 14-20 region of amylin located at the amphipathic  $\alpha$ -helical segment (Nanga *et al.*, 2009) of the molecule may also be of significance.

	1	10	20	30	37
Human CGRP1	<u>A</u> <u>C</u> <u>D</u> TATCVT	<u>H</u> <u>R</u> <u>L</u> <u>A</u> <u>G</u> <u>L</u> <u>L</u> <u>S</u> <u>R</u> <u>S</u>	<u>G</u> <u>G</u> <u>V</u> <u>V</u> <u>K</u> <u>N</u> <u>N</u> <u>F</u> <u>V</u> <u>P</u>	TNVGS <u>K</u> <u>A</u> <u>F</u>	
Human CGRP2	<u>A</u> <u>C</u> <u>N</u> TATCVT	<u>H</u> <u>R</u> <u>L</u> <u>A</u> <u>G</u> <u>L</u> <u>L</u> <u>S</u> <u>R</u> <u>S</u>	<u>G</u> <u>G</u> <u>M</u> <u>V</u> <u>K</u> <u>S</u> <u>N</u> <u>F</u> <u>V</u> <u>P</u>	TNVGS <u>K</u> <u>A</u> <u>F</u>	
Human	KCNTATCAT	QRLANFLVHS	SNNFGAILSS	TNVGSNTY	
Rat	KCNTATCAT	QRLANFLVRS	SNNLGPVLP	TNVGSNTY	
Bear	KCNTATCAT	QRLANFLVRS	GNNLGAILSP	TNVGSNTY	
Puffer fish	KCNTATCVT	QRLADFLVRS	SNTIGTVYAP	TNVGSITY	
Monkey	KCNTATCAT	QRLANFLVRS	SNNFGTILSS	TNVGSNTY	
Macaque	KCNTATCAT	QRLANFLVRS	SNNFGTILSS	TNVGSNTY	
Baboon	ICNTATCAT	QRLANFLVRS	SNNFGTILSS	TNVGSNTY	
Porcine	KCNMATCAT	QHLANFLDRS	RNNLGTIFSP	TKVGSNTY	
Cow	KCGTATCET	QRLANFLAPS	SNKLGAIKSP	TKMGSNTY	
Cat	KCNTATCAT	QRLANFLIRS	SNNLGAAILSP	TNVGSNTY	
Dog	KCNTATCAT	QRLANFLVRT	SNNLGAAILSP	TNVGSNTY	
Mouse	KCNTATCAT	QRLANFLVRS	SNNLGPVLP	TNVGSNTY	
Guinea pig	KCNTATCAT	QRLTNFLVRS	SHNLGAAILP	TDVGSNTY	
Hamster	KCNTATCAT	QRLANFLVHS	NMNLGPVLP	TNVGSNTY	
Degu	KCNTATCAT	QRLTNFLVRS	SHNLGAAILP	TKVGSNTY	
Ferret	KCNTATCVT	QRLANFLVRS	SNNLGAAILP	TDVGSNTY	
Rabbit	CNTVTCAT	QRLANFLIHS	SNNFGAFLPP	<u>S</u>	
Hare	T	QRLANFLIHS	SNNFGAFLPP	T	

**Table 1.1:** The primary amino acid sequences of human CGRP and amylin of different species. Amylin is highly conserved but with clear variation in the 20–29 region. This corresponds to residues 31–40 of proAmylin. The biologically active mature amino acid sequences all have a disulfide bridge between Cys-2 and Cys-7 as well as an amidated C-terminus. Primates and cats have been shown to form islet amyloid, while cows, rodents, and dogs do not. Ferret and porcine amylin has been reported to be significantly less amyloidogenic than human amylin. Islet amyloid is found in the degu, but it is insulin-derived rather than being formed from amylin. The sequences for rabbit and hare are incomplete (Adapted from Akter *et al.* 2015).

## 1.4 Expression of Amylin

Amylin is initially expressed as part of an 89- amino acid residue pre proprotein, made up of a 22 amino acid signal peptide and two short peptides adjacent to each other, which are cut off at double basic amino acid residues (Betsholtz *et al.*, 1989; Mosselman *et al.*, 1989; Sanke *et al.*, 1988), in a similar way to proinsulin (Nolan, 1971). A single-copy gene on the short arm of chromosome 12 expresses amylin, in contrast to insulin and other members of the calcitonin family, including CGPR and calcitonin, which are encoded by evolutionarily conserved genes on chromosome 11 (Wimalawansa, 1997). PreproAmylin has three exons, with the last two coding for the full length prepro molecule (Christmanson *et al.*, 1990, Nishi *et al.*, 1989). In the endoplasmic reticulum (ER), the signal peptide is cut off, and proAmylin is converted to amylin in the secretory vesicles. Two endoproteases, prohormone convertase 2 (PC2) and prohormone convertase 1/3 (PC1/3), as well as carboxypeptidase E (CPE), control the course of action of ProAmylin and proinsulin (figure 1.4). This process is pH dependent and occurs in the Golgi and secretory granules. The carboxyl edge of Arg31 and Arg32 of human proinsulin is cleaved by PC1/3, and cleavage after Lys64 Arg65 is facilitated by PC2 (Smeekens *et al.*, 1992). The carboxyl terminal of the dibasic amino acids is removed by CPE (Davidson *et al.*, 1987). ProAmylin is processed by PC2 at position Lys10 Arg11 and at position Lys50 Arg51 by PC1/3 (Marzban *et al.*, 2004; Cao *et al.*, 2013). PC2 can process proAmylin at the carboxyl terminal, when PC1/3 is absent (Wang *et al.*, 2001). The carboxyl terminal glycine residue in several hormonal peptides is used for amidation which, along with the disulphide bridge between residues 2 and 7, is a requirement for complete biological activity.

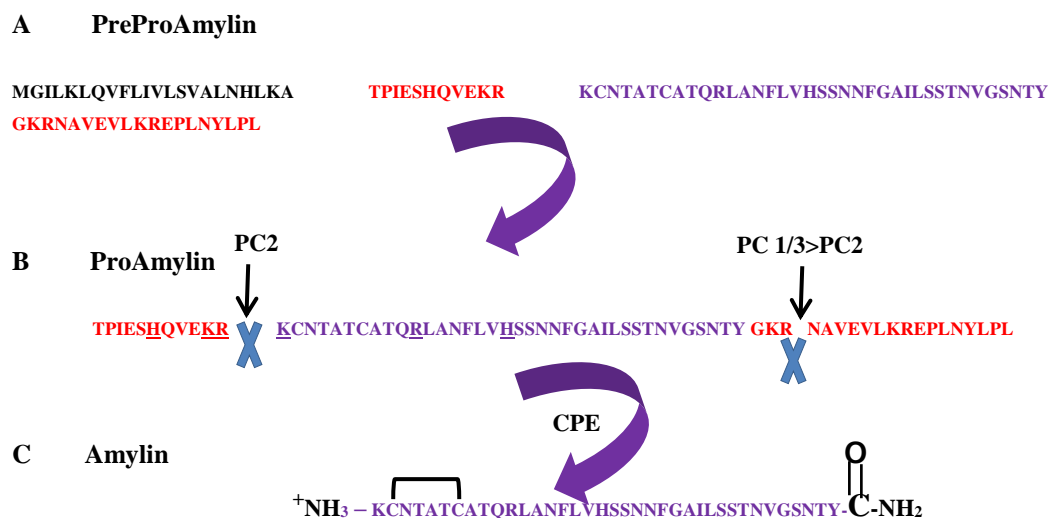


**Figure 1.2:** Processing of human PreProAmylin to form mature Amylin. (A) The primary amino acid sequence of human PreProAmylin, the peptide length is 89 residues. The 22 residue signal sequence is shown in black, the N- and C-terminal proAmylin flanking regions are shown in red, and the mature amino acid sequence is shown in purple. (B) The primary sequence of the 67-residue human proAmylin with cleavage site for PC(1/3) at the COOH terminus and PC2 at the NH<sub>2</sub> terminus, indicated by the arrows. CPE/PAM processed the amidation of the C-terminus of Amylin. (C) The amino acid sequence of the mature 37-residue human Amylin. The biologically active peptide possesses an amidated C-terminus and a disulfide bridge between Cys-2 and Cys-7.

The two flanking peptides from proAmylin and the C peptide from proinsulin stay in the secretory granule, resulting in exocytosis and discharge of equimolar concentrations of the isolated peptides and their ultimate hormonal products.

Insulin and amylin genes contain similar promoter elements (German *et al.*, 1992) and the pancreatic and duodenal homeobox 1 (PDX1) transcription factor controls the effect of glucose on both genes (German *et al.*, 1995; Watada *et al.*, 1996). In rats, glucose stimulation results in a synchronized increase in protein expression for amylin and insulin from the islet  $\beta$  cells (Kahn *et al.*, 1991; Mulder *et al.*, 1996). This linked expression pattern for insulin and amylin is, however, modified in experimental animal models of T2DM. In the presence of dexamethasone, more amylin was secreted by perfused rat pancreas than insulin (O'Brien *et al.*, 1991), and insulin secretion was also less than that of amylin at high doses of streptozotocin and alloxan (Mulder *et al.*, 1995). The expression of amylin and insulin is also regulated differently by fatty acids; for example, in MIN6 cells, oleate and palmitate increased the expression of amylin, but not insulin (Qi *et al.*, 2010). However, mice refed with intralipid showed significantly higher levels of amylin and insulin compared to those refed with saline (Qi *et al.*, 2010). Furthermore, plasma amylin was found to be 4.5 times greater than insulin in mice fed for 6 months with a high fat diet, compared with mice fed with standard food containing 4% fat (Westermarck *et al.*, 1998). These examples show that under certain conditions, the precise synchronized expression of insulin and amylin may be interrupted.

Furthermore, amylin is expressed in the gut of all mammals including cats, mice and rats (Miyazato *et al.*, 1991; Mulder *et al.*, 1996; Mulder *et al.*, 1994; Toshimori *et al.*, 1990), and in the sensory neurons of rats and mice (Gebre-

Medhin *et al.*, 1998; Mulder *et al.*, 1995). In the rat gastrointestinal tract, amylin is detected beginning from the pyloric antrum to the large intestine, with the antrum having the highest concentration (Miyazato *et al.*, 1991). However, the pyloric amount of amylin is only about 1 % of that found in the pancreas (Miyazato *et al.*, 1991). On the other hand, in the brain and intestine of the chicken, amylin is more highly expressed than in the pancreas (Fan *et al.*, 1994). It is, however, unclear how these extra-pancreatic sites regulate synthesis, storage and release of amylin (Fan *et al.*, 1994), but this suggests a common origin for the amylin and CGRP genes.

In healthy adults, the molar ratio of amylin to insulin is approximately 1:100. However, in T2DM, the molar ratio of amylin to insulin is approximately 1:20 (Knight *et al.*, 2008; Hull *et al.*, 2004), and it is therefore no surprise that small changes in the relative amounts of amylin and other  $\beta$  cell granule constituents can stimulate amylin aggregation and initiate amyloid fibril formation. The presence of amyloid-like fibrils in  $\beta$  cells during the initial stages of the disease (Paulsson *et al.*, 2006) also supports this finding. Human amylin is highly fibrillogenic in a spontaneous fashion, and thus should be protected from aggregation (Abedini *et al.*, 2007).

Amylin works together with insulin in maintaining circulating glucose concentrations in quite a narrow range, thus impeding an abnormal rise in glucose concentrations (Hirsch, 1999). The pathogenesis of T2DM is characterised by decreased insulin sensitivity and  $\beta$ -cell function (Porte and Kahn, 1991). Alterations in  $\beta$ -cell function involve a decrease in insulin

secretion in response to glucose (Porte, 1999). In addition to decreased insulin secretion, there is also a decrease in amylin response. Studies have shown that a decrease in insulin and amylin responses are seen in patients with high diabetes risk is an indication of early alterations in  $\beta$ -cell function. Amylin deposits have been found in patients with T2DM and studies suggest that an increase in amylin secretion may be involved in the development of these deposits (Westermarck *et al.*, 1987; Cooper *et al.*, 1987). Although the relationship between insulin sensitivity and amylin response is still being argued, amylin secretion from the  $\beta$ -cell of the pancreas may not be regulated by insulin sensitivity. However, amylin which is co-secreted with insulin by the pancreatic  $\beta$ -cells (Lukinius *et al.*, 1989), have been shown to be elevated in insulin-resistant conditions such as obesity (Kautzky-Willer *et al.*, 1994; Kahn *et al.*, 1998). This suggest a relationship between insulin resistance and amylin levels and since increased levels of amylin which results in the formation of amylin aggregates is a main pathological feature of T2DM, it could be thought that inhibiting amylin elevation and aggregation may also impact on insulin resistant states. Given that insulin and amylin have a hyperbolic (Landchild *et al.*, 2000) relationship, it could be assumed the secretion of insulin-containing granules as rmodulated by insulin sensitivity could also be applied to amylin.

It is likely that the interaction with other components such as proinsulin and insulin defends against amylin aggregation (Westermarck *et al.*, 1996). Insulin has been shown to act as a natural inhibitor of amylin (Gilead *et al.*, 2006) and to strongly impede the formation of amylin fibrils (Westermarck *et al.*, 1996) when its concentration is in excess of that of amylin (Janciauskiene *et al.*, 1997).

These findings have been supported by several studies which elucidate the inhibitory ability of insulin on amylin aggregation (Jaikaran *et al.*, 2004; Larson *et al.*, 2004; Sellin *et al.*, 2010). The 9-20 segment of the insulin  $\beta$ -chain binds to amylin and this appears to be responsible for the inhibition (Larson *et al.*, 2004). However, other studies have shown contradictory effects on amylin aggregation. One study showed that although insulin is a kinetic inhibitor of amylin aggregation, its inhibitory effect on amylin is only apparent for a limited time period (Cui *et al.*, 2009). It was also reported that insulin copolymerizes with amylin monomers and oligomers, instead of amylin fibrils (figure 1.2). This interaction results in inhibition of amylin aggregation, but, in diabetic conditions, can stimulate the aggregation of amylin over time (Cui *et al.*, 2009). These results suggest that insulin could play different roles in amylin aggregation, by inhibiting amylin aggregation in healthy people while promoting amylin aggregation during the pathogenesis of T2DM. Given these contradictory effects, insulin cannot be used to develop peptide inhibitors of amylin aggregation, and more study is required to elucidate the interactions of insulin and amylin in both healthy and type 2 diabetic individuals.

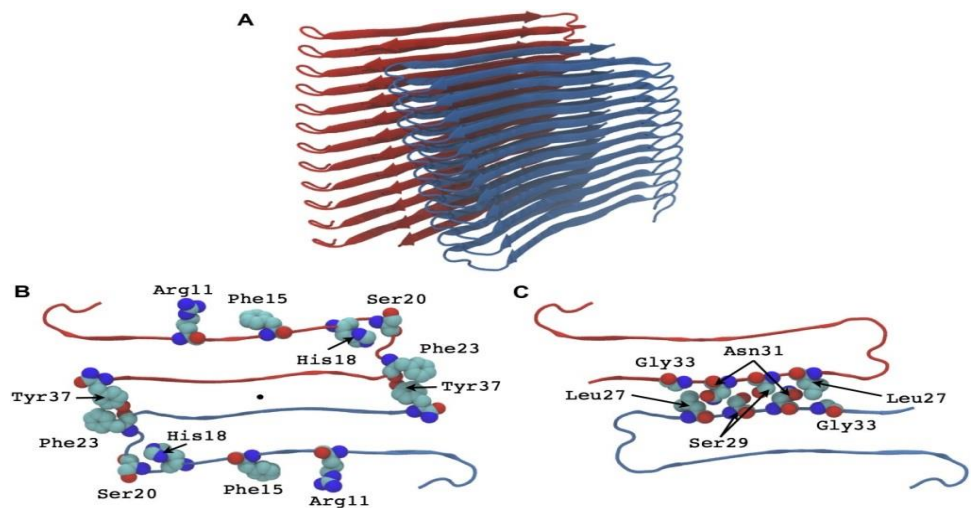


**Figure 1.3:** Structural model of the amylin fibril derived from steric zipper studies. (A) Ribbon diagram of human amylin fibril structure showing the two stacks of symmetry related monomers. (B) Cross section of a single fibril layer, viewing inside the fibril axis, reveals several key residues. The aromatic residues Phe15, Phe23 and Tyr37 are shown in space filling format together with Arg11, His18 and Ser20. (C) Cross section of a single layer showing the tight “steric zipper” interface between two human amylin monomers. Interdigitated residues Leu27, Ser29, Asn31 and Gly33 are shown in space filling representation (Cao *et al.*, 2013).

## **1.5 Effects of Amylin**

### **1.5.1 General Effects of Amylin**

The fact that amylin is conserved across several animal species suggests that it has an important function. The role of amylin is not fully understood, a major difficulty being the complexity in differentiating its pathological and physiological roles, as well as its pharmacological impact in experiments. Since amylin is co-secreted and co-stored with insulin, it is logical to think that amylin could play a role in the regulation of glucose metabolism, by acting as a paracrine molecule in the islets of Langerhans, and there is good evidence to support this. There is also evidence that amylin can act as a hormone with impact on the central nervous system (Barth *et al.*, 2003; Lutz, 2006).

### **1.5.2 Anorectic Effects of Amylin**

Studies in humans and animals have proven that amylin has an inhibitory effect on eating (Arnelo *et al.*, 1996; Barth *et al.*, 2003; Lutz, 2006). Pramlintide, a drug which consists of human amylin with amino acid substitutions that change its solubility, has been shown to decrease both meal duration and calorie intake in healthy men (Chapman *et al.*, 2007). Amylin binding sites have been found in some parts of the brain, including the nucleus accumbens and the postrema area (Potes and Lutz, 2010; Christopoulos *et al.*, 1995). Additionally, the postrema is outside of the blood-brain barrier and may, perhaps, be a target for amylin secreted by the pancreatic islets of Langerhans. Although early studies suggested that amylin has no cerebral production, further studies have revealed

amylin immunoreactivity in the basal ganglia and hypothalamus (D'Este *et al.*, 2000; D'Este *et al.*, 2001; Skofitsch *et al.*, 1995). Additionally, amylin mRNA was found in the preoptic region of the lactating rat (Dobolyi, 2009). Amylin inhibits gastric emptying (Reidelberger *et al.*, 2001) and it does this by binding to the brain (Arnelo *et al.*, 1996). In type 1 diabetes, gastric emptying is fast and this is thought to promote the postprandial hyperglycemia observed in the disease (Woerle *et al.*, 2008). It is assumed that insufficient islet amylin secretion in type 1 diabetes may play a key role in these gastric actions (Woerle *et al.*, 2008).

### **1.5.3 Effects of Amylin on Pancreatic Islet Cells**

Following the discovery of amylin, it was found that amylin impedes insulin-stimulated glucose uptake and the synthesis of glycogen in incubated rat skeletal muscle (Cooper *et al.*, 1988). A study also revealed that amylin impedes insulin-stimulated glucose transport *in vitro* through a post-insulin-receptor effect (Zierath *et al.*, 1992). This inhibition may be regulated by the influence of some enzymes including glycogen phosphorylase and glycogen synthase (Deems *et al.*, 1991). Originally, it was thought that the basic mechanism behind insulin resistance in T2DM had been realised with the discovery of amylin, as *in vivo* studies also began to reveal that infiltration of amylin stimulates insulin resistance (Johnson *et al.*, 1990). However, these results were attained at very high concentrations of amylin compared to those observed physiologically, and were thus considered to be pharmacological rather than physiological. Although the role of amylin in altering the effect of insulin on peripheral tissues is still

disputed, this activity cannot be disregarded. High amylin plasma concentrations compared to those observed in physiological conditions have also been found to suppress insulin response to glucose load in humans (Bretherton-Watt *et al.*, 1992; Cooper *et al.*, 1988). Additionally, studies have shown an inhibition of insulin secretion by amylin (Degano *et al.*, 1993; Kogire *et al.*, 1991; Sandler and Stridsberg, 1994), even at low concentrations (Silvestre *et al.*, 1997), although other studies have shown that there is no inhibitory effect of amylin on insulin secretion (Broderick *et al.*, 1991; O'Brien *et al.*, 1990; Pettersson and Ahrén, 1990). The reason for these discrepancies is unclear, but the strong tendency of amylin to form amyloid-like fibrils may be responsible.

#### **1.5.4 Other Effects of Amylin**

The fact that amylin and calcitonin are structurally similar suggests that amylin may also play a role in the regulation of calcified tissues (MacIntyre, 1989). Studies have shown that amylin inhibits osteoclastic activity (Zaidi, 1990), and plays a role in inhibiting bone resorption (Naot and Cornish, 2008). Amylin also possesses vasodilative properties, likely based on its binding with CGRP receptors, but amylin is two times less effective at this than its relative CGRP (Brain *et al.*, 1990). Early findings showed strong binding of radio-labelled amylin to the renal cortex (Stridsberg *et al.*, 1993). This binding was initially considered to be an unspecific radioactivity uptake owing to reabsorption of labelled amylin in the proximal tubules. However, further studies have reported specific binding (Wookey *et al.*, 1996). This suggests that amylin may play a role in kidney function.

## 1.6 Amylin and Oxidative Stress

In about 90% of patients with T2DM, amylin aggregates into insoluble extracellular amyloid deposits (Cooper *et al.*, 1987). It is not clear why amylin forms these deposits; however, an increased demand for  $\beta$  cell secretory function during T2DM may play a fundamental role in this process (Aston-Mourney *et al.*, 2011). Changes in glycosylation and deficient enzymatic processing of the pro-Amylin precursor may also play a role in the aggregation of amylin (Marzban *et al.*, 2003; Park and Verchere, 2001). Amylin aggregates, particularly the soluble oligomeric forms, are likely to contribute to the destruction of pancreatic  $\beta$  cells in the late phase of T2DM (Lorenzo *et al.*, 1994). The cytotoxicity of amyloidogenic assemblies may be due to the presence of these oligomers (Lorenzo *et al.*, 1994; Lorenzo and Yankner, 1994; Konarkowska *et al.*, 2006). Human amylin is thought to form ionic channels in the lipid bi-layers of  $\beta$  cells (Mirzabekov *et al.*, 1996). Additionally, studies suggest that oxidative stress may play a role in amyloid formation, which ultimately results in the destruction of pancreatic islet cells (Zraika *et al.*, 2009). Amylin has been shown to generate reactive oxygen species (ROS) directly, which could explain some of its damaging effects on the islets of individuals with T2DM (Masad *et al.*, 2011).

The aggregation of amylin has been studied extensively *in vitro* and is due in part to intermolecular hydrophobic interactions that occur between the protein molecules (Fink, 1998; Vieira *et al.*, 2006). Therefore, hydrophobic compounds which block the self-assembly of amylin are a potential therapeutic approach for treating or preventing diabetes. Since oxidative stress has been shown to be

linked with amyloid formation, inhibition of oxidative stress may also be a viable therapeutic strategy.

## **1.7 Amylin Toxicity**

Amyloid is characterised by the presence of fibrils with a diameter of 7-10 nm (Goldsbury *et al.*, 2000), with the integral monomers being arranged vertically into  $\beta$ -sheet structures. The formation of amyloid is nucleation dependent and is divided into three distinct phases (figure 1.5). The first phase, being the lag phase, is the rate-limiting step where the nucleation of monomeric peptides occurs (Wilson *et al.*, 2008). This phase spans from a few minutes to a life time subject to variable conditions such as temperature and concentration (Wilson *et al.*, 2008). The elongation phase is the second phase in which amyloid fibrils are generated. The third phase is the plateau phase where fibrillation is in a steady condition, and the fibrillar mass is stable (Wilson *et al.*, 2008). Amyloid formation is a spontaneous process which, after initiation, continues if there is a satisfactory concentration of amyloidogenic protein (Wilson *et al.*, 2008). In systemic amyloidosis, significant quantities of amyloid deposits are formed in various organs such as heart, kidney, liver or spleen, and these deposits are capable of triggering severe diseases (Merlini and Westermark, 2004; Pepys, 2006).

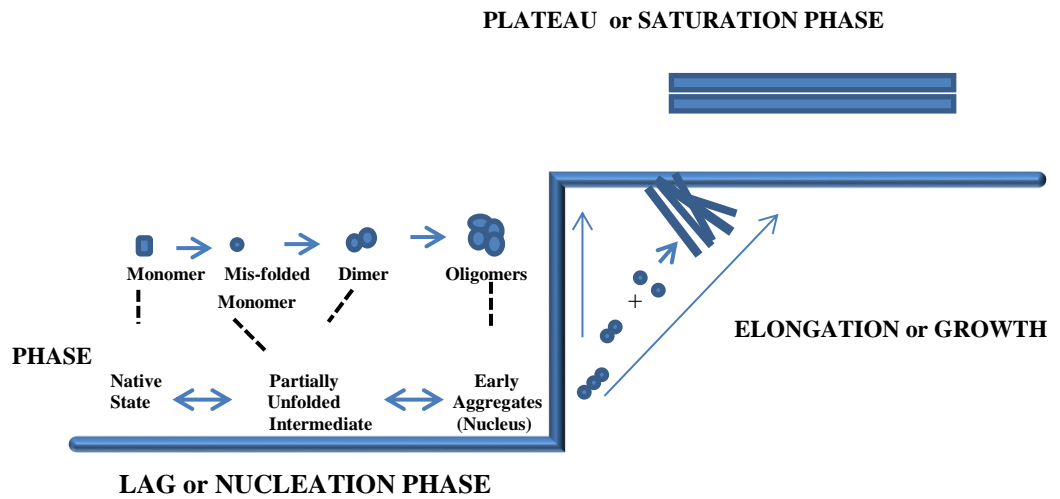


**Figure 1.4:** Schematic representation of the amyloid forming phases. The formation of amyloid fibrils is nucleation dependent. During the lag phase, the soluble prefibrillar oligomers or nuclei are formed. The elongation phase is the phase in which the nuclei grows rapidly by the addition of monomers and subsequently forming insoluble mature amyloid fibrils. The plateau phase is the steady stage where maximum fibril growth has been attained.

In Alzheimer's disease, the amyloid fibril protein found in senile plaques and in the walls of cerebral blood vessels is A $\beta$ , which constitutes a 40-42 amino acid segment of the A $\beta$  precursor protein (De Strooper, 2010). Early studies revealed A $\beta$  to be neurotoxic *in vitro* (Yankner *et al.*, 1989; Yankner *et al.*, 1990). A $\beta$  molecules naturally exist as soluble monomers, but in the early stages of development of Alzheimer's disease (Teich and Arancio, 2012), they begin to aggregate into small oligomers which remain soluble, but eventually coalesce to form the insoluble amyloid plaques which are one of the hallmarks of this disease. A $\beta$  oligomers can impair synaptic function, and, together with the plaques, presumably contribute to nerve cell damage (Pimplikar *et al.*, 2010). The protein Tau has also been implicated in Alzheimer's disease, due to the formation of intracellular neurofibrillary tangles composed of a heavily phosphorylated form of this protein. Tau is a microtubule-binding protein that helps to link neuronal microtubules together in a parallel position, so aiding in the transport of nutrients and organelles from the cell body to the axon, and in the elimination of any accumulated toxic proteins from nerve cells, as part of the axonal transport process (Lonskaya *et al.*, 2014). Failure of this transport system would inevitably lead to degeneration of the neuron (Caughey *et al.*, 2003). The reason for Tau malfunction in Alzheimer's disease is not clearly understood, but there may be a link between A $\beta$  accumulation and neurofibrillary tangle formation (Hardy and Selkoe, 2002) since A $\beta$  can influence the signaling pathways that control phosphorylation of Tau (Hardy and Selkoe, 2002; Lonskaya *et al.*, 2014) and also inhibit the degradation of hyperphosphorylated Tau (Lonskaya *et al.*, 2014). The two closely related proteins A $\beta$  and Tau are both therapeutic targets for Alzheimer's disease.

Early studies elucidating the role of protein toxicity in T2DM (Lorenzo *et al.*, 1994) demonstrated the toxicity of human amylin to cultured islet cells, apparently through induction of membrane damage and apoptosis. These background findings initially suggested that the toxic forms of both A $\beta$  and amylin are the amyloid fibrils themselves (Hiddinga and Eberhardt, 1999; Kapurniotu *et al.*, 1998; Lorenzo and Yankner, 1996; Yan *et al.*, 2007). However, more recent studies have shown that soluble oligomers are more likely to be the toxic form of these molecules (Aitken *et al.*, 2010; Ritzel *et al.*, 2007).

The role of amylin toxicity is currently an important subject in the pathogenesis of T2DM but a key issue is the ill-defined nature of the oligomers, which have been studied *in vitro* to a large extent (Glabe, 2008; Kaye *et al.*, 2009). The first identified toxicity process is the disruption of the plasma membrane, resulting in effects on intracellular homeostasis (Westermarck *et al.*, 1990; Lorenzo *et al.*, 1994). Some studies reveal that oligomers are incorporated into the cell membrane, where they form channel-like pores that are permeable to certain ions, particularly Ca<sup>2+</sup> (Anguiano *et al.*, 2002; Mirzabekov *et al.*, 1996; Porat *et al.*, 2003). The cytotoxicity of amyloid proteins have been associated with this pore forming ability, and lipid bilayers have been found to contain oligomeric complexes ranging from trimers to octamers, depending on the amyloid protein type (Quist *et al.*, 2005). The incorporated complexes in the case of amylin are mainly trimeric and hexameric (Quist *et al.*, 2005). Although it has been proposed that amylin permeabilizes membranes by formation of these doughnut-like pores, physical membrane disruption could also be important due to the extreme negative curvature strain present in small pre-fibrillar aggregates (Smith *et al.*, 2009). A number of prefibrillar structures can

be identified *in vitro*, with only a few being annular shaped (Kayed *et al.*, 2009). Antibodies specific to oligomers have been identified that can recognize these structures independent of the type of amyloid protein (Kayed *et al.*, 2003), demonstrating the existence of a common structural backbone epitope, and hinting at a possible common toxic mechanism. *In vivo* studies have identified soluble oligomers in the brain in transgenic mouse models of Alzheimer mice (Lesné *et al.*, 2006) as well as in post-mortem human brain tissue (Tomic *et al.*, 2009). Likewise, *in vivo* studies have confirmed the formation of human amylin oligomers in transgenic mice (Lin *et al.*, 2007) and in human pancreatic tissue (Gurlo *et al.*, 2010). Although, the pathological role of amylin oligomers is still being debated, the role of mature amylin fibrils in the destruction  $\beta$  cells in T2DM should not be disregarded (Zraika *et al.*, 2010).

Several factors including protein concentration, pH, temperature, and the presence of other proteins such as chaperones, play a key role in protein aggregation and amyloid formation (Calloni *et al.*, 2008). It is also likely that the lipid environment of the cell membrane is particularly conducive to induction of aggregation. The kinetic profile of amyloid formation by amylin is very dependent on pH and appears to be regulated by protonation of the His-18 residue and the N-terminus (Charge *et al.*, 1995; Abedini and Raleigh, 2005). Amylin is stored together with insulin at very high concentrations within the secretory granules of pancreatic  $\beta$  cells, with an acidic pH of 5.5 (Fox *et al.*, 2010). This acidic environment impedes amylin aggregation and protects the cells (Brender *et al.*, 2013; Jha *et al.*, 2014). However, the extracellular matrix into which amylin is secreted has a physiological pH of 7.4 and this environment

promotes fibril formation (Jha *et al.*, 2014). In general, the lower the pH, the longer the time it takes for amyloid formation (Abedini and Raleigh, 2005). In addition, cholesterol and other lipids have been reported to play a role in the aggregation and toxicity of human amylin (Jean *et al.*, 2010). In the presence of cholesterol, exogenic human amylin aggregates within ganglioside-rich lipid rafts in the plasma membrane of the cell (Wakabayashi and Matsuzaki, 2009). In contrast, cholesterol impedes the aggregation of human amylin on synthetic membranes (Cho *et al.*, 2009). Another study has revealed that human amylin may induce apoptosis through stimulation of acid sphingomyelinase, resulting in ceramide production (Zhang *et al.*, 2009). Amylin could also stimulate the inflammasome to release interleukin-1 $\alpha$  and interleukin-1 $\beta$ , which would lead to inflammation and  $\beta$  cell damage (Masters *et al.*, 2010). In one particular amylin cytotoxicity model, once amylin was absorbed into the lipid membrane, the 19 amino-terminal residues were incorporated into the membrane (Engel *et al.*, 2006; Khemtémourian *et al.*, 2008), which allowed the amyloidogenic region of residues 20-29 to aggregate, with growth of the fibril causing the membrane to rupture (Engel *et al.*, 2006; Engel *et al.*, 2008). A significant variation from other toxicity models is that this involves monomeric amylin rather than oligomers or fibrils.

## 1.8 Amylin and Type 2 Diabetes

Islet amyloid has been strongly associated with T2DM (Clark *et al.*, 1998). It can also be found in non-diabetic individuals but affects few islets, apparently with no adverse impact (Bell, 1959; Pearse *et al.*, 1972). The evidence of islet amyloid in non-diabetic individuals and the fact that overt amyloid deposition is not found in all individuals with T2DM, initially led to a rather hasty conclusion that islet amyloid plays no significant role in the pathogenesis of this disease. However, further careful studies demonstrated that the degree of amyloid deposition is linked with the decrease in  $\beta$  cell mass (Clark *et al.*, 1998), and that  $\beta$  cells found around amylin deposits show numerous fibrils penetrating deep into the cells (Westermarck, 2005), suggesting that the function of these cells is likely to be compromised. As noted previously, disruption of the cell membrane by amyloid oligomers or fibrils results in the upregulation of  $\text{Ca}^{2+}$  influx, which can severely alter the function of cells (Kawahara *et al.*, 2000). In type 1 diabetes, the  $\beta$  cell mass has been reported to be decreased by only 10% compared to normal, suggesting that individuals with this disease still have a significant number of cells that could potentially produce insulin (Willcox *et al.*, 2009). Similarly, in T2DM the islets with amyloid still possess a significant number of insulin-containing  $\beta$  cells. However, in both types of diabetes, the remaining islet  $\beta$  cells are likely to be damaged so that they cannot function properly (Westermarck and Wilander, 1978).

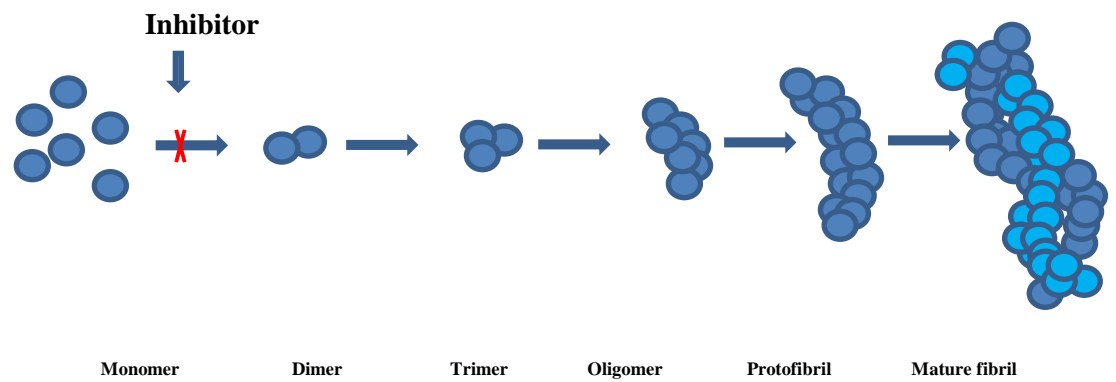


**Figure 1.5:** General representation of fibril formation from natively unfolded monomers. Oligomers are the most toxic form of these aggregates. Inhibiting the progression of amyloid formation at the initial monomeric stage is an attractive therapeutic target for T2DM.

## 1.9 Purpose of Study

In conclusion, under normal physiological conditions human amylin is present as a soluble monomer, but in T2DM it self-associates to form oligomeric structures, protofibrils, and insoluble amyloid fibrils (figure 1.6). The oligomers in particular are toxic to pancreatic  $\beta$  cells (Kodali and Wetzel, 2007), potentially resulting in their malfunction and destruction. The destruction of pancreatic  $\beta$  cells leads to a reduction in insulin production, and is presented as T2DM. Therefore, compounds that inhibit the self-assembly of amylin are a potential therapeutic target for treating this disease. As noted above, amylin and its aggregation could also play a role in insulin resistance, which is the second important aspect of T2DM. The overall objective of this study is to develop novel peptide based inhibitors of amylin aggregation that impede the spontaneous aggregation of amylin into oligomers and fibrils.

It has been challenging to find suitable drug-like therapeutic agents that inhibit the aggregation of various amyloid proteins. However, small organic molecules, peptides, peptidomimetics and nanoparticles have all been developed for this purpose. These inhibitors can interact in different ways involving specific or non-specific binding or colloidal inhibition (Mata-Cantero *et al.*, 2015).

In the case of Alzheimer's disease, a number of inhibitors of A $\beta$  aggregation, including small molecules and peptides, have been developed over the years, but none of these compounds have been successful in human clinical trials. This is partly due to the fact that inhibition of amyloid aggregation involves impeding the interactions between protein monomers, and protein-protein interactions are

recognized as difficult therapeutic targets (Whitty and Kumaravel, 2006; Hajduk and Burns, 2002). Generally, regions for protein-protein interactions are 1500–3000 Å in size (Keskin *et al.*, 2008; Teichmann, 2002), while the region for protein-small molecule interactions is only 300–1000 Å (Smith *et al.*, 2006; Cheng *et al.*, 2007). Therefore, small molecules are generally not able to build adequate steric interruptions to inhibit protein aggregation (Wells and McClendon, 2007). Also, the plasticity of protein surfaces can lodge small molecules, thereby obstructing inhibition (Gestwicki *et al.*, 2004). Altogether, these challenges make it difficult to develop potent and selective small molecule inhibitors of amyloid aggregation.

A growing strategy for inhibition of amyloid aggregation is the use of peptide-based inhibitors. A number of peptide fragments that bind to critical regions of A $\beta$  have been used to target inhibition of amyloid aggregation (Liu *et al.*, 2012; Gibson and Murphy, 2005; Lowe *et al.*, 2001; Taylor *et al.*, 2010). Studies on electrostatic interactions to develop new inhibitors of amylin aggregation have shown that charge-loaded peptides can impede the elongation of amylin fibrils (Sharadrao *et al.*, 2015). Peptide-based inhibitors which target specific amyloid sub-regions represent the first generation of amyloid-based therapeutics which can then be developed further into more drug-like molecules, and this could be a promising avenue for development of a new disease-modifying therapy for T2DM.

The main objective of this study was to develop novel peptide-based inhibitors of amylin aggregation. Previous studies have focused almost exclusively on the amyloidogenic region of human amylin (amino acid residues 22-27, with

sequence NFGAIL), which is the main region involved in protein misfolding into the toxic  $\beta$ -sheet conformational structure (Goldsbury *et al.*, 2000; Tenidis *et al.*, 2000). These peptide inhibitors are designed to act as  $\beta$ -sheet breakers, and are typically compounds that consist of the amyloidogenic motif in combination with a  $\beta$ -sheet breaker element. The latter can be comprised, for example, of methylated amino acids or prolines (Elgersma *et al.*, 2006; Soto *et al.*, 1996). However, these ' $\beta$ -breaker' peptides do not completely inhibit fibril formation and their inhibitory effects are often only seen at very high concentrations, when the peptides are present in molar excess (Westermarck *et al.*, 1990; Abedini *et al.*, 2007; Scrocchi *et al.*, 2002). In contrast, the peptide inhibitors described here are designed to interact with amylin at the binding region 11-20 (with sequence RLANFLVHSS), peptide derivatives from which show maximum binding to full length human amylin (Mazor *et al.*, 2002). This binding region is implicated in the interactions that occur when two or more misfolded amylin molecules associate together to form oligomers and amylin fibrils. Preventing this interaction should impede aggregation.

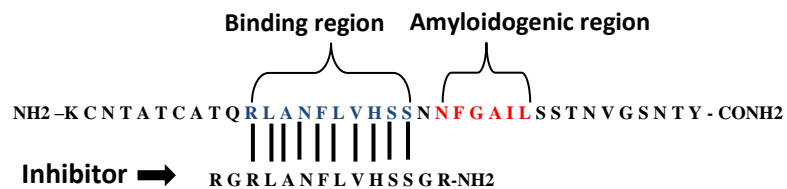


**Figure 1.6:** Design of peptide inhibitors. Amino acid sequence of human amylin showing binding sites for amylin association and the main amyloidogenic region. The short peptide inhibitors are designed to interact with full-length amylin. The binding region (Mazor *et al.*, 2002) is the region involved when two misfolded amylin molecules bind together, after which they continue to aggregate into oligomers and fibrils. The amyloidogenic region (Goldsbury *et al.*, 2000) is the main region involved in protein misfolding into the toxic  $\beta$ -sheet conformational structure. The arginine-glycine residues (RG-GR) residues on either side of the peptides contain positively charged amino acids which impede self-aggregation and repel the next amylin molecule from binding.

Most peptides face the challenge of insolubility in aqueous solution. It is important to keep peptides soluble in aqueous solution and protected from proteolytic degradation. To improve the solubility of these peptides, the arginine-glycine residues (RG-GR) were placed at the ends of the peptides (figure 1.7), containing positively charged residues. This was done to improve the solubility of the peptides as well as inhibit self-aggregation of the amylin molecule. This approach is different from the  $\beta$  sheet blockers as seen in other studies (Nie *et al.*, 2011; Aitken *et al.*, 2003; Ono *et al.*, 2003), and aims at impeding interactions between amylin molecules. This rationale is based on previous research at Lancaster University where a peptide inhibitor (OR2) with the sequence H<sub>2</sub>N-R-G-K-L-V-F-F-G-R-NH<sub>2</sub>, was developed for the inhibition of A $\beta$  oligomerisation in Alzheimer's disease (Taylor *et al.*, 2010). A retro-inverso version (RI-OR2), with sequence reversal and substitution of L-amino acids with D-amino acids, H<sub>2</sub>N-rrGrkrlrvrfrfrGrr-Ac (shown in lower case), was made based on the previous inhibitor, OR2 (Taylor *et al.*, 2010). These peptides showed significant inhibition of A $\beta$  fibril formation and the retro-inverso version was found to be highly stable to proteolysis. The presence of D-amino acids, render the inhibitor stable to proteolysis, and are thus more stable to be used as drugs. Seeing that amyloid proteins show numerous similarities in structure and biological activities, potential inhibition strategies developed for targeting one amyloid disease can be applied for other amyloid aggregation diseases.

### 1.9.1 Objectives of Study

- To find and develop a suitable peptide-based inhibitor of amylin aggregation as a potential therapeutic for the treatment of T2DM. Peptides were developed from the binding region of the human amylin sequence and assessed at a wide range of concentrations using various biochemical and biophysical methods.
- To assess the ability of the peptides to disaggregate pre-formed amylin fibrils.
- To make the peptides suitable as drug candidates by protecting them from proteolytic degradation through retro-inversion and N-methylation.
- To assess the possible cytotoxic effects of the peptides on PANC-1 human pancreatic islet cells, and the ability of the peptides to protect cells from the cytotoxic effects of human amylin.
- To assess the ability of the peptides to penetrate the cell membrane, and determine their intracellular localisation.

## 2.0 Materials and Methods

### 2.1 Suppliers and Equipment

Short Name	Full Name and Location
American Peptide	American Peptide Co. California, USA
Anaspec	Anaspec EGT Group. California, USA
BioTek	BioTek Instruments Inc. Bedfordshire, UK
BOC	BOC Industrial gases. Surrey, UK
China Peptide	ChinaPeptide Co. Ltd. Shanghai, China
Corning	Corning Inc. Corning. New York, USA
Eppendorf	Eppendorf (UK) Ltd. Cambridge, UK
Excel	Excel Scientific Inc. California, USA
Millipore	Millipore (UK) Ltd. Watford, UK
Nunc	Nalge Nunc International. New York, USA
Pechiney	Pechiney Plastic Packaging Company, Illinois, USA
Sigma-Aldrich	Sigma-Aldrich Company Ltd. Dorset, UK
Thermo Electron	Thermo Electron Corporation Inc. Gloucestershire, UK
PerkinElmer	PerkinElmer Inc. Massachusetts, USA

**Table 2.1:** List of suppliers used and location.

<b>Equipment</b>
Joel JEM-1010 electron microscope (Joel)
Milli-Q deionised water (Millipore)
Zeiss LSM880 laser scanning confocal microscope (Zeiss)
Nanodrop 200c Spectrophotometer (Thermo Scientific)
Savant ISS110 SpeedVac Concentrator (Thermo Electron Corporation)
Synergy 2 multi-label microtitre plate reader (BioTek)
Wallac Victor <sup>2</sup> 1420 multilabel counter (PerkinElmer).
Dionex HPLC GP50 Gradient pump (Dionex)

**Table 2.2:** List of equipment used.

## 2.2 Peptides

Full length human amylin peptide (1-37), was obtained from American Peptide Company (lot numbers 1306086T, 1301022T) with purity of >95% as determined by high performance liquid chromatography-mass spectrometry (HPLC-MS). The amino acid sequence is given as:



The amylin was amidated in a similar way to the amylin formed *in vivo* with a disulphide bridge between Cys 2 and Cys 7. The first batch of peptide inhibitors (IO1 – IO8) was made by conventional peptide synthesis and purchased from ChinaPeptide Company. The peptides were analysed for purity by HPLC-MS by Dr. Fuyuki Kametani (Tokyo, Japan) (Appendix C). Seven peptide inhibitors were first designed from the 11-20 amylin binding region (table 2.3). Based on the results obtained from these peptides, 2 more peptides were designed from the combined amino acid sequence of IO4 and IO5 (table 2.4). The effects of two previously published amylin-derived inhibitors on amylin aggregation were compared with our own peptide inhibitors. The first peptide, NMeG24 NMeI26, is a modification of the amylin 22-27 fragment (NFGAIL), with an N-methylation of the amide bonds at G24 and I26 (Sellin *et al.*, 2010), and was purchased from Anaspec EGT group. The second peptide, with amino acid sequence ANFLVH (Potter *et al.*, 2009), was made by conventional peptide synthesis and was purchased from ChinaPeptide Company. These peptides were also analysed for purity by HPLC-MS by Dr. Fuyuki Kametani (Tokyo, Japan).

Peptide inhibitor ID	Sequence	Purity %
IO1	R G <u>R L A N F L V H S S</u> G R-NH <sub>2</sub>	=95%
IO2	R G <u>R L A N F</u> G R-NH <sub>2</sub>	=95%
IO3	R G <u>L A N F L</u> G R-NH <sub>2</sub>	=93.094%
IO4	R G <u>A N F L V</u> G R-NH <sub>2</sub>	=95%
IO5	R G <u>N F L V H</u> G R-NH <sub>2</sub>	=95%
IO6	R G <u>F L V H S</u> G R-NH <sub>2</sub>	=96%
IO7	R G <u>L V H S S</u> G R-NH <sub>2</sub>	=95%

**Table 2.3:** Peptide inhibitors of amylin aggregation and their sequence (IO1-IO7). These peptides were designed from the binding region of human amylin (RLANFLVHSS, residues 11-20), which is responsible for self-association. However, to promote solubility of these peptide inhibitors, while preventing them from self-aggregating, a cationic Arg was added at their N- and C-termini, in each case via a Gly spacer. The Gly residues were placed as spacers between Arg and the RLANFLVHSS binding sequence to facilitate the interaction between amylin and the peptide inhibitors. The part of the peptides that is derived from the amylin sequence is underlined. We hypothesize that the binding of these peptides to amylin could prevent another amylin molecule from interacting, thus preventing protein aggregation.

Peptide inhibitor ID	Sequence	Purity %
IO8	RG <u>ANFLVH</u> GR-NH <sub>2</sub>	=95%
RI-IO8	Ac-r <u>Ghvlfn</u> aGr-NH <sub>2</sub>	= 96%

**Table 2.4:** IO8 and RI-IO8 inhibitors. The IO8 inhibitor was made from the combination of IO4 and IO5 inhibitors (table 2.3). IO8 was retro-inverted with the amino acid sequence reversed, and L-amino acids replaced with D-amino acids (lower case) to give RI-IO8. The part of the peptides that is derived from the amylin binding sequence is underlined. Retro-inverted peptides are more stable to proteolysis.

Peptide inhibitor	Purity %
NMeG24 NMeI26	=95%
ANFLVH	=95%

**Table 2.5:** Peptide inhibitors reported in literature to inhibit amylin aggregation. The effects of these inhibitors were assessed alongside our own peptide inhibitors.

Following the results obtained from these inhibitors, it was important that our most effective inhibitor IO8 was protected from proteolytic degradation. The first attempt at this was made by designing a retro-inverso version of IO8 where the L-amino acids were replaced with D- amino acids and the sequence was reversed. Retro-inverso peptides, also known as a retro-all-D- or retro-enantiopeptides, exhibit a side chain topology in its expanded conformation that resembles the native L-sequence, therefore modelling biological characteristics of the parent molecule, and at the same time being protected against proteolytic degradation (Chorev and Goodman, 1979). Other inhibitory peptides designed were NH<sub>2</sub>-RGANFLVHSSNNFGR-NH<sub>2</sub> and its retro inverso form Ac-rGfnssshvlfnaGr-NH<sub>2</sub>.

Another approach for stabilising the IO8 peptide was to replace the first R residue ( $\text{H}_2\text{N-RGANFLVHGR-NH}_2$ ) with homoarginine [ $\text{H}_2\text{N-HarGANFLVHGHar-NH}_2$  (HIO8)], an unnatural analogue of arginine. Substituting arginine with homoarginine protects proteins against proteolytic degradation by trypsin. The HIO8 peptide was purchased from Cambridge Peptides UK.

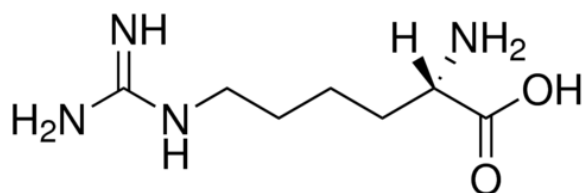


**Figure 2.1:** Structure of L-homoarginine.

The final method for protecting our peptides against proteolytic degradation was through the N methylation of certain amino acid residues. Methylation is the addition of a methyl group to a substrate, or replacing an atom or group of atoms with a methyl group (Xue *et al.*, 2014). N-methylation is a simple alteration of peptides and proteins to impede the activity of proteolytic enzymes (Chatterjee *et al.*, 2013) and is also used to improve the pharmacokinetic properties of drugs. Our N-methylated peptides (table 2.6) were produced by Cambridge Peptides, UK. We had two different N- methylated peptides made, with the peptides methylated at alternate residues of the amino acid sequence.

Peptide inhibitor ID	Sequence	Purity %
N1-IO8	H <sub>2</sub> N-R G A <sub>m</sub> N F <sub>m</sub> L V <sub>m</sub> H G R-NH <sub>2</sub>	=86.376%
N2-IO8	H <sub>2</sub> N-R G A N <sub>m</sub> F L <sub>m</sub> V H <sub>m</sub> G R-NH <sub>2</sub>	=96.097%

**Table 2.6:** N-methylated peptide inhibitors. The N1-IO8 inhibitor was N-methylated at positions 3, 5 and 6 (i.e. Ala, Phe and Val), whereas the N2-IO8 inhibitor was N-methylated at positions 4, 6 and 8 (i.e. Asn, Leu and His). N-methylated peptides are relatively stable to proteolysis and improve the pharmacokinetic properties of peptides.

## 2.3 Solutions and Buffers

### 2.3.1 10 mM Phosphate buffer, pH 7.4, containing 150 mM NaCl (PBS)

For 100 ml, 0.81 ml of 1 M Na<sub>2</sub>HPO<sub>4</sub> (monobasic salt) was added to 0.19 ml of 1 M KH<sub>2</sub>PO<sub>4</sub> (dibasic salt) and 0.876 g of NaCl was added. This solution was made up to 100 ml with distilled water, which brings the final concentration of NaCl in the buffer to 150 mM. This buffer was then stored at room temperature for up to 2 months.

### 2.3.2 10 mM Phosphate buffer, pH 7.4, containing 300 mM NaCl (PB 2.S)

For 100 ml, 0.81 ml of 1 M Na<sub>2</sub>HPO<sub>4</sub> (monobasic salt) was added to 0.19 ml of 1 M KH<sub>2</sub>PO<sub>4</sub> (dibasic salt) and 1.752 g of NaCl was added. This solution was made up to 100 ml with distilled water, which brings the final concentration of NaCl in the buffer to 300 mM. This buffer was then stored at room temperature for up to 2 months.

### **2.3.3 10 mM Phosphate Buffer, pH 7.4 (PB)**

For 100 ml, 0.81 ml of 1 M  $\text{Na}_2\text{HPO}_4$  (monobasic salt) was added to 0.19ml of 1 M  $\text{KH}_2\text{PO}_4$  (dibasic salt). The solution was made up to 100 mls with distilled water and stored at room temperature for up to 2 months.

### **2.3.4 15 mM Thioflavin-T (Th-T) Solution**

Th-T stock solution was made by dissolving 23.9 mg of Th-T powder (Sigma-Aldrich) in 5 ml of 10 mM Phosphate buffer (PB). The tube was wrapped in tin foil and stored at 4 °C for up to 6 weeks before being replaced with fresh ThT solution.

### **2.3.5 2% Phosphotungstic Acid (solution)**

The 2% phosphotungstic acid was made by dissolving 2 g of phosphotungstic acid powder (Sigma-Aldrich) in 100 ml distilled water. The pH was adjusted to 7.3 using 1N NaOH and the solution was stored in the fridge at 4 °C for up to 8 weeks.

## 2.4 Peptide Preparation

### 2.4.1 Deseeding Human Amylin

Previous studies have revealed that the presence of pre-existing aggregates ('seeds') in a starting peptide solution speeds up the formation of amyloid fibrils (Cho *et al.*, 2009). Thus the following protocol was used to 'deseed' or remove any preformed amylin aggregates from the synthetic human amylin (1-37) for future experiments. In a fume cupboard, 45  $\mu$ l of thioanisole was added to a glass vial containing 1 ml trifluoroacetic acid (TFA). The mixture was then added to 1 mg of human amylin peptide. Due to the corrosive nature of TFA, only glass materials were used for this step. A lid of a chemically resistant eppendorf tube was used to seal the glass vial, which was further sealed with parafilm. This was left for 1 hr, and at every 10 mins, was vortexed, sonicated, and vortexed again, for 2 mins each. The liquid was then blown off by passing a stream of nitrogen gas over it. After drying, 1 ml of 1,1,1,3,3,3-hexafluoro-2-propanol (HFIP) was added to the glass vial and allowed to stand for 10 mins, after which it was vortexed, sonicated and vortexed again, for 2 mins each. The liquid was then transferred to a 1.7 ml chemically resistant eppendorf tube and the HFIP removed using a centrifugal concentrator for 30 mins. 1 ml HFIP was added again and left for 10 mins after which it was vortexed, sonicated, and vortexed again, for 2 mins each. This was then centrifuged at 10,000  $\times$  *g* for 15 mins, and aliquots of 50  $\mu$ g were transferred to chemically resistant eppendorf tubes. HFIP was then removed using a centrifugal concentrator, for 15 mins. After being fully dried, the samples were stored at -20 °C. To make a 100  $\mu$ M

solution of amylin peptide, 128  $\mu$ l of PB was added to 50  $\mu$ g of amylin in an eppendorf tube.

#### 2.4.2 Preparation of Peptide Inhibitors

1mM stock solutions of the peptide inhibitors (table 2.7) were prepared and stored in the fridge, as follows:

Peptide ID	Stock solution (1mM)
IO1	1.6 mg in 1 ml PBS
IO2	1.0 mg in 1ml PBS
IO3	1.0 mg in 1 ml PBS
IO4	0.9 mg in 1 ml PBS
IO5	1.0 mg in 1 ml PBS
IO6	1.0 mg in 1 ml PBS
IO7	0.9 mg in 1 ml PBS
IO8	1.1 mg in 1 ml PBS
HIO8	1.15 mg in 1 ml PBS
RI-IO8	1.2 mg in 1 ml PBS
NFG	1.1 mg in 1 ml PBS
N1-IO8	1.17 mg in 1 ml PBS
N2-IO8	1.17 mg in 1 ml PBS

**Table 2.7:** Preparation of 1 mM of each of the peptide inhibitors.

## 2.5 Thioflavin-T (Th-T) Assays

### 2.5.1 Mechanism of Th-T Assay

Th-T is a yellow, cationic, benzothiazole salt which is obtained by the methylation of dehydrothiolumidine with methanol in the presence of hydrochloric acid. It is used as a dye to visualize and measure *in vivo* and *in vitro* fibrillization of misfolded protein aggregates known as amyloid. The interaction of the polar and hydrophobic regions increases the possibility of Th-T molecules forming micelles in aqueous solution, with the positively charged hydrophobic interior N<sup>+</sup> (figure 2.1), pointing in the direction of the solvent (Khurana *et al.* 2005). Several studies have elucidated the binding of Th-T to amyloid proteins and have suggested that Th-T binds specifically to  $\beta$ -sheet structures of the amyloid protein (Biancalana and Koide, 2010; Groenning, 2010); however, this is not fully understood. Thus, the interaction between negatively charged compounds and positively charged Th-T could be responsible for Th-T binding (Khurana *et al.* 2005).

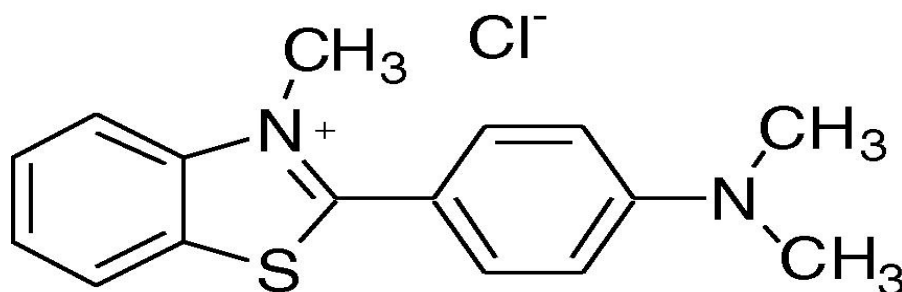


**Figure 2.2:** The structure of Th-T. The hydrophobic region terminates with a dimethylamino group attached to a phenyl group on the right, and the polar region is a benzothiazole group containing the polar N and S. (Khurana *et al.* 2005).

### **2.5.2 Th-T Assay Protocol**

The Th-T assay was used to measure the aggregation of the amylin peptide. The Th-T assay measures differences in fluorescence intensity when it binds to amyloid fibrils. The Th-T assays were carried out in 384-well clear-bottomed microtiter plates (NUNC) by incubating the amylin peptides (25  $\mu$ M) in the presence of Th-T (15  $\mu$ M) in 10 mM PBS (pH 7.4). The inhibitors were present at varying molar ratios relative to amylin, with the total volume of solution in each well set at 60  $\mu$ l. The plates were shaken and the fluorescence read every 10 mins ( $\lambda_{ex}$  = 442 nm, and  $\lambda_{em}$  = 483 nm) in a BioTek Synergy 2 plate reader, at 30°C for 48 hrs. Triplicate readings were taken for each condition and each experiment was repeated three times.

## **2.6 Cell Culture**

### **2.6.1 Cell Maintenance**

Human pancreatic  $\beta$  cells; PANC-1 Human pancreatic 1.4E7 (ECACC 10070102) insulin-secreting cells were obtained from Public Health England Culture Collection. The PANC-1 cells were routinely grown in RPMI-1640 medium with L-Glutamine (Gibco Life Technologies), supplemented with 10% fetal calf serum and 1% penicillin/streptomycin. Cell culture was carried out in a safety hood which was sterilised with 70% ethanol, and utilised pre-warmed media. Monolayers of cells were grown in 75 cm<sup>3</sup> flasks at a ratio of 1:10 cells to media and incubated at 37 °C, 5% CO<sub>2</sub>. Cell splitting was required when cells reached confluence, often after 1 week of incubation at 37 °C, 5% CO<sub>2</sub>. At this

time, growth medium was removed from the flask using a 10 ml stripette and the cell monolayer was washed with 2 mls of trypsin (Gibco Life Technologies) for 30 secs to remove the serum, and then re-incubated with 2 mls of trypsin at 37 °C, 5% CO<sub>2</sub> for 5 mins. Following this, the cells detach from the bottom of the plate. The activity of trypsin was stopped by the addition of 8 mls of media, taking the total volume in the flask to 10 mls, then 9 mls of fresh media was added to a clean 75 cm<sup>3</sup> flask and 1 ml of the cell mixture was added to it (1: 10 dilution). This was left to grow in the incubator at 37 °C, 5% CO<sub>2</sub>. Every 2 days, media was removed from flask and 10 mls of fresh media was replaced to keep the cells healthy.

### **2.6.2 The CellTiter 96 Aqueous One Solution Cell Proliferation (MTS) Assay**

Cell viability was assessed using the CellTiter 96 aqueous one solution cell proliferation assay (Promega). This is a colorimetric method that provides a convenient and sensitive way for determining the number of viable cells in proliferation or cytotoxicity assays. The CellTiter 96 aqueous one solution reagent is made up of a novel tetrazolium compound [3-(4,5-dimethylthiazol-2-yl)-5-(3-carboxymethoxyphenyl)-2-(4-sulfophenyl)-2H tetrazolium, inner salt; MTS] as well as an electron coupling reagent (phenazine ethosulphate; PES) (Promega, 2012). PES combines with MTS to form a stable solution. The MTS tetrazolium compound is converted by cells into a yellow coloured formazan product which is soluble in tissue culture medium. This conversion is probably carried out by NADPH or NADH produced by dehydrogenase enzymes in

metabolically active cells (Promega, 2012). Assays were carried out by adding 20  $\mu$ l of CellTiter 96 aqueous one solution reagent directly to cell culture wells which were incubated for 1-4 hrs and the absorbance at 490 nm was recorded using a Wallac Victor<sup>2</sup> 1420 multilabel counter (PerkinElmer). The number of living cells is directly proportional to the amount of formazan product.

### **2.6.3 Cell Toxicity Protocol for MTS Assay**

The culture medium was removed from cells which had formed a monolayer of non-overlapping confluence in a 75 cm<sup>3</sup> flask, and replaced with 2 mls of trypsin. After 30 secs, the trypsin was removed, replaced with another 2 mls of trypsin, and incubated at 37°C, 5% CO<sub>2</sub> for 5 mins. Culture medium (2 mls) was then added to the flask and the suspended cells were transferred to a 15 ml tube and centrifuged for 5 mins at 3000 xg. The culture medium was removed and cell pellet was resuspended in 2 mls of fresh medium, with mixing. A 10  $\mu$ l sample of this suspension was loaded into a haemocytometer chamber for cell counting. The remaining cells were diluted to 250,000 cells/ml and 100  $\mu$ l of the diluted cell suspension was transferred (at 25,000 cells/well) to a 96-well plate and incubated at 37 °C, 5% CO<sub>2</sub>. After 24 hrs, the medium was replaced with 100  $\mu$ l of fresh medium, with the following conditions: culture medium containing amylin at a final concentration of 20  $\mu$ M in culture medium with or without the peptide inhibitors at 20  $\mu$ M and 5  $\mu$ M. Furthermore, culture medium containing amylin at a final concentration of 10  $\mu$ M with or without the peptide

inhibitors at 10  $\mu$ M and 2.5  $\mu$ M. Each condition was plated in 6 wells and incubated at 37 °C, 5% CO<sub>2</sub>. After 24 hrs, 20  $\mu$ l of CellTiter 96 aqueous one solution reagent was directly added to each cell culture well and incubated for 3 hrs at 37 °C, 5% CO<sub>2</sub> and the absorbance at 490 nm recorded using a Wallac Victor<sup>2</sup> 1420 multilabel counter (PerkinElmer).

#### **2.6.4 The CytoTox-ONE Homogeneous Membrane Integrity (LDH) Assay**

The CytoTox-ONE Homogeneous Membrane Integrity Assay (Promega) is a fluorometric technique to determine the amount of non-viable cells present in a cell based assay. The number of non-viable cells can be measured by the amount of substances release into the cytoplasm following membrane damage. The CytoTox-ONE assay is also known as the of lactate dehydrogenase (LDH) assay, as it involves the secretion of LDH into the culture medium following membrane disruption in an enzymatic reaction where resazurin is converted into resorufin. In this assay, the membranes of healthy cells remain intact thus LDH release can be measured homogeneously in an assay containing both viable and damaged cells. The LDH assay is typically used to examine the cytotoxicity of various compounds. About 100 assays in a 96-well format or 400 assays in a 384-well can be performed with each vial of the CytoTox-ONE Homogeneous Membrane Integrity Assay (Cat no: G7890; Size: 200–800 assays).

The assay kit includes:

- 2 vials Substrate Mix
- 24ml Assay Buffer

- 0.5ml Lysis Solution
- 11ml Stop Solution

All kit components were stored at  $-20^{\circ}\text{C}$  in the dark. The reconstituted CytoTox-ONE Reagent was stored for 6–8 weeks at  $-20^{\circ}\text{C}$ , in the dark.

### **2.6.5 Cell Toxicity Protocol for LDH Assay**

#### Reagent Preparation

- Substrate Mix and Assay Buffer were thawed using a  $37^{\circ}\text{C}$  water bath between 30 seconds to 1 minute.
- CytoTox-ONE Reagent was prepared by adding 11ml of Assay Buffer to each vial of Substrate Mix and then mixed gently to dissolve substrate.

The culture medium was removed from cells which had formed a monolayer of non-overlapping confluence in a  $75\text{ cm}^3$  flask, and replaced with 2 mls of trypsin. After 30 secs, the trypsin was removed and replaced with another 2 mls of trypsin, and then incubated at  $37^{\circ}\text{C}$ , 5%  $\text{CO}_2$  for 5 mins. Culture medium (2 mls) was then added to the flask and the suspended cells were transferred to a 15 ml tube and centrifuged for 5 mins at  $3000\text{ xg}$ . The culture medium was removed and cell pellet was resuspended in 2 mls of fresh medium, with mixing. A  $10\text{ }\mu\text{l}$  sample of this suspension was loaded into a haemocytometer chamber for cell counting. The remaining cells were diluted to 250,000 cells/ml and  $100\text{ }\mu\text{l}$  of the diluted cell suspension was transferred (at 25,000 cells/well) to a 96-well plate and incubated at  $37\text{ }^{\circ}\text{C}$ , 5%  $\text{CO}_2$ . After 24 hrs, the medium was replaced with  $100\text{ }\mu\text{l}$  of fresh medium, with the following conditions: culture

medium containing amylin at a final concentration of 20  $\mu\text{M}$  in culture medium with or without the peptide inhibitors at concentrations of 80, 40, 20, 10, 5 and 2.5 $\mu\text{M}$ . Each condition was plated in 6 wells and incubated at 37 °C, 5%  $\text{CO}_2$ . After 24 hrs, 2  $\mu\text{l}$  of Lysis Solution was added to the positive control wells and 100  $\mu\text{l}$  of CytoTox-ONE™ Reagent was then added to the 100  $\mu\text{l}$  of medium containing cells and incubated at 22°C for 10 mins after which, 50 $\mu\text{l}$  of Stop Solution was then added to each well. Stop Solution was added using the same addition order for CytoTox-ONE Reagent to maintain consistency in incubation times. The plate was shaken in the Wallac Victor<sup>2</sup> 1420 multilabel counter (PerkinElmer) plate reader for 10 seconds and fluorescence recorded with an excitation wavelength of 560nm and an emission wavelength of 590nm aqueous one solution reagent was directly added to each cell culture well and incubated for 3 hrs at 37 °C, 5%  $\text{CO}_2$  and the absorbance at 490 nm recorded using a Wallac Victor<sup>2</sup> 1420 multilabel counter (PerkinElmer). Appropriate controls were used for this experiment. To detect background fluorescence, negative controls having wells without cells were used. The untreated cells control contained cells in culture without the peptides. The LDH release control was setup by adding 2  $\mu\text{l}$  of lysis buffer to the positive control wells (Cells with treatment). Each experimental condition was set up in triplicates.

#### **2.6.6 Cell Penetration Assay**

The cell penetration assay was carried out to access the cellular uptake and intracellular localization of our peptide inhibitors. Described below is the

protocol used for delivery of amylin peptide-based inhibitors to adherent cultured human pancreatic PANC-1 cells.

### **2.6.7 Cell Penetration Assay Protocol**

Peptides were fluorescently tagged according to manufacturer's instructions using the protein labelling kit from Thermo Fisher Scientific, Alexa Fluor 488, as follows:

1 M sodium bicarbonate solution was prepared by adding 1 ml deionized water (dH<sub>2</sub>O) to the vial of sodium bicarbonate (Component B) and vortexed until the reagent was fully dissolved. The bicarbonate solution had a pH of ~8.3 and was stored at 4°C for up to two weeks. 50 µl of a 1 mg/ml solution of peptide was transferred to a reaction tube (Component C) and 5 µl of 1 M sodium bicarbonate added and mixed by pipetting up and down several times. 11.3 nmol of the reactive dye was prepared immediately prior to use by adding 10 µl of dH<sub>2</sub>O to one vial of Alexa Fluor® 488 TFP ester (Component A). 1 µl of reactive dye was added to the reaction tube containing the pH-adjusted protein and mixed thoroughly by pipetting up and down several times. The reaction mixture was then incubated for 15 mins at room temperature. The conjugate was purified by separating labelled protein from unreacted dye by using purification spin filters containing gel resin (Component E). The upper chamber of the spin filter was filled with 800 µl of suspended gel resin, and the spin filter centrifuged at 16,000 xg in a microcentrifuge for a total of 15 secs. After preparation of the spin filter, 50 µl of the conjugate reaction mixture was added onto the centre of the resin bed surface. The collection tube now contained

purified dye-labelled protein in approximately 60–100  $\mu\text{l}$  of buffer. The unreacted dye is retained on the filter and the resin has a yellow-green colour

For cell penetration experiments, 100  $\mu\text{l}$  of the diluted cell suspension (25,000 cells/well) were grown on cover slips in a 6 well plate for 24 hours, the fluorescein-tagged peptides, at a concentration of 10  $\mu\text{M}$ , was then added to cell growth medium on a slide containing cultured PANC-1 cells and incubated for 10 mins, 30 mins and 1 hr. After incubation, cells were mounted on slides using Fluoroshield mounting medium containing DAPI as a nuclei stain. Labelled samples were excited using the 488nm laser and emission collected 495 – 630nm with DAPI visualised using 405 laser and emissions collected 410 – 490nm wavelengths. Confocal micrographs were taken using the Zeiss LSM880 laser scanning confocal microscope.

## **2.7 Congo Red Assay**

The Congo Red (CR) spectrophotometric assay was used to examine amylin samples in the presence of inhibitors. The CR spectrophotometric assay is relatively objective, and can be easily combined with the microscopic analysis

### **2.7.1 Protocol for Procedures for Congo Red Spectroscopic Assay:**

Amylin peptide (25  $\mu\text{M}$ ) with and without inhibitors (at varying concentrations) was incubated for 48 hrs at 37  $^{\circ}\text{C}$  prior to the experiment.

A 7 mg/mL solution of CR was prepared in buffer (5 mM potassium phosphate, 150mM NaCl, pH7.4) and filtered through a 0.2  $\mu$ m syringe filter immediately prior to use.

The UV-Vis Nanodrop 200c spectrophotometer was first zeroed between 400 and 700 nm at room temperature with a sample of 1 mL phosphate buffer in a disposable cuvette.

To measure the spectrum for CR, 5 $\mu$ L of the CR solution was added to 1 mL phosphate buffer in a disposable cuvette and scanned between 400 and 700 nm.

10  $\mu$ L of protein sample was then added to disposable cuvette containing 5  $\mu$ L of CR solution in 1 mL of phosphate buffer and incubated for 30 mins at room temperature. At this stage, a red precipitate becomes visible. The contents of the cuvette were then mixed by pipetting the solution up and down and then the spectrum was recorded, between 400 and 700 nm.

A maximal spectral difference at 540 nm is indicative of amyloid fibrils. This is calculated mathematically by subtracting the CR spectrum from the protein + CR spectrum.

## **2.8 Stability Assay using High Performance Liquid Chromatography**

High performance liquid chromatography (HPLC) is a more advanced and highly sensitive form of column chromatography where the solvent is forced through under high pressures. This permits the passage of smaller sized particles as well as giving a finer separation of the components of the mixture. Here, reverse-phase HPLC was used to determine the stability of the peptide inhibitors in plasma, and in the presence of various proteolytic enzymes. In this form of HPLC, the silica column is modified to make it non-polar by linking long hydrocarbon chains to its surface. Hydrophobic molecules are adsorbed onto this type of column in the presence of a polar solvent, and are eluted by employing increasing concentrations of a non-polar organic solvent. The HPLC equipment used for these experiments was the Dionex GP50 Gradient pump. The column used for these experiments was the C18 x 2.0mm column and the solvent consisted of a gradient produced from 0.01% trifluoro acetic acid in dH<sub>2</sub>O (Solvent A) versus 0.01% trifluoro acetic acid in acetonitrile (Solvent B). Reversed-Phase High-Performance Liquid Chromatography (RP-HPLC) is concerned with the dissociation of molecules by reason of their hydrophobicity. This dissociation is influenced by the hydrophobic binding of the solute molecule between the mobile phase and the immobilized hydrophobic ligands connected to the stationary phase in other words, sorbent. Firstly, the solute mixture is added to the sorbent in the presence of aqueous buffers, the presence of organic solvent at the mobile phase elutes the solutes, this can be isocratic, where there is a constant concentration of organic solvent or it can be by gradient conditions where there the amount of organic solvent accumulates over

a period of time. The solutes are thus eluted in an increasing succession of molecular hydrophobicity.

RP-HPLC is an especially important approach for peptide and protein analysis because chromatographs can be altered without difficulty via changes in mobile phase attributes. Also, RP-HPLC also possesses high resolution for both similar and dissimilar molecules attained through its variety of chromatographic conditions. In addition, RP-HPLC produces high quality repetitive separations as well as high recoveries (Aguilar and Hearn, 1996; Mant and Hodges, 1996). RP-HPLC can however result in irreversible denaturing of protein samples thus the chances of recovering biologically active materials is greatly diminished.

Human plasma samples were obtained, with ethical approval including informed consent (Oldham Ethics Committee), from Prof. David Mann (University of Manchester). The frozen plasma sample (stored at  $-80^{\circ}\text{C}$ ) was thawed in a water bath ( $25^{\circ}\text{C}$ ) for 5 min. To assess the stability of the peptide inhibitors in plasma, 5 $\mu\text{l}$  of peptide was added to 95  $\mu\text{l}$  of thawed plasma in a microfuge tube and incubated for 0 hrs, 1hr, 3hrs, 24hrs, 48hrs and 72 hrs at  $37^{\circ}\text{C}$ . To assess the stability of peptides in the presence of proteolytic enzymes (table 2.8), 2  $\mu\text{l}$  of enzyme was added to 98  $\mu\text{L}$  of peptide. After incubation at 0 hrs, 1hr, 3hrs, 24hrs, 48hrs and 72 hrs, 100  $\mu\text{l}$  of sample was injected into the HPLC injector column and monitored at a flow rate of 1ml/min for a total run time of 40 mins at a linear gradient of 0-60% solution B, with the absorbance measured at a wavelength of 220nm.

<b>Enzyme</b>	<b>Concentration</b>
Trypsin	1mg/ml
Chymotrypsin	1mg/ml
Cathepsin G	1mg/ml
Elastase	1mg/ml
Thrombin	1mg/ml
Kallikrein	1mg/ml
Plasmin	1mg/ml
Factor X	1mg/ml

Table 2.8: List of proteolytic enzymes used.

## **2.9 Transmission Electron Microscopy**

Solutions of amylin at 25  $\mu$ M and amylin in the presence of inhibitors at varying concentrations were prepared and incubated in PBS for 48 hrs. After incubation, 5  $\mu$ l of the mixture was pipetted onto carbon-coated formvar grids held using forceps and left for 3 mins. The edges of the grids were touched with filter paper to draw off the liquid, then 5  $\mu$ l of 2% aqueous phosphotungstic acid (adjust pH to 7.3 using 1N NaOH) was applied immediately (before the sample had dried) and left for 1 min. The excess liquid was removed as before, the grid was allowed to dry overnight (in the grid box) before observation. Five fields for each sample were randomly photographed at 5000x magnification, after first examining the grid for uniformity. The negatives were enlarged 3.0x to a final magnification of 15000x. Five photographs were examined for each sample.

### 2.9.1 Statistical analysis

The Th-T assays were performed in triplicate, while the cell toxicity assays were performed in replicates of six. The data are expressed as mean  $\pm$  standard error of mean (SEM), or representative data are shown. Statistical analysis with SPSS was performed using One-way ANOVA, Tukey's post hoc test, and confidence interval (CI) analysis ( $P < 0.05 + 95\%$  CI) was used to compare mean values.

For the quantitative studies in chapter 3, a one-way between samples ANOVA was conducted to compare the effect of peptide inhibitors at varying concentrations on amylin aggregation, inhibitor only (no amylin) and the amylin only (no inhibitor) conditions. Significance was recorded at \* $P < 0.05$ , \*\* $P < 0.01$ , \*\*\* $P < 0.001$ . Post hoc comparisons using the Tukey's post hoc test indicated the significant difference between the mean scores for the peptide conditions at varying concentrations, the inhibitor only (no amylin) and the amylin only (no inhibitor) conditions.

## Chapter 3

### Quantitative analysis of peptide-based inhibitors on amylin aggregation

This chapter is focused on the hypothesis that the deposition of amylin in the pancreatic islets leads to the development of T2DM and that developing peptide-based inhibitors which interact with the binding region of human amylin may stop amylin from misfolding and/or prevent its subsequent aggregation. Amylin exists as monomers in its normal physiological state. However, in T2DM, amylin begins to aggregate to form dimers, oligomers and ultimately fibril-like structures. The inhibition of amylin aggregation at the initial monomeric state may hold considerable potential for the treatment of T2DM. In this Chapter, peptide inhibitors developed from the binding region of human amylin were tested using Thioflavin-T (Th-T) and Congo Red (CR) assay techniques to investigate their effects on the aggregation of human amylin.

#### 3.1 Thioflavin T assay

The Th-T assay is a fluorescence-based assay used for the detection of misfolded protein aggregates, as described previously (section 2.5.2). This assay has been used to assess the extent of amyloid fibril formation *in vitro* (Khurana *et al.*, 2005; Lindberg *et al.*, 2015) and stains such as Th-T are also used to examine histological tissue samples for the presence of amyloids in general (LeVine, 1993; Groenning, 2010). A common feature of all amyloid proteins is

the formation of long misfolded  $\beta$ -sheet structures (Sunde *et al.*, 1997) which are targets for Th-T binding. Resulting changes in Th-T fluorescence can be used to identify and distinguish varying surface characteristics of amyloid fibrils (Cohen *et al.*, 2013; Bolognesi *et al.*, 2014). It also appears that Th-T has some predisposition for interacting with aromatic side chains (Biancalana *et al.*, 2009; Wolfe *et al.*, 2010). Nevertheless, the intensity of Th-T fluorescence varies significantly between samples of different amyloid proteins and also differs when comparing fibrils formed from normal and mutant forms of the same protein (Adler *et al.*, 2014; Walsh *et al.*, 2009). Here, the Th-T assay was used to measure changes in fluorescence intensity of Th-T upon binding to amylin fibrils in the presence and absence of varying concentrations of the different peptide-based inhibitors.

### **3.1.1 Peptide based inhibitors show inhibitory effects on amylin aggregation**

In order to find a suitable inhibitor of amylin aggregation, peptides spanning the binding region of human amylin, named IO1, IO2, IO3, IO4, IO5, IO6 and IO7, were tested. The aggregation of amylin in the presence of these peptides was assessed using the Th-T assay. Amylin was incubated at 25  $\mu$ M in PBS in the continuous presence of Th-T for 48 hrs, with shaking, and fluorescence measurements were taken every 10 mins in a BioTek Synergy 2 plate reader at 30°C. The IO1-IO7 peptide inhibitors were incubated at varying concentrations of 0  $\mu$ M, 0.6  $\mu$ M, 2.5  $\mu$ M, 5  $\mu$ M, 12.5  $\mu$ M, 25  $\mu$ M, 50  $\mu$ M and 100  $\mu$ M, while the concentration of amylin was kept constant at 25  $\mu$ M. All experiments were carried out in triplicate and repeated three times. This is the case for all of the Th-T experiments presented in this Chapter, and the results show mean +/-

standard error of the mean (SEM) for one representative experiment. Figure 3.1.1 presents aggregation curves showing a typical sigmoidal shape, with lag, sigmoidal and plateau phases of fibril formation. Amylin alone showed a characteristic increase in fluorescence, while the presence of inhibitors, at varying concentrations, had different effects on amylin aggregation. Figure 3.1.1.1 shows data for the percentage aggregation of amylin in the presence of IO1, IO2, IO3, IO4, IO5, IO6 and IO7 peptide inhibitors at the above concentrations, relative to a non-inhibitor control. IO5 significantly inhibited amylin aggregation at 12.5  $\mu\text{M}$ , 25  $\mu\text{M}$ , 50  $\mu\text{M}$  and 100  $\mu\text{M}$ . IO4 significantly inhibited amylin aggregation at 25  $\mu\text{M}$  and 100  $\mu\text{M}$ . IO2 significantly inhibited amylin aggregation at 12.5  $\mu\text{M}$  and 100  $\mu\text{M}$ . IO3 and IO7 only showed inhibitory effects on amylin aggregation at 100  $\mu\text{M}$ , the highest concentration tested. On the other hand, IO1 and IO6 showed no inhibitory effect on amylin aggregation. At lower concentrations, all peptides appeared to stimulate amylin aggregation.

IO5 is considered to be the best inhibitor, since it inhibits amylin aggregation at 12.5  $\mu\text{M}$ , 25  $\mu\text{M}$ , 50  $\mu\text{M}$  and 100  $\mu\text{M}$ . Data from IO1, IO2, IO6 and IO7 showed unusual curves quite unlike the others (figure 3.1.1.1), revealing a ‘hump’ along the curve and not the characteristic “sigmoidal” shape expected of an inhibition curve. However, curves from IO4 and IO5 looked more convincing, with a dose-dependent effect. In fact the shape of all of the graphs was rather unusual and did not show the characteristic “sigmoidal” shape often expected for an inhibition curve. Since IO4 and IO5 showed the most promising results, they were chosen for further studies.

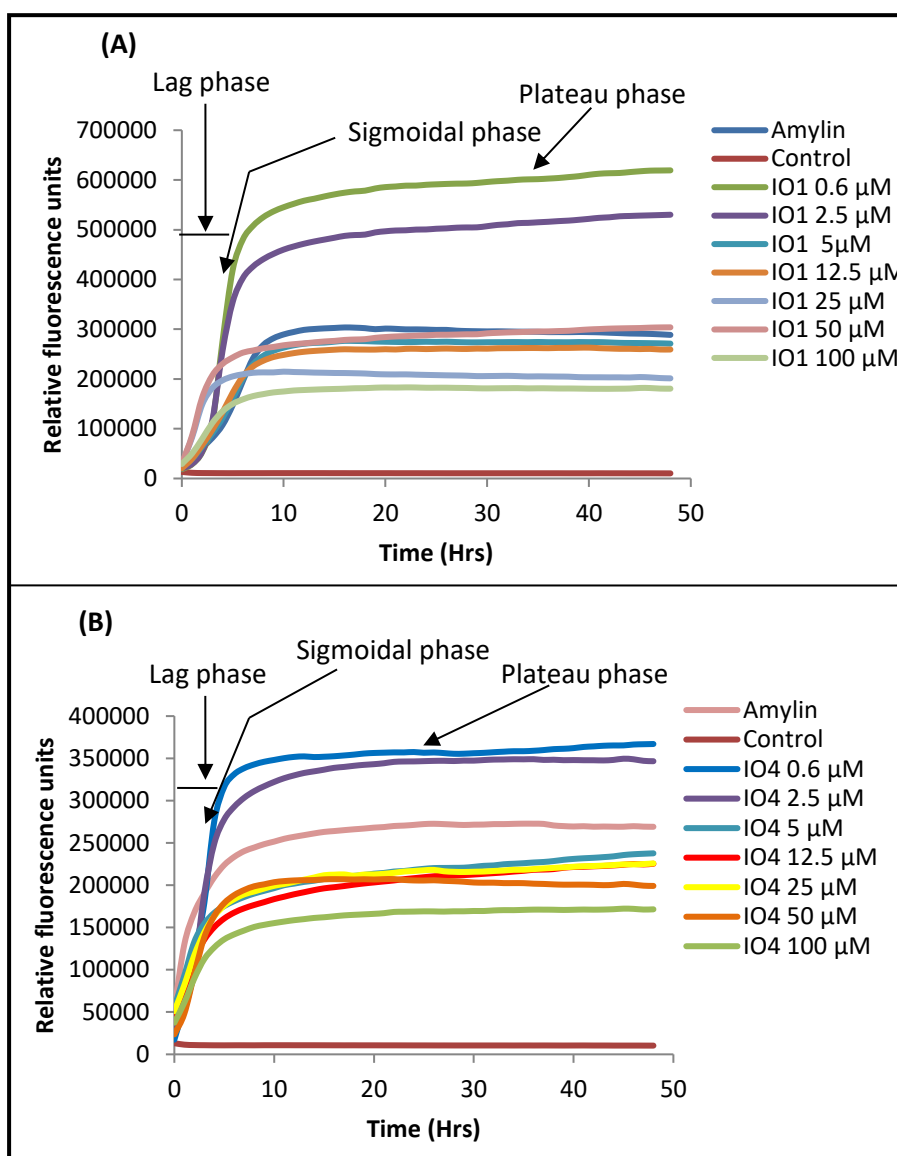


**Figure 3.1.1:** Examples of Th-T fluorescence curves for time-dependent aggregation of human amylin in the presence of two representative inhibitors, IO1 (A) and IO4 (B). Amylin alone at 25 μM displayed a characteristic increase in Th-T fluorescence corresponding to the lag, sigmoidal and plateau phases of fibril formation, while the addition of inhibitors, at varying concentrations, had clear effects on amylin aggregation. Buffer PBS controls ('Control') contained neither amylin nor inhibitors.

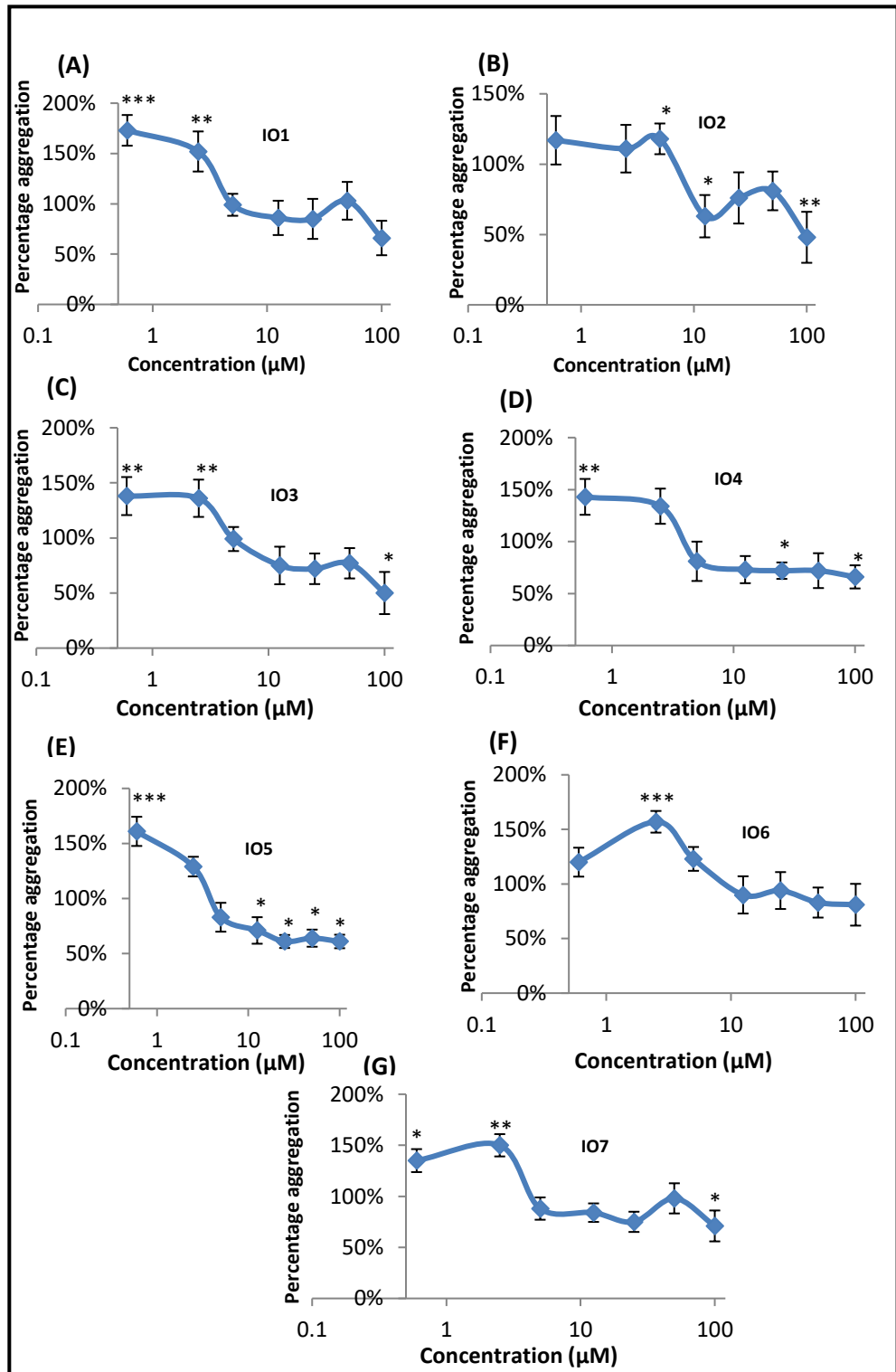


**Figure 3.1.1.1:** Effects of IO1, IO2, IO3, IO4, IO5, IO6 and IO7 peptides on amylin aggregation. Percentage aggregation of amylin, in the presence of (A) IO1, (B) IO2, (C) IO3, (D) IO4, (E) IO5, (F) IO6 and (G) IO7 peptides. All peptides were tested at 0.6 μM, 2.5 μM, 5 μM, 12.5 μM, 25 μM, 50 μM and 100 μM, with amylin at 25 μM. The peptides and amylin were incubated for 48 hrs in the presence of Th-T. Triplicate readings were taken for each condition and results are means +/- SEM. One-way ANOVA, Tukey's post hoc test \*P<0.05, \*\*P<0.01, \*\*\*P<0.001, compared to 100% control (amylin alone). [Percentage aggregation = fluorescent reading of amylin alone minus (-) fluorescence of amylin in the presence of peptide multiplied by (X) 100. Calculated for each peptide concentration].

### **3.1.2 Effect of amylin derived peptide inhibitors (IO8 and RI-IO8) on amylin aggregation**

The IO8 inhibitor was designed using the combined amino acid sequences of IO4 and IO5 as they appeared to be more potent inhibitors compared to other previously tested inhibitors (see sections 2.2 and 3.1.1). In order to stabilise IO8 and preserve it from proteolytic degradation, a retro-inverso version of IO8 (RI-IO8) was made. This was achieved by reversing the peptide sequence and replacing the L-amino acids with D-amino acids. The Th-T assay was used to monitor the effects of IO8 and RI-IO8 on amylin aggregation, carried out under similar experimental conditions to those described above (Section 3.1.1). Figure 3.1.2 shows data for the percentage aggregation of amylin in the presence of IO8 and RI-IO8 peptides. IO8 displayed inhibitory effects on amylin aggregation at all concentrations  $\geq 1 \mu\text{M}$  (1:25 molar ratio of inhibitor to amylin). At an equimolar concentration of amylin, IO8 reduced the development of Th-T fluorescence to 16% of the non-inhibited control (figure 3.1.2). At 50  $\mu\text{M}$  (2:1 molar ratio of IO8 to amylin) and 100  $\mu\text{M}$  (4:1 molar ratio of IO8 to amylin), IO8 significantly decreased the Th-T fluorescence to 11% and 8% respectively ( $p < 0.001$ ); levels comparable with buffer control (figure 3.1.2). In complete contrast, the addition of RI-IO8 peptide to amylin under the same experimental conditions showed no inhibitory effects on amylin aggregation and in fact appeared to enhance fibril formation at all concentrations mentioned above, with the exception of 100  $\mu\text{M}$  (4:1 molar ratio inhibitor to amylin), where RI-IO8 ( $p < 0.05$ ) decreased amylin aggregation to 77% of control (figure 3.1.2). Therefore, IO8 acts as an inhibitor, whereas RI-IO8 does not and may even stimulate aggregation.

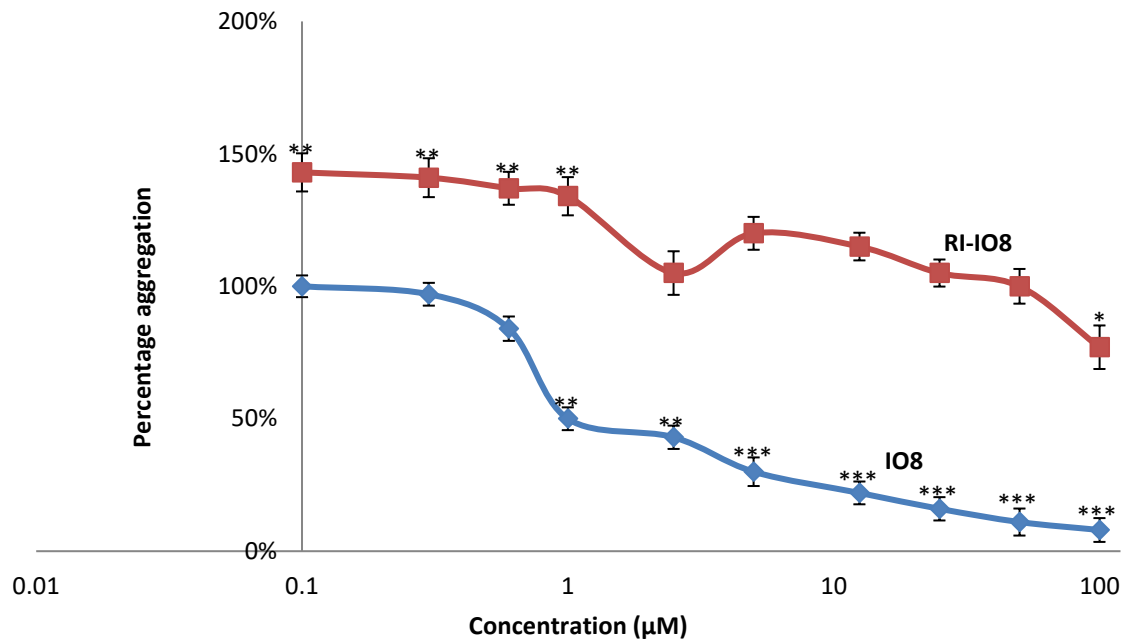


**Figure 3.1.2:** Percentage aggregation of amylin in the presence of IO8 and RI-IO8 peptides. The peptides, at 0.1 µM, 0.3 µM, 0.6 µM, 1 µM, 2.5 µM, 5 µM, 12.5 µM, 25 µM, 50 µM and 100 µM, along with amylin at 25 µM, were incubated for 48 hrs in the presence of Th-T. Triplicate readings were taken for each condition and results are means +/- SEM. One-way ANOVA, Tukey's post hoc test \*P<0.05, \*\*P<0.01, \*\*\*P<0.001, compared to 100% control (amylin alone). [Percentage aggregation = fluorescent reading of amylin alone minus (-) fluorescence of amylin in the presence of peptide multiplied by (X) 100. Calculated for each peptide concentration].

### 3.1.3 Effect of IO8, NMeG24NMeI26 and ANFLVH on amylin aggregation

Given that IO8 is the most promising inhibitor of amylin aggregation, compared to the other peptides, the effects of this inhibitor on amylin aggregation were monitored alongside NMeG24 NMeI26 (Sellin *et al.*, 2010) and ANFLVH (Potter *et al.*, 2009), which are inhibitors reported to reduce amylin fibril formation in the literature. However, ANFLVH did not dissolve in aqueous solution, and so could not be used for this experiment. The Th-T assay was carried out under similar experimental conditions to those described above. Figure 3.1.3 shows data for the percentage aggregation of amylin in the presence of IO8 and NMeG24 NMeI26 peptides, relative to a non-inhibited control. IO8 displayed strong inhibitory effects on amylin aggregation at all concentrations  $\geq 1 \mu\text{M}$ , and at  $2.5 \mu\text{M}$  (1:10 molar ratio inhibitor to amylin), IO8 decreased amylin aggregation to 35% ( $p < 0.01$ ) of the non-inhibited control (figure 3.1.3). On the other hand, the addition of NMeG24 NMeI26 peptide to amylin under the same conditions showed no inhibitory effect on amylin and significantly accelerated fibril formation at  $0.05 \mu\text{M}$ ,  $0.1 \mu\text{M}$  and  $0.3 \mu\text{M}$ . The data confirm the inhibitory effects of IO8, but fail to demonstrate any inhibition with NMeG24 NMeI26.

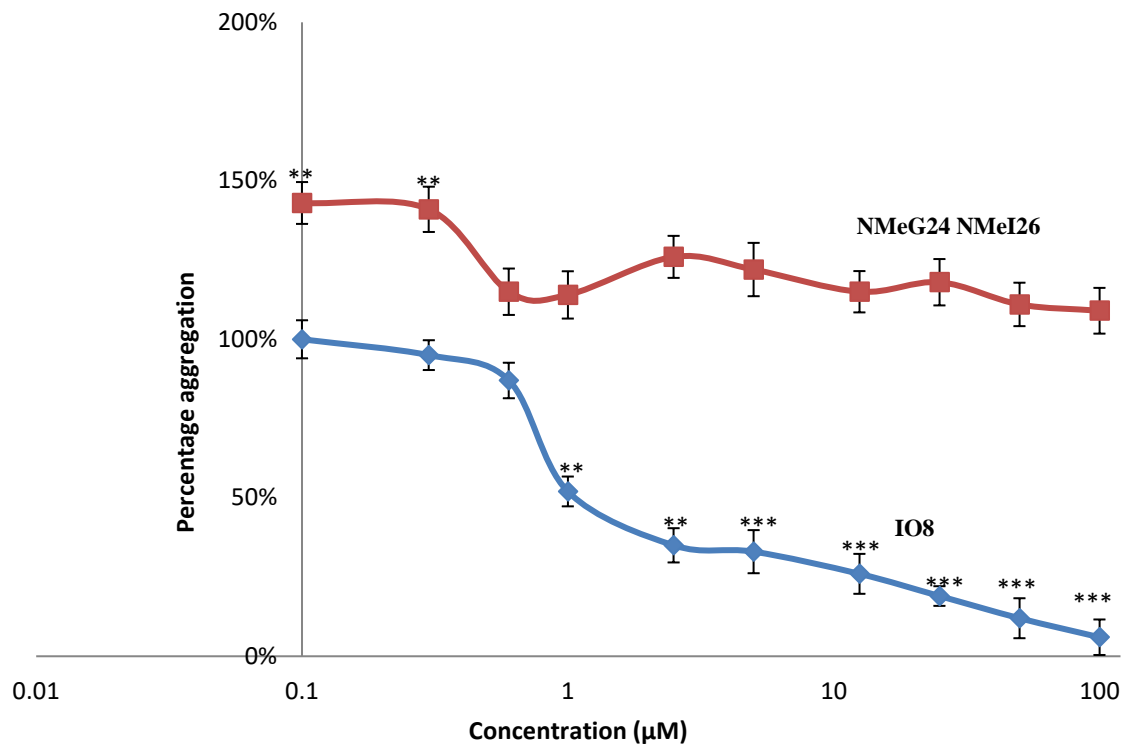


**Figure 3.1.3:** Effects of IO8 and NMeG24 NMeI26 peptides on amylin aggregation. Percentage aggregation of amylin (at 25 µM) in the presence of IO8 and NMeG24 NMeI26 peptides at 0.1 µM, 0.3 µM, 0.6 µM, 1 µM, 2.5 µM, 5 µM, 12.5 µM, 25 µM, 50 µM and 100 µM. The peptides and amylin were incubated for 48 hrs and then monitored by Th-T assay. One-way ANOVA, Tukey's post hoc test \*P<0.05, \*\*P<0.01, \*\*\*P<0.001, compared to 100% control (amylin alone). [Percentage aggregation = fluorescent reading of amylin alone minus (-) fluorescence of amylin in the presence of peptide multiplied by (X) 100. Calculated for each peptide concentration].

### 3.1.4 Effect of H<sub>2</sub>N-RGNFGAILSGR-NH<sub>2</sub> on amylin aggregation

Inhibitor IO8 (directed at the binding region of amylin) was then compared with another peptide directed at the amyloidogenic region (H<sub>2</sub>N-RGNFGAILSGR-NH<sub>2</sub>), the latter being the region focused on in most of the other peptide inhibitors described the literature (Potter *et al.*, 2009; Sellin *et al.*, 2010; Andreasen *et al.* 2012). Again, the Th-T assay was carried out under similar experimental conditions to those described above. Figure 3.1.4 shows data for the percentage aggregation of amylin in the presence of the IO8 and H<sub>2</sub>N-RGNFGAILSGR-NH<sub>2</sub> peptides. IO8 displayed strong inhibitory effects on amylin aggregation at all concentrations  $\geq 1 \mu\text{M}$ . At 100  $\mu\text{M}$  (4:1 molar ratio inhibitor to amylin), this peptide decreased amylin aggregation to 8% of the non-inhibited control, and at 25  $\mu\text{M}$  (1:1 molar ratio inhibitor to amylin), it decreased amylin aggregation to 18% ( $p < 0.001$ ). On the other hand, the H<sub>2</sub>N-RGNFGAILSGR-NH<sub>2</sub> peptide accelerated amylin aggregation at 100  $\mu\text{M}$  (4:1 molar ratio of inhibitor to amylin), 50  $\mu\text{M}$  (2:1 molar ratio), and 25  $\mu\text{M}$  (1:1 molar ratio).

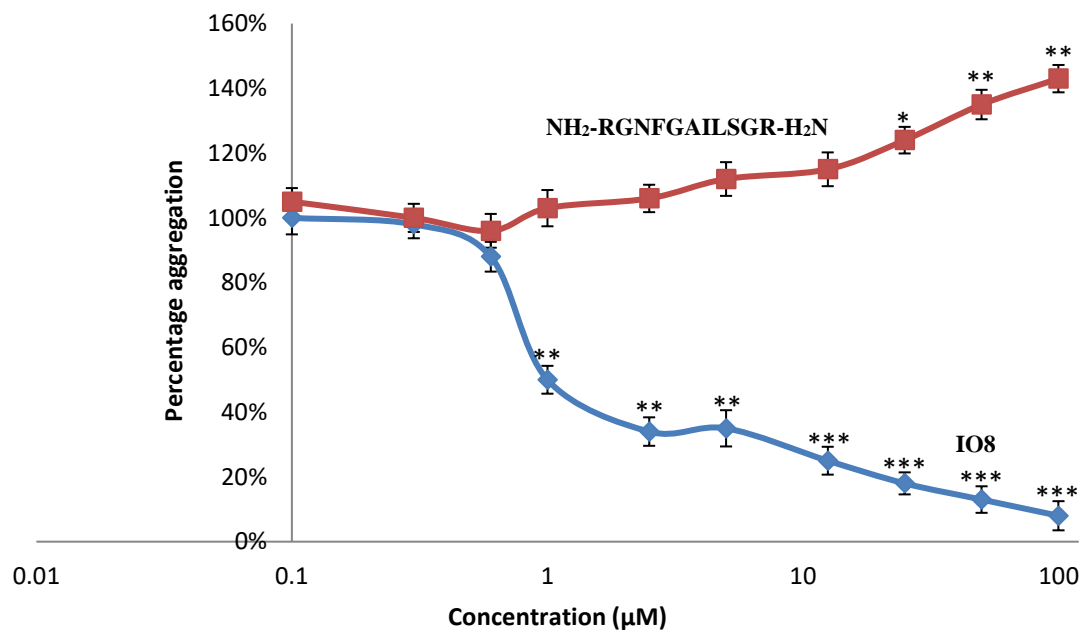


**Figure 3.1.4:** Effects of IO8 and H<sub>2</sub>N-RGNFGAILSGR-NH<sub>2</sub> peptides on amylin aggregation. Data show percentage aggregation of amylin (at 25 µM) in the presence of 0.1 µM, 0.3 µM, 0.6 µM, 1 µM, 2.5 µM, 5 µM, 12.5 µM, 25 µM, 50 µM and 100 µM of each peptide inhibitor, by Th-T assay. The peptides and amylin were incubated for 48 hrs and results show means  $\pm$  SEM, n=3. One-way ANOVA, Tukey's post hoc test \*P<0.05, \*\*P<0.01, \*\*\*P<0.001, compared to 100% control (amylin alone). [Percentage aggregation = fluorescent reading of amylin alone minus (-) fluorescence of amylin in the presence of peptide multiplied by (X) 100. Calculated for each peptide concentration].

### 3.1.5 Effect of HIO8 on amylin aggregation

Given that the retro-inverso peptide RI-IO8 failed to inhibit amylin aggregation, but instead stimulated the aggregation of amylin, we devised a new strategy to protect IO8 (H<sub>2</sub>N-**R**GANFLVH**G**R-NH<sub>2</sub>) from proteolytic degradation. Thus peptide HIO8, with amino acid sequence H<sub>2</sub>N-**Har**-GANFLVHG-**Har**-NH<sub>2</sub>, was designed. In HIO8, the arginine residues of IO8 (coloured red) were replaced with homoarginine (coloured blue), which is an unnatural analogue of arginine. This replacement was designed to protect the peptide from proteolytic degradation by trypsin as an initial step to protect the peptide, although still susceptible to degradation by other proteases like chymotrypsin. The Th-T assay was carried out under similar experimental conditions to those described above. Figure 3.1.5 shows data for the percentage aggregation of amylin in the presence of IO8 and HIO8 peptides. Again, IO8 displayed strong inhibitory effects on amylin aggregation at all concentrations  $\geq 1 \mu\text{M}$ . At 100  $\mu\text{M}$  (4:1 molar ratio inhibitor to amylin), it decreased amylin aggregation to 10% of the non-inhibited control ( $p < 0.001$ ). At a concentration of 25  $\mu\text{M}$  (1:1 molar ratio), IO8 decreased amylin aggregation to 15%. In addition, HIO8 showed similar inhibitory effects on amylin aggregation to IO8. At 100  $\mu\text{M}$  (4:1 molar ratio of inhibitor to amylin), HIO8 decreased amylin aggregation to 13% ( $p < 0.001$ ). At a concentration of 25  $\mu\text{M}$  (1:1 molar ratio), HIO8 decreased amylin aggregation to 25%. Thus IO8 and HIO8 are both effective inhibitors of amylin aggregation.

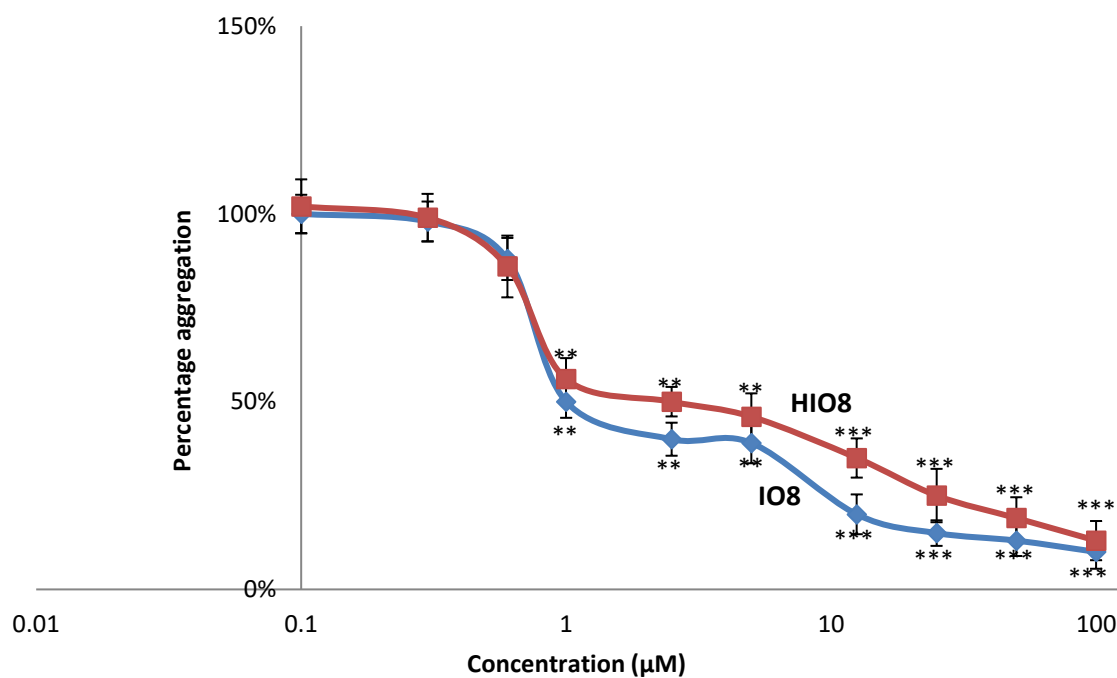


**Figure 3.1.5:** Effects of IO8 and HIO8 peptides on amylin aggregation. Percentage aggregation of IO8 and HIO8 peptides at 0.1 µM, 0.3 µM, 0.6 µM, 2.5 µM, 1 µM, 5 µM, 12.5 µM, 25 µM, 50 µM and 100 µM in the presence of amylin at 25 µM, with aggregation monitored by Th-T assay after 48 hrs incubation. One-way ANOVA, Tukey's post hoc test \*P<0.05, \*\*P<0.01, \*\*\*P<0.001, compared to 100% control (amylin alone). [Percentage aggregation = fluorescent reading of amylin alone minus (-) fluorescence of amylin in the presence of peptide multiplied by (X) 100. Calculated for each peptide concentration].

### 3.1.6 Effect of N1-IO8 and N2-IO8 on amylin aggregation

For peptides to be used as effective drug candidates, it is important to protect them from proteolytic degradation. One method to improve the physiochemical properties of IO8 is through N-methylation of particular amino acid residues, and so the next step was to carry out Th-T assays under similar experimental conditions to those described above with two different N-methylated peptides. Figure 3.1.6 shows data for the percentage aggregation of amylin in the presence of these N1-IO8 (**H<sub>2</sub>N-R G Am N Fm L Vm H G R-NH<sub>2</sub>**) and N2-IO8 (**H<sub>2</sub>N-R G A Nm F Lm V Hm G R-NH<sub>2</sub>**) peptides. Both N1-IO8 and N2-IO8 showed clear dose-dependent inhibition of amylin aggregation, with very similar inhibition curves. Both inhibitors showed highly significant inhibition of aggregation ( $p < 0.001$ ) at concentrations of  $\geq 25 \mu\text{M}$ . At  $100 \mu\text{M}$  (4:1 molar ratio of inhibitor to amylin), N1-IO8 decreased amylin aggregation to 15% of the non-inhibited control. At a concentration of  $25 \mu\text{M}$  (1:1 molar ratio), N1-IO8 inhibited amylin aggregation to 34%. At  $100 \mu\text{M}$  (4:1 molar ratio of inhibitor to amylin), N2-IO8 decreased amylin aggregation to 12%. At a concentration of  $25 \mu\text{M}$  (1:1 molar ratio), N2-IO8 inhibited amylin aggregation to 36%. Thus N1-IO8 and N2-IO8 inhibited amylin aggregation in a similar way and they are both effective inhibitors of amylin aggregation.

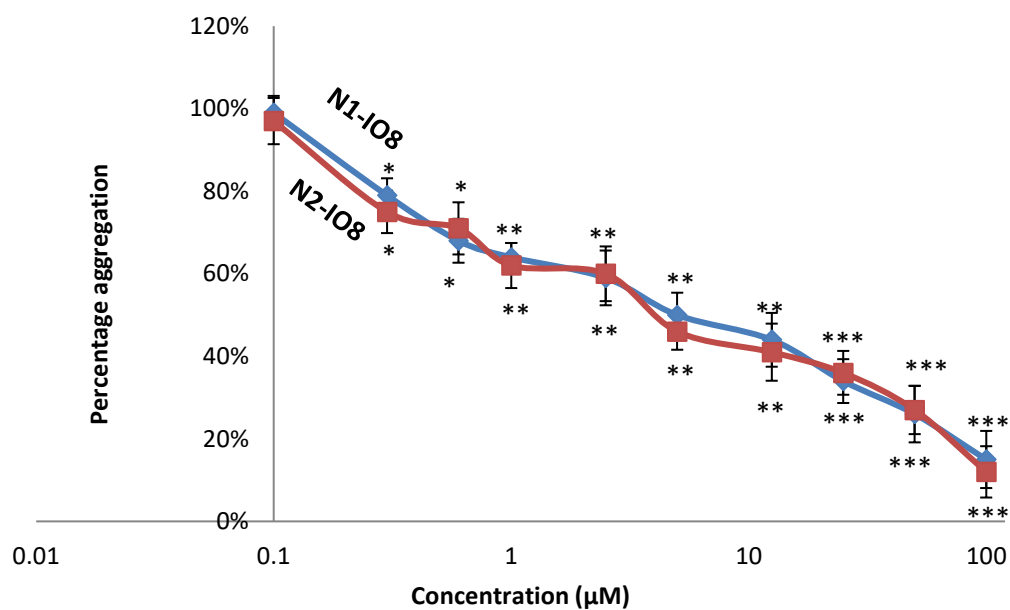


**Figure 3.1.6:** Effects of N1-IO8 and N2-IO8 peptides on amylin aggregation. Percentage aggregation of amylin (at 25 µM) in the presence of N1-IO8 and N2-IO8 peptides at 0.1 µM, 0.3 µM, 0.6 µM, 2.5 µM, 1 µM, 5 µM, 12.5 µM, 25 µM, 50 µM and 100 µM, relative to a control without inhibitor. The peptides and amylin were incubated for 48 hrs and aggregation was monitored by Th-T assay. One-way ANOVA, Tukey's post hoc test \*P<0.05, \*\*P<0.01, \*\*\*P<0.001, compared to 100% control (amylin alone). [Percentage aggregation = fluorescent reading of amylin alone minus (-) fluorescence of amylin in the presence of peptide multiplied by (X) 100. Calculated for each peptide concentration].

### **3.2 Quantifying amylin aggregation using the Congo Red Spectrophotometric Assay**

Congo Red (CR) is a dye which binds to the  $\beta$ -pleated sheet of all amyloid fibrils and gives a characteristic green/red birefringence when a histology tissue sample is examined by polarisation microscopy. This study was aimed at confirming the effects of peptide-based inhibitors on amylin aggregation by quantifying this process using CR stain and measuring the characteristic change in colour absorbance on binding to amyloid fibrils. Amylin at 25  $\mu$ M was incubated in the absence and presence of peptides at varying concentrations for 48 hrs as described in the Methods section 2.7.1. UV-VIS measurements were carried out using the NANODROP 2000C spectrophotometer. These sets of experiments were focused on the most promising peptides, IO8, N1-IO8 and N2-IO8, as well as the retroinverso peptide RI-IO8 which appeared to stimulate amylin aggregation when this was monitored by Th-T assay.

### **3.2.1 Congo red binding studies of amylin aggregation in the presence of IO8 inhibitor**

The effect of IO8 on amylin fibril formation was monitored by using the CR binding assay. IO8 was incubated with amylin (25  $\mu\text{M}$ ) at inhibitor concentrations of 0  $\mu\text{M}$ , 0.1  $\mu\text{M}$ , 0.3  $\mu\text{M}$ , 0.6  $\mu\text{M}$ , 1  $\mu\text{M}$ , 2.5  $\mu\text{M}$ , 5  $\mu\text{M}$ , 12.5  $\mu\text{M}$ , 25  $\mu\text{M}$ , 50  $\mu\text{M}$  and 100  $\mu\text{M}$ , for 48 hrs at 37°C with continuous shaking and then addition of CR solution. The absorbance spectrum was read between 400 to 700 nm using the UV-VIS Spectrophotometer. The spectrum obtained with CR alone was subtracted from the 'protein plus CR' spectrum, with spectral difference at the optimal wavelength of 540 nm indicating the presence of amyloid fibrils. Figure 3.2.1 shows the effects of IO8 on amylin fibril formation. Similar to the Th-T results, the data suggest that IO8 at concentrations of 100  $\mu\text{M}$  (4:1 molar ratio of inhibitor to amylin) and 50  $\mu\text{M}$  (2:1 molar ratio of inhibitor to amylin) inhibits amylin fibril formation to around 13% of a non-inhibited control, which is comparable with a buffer alone control. IO8 on its own did not alter the absorbance of CR. These data also confirm that the inhibitory effect of IO8 on amylin fibril formation is dose dependent.

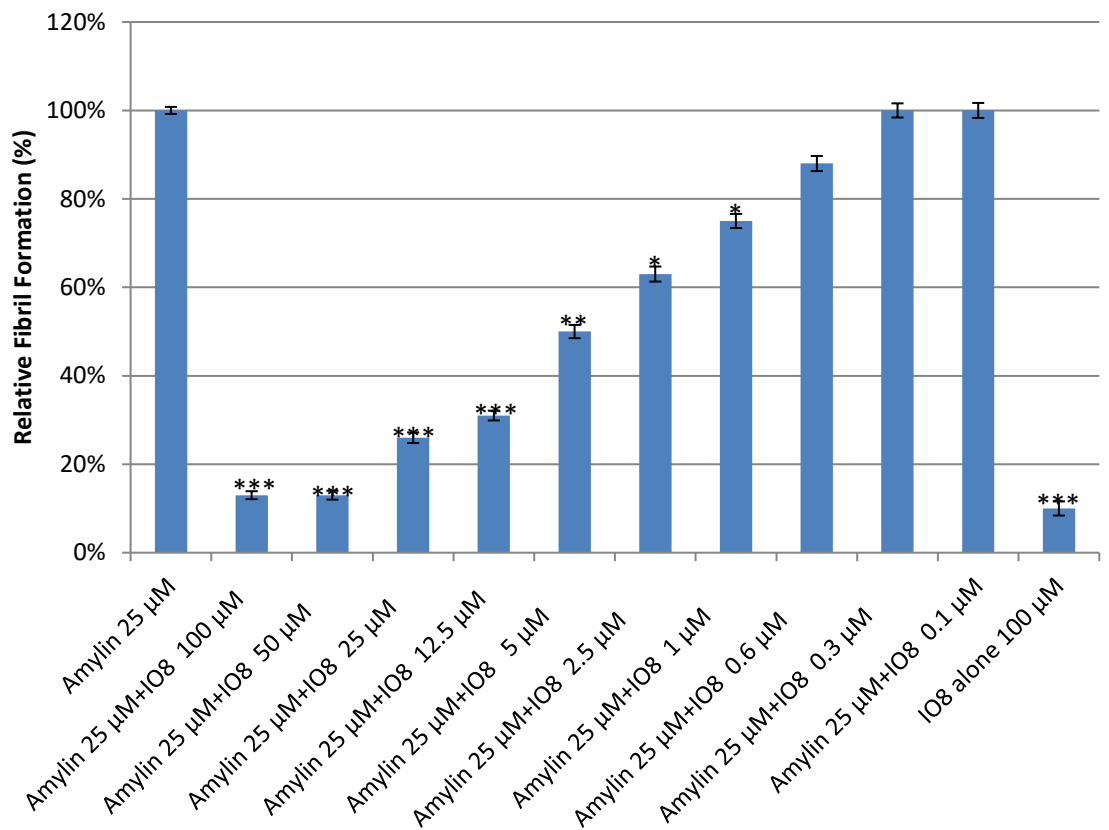


**Figure 3.2.1:** Effect of IO8 on human amylin fibril formation as monitored by Congo red assay. Relative fibril formation of 25 µM amylin in the presence IO8 at 0.1 µM, 0.3 µM, 0.6 µM, 2.5 µM, 1 µM, 5 µM, 12.5 µM, 25 µM, 50 µM and 100 µM. The peptides and amylin were incubated for 48 hrs at 37 °C and then analysed by Congo red assay. The results show means +/- SEM, n =3. One-way ANOVA, Tukey's post hoc test \*P<0.05, \*\*P<0.01, \*\*\*P<0.001, compared to 100% control (amylin alone).

### **3.2.2 Congo red binding studies of amylin aggregation in the presence of RI-IO8**

The effect of RI-IO8 on amylin fibril formation was also monitored by using the CR binding assay, with similar experimental conditions to those described above. Figure 3.2.2 shows the percentage fibril formation of amylin in the presence of different concentrations of RI-IO8. Similar to the Th-T fluorescence results, the data suggest that RI-IO8 significantly stimulated the formation of amylin fibrils. However, at a concentration of 100  $\mu$ M (4:1 molar ratio of inhibitor to amylin), a decreased CR spectrum at 540 nm was observed, with RI-IO8 decreasing fibril formation to 74%. RI-IO8 on its own did not alter the binding absorbance of CR. These data confirm that RI-IO8, at all but the highest concentration tested, is apparently a stimulator of amylin fibril formation.

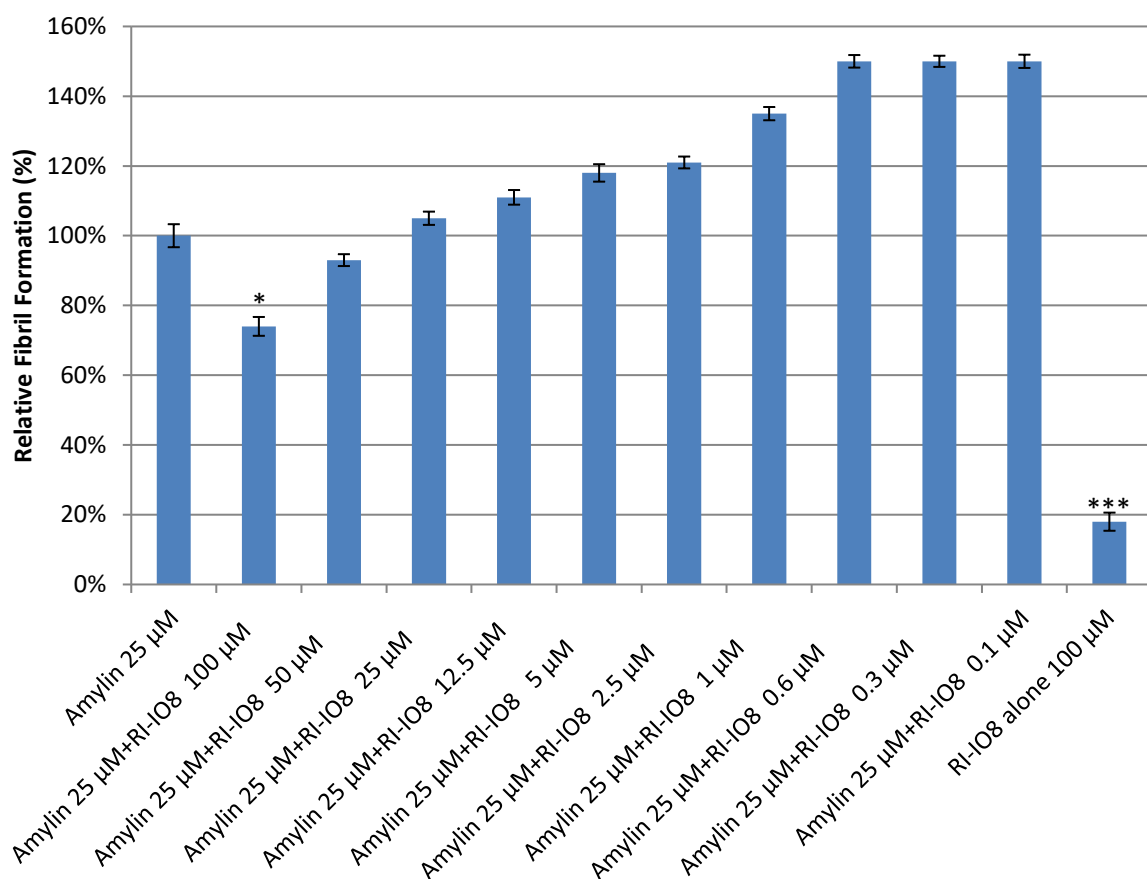


**Figure 3.2.2:** Effect of RI-IO8 on human amylin fibril formation as monitored by Congo red assay. Relative fibril formation of 25 µM amylin in the presence RI-IO8 at 0.1 µM, 0.3 µM, 0.6 µM, 2.5 µM, 1 µM, 5 µM, 12.5 µM, 25 µM, 50 µM and 100 µM. The peptides and amylin were incubated for 48 hrs at 37 °C and analysed by Congo red assay. The results are means  $\pm$  SEM, n =3. One-way ANOVA, Tukey's post hoc test \*P<0.05, \*\*P<0.01, \*\*\*P<0.001, compared to 100% control (amylin alone).

### **3.2.3 Congo red binding studies of amylin aggregation in the presence of N1-IO8 inhibitor**

The effect of N1-IO8 on amylin fibril formation was monitored by using the CR binding assay, with similar experimental conditions to those described above. Figure 3.2.3 shows the relative fibril formation of amylin in the presence of different concentrations of N1-IO8. Similar to Th-T fluorescence results, the data suggest that N1-IO8 at concentrations of 100  $\mu$ M (4:1 molar ratio of inhibitor to inhibitor) and 50  $\mu$ M (2:1 molar ratio of amylin to inhibitor), decreased CR spectra at 540 nm, confirming their inhibitory effect on amylin fibril formation. At these concentrations, amylin fibril formation was decreased to 17% and 29%, respectively, levels comparable with buffer control. N1-IO8 on its own did not alter the binding absorbance of CR. These data also confirm that the inhibitory effect of N1-IO8 on amylin fibril formation is dose dependent.

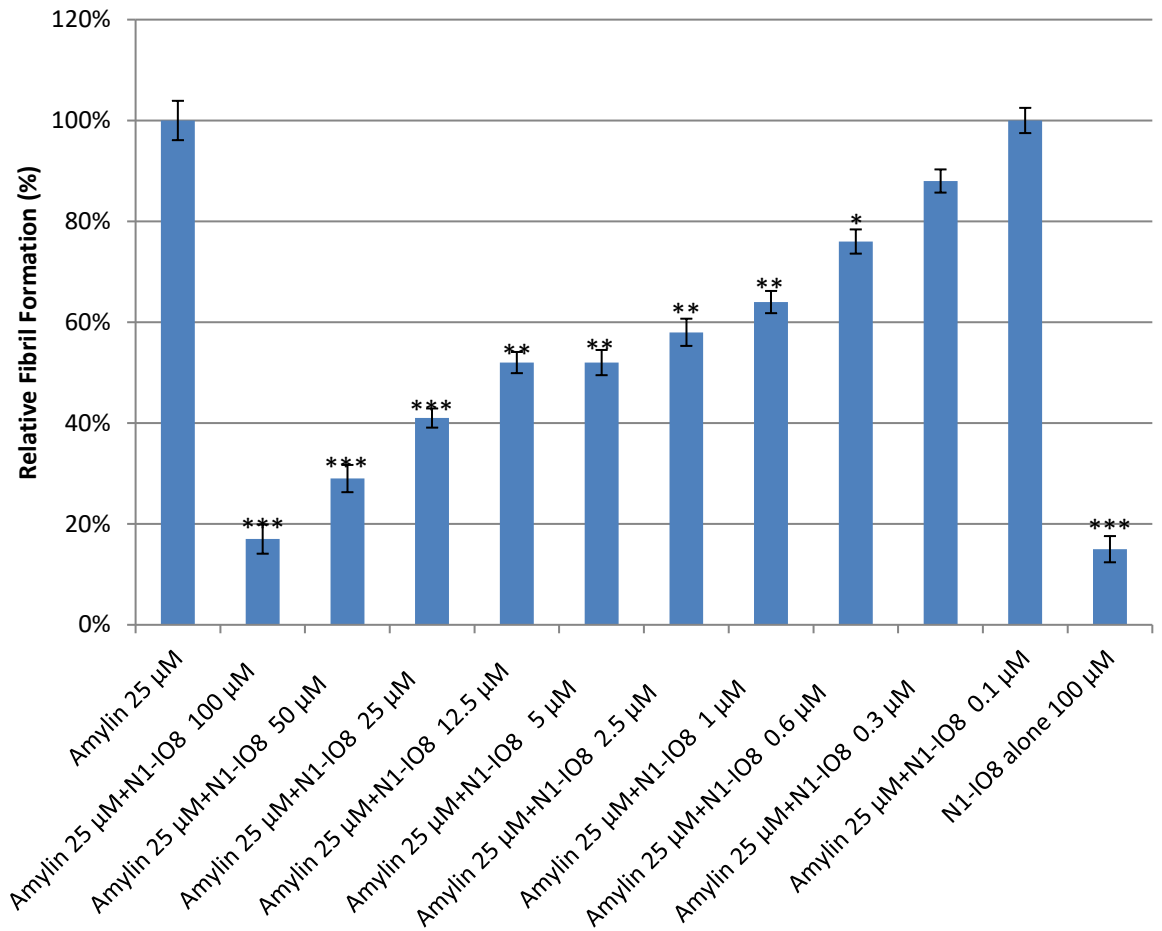


**Figure 3.2.3:** Effect of N1-IO8 on human amylin fibril formation, as monitored by Congo red assay. Relative fibril formation of 25  $\mu$ M amylin in the presence N1-IO8 at 0.1  $\mu$ M, 0.3  $\mu$ M, 0.6  $\mu$ M, 2.5  $\mu$ M, 1  $\mu$ M, 5  $\mu$ M, 12.5  $\mu$ M, 25  $\mu$ M, 50  $\mu$ M and 100  $\mu$ M. The peptides and amylin were incubated for 48 hrs at 37  $^{\circ}$ C and analysed by Congo red assay. Results are means  $\pm$  SEM, n=3. One-way ANOVA, Tukey's post hoc test \*P<0.05, \*\*P<0.01, \*\*\*P<0.001, compared to 100% control (amylin alone).

### **3.2.4 Congo red binding studies of amylin aggregation in the presence of N2-IO8 inhibitor**

The effect of N2-IO8 on amylin fibril formation was also monitored using the CR binding assay, as before. Figure 3.2.4 shows the relative fibril formation of amylin in the presence of different concentrations of N2-IO8. Similar to Th-T fluorescence results, the data show that N2-IO8 at concentrations of 100  $\mu\text{M}$  (4:1 molar ratio of inhibitor to amylin) and 50  $\mu\text{M}$  (2:1 molar ratio of inhibitor to amylin), decreased CR spectra at 540 nm, confirming their inhibitory effect on amylin fibril formation. At these concentrations, amylin fibril formation was decreased to 23% and 35% respectively, levels comparable with buffer control. N2-IO8 on its own did not alter the binding absorbance of CR. These data also confirm that the inhibitory effect of N2-IO8 on amylin fibril formation is dose dependent.

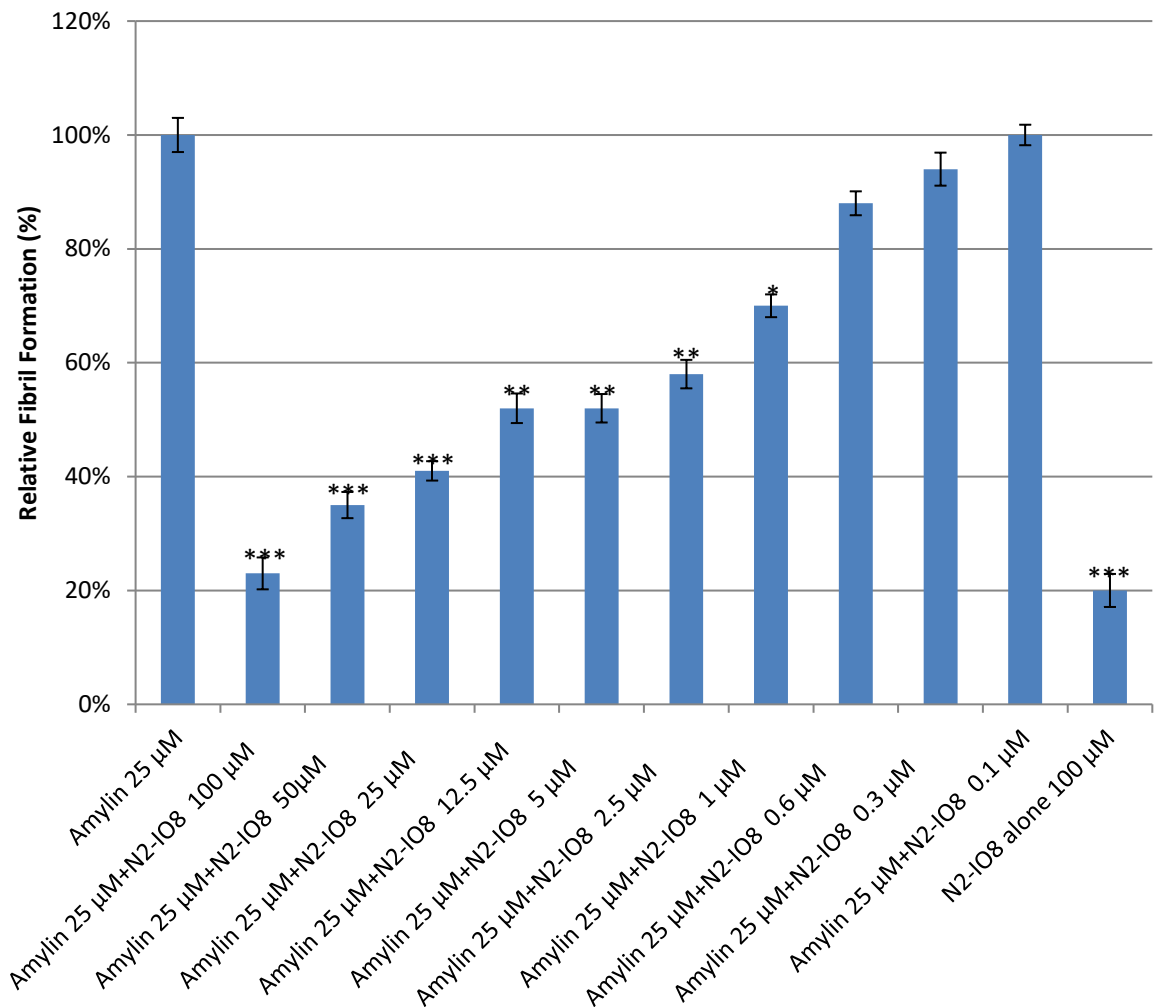


**Figure 3.2.4:** Effect of N2-IO8 on human amylin fibril formation as monitored by Congo red assay. Relative fibril formation of 25 µM amylin in the presence N2-IO8 at 0.1 µM, 0.3 µM, 0.6 µM, 2.5 µM, 1 µM, 5 µM, 12.5 µM, 25 µM, 50 µM and 100 µM in the presence of amylin at 25 µM. The peptides and amylin were incubated for 48 hrs at 37 °C and analysed using the Congo red assay. The results are means +/- SEM, n =3. One-way ANOVA, Tukey's post hoc test \*P<0.05, \*\*P<0.01, \*\*\*P<0.001, compared to 100% control (amylin alone).

### 3.3 Discussion

Most patients with T2DM have amyloid deposits in their pancreatic islets (Westermarck, 1972). This leads to a reduction of  $\beta$  cell mass and function (Hull *et al.*, 2004; Jurgens *et al.*, 2011). Although many different peptide-based inhibitors have been designed for the inhibition of amyloid beta ( $A\beta$ ) aggregation, less work has been done on the inhibition of amylin aggregation. Research has shown that the highly amyloidogenic region of human amylin (NFGAIL) resides in residues 22-27 (Westermarck *et al.*, 1990); whereas in rodent amylin, proline substitutions impede  $\beta$ -sheet formation (Moriarty and Raleigh, 1999). This has led to the design of ‘ $\beta$ -sheet breaker’ peptide inhibitors based on this amyloidogenic region. In contrast, the study reported here was focused instead on investigating potential inhibitors of human amylin derived from the binding region corresponding to residues 11-20 of the molecule (RLANFLVHSS), and determining their effects on the fibrillogenesis of full-length human amylin. A series of overlapping small peptides was designed to target this binding region, and the ability of each of these peptides to prevent amylin aggregation was investigated. The rationale here is that prevention of the interaction between two amylin monomers, even if they are already misfolded, should impede their further aggregation. The ability of these peptide inhibitors to interfere with the formation of  $\beta$ -sheet amylin fibrils was examined using both Th-T and CR assay methods. Firstly, the inhibitory effects of IO1, IO2, IO3, IO4, IO5, IO6 and IO7 peptides on 25  $\mu$ M amylin were determined at a wide range of different inhibitory peptide concentrations (figure 3.1.1.1). Th-T analysis revealed that IO2, IO3 IO4, IO5 and IO7 showed some inhibitory

effects on amylin aggregation, but even at 100  $\mu\text{M}$ , the highest concentration tested, amylin aggregation was only inhibited by around 50% relative to non-inhibited controls. Peptides IO1 and IO6 showed no inhibitory effect on amylin aggregation, and at lower concentrations, all of the peptides appeared to stimulate amylin aggregation. The most convincing inhibition was achieved with peptides IO4 and IO5, and so their amino acid sequences were combined to make IO8, with the aim of enhancing their inhibitory effects. Th-T analysis showed that the IO8 peptide had a strong inhibitory effect on human amylin aggregation (figure 3.1.2). Incubating human amylin with IO8 at concentrations of 100  $\mu\text{M}$  (4:1 molar ratio of inhibitor to amylin), 50  $\mu\text{M}$  (1:2 molar) and 25  $\mu\text{M}$  (1:1 molar ratio) had a highly significant inhibitory effect on amylin aggregation, and the Th-T assay showed that IO8 inhibits the formation of amylin aggregates with an  $\text{IC}_{50}$  of around 1  $\mu\text{M}$ , which is very encouraging. Moreover, the inhibitory action of IO8 was clearly concentration dependent and almost complete inhibition (down to levels comparable with buffer only controls) was now achievable. However, the retro-inverso version of IO8 (RI-IO8) showed no inhibitory effect on human amylin aggregation, rather, an increase in the aggregation of human amylin was observed. CR experiments confirmed the results obtained for both IO8 and RI-IO8 (figure 3.2.1; figure 3.2.2). Although the mechanism of inhibition of IO8 has not been investigated, it is likely that this is due to binding of IO8 to monomeric amylin. Also, it is not clear why RI-IO8 actually enhanced amylin aggregation, as all of the peptides on their own at 100  $\mu\text{M}$  did not appear to form  $\beta$  sheets as assessed by Th-T assay (Appendix D). This result was surprising since previous studies at Lancaster have shown that a retro-inverso peptide (RI-OR2) can successfully

inhibit the aggregation of A $\beta$  associated with Alzheimer's disease (Taylor *et al.*, 2010). Most inhibitors of amylin aggregation are designed to target the aggregation prone region of amylin. However our peptides were designed to target the binding region of the human amylin peptide. The residues on the N- and C- termini are designed to act to facilitate aggregation inhibition and impede the binding of additional amylin-peptide complex. The N- and C- termini of all our peptides are capped with the GR-NH<sub>2</sub> side chains to improve solubility of the peptides. Solubility is important when choosing side chains and Ramírez-Alvarado *et al.*, 1999 have previously used the Ac-RG- and -GR NH<sub>2</sub> Side chains to improve solubility of peptides. Our results add to previous research which has elucidated the effects of peptides and small molecule inhibitors on amylin aggregation. Small molecule inhibitors such as resveratrol have been shown to inhibit membrane bound human amylin at a ratio of 1:2 amylin:resveratrol complex /membrane interphase (Lolicato *et al.*, 2015). Molecular dynamics simulations for human amylin pentamer with resveratrol also showed that resveratrol binding with human amylin resulted in significant conformational changes of human amylin pentamer (Wang *et al.*, 2015). Another molecule, acid fuchsin (Meng *et al.*, 2010) have been previously used to impede amylin amyloid formation. Also, small molecules comprising of polyphenols and aromatic groups have been shown to impede amylin amyloid formation, but this was only achieved by using molar excess of the inhibitory compounds (Cheng *et al.*, 2011; Sinha *et al.*, 2011; Mishra *et al.*, 2009). In addition, tetracycline showed little inhibitory effect on human amylin, with some inhibition being achieved only at a molar ratio of 20 fold excess of the inhibitory molecules (Aitken *et al.*, 2003). Other small molecules such as

Acridine Orange and Methylene Blue were able to bind to oligomeric forms of human amylin but showed no inhibitory effect on human amylin aggregation even at 20-fold molar excess concentrations of the inhibitory compounds (Aitken *et al.*, 2003). Although small molecule inhibitors have potential advantages including easy penetration into a large population of cells, they are not good candidates as amyloid aggregation inhibitors because inhibiting amylin aggregation requires impeding interactions between relatively large amylin monomers. Due to the size and geometry of the protein interaction surface, the small molecule would need to be the size of a peptide to work as an aggregation inhibitor. Protein-protein interaction regions are generally of the size 1500–3000 Å (Keskin *et al.*, 2008), while protein–small molecule interaction regions are approximately 300–1000 Å (Cheng *et al.*, 2007; Smith *et al.*, 2006). Therefore, small molecules are mostly incapable of generating sufficient steric hindrance to impede amylin aggregation. Thus peptide-based inhibitors are a better choice for aggregation inhibitor drugs. Full-length amylin with a single proline substitution in the 20–29 region has been shown to inhibit amylin fibril formation and toxicity, so converting amylin into a potent amyloid inhibitor (Abedini *et al.*, 2007; Meng *et al.*, 2010); furthermore, a double N-methylated variant of human amylin effectively inhibited the formation and cytotoxicity of amylin amyloid formation (Yan *et al.*, 2006). Although the mechanism of action of these compounds is yet to be understood, they may carry out their activity through interaction with helical oligomers (Stefani and Rigacci, 2013). However, full length amylin is expensive and difficult to synthesize. There could also be a risk for immunogenic responses. Thus full length amylin may not be the best peptide for amylin aggregation inhibitors.

Next, we compared the effects of IO8 with a previously reported inhibitor of amylin aggregation in literature, NMeG24 NMeI26 (Sellin *et al.*, 2010) which is a modified form of amylin 22-27 amyloidogenic fragment (NFGAIL), with N-methylation at the amide bonds G24 and I26. Although IO8 showed significant inhibition of amylin aggregation, NMeG24 NMeI26 was found to have no inhibitory effect on amylin aggregation, and actually showed the capacity to enhance amylin aggregation (figure 3.1.3). We also attempted to test the peptide ANFLVH (Potter *et al.*, 2009) which has been reported in literature to show inhibitory effects on amylin aggregation. However, this peptide was found to be insoluble in aqueous solution, and therefore could not be used in this study. A possible explanation for this could be the absence of arginine and glycine (RG) residues at both ends of the ANFLVH peptide, which are present in IO8. In search of other inhibitory peptides of amylin aggregation, we designed peptides with longer sequences spanning through the binding region; namely H<sub>2</sub>N-RGANFLVHSSNNFGR-NH<sub>2</sub> and its retro inverso form Ac-rGfnssshvlfnaGr-NH<sub>2</sub>. The inhibitory effects of these peptides could also not be assessed as they were insoluble in aqueous and non-aqueous solutions, and so no data is shown. It should be noted that as peptide length increases, generally the purity of the peptide becomes lower (Milton *et al.*, 1990). Probably shortening the sequence to eliminate some hydrophobic residues could help increase peptide polarity, as the greater the polarity, the more likely it is that the peptide will be soluble in aqueous solution.

Given that IO8 was the best inhibitor, efforts were made to stabilise IO8 from proteolytic degradation by replacing the arginines in IO8 (H<sub>2</sub>N-RGANFLVHGR-NH<sub>2</sub>) with homoarginine, to give HIO8 (H<sub>2</sub>N-Har-GANFLVHG-Har-NH<sub>2</sub>). This was to protect IO8 from degradation by trypsin. HIO8 showed inhibition of amylin aggregation comparable to that seen with IO8, and at a concentration of 100 μM (4:1 molar ratio of inhibitor to amylin), amylin aggregation was decreased to 13 % (figure 3.1.5). However, to completely stabilise IO8, it must be protected from proteolytic degradation by other proteolytic enzymes, and not just trypsin.

In the search for a more potent peptide than IO8, and to compare two different strategies (i.e. targeting of amyloidogenic versus binding regions of amylin), we designed another peptide, H<sub>2</sub>N-RGNFGAILSGR-NH<sub>2</sub> containing the ‘core’ of the 20-29 amyloidogenic region (NFGAIL). Our rationale was to investigate if the addition of positively charged RG (arginine-glycine) groups on either side of this peptide could confer inhibitory properties on the peptide, as they have been reported to improve peptide solubility and upon binding with the amyloid protein, prevents other molecules from binding to the amyloidogenic protein (Taylor *et al.*, 2010). However, the H<sub>2</sub>N-RGNFGAILSGR-NH<sub>2</sub> peptide showed no inhibitory effect on human amylin aggregation and even seemed to enhance aggregation (figure 3.1.4). Previous studies have shown that the peptide NFGAIL forms β-sheet containing amyloid fibrils (Tenidis *et al.*, 2000). It could thus be suggested that the presence of the amyloidogenic sequence NFGAIL could account for the increase in amylin aggregation as detected by Th-T assay in the presence of NMeG24 NMeI26 and NH<sub>2</sub>-RGNFGAILSGR-NH<sub>2</sub> peptides.

Another study showed that the addition of N-methyl groups to the peptide NFGAIL (NF(N-Me)GA(N-Me)IL) resulted in its conversion to a non-amyloidogenic and non-cytotoxic peptide (Tatarek-Nossol *et al.*, 2005) and reasonably impeded amylin amyloid formation, suggesting that N-methylation of peptides could be a beneficial approach in the design of amyloid therapeutics for T2DM. N-methylated peptides are designed to repress the H-bonding capacity of a NH group, to control the peptide backbone, and to assemble cylindrical  $\beta$ -sheet dimers (Vitoux *et al.*, 1986; Manavalan and Mormany, 1980; Clark *et al.*, 1998; Sun and Lorenzi, 1994). Considering the fact that our IO8 peptide was our most potent inhibitor of amylin aggregation, we thought to stabilize IO8 to proteolytic degradation and possibly improve its inhibitory properties through the selective N-methylation of alternate amino acid residues within the IO8 primary sequence. These N-methylated peptides, N1-IO8 (H<sub>2</sub>N-RGAmNFmLVmHGR-NH<sub>2</sub>) and N2-IO8 (H<sub>2</sub>N-RGANmFLmVHm R-NH<sub>2</sub>), gave significant inhibition of amylin aggregation, and at a concentration of 100  $\mu$ M (4:1 molar ratio of inhibitor to amylin), N1-IO8 decreased amylin aggregation to 15 % (figure 3.1.6). At a similar concentration, N2-IO8 decreased amylin aggregation to 12 % (figure 3.1.6). The Th-T assay showed that N1-IO8 and N2-IO8 inhibited the formation of amylin aggregates with IC<sub>50</sub> values of around 1.6  $\mu$ M and 1.5  $\mu$ M, respectively. They are, therefore, no more potent than IO8, which gave an IC<sub>50</sub> of 1  $\mu$ M. The inhibitory action of both N1-IO8 and N2-IO8 was very similar and showed clear concentration dependence. These results were also confirmed by CR experiments (figure 3.2.3; figure 3.2.4). These N- methylated peptides show better inhibitory properties than those described in literature as they inhibit amylin aggregation even at very low

concentrations. N1-IO8 and N2-IO8 are presumably capable of interacting with the full length human amylin, leading to inhibition of  $\beta$ -sheet formation and/or amyloidogenesis. *N*-Methylation has been thought to enhance  $\beta$ -sheet formation by converting the residue to a  $\beta$  conformation thereby producing soluble monomeric  $\beta$ -sheet peptides. *N*-methylation of the amide NH groups may impede intermolecular hydrogen bonding and possibly amyloid aggregation (Hughes *et al.*, 2000). These results suggest that there are definite structural rules that dictate protein self-assembly into amyloid (Dobson *et al.*, 1999), and illustrate the significance of adopting a rational approach to inhibitor design, and specific structural models of the amyloid core, when using native sequences as scaffolds to design amyloid inhibitors. For example, it is likely that the insolubility of the ANFLVH peptide is due to the predominance of hydrophobic residues which can sometimes lead to assembly problems (Fauchere and Pliska, 1983). This suggests that adding a polar residue like Arginine as seen in our IO8 peptide (H<sub>2</sub>N-RGANFLVHGR-NH<sub>2</sub>), could help to alter regular peptide structure thereby increasing polarity and solubility. Although the IO8 peptide has a similar sequence with the peptide in literature ANFLVH, it showed high solubility in aqueous solution, along with a greater inhibitory ability on amylin aggregation, thus making IO8 the better drug candidate.

Fluorescent dye-binding assays, like Congo red and Th-T are generally used to probe the aggregation of amyloidogenic proteins and for assessing inhibitors of amyloid aggregation and fibrillization (Hawe *et al.*, 2008; Buell *et al.*, 2010). This plays a key role in the understanding of numerous human diseases linked with protein aggregation. Following binding to protein aggregates, these dyes

show distinct spectral shifts when compared to their unbound state and thus can be used as good reporters of protein aggregation states (Nilsson, 2004; Eisert *et al.*, 2006). It is generally assumed that emission at 490 nm is directly proportional to the amount of amyloid fibrils present, and thus, the kinetics of fibril formation can be assessed by measuring the time dependent increase in fluorescence. On the other hand, a decrease in Th-T fluorescence generally denotes an inhibition of the amyloid self-assembly process (Buell *et al.*, 2010; Hawe *et al.*, 2008). It has however been shown that Th-T fluorescence may sometimes not give accurate assessment of the kinetics of the amyloid aggregation (Middleton *et al.*, 2012). For example, Middleton *et al.* (2012), reported that after 8 hours of amyloid aggregation, Th-T fluorescence attained a plateau state and continued in that state for up to 30 hours, which indicates the presence of a stable  $\beta$ -sheet content. However, 2D IR measurements showed that  $\beta$ -sheet structural and content changes occurred throughout a 24 hour period (Middleton *et al.*, 2012). Also, Th-T does not detect soluble amyloid oligomers, as observed from a characteristic lag phase in the time-dependent studies (figure 3.1), but predominantly detects the insoluble fibrillar aggregates in the  $\beta$ -sheet conformation (Bartolini *et al.*, 2011; Amaro *et al.*, 2011). Some studies have however reported that Th-T can differentiate between oligomeric and fibrillar A $\beta$  species (Maezawa *et al.*, 2008; Ryan *et al.*, 2010). These differences in reports can be attributed to variations in preparation methods for the A $\beta$  oligomers (Reinke and Gestwicki, 2011).

Another draw-back with dye-binding assays is, competitive binding of the dye and the inhibitors to the amyloidogenic proteins (Klunk *et al.*, 1999). If the

binding site of the inhibitor to the aggregating protein is the same as the binding site of the dye to the aggregating protein, the inhibitor and dye would have to compete for the binding site, which may result in inadequate binding of the dye to the aggregating protein. This may cause changes in signal intensity resulting in artifacts or false positives (Klunk *et al.*, 1999). Thus, when assessing the inhibitory effect of inhibitors on amylin aggregation and fibril formation, it is important to examine the impact of the inhibitors on the fluorescence of the dye in the absence of the aggregating peptide. In this study, inhibitors alone, in the presence of the dye indicated the absence of aggregation, with results similar to PBS buffer controls.

Considering the ease of manipulation and high throughput screening of potential inhibitors, dye-binding assays are usually used as the fundamental test of aggregation inhibiting peptides. Compounds that show inhibitory effects on amylin aggregation are considered for further testing, while compounds that do not show any inhibitory effect are not considered for further testing. Further testing of inhibitory molecules using biophysical methods like atomic force microscopy (AFM) and Transmission Electron Microscopy (TEM) are therefore required to confirm the effects of inhibitors on amyloid proteins.

### 3.3.1 Conclusion

Previous studies have focused on developing inhibitors of amylin amyloid aggregation by targeting the amyloidogenic region (Scrocchi *et al.*, 2002; Porat *et al.*, 2004; Kapurniotu *et al.*, 2002; Tatarek-Nossol *et al.*, 2005), which on its own can form fibrillar structures exhibiting a  $\beta$ -sheet conformation (Glennner *et al.*, 1988; Westermark *et al.*, 1990). However, in general these inhibitors were only found to work when they were in high molar excess compared to the amylin peptide (Scrocchi *et al.*, 2002; Porat *et al.*, 2004). Here, the effects on fibrillogenesis of full-length human amylin of a series of overlapping human amylin peptides derived from the binding region of amylin was examined, the objective being to determine if these fragments are capable of interacting with human amylin and altering the aggregation pathway. IO8, HIO8, N1-IO8 and N2-IO8 peptides were the most potent inhibitors and were shown to be significantly better than the peptide-based and small molecule inhibitors reported in literature. Even at a molar ratio of 1:10 inhibitor to amylin, these peptides are still potent inhibitors of amylin aggregation. It is important to note that for a peptide to be a good drug candidate, it must not only inhibit amyloid aggregation, but must also be stable to proteolytic degradation and be non-toxic. Applying this approach could lead to the development of new therapeutics capable of affecting amylin aggregation and further contribute information on the sequence-dependent mechanisms of amyloid formation.

## Chapter 4

### Qualitative analysis of the effects of peptide-based inhibitors on amylin aggregation

Transmission Electron Microscopy (TEM) has been used extensively for monitoring the formation of amyloid fibrils from proteins *in vitro*. TEM can be used qualitatively to assess characteristics such as fibril curvature and surface smoothness as well as bends and twists in the ribbon-like fibrils (Thorn *et al.*, 2008). Also, quantitative data such as the length of seeds and early aggregates, the amount of protofilaments, as well as the diameter of fibrils, can be obtained using TEM (Goldsbury *et al.*, 2000). Human amylin has been shown previously by TEM to assemble into amyloid fibrils from its initial monomeric stage, through to oligomers (Lee *et al.*, 2016). In order to confirm the effects of the peptide inhibitors on amylin aggregation, the aggregation of human amylin with and without inhibitors was examined, focussing specifically on IO8, N1-IO8, N2-IO8 and RIO8. The ultrastructural morphology of amylin aggregates was determined by using TEM to compare the effects of IO8 with its stable forms, N1-IO8, N2-IO8, as well as with RI-IO8 which appeared to stimulate amylin aggregation as observed in the Th-T assay. Although the Th-T assay has the advantage of showing the kinetics of amylin amyloid formation, it can give misleading results since it is dependent on the binding of an extrinsic probe (Meng *et al.*, 2008), and can lead to false positives result since a range of factors can result in the loss of Th-T fluorescence in addition to inhibition of amyloid formation (Jaikaran *et al.*, 2004). Therefore it was important to validate the Th-T

data by use of TEM to compare the ultrastructural morphology of human amylin fibrils in the presence and absence of the peptide-based inhibitors.

#### **4.1 IO8 inhibits amylin aggregation**

TEM was used to monitor the effects of IO8 on human amylin aggregation, with samples being negatively stained with 2% phosphotungstic acid (PTA). The effect of IO8 on the aggregation of 25  $\mu\text{M}$  amylin was examined at varying IO8 concentrations of 100  $\mu\text{M}$ , 50  $\mu\text{M}$ , 25  $\mu\text{M}$ , 5  $\mu\text{M}$  and 0  $\mu\text{M}$  (non-inhibited control). All experiments were repeated three times with similar results. Figure 4.1 shows the ultrastructural morphology of human amylin in the presence and absence of IO8 inhibitor. Figure 4.1A shows clearly that amyloid fibrils were formed after 48 hrs incubation of human amylin alone. With addition of 100  $\mu\text{M}$ , 50  $\mu\text{M}$ , or 25  $\mu\text{M}$  IO8 (4:1, 2:1 and 1:1 molar ratios of IO8 to amylin), no fibrils were observed after 48 hrs incubation (Figure 4.1B, 4.1C and 4.1D). It should be noted that at 100  $\mu\text{M}$ , an altered crystal-like morphology was observed. At a concentration of 5  $\mu\text{M}$  IO8 (1:5 molar ratio of IO8 to amylin), the presence of relatively less dense fibrils with a morphology similar to that of amylin fibrils was observed (Figure 4.1E). IO8 alone at 100  $\mu\text{M}$  showed no tendency to aggregate (Figure 4.1F). These results confirm that IO8 is an effective inhibitor of amylin aggregation.

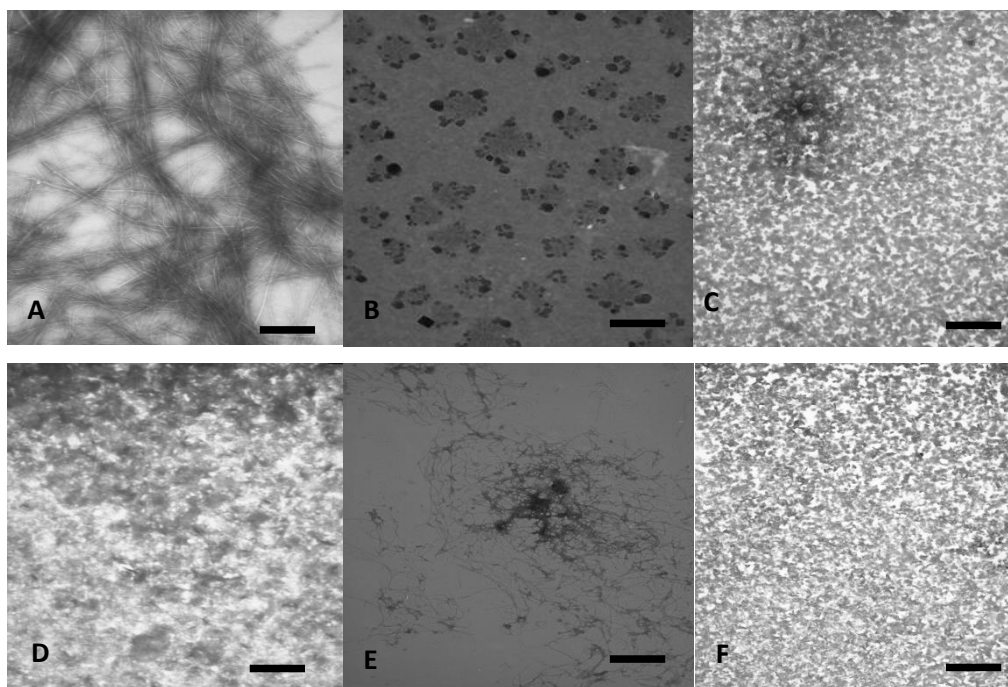


**Figure 4.1:** TEM examination of the effects of IO8 on amylin fibril formation. Samples of 25  $\mu\text{M}$  amylin in the presence and absence of IO8 at varying concentrations were incubated with continuous shaking for 48 hrs at 37°C in distilled water, negatively stained with phosphotungstic acid (2% w/v) and visualized using TEM. (A) Amylin alone; (B) Amylin + IO8 (100  $\mu\text{M}$ ); (C) Amylin + IO8 (50  $\mu\text{M}$ ); (D) Amylin + IO8 (25  $\mu\text{M}$ ); (E) Amylin + IO8 (5  $\mu\text{M}$ ); (F) IO8 peptide alone (100  $\mu\text{M}$ ). n=3 (3 replicates for each sample). Magnification = X15000. Scale bar = 500 nm.

## 4.2 RI-IO8 stimulates amylin aggregation

Studies from the Th-T assays showed that RI-IO8 appeared to stimulate amylin aggregation. To confirm these results, TEM was used to monitor the effects of RI-IO8 on amylin aggregation. The samples were negatively stained with 2% PTA. The effect of RI-IO8 on amylin aggregation was examined at varying concentrations of 100  $\mu\text{M}$ , 50  $\mu\text{M}$ , 25  $\mu\text{M}$  and 5  $\mu\text{M}$ , with amylin at a constant concentration of 25  $\mu\text{M}$ . All experiments were repeated three times with similar results. Figure 4.2 shows the ultrastructural morphology of human amylin in the presence and absence of RI-IO8. Figure 4.2A shows clearly that amyloid fibrils were formed after 48 hrs incubation of human amylin alone. These electron micrographs confirm the presence of amyloid fibrils/aggregated species in all samples of amylin. As can be seen in Figure 4.2A-F, there was a slight morphological variation among the aggregates/fibrillar species seen in these samples. On addition of 100  $\mu\text{M}$  RI-IO8 (4:1 molar ratio of RI-IO8 to amylin), relatively dense fibrillar aggregates with a similar morphology those seen with amylin alone were observed (Figure 4.2B). At 50  $\mu\text{M}$  RI-IO8 (2:1 molar ratio of RI-IO8 to amylin), dense fibrils with a more 'rigid' morphology than amylin fibrils were observed (Figure 4.2C). These rigid fibrils were denser and more numerous at 25  $\mu\text{M}$  and 5  $\mu\text{M}$  of RI-IO8 (1:1 and 1:5 molar ratios of RI-IO8 to amylin) (Figure 4.2D, 4.2E). RI-IO8 alone showed no tendency to aggregate (Figure 4.2F). These results support the Th-T data and confirm that RI-IO8 has no inhibitory effect on amylin aggregation, but rather stimulates the amylin aggregation process.

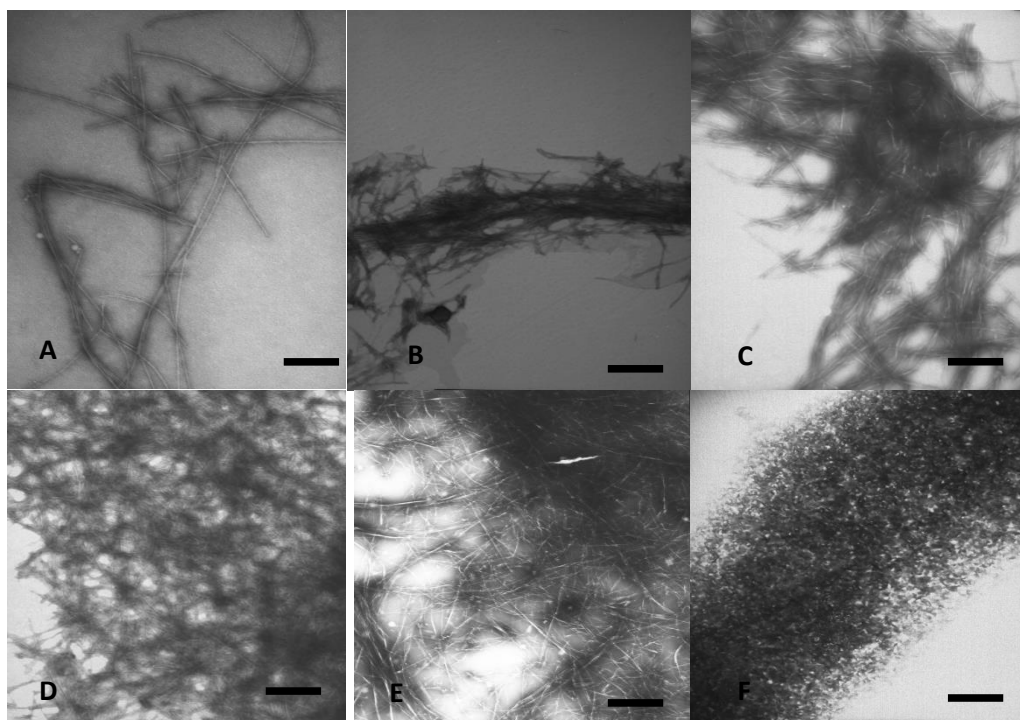


**Figure 4.2:** TEM examination of the effects of RI-IO8 on amylin fibril formation. Samples of 25  $\mu\text{M}$  of amylin in the presence and absence of RI-IO8 at varying concentrations were incubated with continuous shaking for 48 hrs at 37°C in distilled water, negatively stained with phosphotungstic acid (2% w/v) and visualized using TEM. (A) Amylin alone; (B) Amylin + RI-IO8 (100  $\mu\text{M}$ ); (C) Amylin + RI-IO8 (50  $\mu\text{M}$ ); (D) Amylin + RI-IO8 (25  $\mu\text{M}$ ); (E) Amylin + RI-IO8 (5  $\mu\text{M}$ ); (F) RI-IO8 alone (100  $\mu\text{M}$ ). n=3 (3 replicates for each sample) Magnification = X15000. Scale bar = 500 nm.

### **4.3 N1-IO8 inhibits amylin aggregation**

Following examination of the effects of N1-IO8 on amylin aggregation using the Th-T assay, we used the TEM to monitor its effects on amylin aggregation. The samples were negatively stained with 2% PTA, with the same conditions as before. The data shown are representative of at least two different experiments with similar results. Figure 4.3 shows the ultrastructural morphology of human amylin in the presence of N1-IO8 inhibitor. Figure 4.3A shows clearly the formation of amyloid fibrils following 48 hrs incubation of human amylin alone. In the presence of 100  $\mu\text{M}$ , 50  $\mu\text{M}$  and 25  $\mu\text{M}$  of N1-IO8 (4:1, 2:1 and 1:1 molar ratios of N1-IO8 to amylin), no fibrils were seen after 48 hrs incubation (Figure 4.3B, C and D). At 5  $\mu\text{M}$  of N1-IO8 (1:5 molar ratio of N1-IO8 to amylin), the presence of relatively less dense fibrils with a morphology similar to that of amylin fibrils was observed (Figure 4.3E). N1-IO8 showed no tendency to aggregate (Figure 4.3F). These results confirm that N1-IO8 is an effective inhibitor of amylin aggregation.

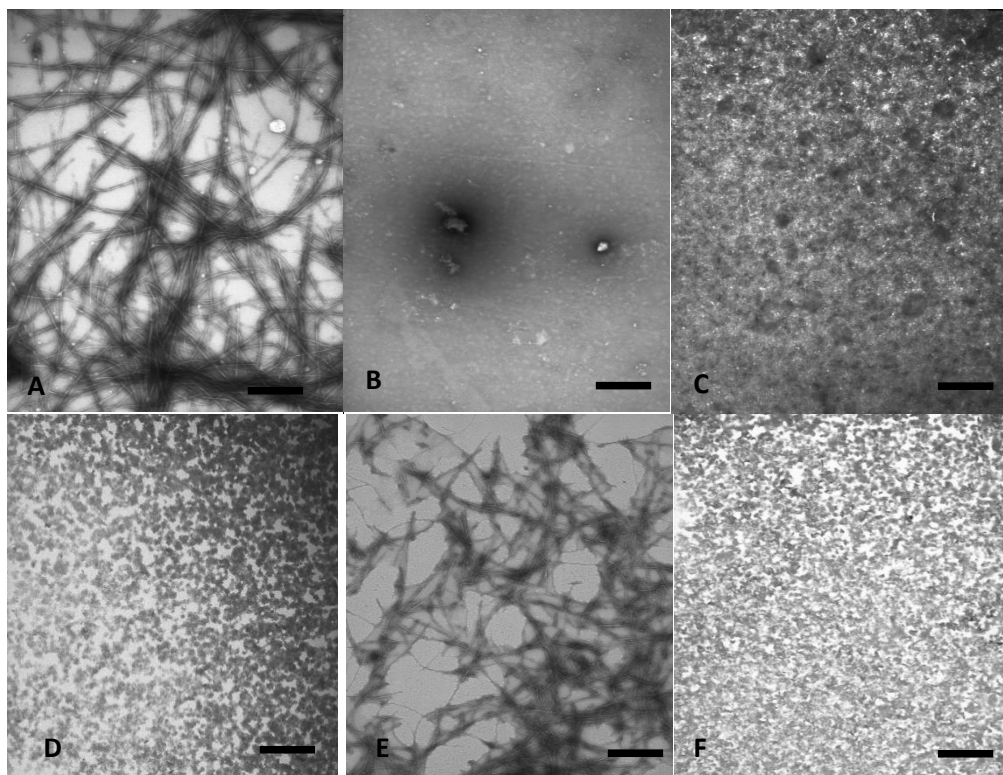


**Figure 4.3:** TEM examination of the effect of N1-IO8 on amylin fibril formation. Samples of 25  $\mu\text{M}$  of amylin in the presence and absence of RI-IO8 at varying concentrations were incubated with continuous shaking for 48 hrs at 37°C in distilled water, negatively stained with phosphotungstic acid (2% w/v) and visualized using TEM. (A) Amylin alone; (B) Amylin + RI-IO8 (100  $\mu\text{M}$ ); (C) Amylin + N1-IO8 (50  $\mu\text{M}$ ); (D) Amylin + N1-IO8 (25  $\mu\text{M}$ ); (E) Amylin + N1-IO8 (5  $\mu\text{M}$ ); (F) N1-IO8 peptide alone (100  $\mu\text{M}$ ). n=3 (3 replicates for each sample) Magnification = X15000. Scale bar = 500 nm.

#### **4.4 N2-IO8 inhibits amylin aggregation**

Following examination of the effects of N2-IO8 on amylin aggregation using the Th-T assay, TEM was used to monitor its effects on amylin aggregation, with the same experimental conditions as those described above. The data shown are representative of at least two different experiments with similar results. Figure 4.4 shows the ultrastructural morphology of human amylin in the presence of N2-IO8 inhibitor. Figure 4.4A shows clearly the formation of amyloid fibrils following 48 hrs incubation of human amylin. In the presence of 100  $\mu$ M, 50  $\mu$ M, 25  $\mu$ M or 5  $\mu$ M N2-IO8 (4:1, 2:1, 1:1, 1:5 molar ratios of N2-IO8 to amylin), no fibrils were seen after 48 hrs incubation (Figure 4.4B, 4.4C, 4.4D, 4.4E). N2-IO8 on its own at 100  $\mu$ M failed to aggregate (Figure 4.4F). These results confirm that N2-IO8 is an effective inhibitor of amylin aggregation.

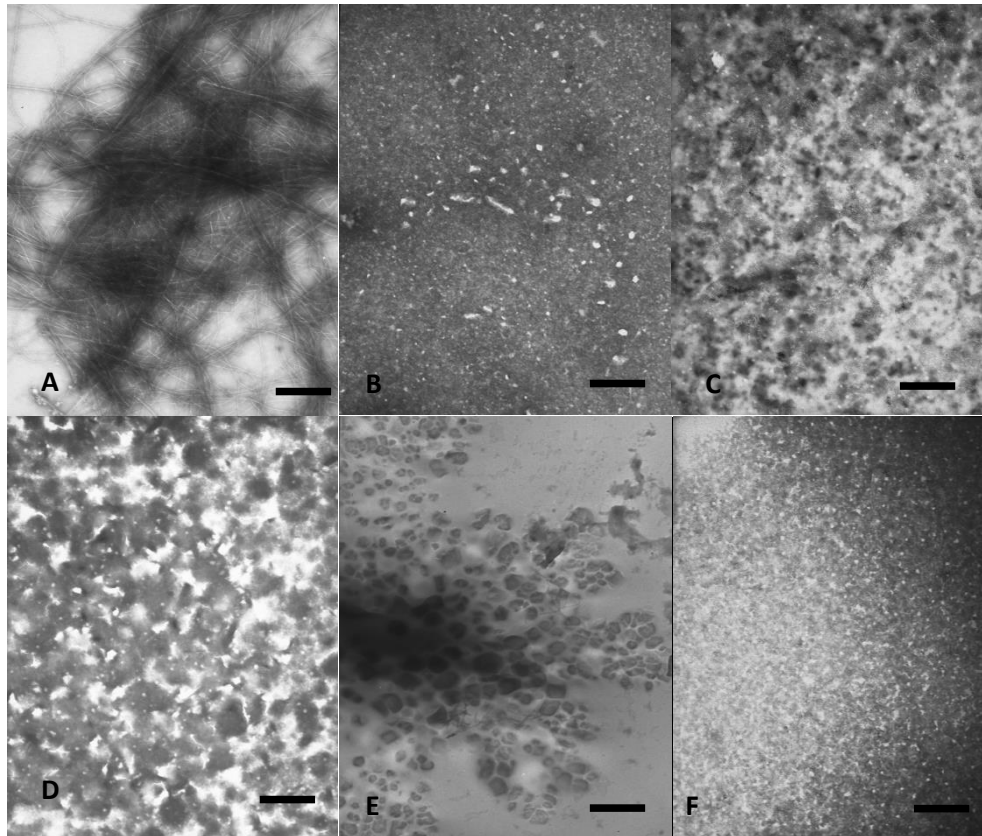


**Figure 4.4:** TEM examination of the effects of N2-IO8 on amylin fibril formation. Samples of 25  $\mu\text{M}$  of amylin in the presence and absence of N2-IO8 at varying concentrations were incubated with continuous shaking for 48 hrs at 37°C in distilled water, negatively stained with phosphotungstic acid (2% w/v) and visualized using TEM. (A) Amylin alone; (B) Amylin + N2-IO8 (100  $\mu\text{M}$ ); (C) Amylin + N2-IO8 (50  $\mu\text{M}$ ); (D) Amylin + N2-IO8 (25  $\mu\text{M}$ ); (E) Amylin + N2-IO8 (5  $\mu\text{M}$ ); (F) N2-IO8 peptide alone (100  $\mu\text{M}$ ). n=3 (3 replicates for each sample) Magnification = X15000. Scale bar = 500 nm.

#### **4.5 Disaggregation of pre-formed amyloid fibrils**

The ability of IO8, RI-IO8, N1-IO8 and N2-IO8 to disaggregate pre-formed amylin amyloid fibrils was then monitored using the TEM. Human amylin was pre-aggregated at 25  $\mu\text{M}$  for 48 hrs and a sample was prepared immediately for TEM after which 100  $\mu\text{M}$  or 50  $\mu\text{M}$  (final concentration) of IO8, RI-IO8, N1-IO8 or N2-IO8 peptides were added to the pre-formed fibrils and incubated for a further 48 hrs with continuous shaking at 37°C and another TEM sample was prepared. The samples were negatively stained with 2% PTA. Figure 4.5.1 to 4.5.4 illustrate the effects of IO8, RI-IO8, N1-IO8 and N2-IO8, respectively, on pre-aggregated amylin. All amylin controls clearly showed the formation of amyloid fibrils, following incubation of 25  $\mu\text{M}$  human amylin for 48 hrs (e.g. Figure 4.5.1A; 4.5.1C). After 48 hrs incubation of fibrils in the presence IO8 at 100  $\mu\text{M}$  or 50  $\mu\text{M}$ , less amylin fibrils fibrils were observed (Figure 4.5.1B; 4.5.1D) compared to the amylin control samples (Figure 4.5.1A; 4.5.1C).

Upon addition of 100  $\mu\text{M}$  or 50  $\mu\text{M}$  RI-IO8 to pre-aggregated amylin, no disaggregation was observed (Figure 4.5.2 B; 4.5.2 D) as compared to the amylin control samples (Figure 4.5.2A; 4.5.2C). In fact, the number of fibrils after 48 hrs post-incubation seemed to be increased after the addition of RI-IO8 (Figure 4.5.2B; Figure 4.5.2D) when compared to the amylin control samples (Figure 4.5.2A; Figure 4.5.2C). The addition of 100  $\mu\text{M}$  of N1-IO8 to pre-aggregated amylin resulted in the disaggregation of pre-formed fibrils (Figure 4.5.3B), as compared to the amylin control samples (Figure 4.5.3A). Also, the addition of 50  $\mu\text{M}$  of N1-IO8 to pre-aggregated amylin resulted in the

disaggregation of pre-formed fibrils (Figure 4.5.3D) leaving a less dense fibril mass when compared to the amylin control samples (Figure 4.5.3C). The addition of N1-IO8 noticeably gave rise to fragmented fibrils with a shorter length. N2-IO8 also showed significant disaggregation of pre-formed amylin fibrils upon incubation of pre-aggregated amylin with 100  $\mu$ M of N2-IO8 (Figure 4.5.4B), as compared to the amylin control samples (Figure 4.5.4A). A similar result was also obtained with 50  $\mu$ M of N2-IO8 (compare Figure 4.5.4D with the control Figure 4.5.4C).

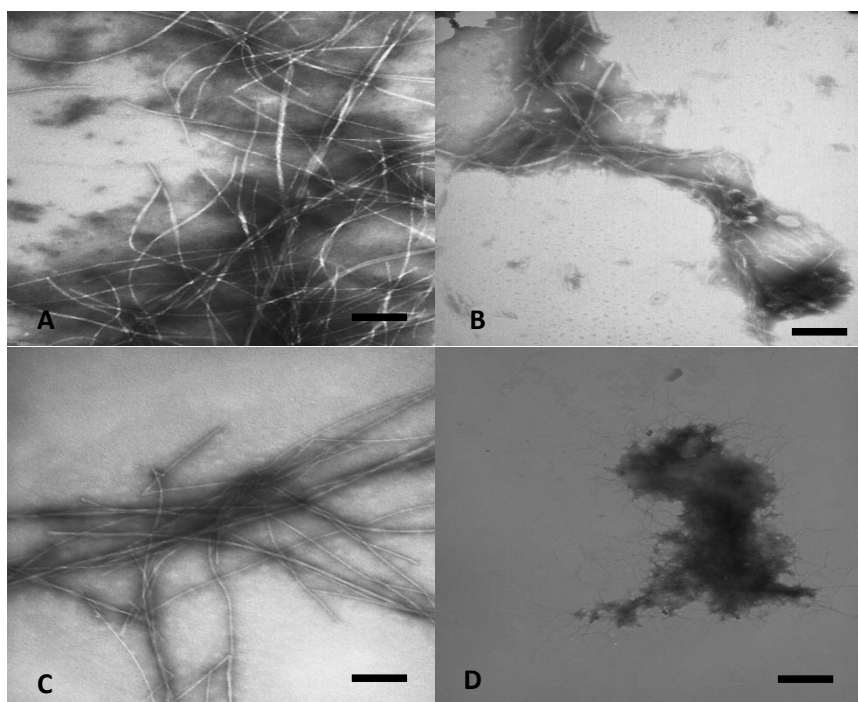


**Figure 4.5.1:** Experiment to monitor possible disaggregation of pre-formed amylin fibrils by IO8. (A) 25  $\mu\text{M}$  amylin incubated for 48 hrs, negatively stained with 2% (w/v) phosphotungstic acid and immediately taken for TEM imaging. (B) 100  $\mu\text{M}$  of IO8 added to the pre-aggregated amylin in “A” and sample incubated for 48 hrs at 37°C before TEM imaging. (C) 25  $\mu\text{M}$  amylin incubated for 48 hrs and immediately taken for TEM imaging (D) 50  $\mu\text{M}$  of IO8 added to the pre-aggregated amylin in “C” and sample incubated for 48hrs at 37 °C before TEM imaging . n=3 (3 replicates for each sample) Magnification = X15000. Scale bar = 500 nm.

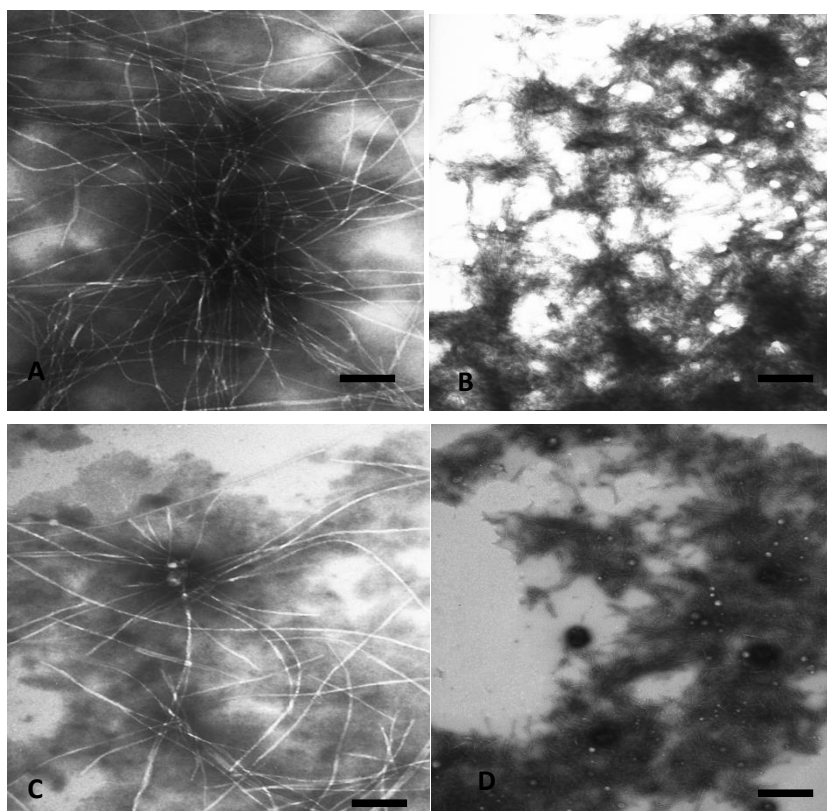


**Figure 4.5.2:** Experiment to monitor possible disaggregation of pre-formed amylin fibrils by RI-IO8. (A) 25  $\mu\text{M}$  amylin incubated for 48 hrs, negatively stained with 2% (w/v) phosphotungstic acid and immediately taken for TEM imaging. (B) 100  $\mu\text{M}$  of RI-IO8 added to the pre-aggregated amylin in “A” and sample incubated for 48 hrs at 37°C before TEM imaging. (C) 25  $\mu\text{M}$  amylin incubated for 48 hrs and immediately taken for TEM imaging (D) 50  $\mu\text{M}$  of RI-IO8 added to the pre-aggregated amylin “C” and sample incubated for 48hrs at 37 °C before TEM imaging . n=3 (3 replicates for each sample) Magnification = X15000. Scale bar = 500 nm.

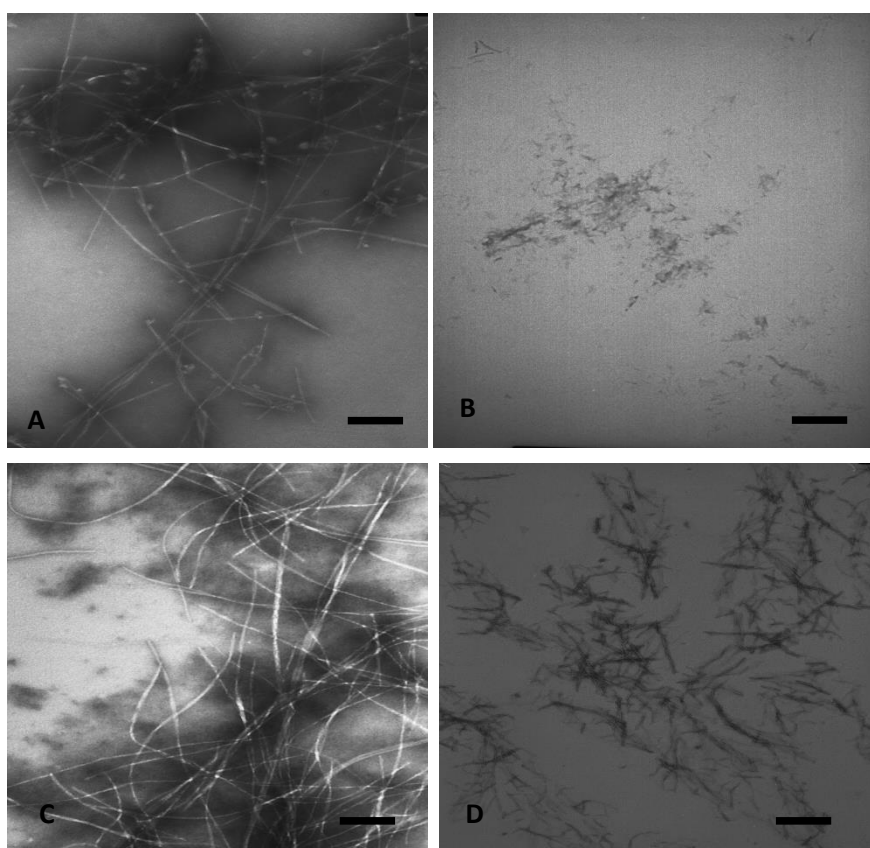


**Figure 4.5.3:** Experiment to monitor possible disaggregation of pre-formed amylin fibrils by N1-IO8. (A) 25  $\mu\text{M}$  amylin incubated for 48 hrs, negatively stained with 2% (w/v) phosphotungstic acid and immediately taken for TEM imaging. (B) 100  $\mu\text{M}$  of N1-IO8 added to the pre-aggregated amylin in “A” and sample incubated for 48hrs at 37  $^{\circ}\text{C}$  before TEM imaging. (C) 25  $\mu\text{M}$  amylin incubated for 48 hrs and immediately taken for TEM imaging (D) 50  $\mu\text{M}$  of N1-IO8 added to the pre-aggregated amylin in “C” and sample incubated for 48hrs at 37  $^{\circ}\text{C}$  before TEM imaging . n=3 (3 replicates for each sample) Magnification = X15000. Scale bar = 500 nm.

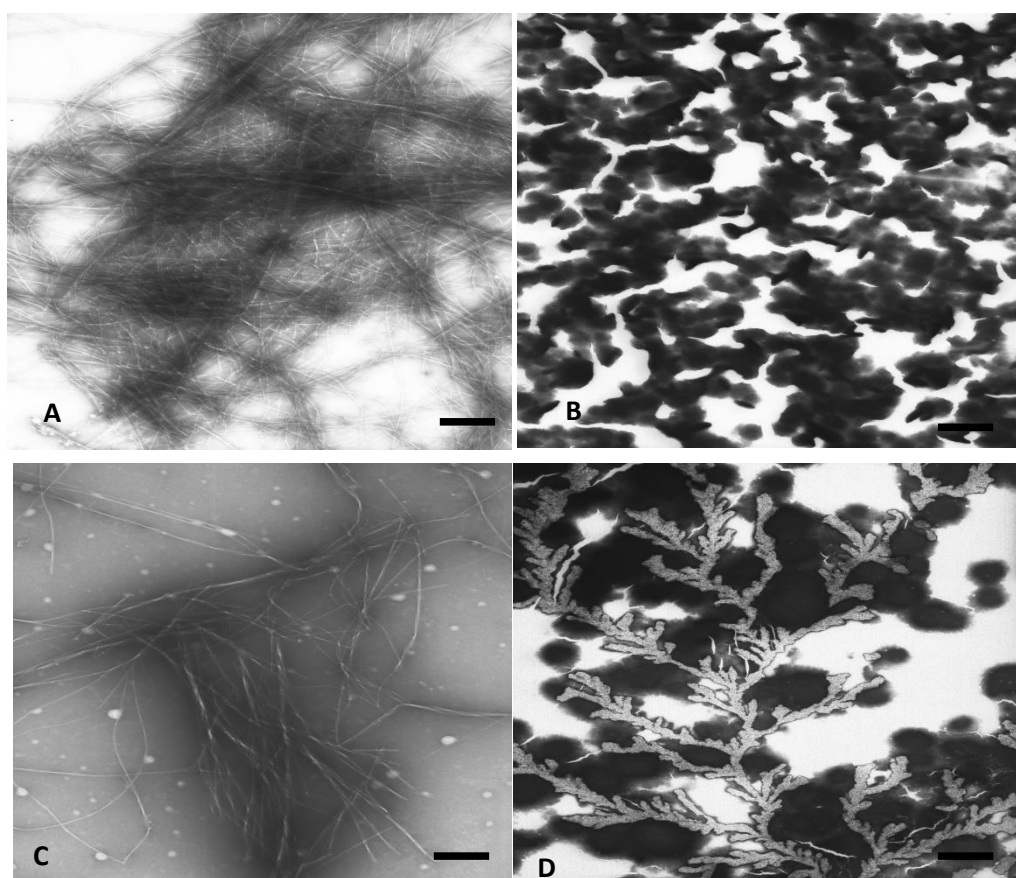


**Figure 4.5.4:** Experiment to monitor possible disaggregation of pre-formed amylin fibrils by N2-IO8 (A) 25  $\mu\text{M}$  amylin incubated for 48 hrs, negatively stained with 2% phosphotungstic acid (w/v) and immediately taken for TEM imaging. (B) 100  $\mu\text{M}$  of N2-IO8 added to the pre-aggregated amylin in “A” and sample incubated for 48 hrs at 37°C before TEM imaging. (C) 25  $\mu\text{M}$  amylin incubated for 48 hrs and immediately taken for TEM imaging (D) 50  $\mu\text{M}$  of N2-IO8 added to the pre-aggregated amylin in “C” and sample incubated for 48hrs at 37 °C before TEM imaging . n=3 (3 replicates for each sample). Magnification = X15000. Scale bar = 500 nm.

## 4.6 Discussion

There have been numerous reports concerning the development of inhibitors of  $\beta$ -amyloid polypeptide ( $A\beta$ ) and prion protein amyloid formation and cytotoxicity (Findeis, 2000; Reixach *et al.*, 2000; Soto *et al.*, 1998). There have, however, been very few reports on inhibitors of amylin amyloid formation. A reason for this could be because amylin is one of the most insoluble and amyloidogenic polypeptides known (Jarrett and Lansbury, 1993). Developing inhibitors of amyloid formation is of therapeutic importance as well as holding potential for understanding the mechanism of amyloid fibril formation. The main objective of this study was to devise a method of impeding the aggregation of amylin into  $\beta$ -sheet oligomers and fibrils. Further to our Th-T and CR experiments, we carried out confirmatory TEM experiments were carried out to examine the ability of the various peptides to influence the aggregation of human amylin. Full-length human amylin assembles into fibrillar structures made up of numerous protofilaments, which are typical of those seen with various forms of amyloid (Serpell *et al.*, 2000), and are characterised by a dense mass of fibrils possessing a mesh-like morphology. The data confirm that IO8, at concentrations of 25, 50 and 100  $\mu$ M, impedes the formation of fibrils derived by incubating amylin at 25  $\mu$ M concentration. At 5  $\mu$ M IO8, thin less compact fibril structures were found. These results are consistent with the Th-T and CR data. Although the Th-T and CR results did not show complete inhibition of fibril formation, TEM analysis revealed an almost complete inhibition of amylin fibril formation by IO8 at 100  $\mu$ M, 50  $\mu$ M and 25  $\mu$ M concentrations. Although IO8 was able to inhibit amylin fibril formation when added to freshly dissolved amylin, it did not completely degrade pre-aggregated amylin fibrils (figure

4.5.1). Inhibiting amylin aggregation has been dependent on using compounds which can bind to amylin (Abedini *et al.*, 2007; Yan *et al.*, 2006; Tatarek-Nossol *et al.*, 2005). The study reported here is consistent with a previous study which showed that two peptides, Ser-Asn-Asn-Phe-Gly-Ala and Gly-Ala-Ile-Leu-Ser-Ser-Thr, moderately inhibit amylin amyloid aggregation at an equimolar ratio with associated protection from amylin cytotoxicity to RIN-1056 cells (Scrocchi *et al.*, 2002). Previous study has also shown the effect of rat amylin as well as mutant forms of rat amylin on human amylin inhibition. Although rat amylin moderately inhibited human amylin aggregation by 85% at a ratio of 10:1 rat amylin to human amylin, the mutant forms of rat amylin were less effective inhibitors (Cao *et al.*, 2010). Even at a molar ratio of 10:1 rat amylin to human amylin, TEM images revealed the presence of fibrils although they were significantly thinner than that observed in the control (Cao *et al.*, 2010). However, the IO8 peptide inhibits amylin aggregation even at low concentrations of the peptide and is thus a considerably better inhibitor than those described above.

On the other hand, the retro-inverso peptide, RI-IO8 had no inhibitory effect on amylin aggregation and in fact increased fibril formation at all concentrations tested. RI-IO8 appeared to enhance amylin aggregation resulting in a denser and more complex amylin fibril mesh (figure 4.2). Although this came as a surprise, previous studies have shown that small peptides can sometimes increase fibril formation, for example the addition of the NFGAIL fragment to amylin greatly enhanced amylin aggregation and fibril formation (Scrocchi *et al.*, 2002). It is likely that the NFGAIL peptide enhances amyloid aggregation because it originates from the amyloidogenic sequence of human amylin and can act as a

seed to promote aggregation, however the mechanism of action by which RI-IO8 enhances amyloid aggregation is currently not known. In addition, RI-IO8 did not degrade already formed fibrils (figure 4.5.2), although a less-defined dense fibril mesh was observed. RI-IO8 on its own did not form any fibrillary structure or aggregates.

The N1-IO8 peptide had a strong effect on  $\beta$  sheet and fibril formation. Incubating 25  $\mu\text{M}$  amylin with either 100  $\mu\text{M}$ , 50  $\mu\text{M}$  or 25  $\mu\text{M}$  of N1-IO8 was sufficient to prevent fibril formation (figure 4.3). However at a concentration of 5  $\mu\text{M}$ , amylin fibril formation was not completely inhibited, although the fibrils present did seem to have an altered morphology with loosely linked ribbon-like structures. This is consistent with a previous study where the peptide fragment AILSST showed inhibitory properties when it was in 5 fold molar excess, but no inhibitory effect at a 1:1 molar ratio (Scrocchi *et al.*, 2002). However, N1-IO8 proved to be the better inhibitor, as it inhibits fibril formation even at a 1:1 molar ratio. N1-IO8 also had a strong effect on  $\beta$  sheet and fibril formation of pre-formed amylin amyloid fibrils. Incubating N1-IO8, at either 100  $\mu\text{M}$  or 50  $\mu\text{M}$  with already formed amylin fibrils was sufficient to degrade pre-formed fibrils (figure 4.5.3). While N1-IO8 could not completely degrade pre-formed fibrils at 50  $\mu\text{M}$ , the aggregates appeared to have an altered morphology and appeared as short thread-like, less compact fibril structures. This suggests that the interaction of human amylin with N1-IO8 peptide altered normal fibril assembly. Furthermore, incubating amylin in the presence of N2-IO8 altered the morphology of the fibrils; no fibril was formed unlike the densely packed fibril clusters observed when amylin was incubated alone (figure 4.4). N2-IO8 also

completely degraded preformed amylin fibrils at both 100 $\mu$ M and 50  $\mu$ M concentrations (figure 4.5.4). N2-IO8 was the only peptide here which completely inhibited amylin fibril formation even at a 1:5 molar ratio of peptide to amylin. These results are consistent with a previous study which showed that incubating amylin in the presence of GAILSS or SNNFGA peptide fragments significantly decreased the density of amylin fibrils formed, but did not completely inhibit the formation of fibrils. This reduced effect was also only observed when the peptides were in 10- or 20- fold excess of amylin (Scrocchi *et al.*, 2002). Double N-methylated peptides derived from the partial human amylin amyloidogenic sequence SNNFGAILSS, including F(N-Me)GA(N-Me)IL, NF(N-Me)GA(N-Me)IL, SNNF(N-Me)GA(N-Me)IL, and SNNF(N-Me)GA(N-Me)ILSS were the first reported to inhibit the short partial human amylin amyloidogenic sequence SNNFGAILSS. Contrary to the parent peptide sequence, the N-methylated derivatives were very soluble and did not aggregate into amyloid fibrils. This suggests that strategies like N-methylation are capable of changing the amyloidogenic amylin into a non-amyloidogenic state. More work is, however, required to study the binding affinity of the peptides reported here to amylin. To completely disaggregate amylin fibrils, these peptides would have to bind to amylin at very high affinity to break the hydrogen bonding between amylin monomers.

Although studies have shown that amyloid deposition is linked with decreased  $\beta$ -cell mass (Clark *et al.*, 1988; Westermark and Grimelius, 1973), controversies have arisen as to whether amylin is a cause or consequence of  $\beta$ -cell dysfunction/hyperglycemia in T2DM as amylin deposits have also been found in

non-diabetic individuals (Bell, 1959; Westermark, 1976). However, it is likely that amylin does play a key role in the  $\beta$ -cell dysfunction/apoptosis seen in T2DM, as previous studies have clearly shown an association between amylin and T2DM. Although the reduction in  $\beta$ -cell mass is not sufficient to explain the defects in insulin dysfunction found in T2DM, it is still likely that these cell functions will be altered, since previous study has shown the presence of amyloid fibrils within cells (Cooper *et al.*, 1987) and these have been shown to be cytotoxic. Amylin is synthesized (in vivo) in the pancreatic  $\beta$  cells and secreted from the secretory granules in soluble form (Serpell *et al.*, 2000). However, certain environmental circumstances such as amylin concentration, pH and molecular binding could alter the conformation of amylin from a random coil to a  $\beta$ -sheet, which stimulates amyloid fibril formation (Janson *et al.*, 1999; Kaye *et al.*, 1999; Hoopener *et al.*, 1999). Studies have suggested that a build-up of insoluble amylin fibrils plays a key role in  $\beta$  cell failure in T2DM (Janciauskiene *et al.*, 1997; de Koning *et al.*, 1993). This is supported by a previous studies which has shown that non-clearance of amylin after secretion as well as a partial pro-amylin processing (Clodi *et al.*, 1998) in patients with T2DM could promote increased fibrillogenesis and aggregation (Park and Verchere, 2001; Higham *et al.*, 2000). It could be thought that IO8, N1-IO8 and N2-IO8 are capable of keeping amylin in soluble form for an extended period of time, and thus impair fibril aggregate formation typical of insoluble amylin. The sudden increase in fibril formation observed when amylin was incubated with RI-IO8 proves the ability of some peptides to increase fibrillogenesis. The results displayed in this present study confirm that peptide sequences found within the human amylin molecule impede  $\beta$  sheet formation and fibrillary

assembly. The data presented here demonstrate that IO8, N1-IO8 and N2-IO8 inhibit amyloid formation by human amylin in a dose-dependent manner and alter the morphology of the fibrils formed. These peptides suggest a potential therapeutic approach for treating already formed amyloid deposition in patients with T2DM.

#### **4.7 Conclusion**

This study investigated the inhibitory effects of IO8, RI-IO8, N1-IO8 and N2-IO8 on in vitro human amylin fibrillogenesis via TEM experiments. The findings demonstrate that IO8, N1-IO8 and N2-IO8 impede amylin amyloid formation and aggregation in a concentration-dependent manner. On the other hand, RI-IO8 enhanced amylin fibril formation. Further investigation on the exact mechanism of action of amylin-inhibitor interactions is required. However the results from this study will promote our understanding of the mechanisms of amyloid self-assembly and design of potential targets for therapeutics designed to prevent amyloid formation associated with T2DM.

## Chapter 5

### Peptide Stability Studies

Peptide stability is an important consideration when developing peptide-based molecules as potential drug candidates. Reversed-Phase High-Performance Liquid Chromatography (RP-HPLC) is an especially important approach for peptide and protein analysis because chromatographs can be tailored to specific requirements via changes in mobile phase attributes. Also, RP-HPLC possesses high resolution for both similar and dissimilar molecules, attained through its variety of chromatographic conditions. In addition, RP-HPLC produces high quality repetitive separations as well as high recoveries (Aguilar and Hearn, 1996; Mant and Hodges, 1996). RP-HPLC can, however, result in irreversible denaturing of protein samples, thus the chances of recovering biologically active materials is greatly diminished, although this is not a consideration in the present study. The presence of eluted peptides or proteins is most often detected by absorbance of ultraviolet (UV) light (typically at 210–220nm) which is strongly absorbed by peptide bonds. Some amino acid residues, however, absorb light at a different wavelength, for example, the aromatic residues phenylalanine, tyrosine and tryptophan absorb UV light between 250–290 nm.

RP-HPLC is the main mode of HPLC used for separating peptides because it is typically more excellent in efficiency and speed compared to other HPLC modes (Richards *et al.*, 1994; Oroszlan *et al.* 1992; Unger, 1990; Henry, 1991; Zhou and Hathaway, 2003; Rusnak and Hathaway, 2002; Masaki *et al.*, 1994). In this study, RP-HPLC was used to assess the stability of peptides in plasma, and after

incubation with various proteolytic enzymes. The chromatographic performance of peptides is impacted by the presence of different counter ions, and the pH value will also affect peptide charge. Anionic counter-ions such as trifluoroacetic acid (TFA) will combine with the positively charged residues of the peptide, while cationic counter-ions, such as triethylammonium, have a tendency to combine with negatively charged residues of the peptide. The solvents employed here all contained 0.01% TFA, which is a commonly used condition for RP-HPLC peptide separations. The resolution of the peptides was optimized by using an appropriate gradient of increasing concentrations of the organic solvent acetonitrile.

Previous chapters have elucidated the effects of RI-IO8 on amylin aggregation; this retro-inverso peptide was designed for the purpose of protecting it from proteolytic degradation. Although RI-IO8 showed no inhibitory effect on amylin aggregation, its stability was examined in order to verify the effect of retro-inversion on the susceptibility of this peptide to proteolytic enzyme attack. The stability of RI-IO8 was assessed in the presence of different proteolytic enzymes, including chymotrypsin and trypsin. RP-HPLC chromatographs (see Appendix A) show that RI-IO8 was stable for at least 24 hrs in human plasma, and in the presence of these proteolytic enzymes. RP-HPLC was also used to examine the stability of HIO8 peptide, derived by substitution of the N-terminal and C-terminal arginines of IO8 with homoarginine. As elucidated in Chapter 3, HIO8 was designed by replacing these arginine residues in IO8 (**N<sub>2</sub>H-RGANFLVHGR-NH<sub>2</sub>**) with homoarginine (**N<sub>2</sub>H-Har-GANFLVHG-Har-NH<sub>2</sub>**) to protect the peptide from trypsin digestion. Chromatographs of HIO8 (see Appendix A) show that HIO8 is indeed stable to proteolytic degradation by

trypsin, but is, however, degraded by other proteases, in particular chymotrypsin. Due to this instability, it is not suitable for therapeutic purposes. On the other hand, although RI-IO8 is stable towards proteases, it is also unsuitable as an amyloid therapeutic, as it appeared to actually stimulate amylin aggregation.

This Chapter is mainly aimed at assessing the stability of the most promising inhibitory peptides (IO8, N1-IO8 and N2-IO8) towards proteases, and in plasma. The peptides were incubated with each proteolytic enzyme and with plasma at 37°C at varying time points, as described in the Methods section (2.3.4), and run on an analytical RP-HPLC system.

### **5.1 The stability of IO8 in the presence of proteolytic enzymes.**

The stability of IO8 peptide was assessed in the presence of various proteolytic enzymes, namely chymotrypsin, cathepsin G, trypsin, elastase, thrombin, kallikrein, plasmin and factor X. IO8 peptide (100  $\mu$ l of 100  $\mu$ M) was incubated at 37°C with 1  $\mu$ l of a 1 mg/ml solution of each enzyme at varying time points of 0 hr, 1 hr and 3 hrs. The stability of IO8 was examined by injecting 100  $\mu$ l of this peptide solution onto a RP-HPLC system (Dionex GP50 Gradient pump, C18 column), followed by elution with a linear gradient of 0–60% acetonitrile containing 0.01% TFA over 40 min, at a flow rate of 1 mL/min. IO8, as detected by a peak corresponding to intact peptide, was found to be degraded in the presence of trypsin and chymotrypsin, as compared to the standard IO8 alone, even after an incubation time with enzyme of zero. No new peaks were seen in the chromatograms of degraded samples of IO8 (figure 5.1.1 – figure 5.1.8). Cathepsin G, elastase, thrombin, kallikrein, plasmin, and factor X, also degraded IO8, but not to the same extent as trypsin and chymotrypsin. Thus, IO8 was unstable in the presence of proteolytic enzymes. Appendix A shows RP-HPLC chromatographs of these latter results.

<b>Protease</b>	<b>IO8</b>
None	√
Chymotrypsin	X
Cathepsin G	X
Trypsin	X
Elastase	X
Thrombin	X
Kallikrein	X
Plasmin	√
Factor X	√

Table 5.1: Susceptibility of IO8 to individual proteases. √ = Stable ; X = Degraded

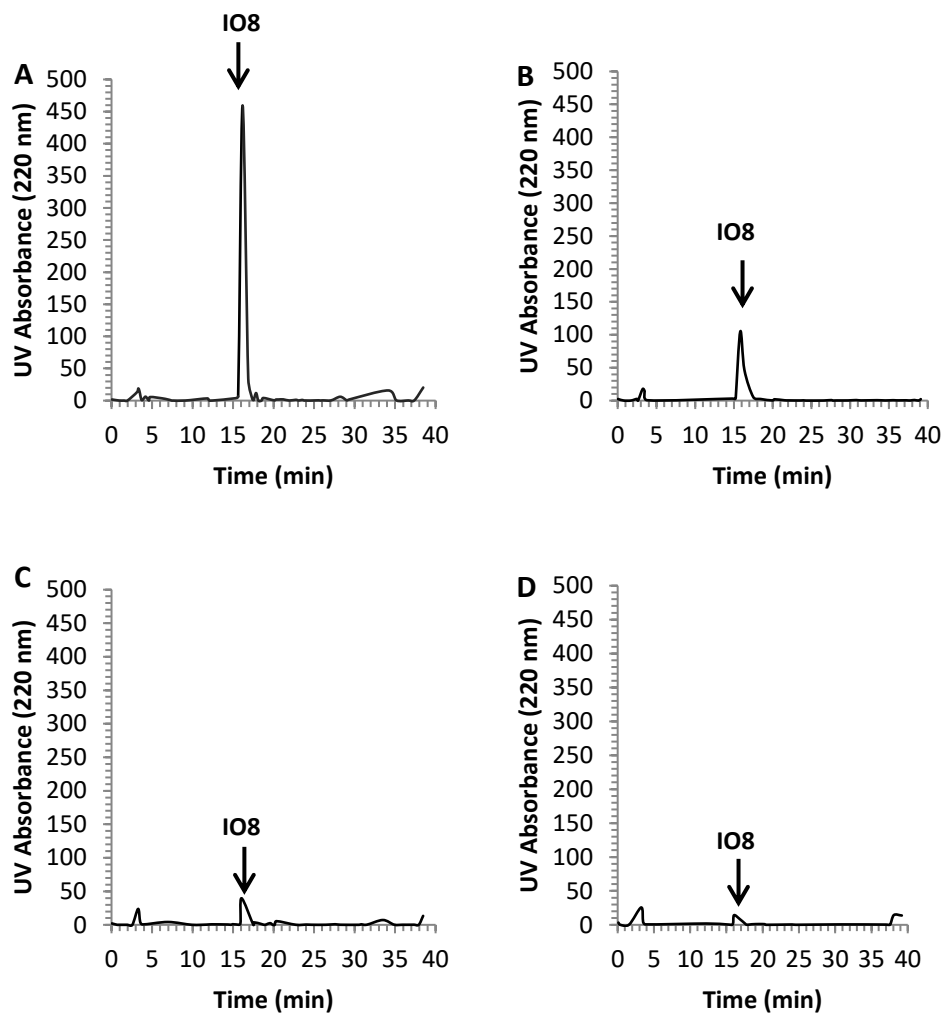


**Figure 5.1.1:** RP-HPLC profile of 100  $\mu$ M IO8 and effects of proteolysis by trypsin. (A) RP-HPLC chromatographs of IO8 in the absence of proteolytic enzymes. RP-HPLC chromatographs of IO8 after incubation with trypsin (B) for 0 hr, (C) for 1 hr, (D) for 3 hrs. Peptides were eluted with a linear gradient of 0–60% acetonitrile containing 0.01% TFA over 40 min, at a flow rate of 1 mL/min. Graphs show absorbance at 220 nm and elution time in mins.

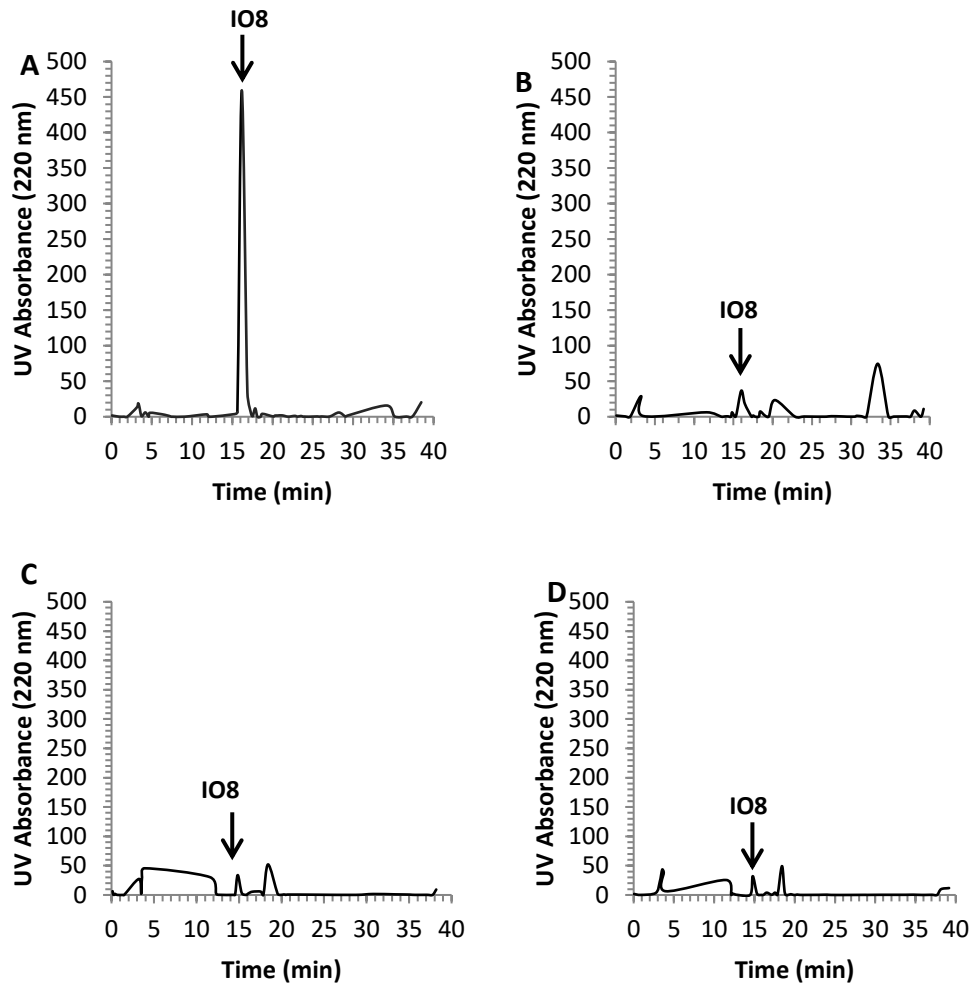


**Figure 5.1.2:** RP-HPLC profile of 100  $\mu$ M IO8 and effects of proteolysis by chymotrypsin. (A) RP-HPLC chromatographs of IO8 in the absence of proteolytic enzymes. RP-HPLC chromatographs of IO8 after incubation with chymotrypsin (B) for 0 hr, (C) for 1 hr, (D) for 3 hrs. Peptides were eluted with a linear gradient of 0–60% acetonitrile containing 0.01% TFA over 40 min, at a flow rate of 1 mL/min. Graphs show absorbance at 220 nm and elution time in mins.

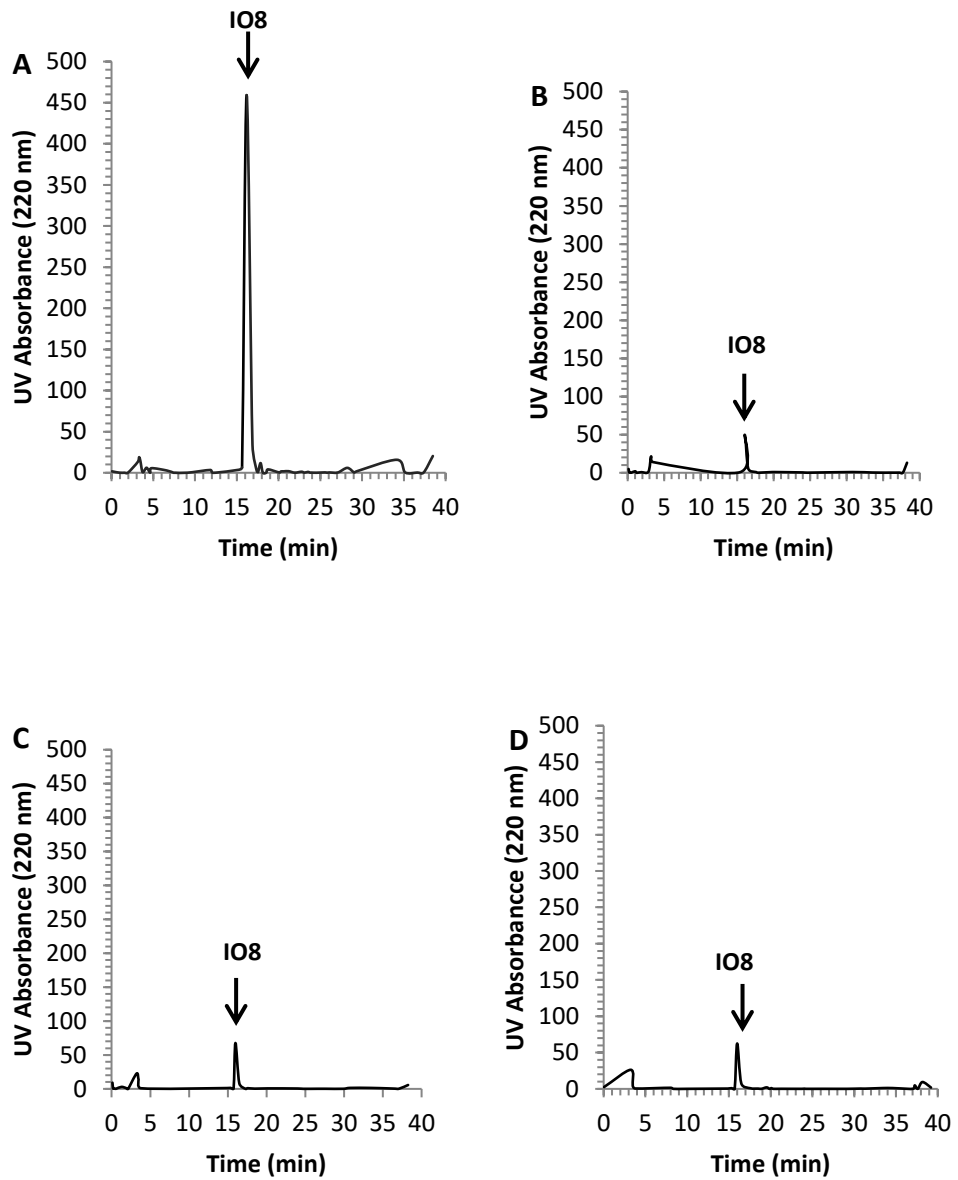


**Figure 5.1.3:** RP-HPLC profile of 100  $\mu$ M IO8 and effects of proteolysis by cathepsin G. (A) RP-HPLC chromatographs of IO8 in the absence of proteolytic enzymes. RP-HPLC chromatographs of IO8 after incubation with cathepsin G (B) for 0 hr, (C) for 1 hr, (D) for 3 hrs. Peptides were eluted with a linear gradient of 0–60% acetonitrile containing 0.01% TFA over 40 min, at a flow rate of 1 mL/min. Graphs show absorbance at 220 nm and elution time in mins.

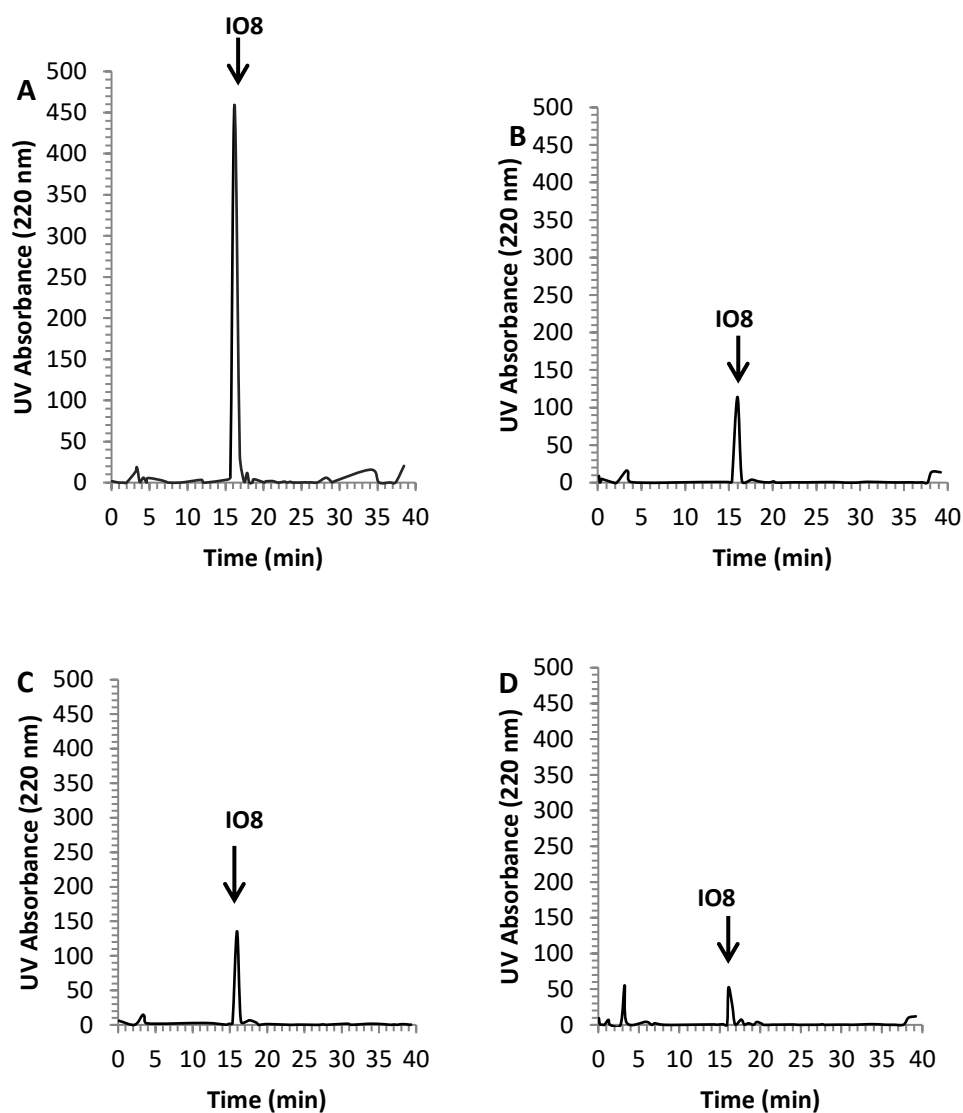


**Figure 5.1.4:** RP-HPLC profile of 100  $\mu\text{M}$  IO8 and effects of proteolysis by Elastase. (A) RP-HPLC chromatographs of IO8 in the absence of proteolytic enzymes. RP-HPLC chromatographs of IO8 after incubation with Elastase (B) for 0 hr, (C) for 1 hr, (D) for 3 hrs. Peptides were eluted with a linear gradient from 0–60% acetonitrile containing 0.01% TFA over 40 min, at a flow rate of 1 mL/min. Graphs show absorbance at 220 nm and elution time in mins.

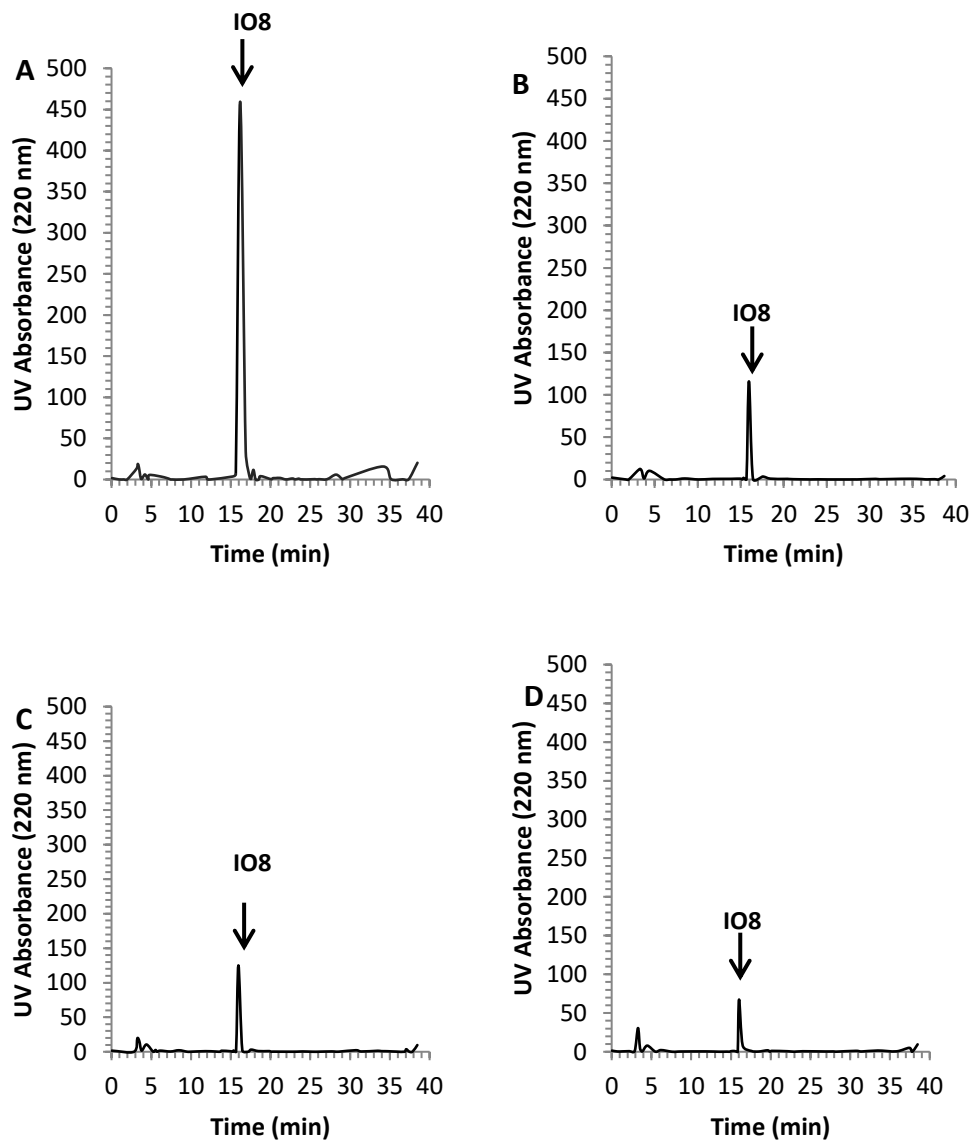


**Figure 5.1.5:** RP-HPLC profile of 100  $\mu$ M IO8 and effects of proteolysis by Thrombin. (A) RP-HPLC chromatographs of IO8 in the absence of proteolytic enzymes. RP-HPLC chromatographs of IO8 after incubation with Thrombin (B) for 0 hr, (C) for 1 hr, (D) for 3 hrs. Peptides were eluted with a linear gradient from 0–60% acetonitrile containing 0.01% TFA over 40 min, at a flow rate of 1 mL/min. Graphs show absorbance at 220 nm and elution time in mins.

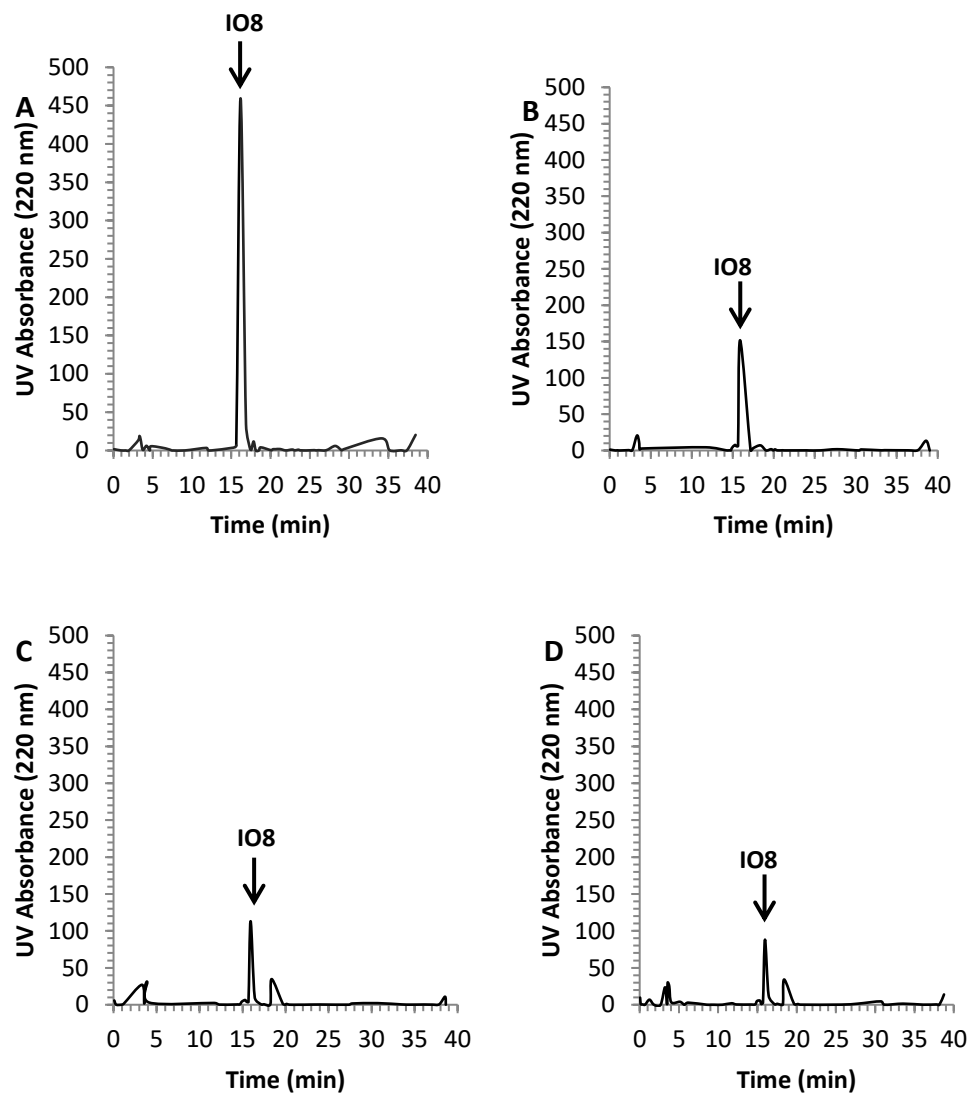


**Figure 5.1.6:** RP-HPLC profile of 100  $\mu$ M IO8 and effects of proteolysis by Kallikrein. (A) RP-HPLC chromatographs of IO8 in the absence of proteolytic enzymes. RP-HPLC chromatographs of IO8 after incubation with Kallikrein (B) for 0 hr, (C) for 1 hr, (D) for 3 hrs. Peptides were eluted with a linear gradient of 0–60% acetonitrile containing 0.01% TFA over 40 min, at a flow rate of 1 mL/min. Graphs show absorbance at 220 nm and elution time in mins.

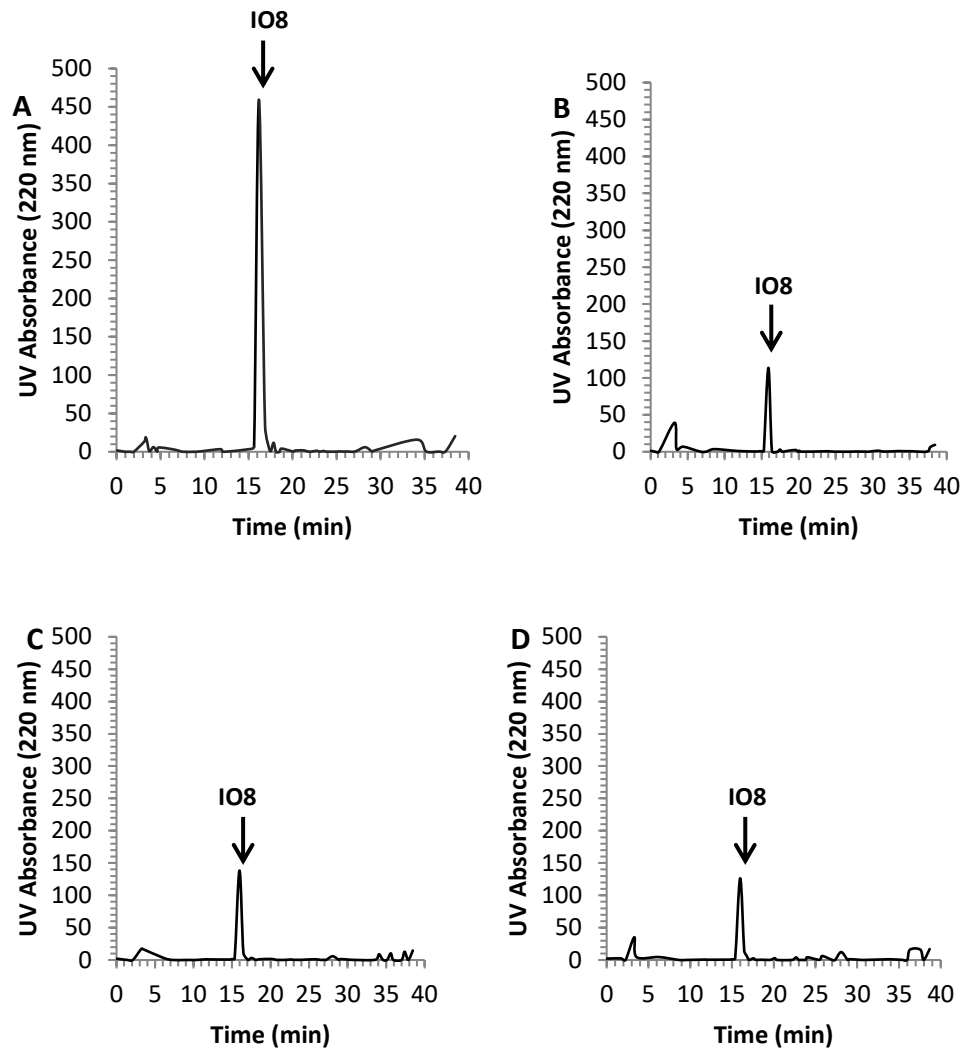


**Figure 5.1.7:** RP-HPLC profile of 100  $\mu$ M IO8 and effects of proteolysis by Plasmin. (A) RP-HPLC chromatographs of IO8 in the absence of proteolytic enzymes. RP-HPLC chromatographs of IO8 after incubation with Plasmin (B) for 0 hr, (C) for 1 hr, (D) for 3 hrs. Peptides were eluted with a linear gradient of 0–60% acetonitrile containing 0.01% TFA over 40 min, at a flow rate of 1 mL/min. Graphs show absorbance at 220 nm and elution time in mins.

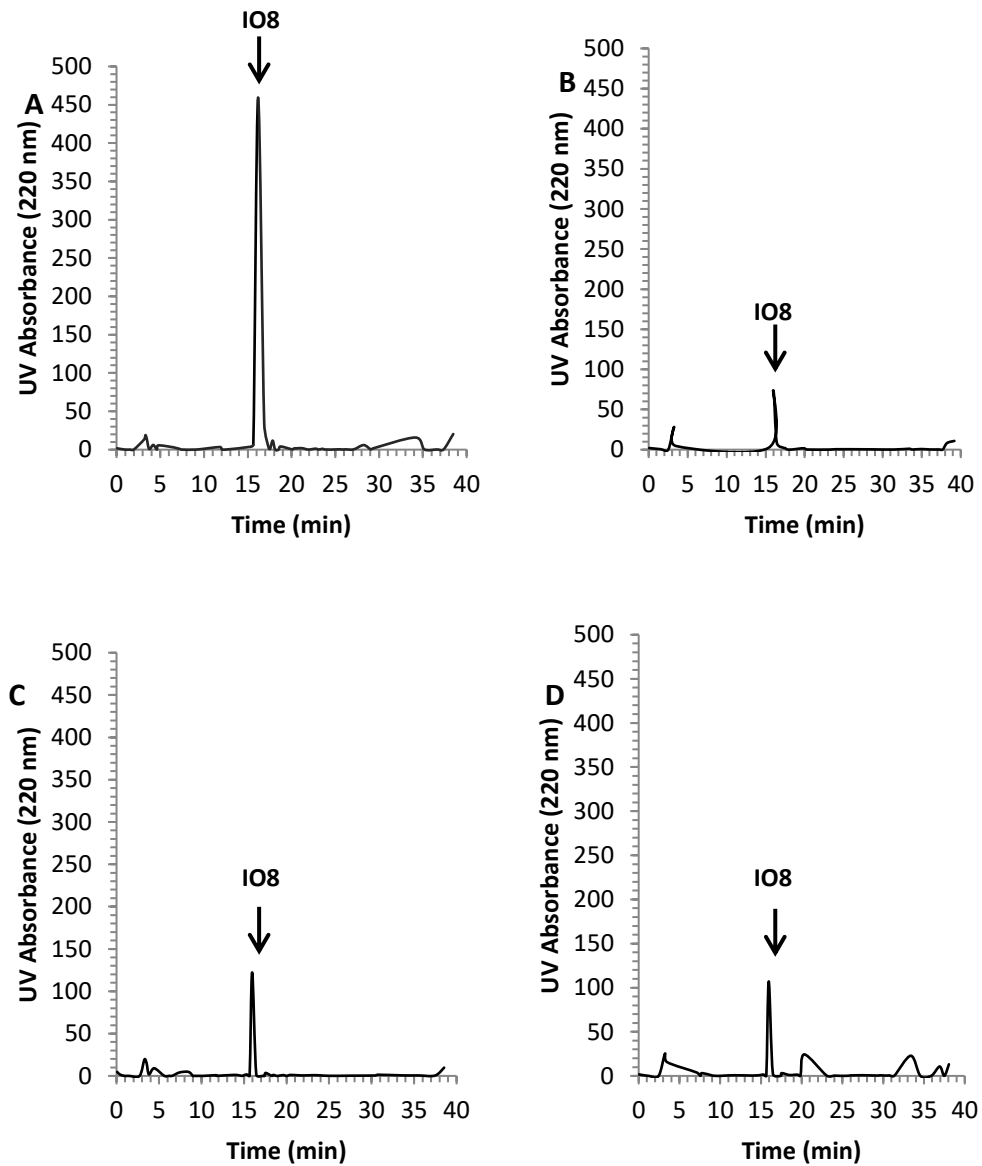


**Figure 5.1.8:** RP-HPLC profile of 100  $\mu$ M IO8 and effects of proteolysis by Factor X. (A) RP-HPLC chromatographs of IO8 in the absence of proteolytic enzymes. RP-HPLC chromatographs of IO8 after incubation with Factor X (B) for 0 hr, (C) for 1 hr, (D) for 3 hrs. Peptides were eluted with a linear gradient of 0–60% acetonitrile containing 0.01% TFA over 40 min, at a flow rate of 1 mL/min. Graphs show absorbance at 220 nm and elution time in mins.

## **5.2 The stability of N1-IO8 in the presence of proteolytic enzymes.**

N1-IO8 was N-methylated at alternate amino acid residues, with the aim of protecting it from proteolytic degradation. The positive inhibitory effects of N1-IO8 on amylin aggregation have been presented previously and here its stability to proteolytic degradation was determined, in the presence of various proteolytic enzymes, namely chymotrypsin, cathepsin G, trypsin, elastase, thrombin, kallikrein, plasmin and factor X. The N1-IO8 peptide was incubated with each enzyme, at varying time points, and examined by RP-HPLC, as before. In the presence of trypsin and chymotrypsin, no apparent degradation of N1-IO8 was observed at up to 3 hrs incubation (figure 5.2.1 B-D; figure 5.2.2 B-D). However, after 24 hrs of incubation, the chromatographic peak area of N1-IO8 was slightly decreased (figure 5.2.1 E; figure 5.2.2 E). Thus, N1-IO8 was considerably more stable than IO8 to the effects of these proteolytic enzymes. Also, cathepsin G, elastase, thrombin, kallikrein, plasmin and factor X had no effect on the chromatographic peak of N1-IO8 (figure 5.2.3-figure 5.2.8), suggesting that these proteolytic enzymes had no effect on N1-IO8. Appendix A shows RP-HPLC chromatographs of these results.

<b>Protease</b>	<b>N1-IO8</b>
None	√
Chymotrypsin	√
Cathepsin G	√
Trypsin	√
Elastase	√
Thrombin	√
Kallikrein	√
Plasmin	√
Factor X	√

Table 5.2: N1- IO8 susceptibility to individual proteases. √ = Stable ; X = Degraded

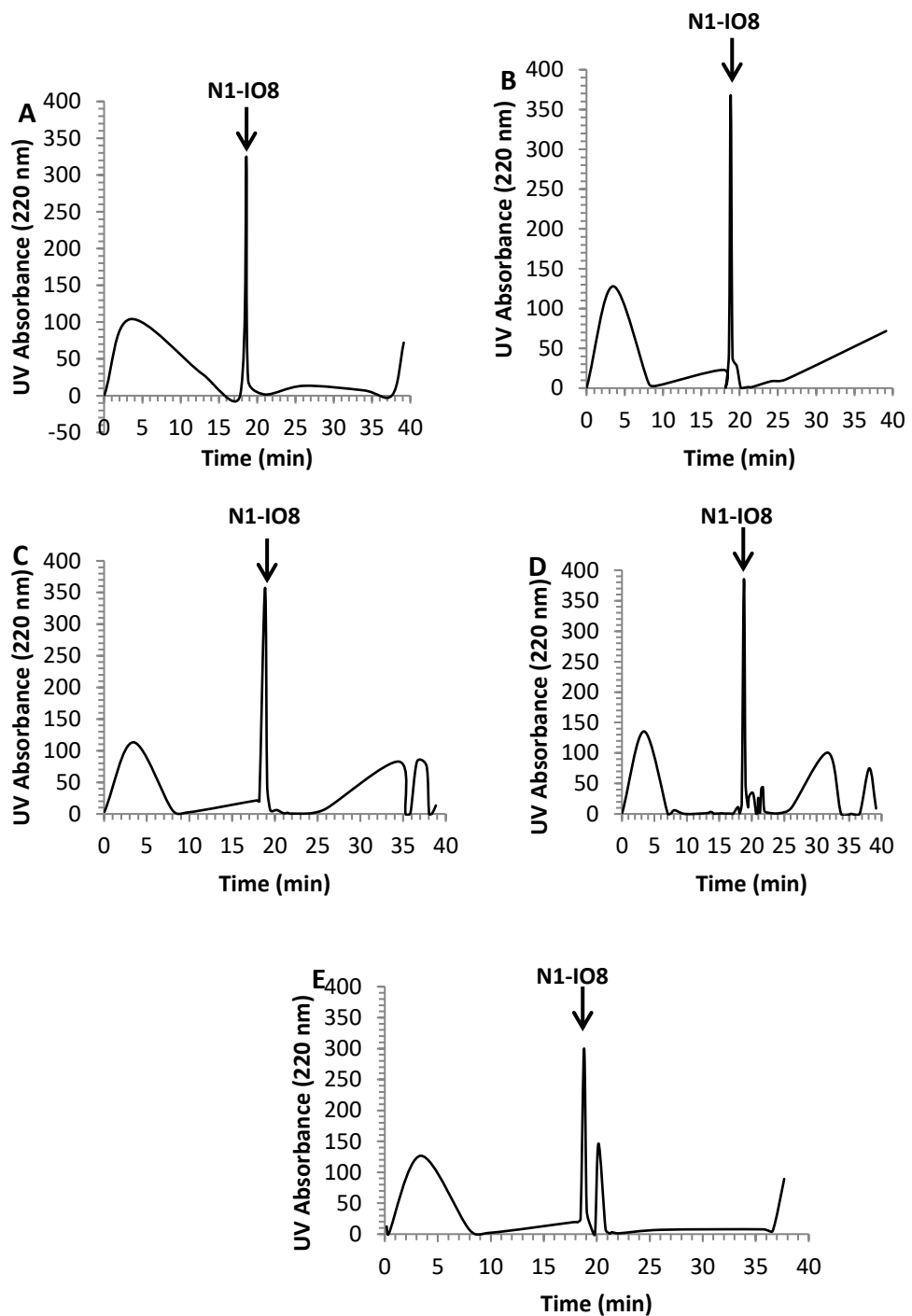


**Figure 5.2.1:** RP-HPLC profile of 100  $\mu$ M N1-IO8 and effects of proteolysis by Trypsin. (A) RP-HPLC chromatographs of N1-IO8 in the absence of proteolytic enzymes. RP-HPLC chromatographs of N1-IO8 after incubation with Trypsin (B) for 0 hr, (C) for 1 hr, (D) for 3 hrs, (E) for 24 hrs. Peptides were eluted with a linear gradient of 0–60% acetonitrile containing 0.01% TFA over 40 min, at a flow rate of 1 mL/min. Graphs show absorbance at 220 nm and elution time in mins.

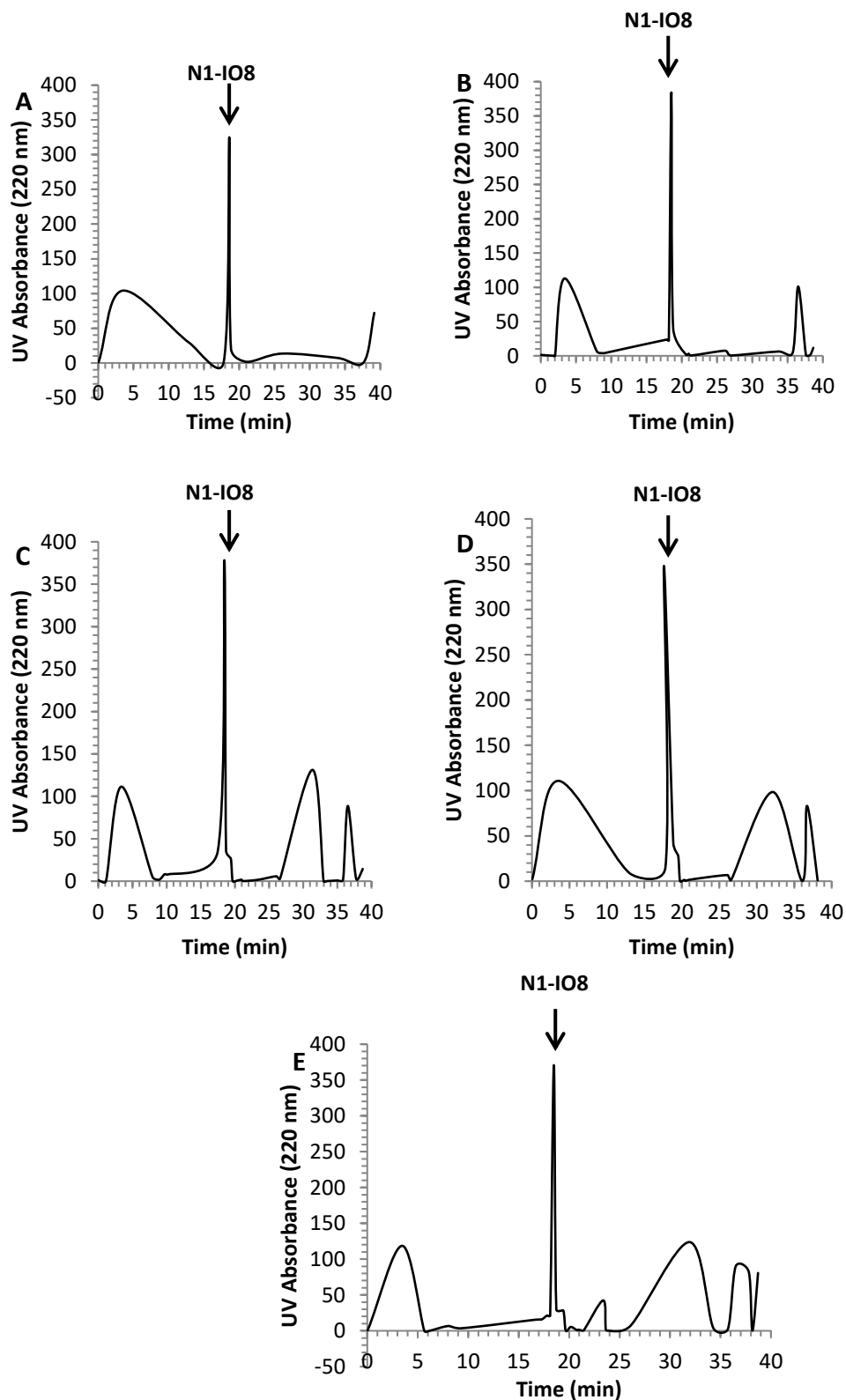


**Figure 5.2.2:** RP-HPLC profile of 100  $\mu$ M N1-IO8 and effects of proteolysis by Chymotrypsin. (A) RP-HPLC chromatographs of N1-IO8 in the absence of proteolytic enzymes. RP-HPLC chromatographs of N1-IO8 after incubation with Chymotrypsin (B) for 0 hr, (C) for 1 hr, (D) for 3 hrs (E) for 24 hrs. Peptides were eluted with a linear gradient of 0–60% acetonitrile containing 0.01% TFA over 40 min, at a flow rate of 1 mL/min, 28 °C. Graphs show absorbance at 220 nm and elution time in mins.

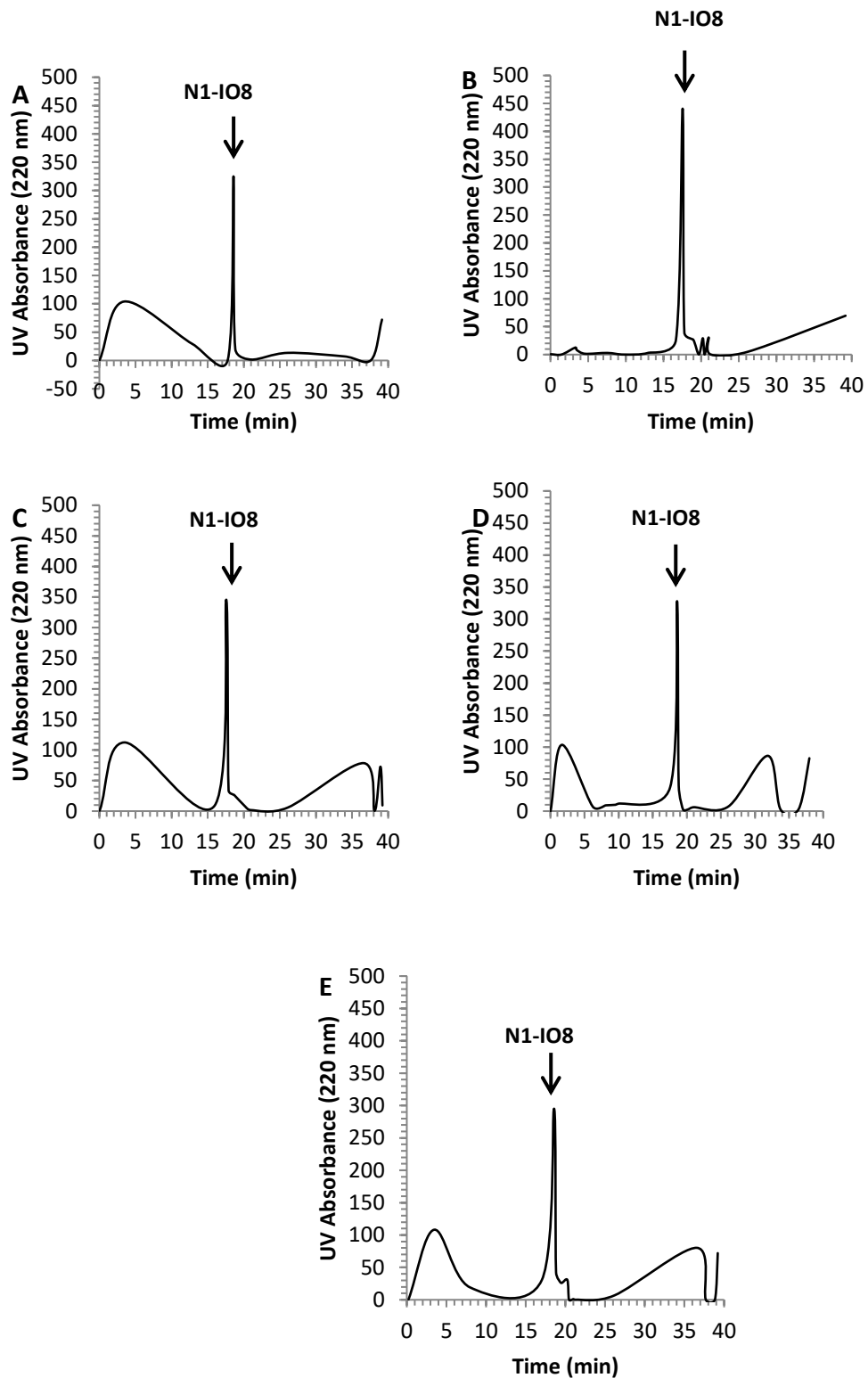


**Figure 5.2.3:** RP-HPLC profile of 100  $\mu\text{M}$  N1-IO8 and effects of proteolysis by Cathepsin G. (A) RP-HPLC chromatographs of N1-IO8 in the absence of proteolytic enzymes. RP-HPLC chromatographs of N1-IO8 after incubation with Cathepsin G (B) for 0 hr, (C) for 1 hr, (D) for 3 hrs, (E) for 24 hrs. Peptides were eluted with a linear gradient of 0–60% acetonitrile containing 0.01% TFA over 40 min, at a flow rate of 1 mL/min. Graphs show absorbance at 220 nm and elution time in mins.

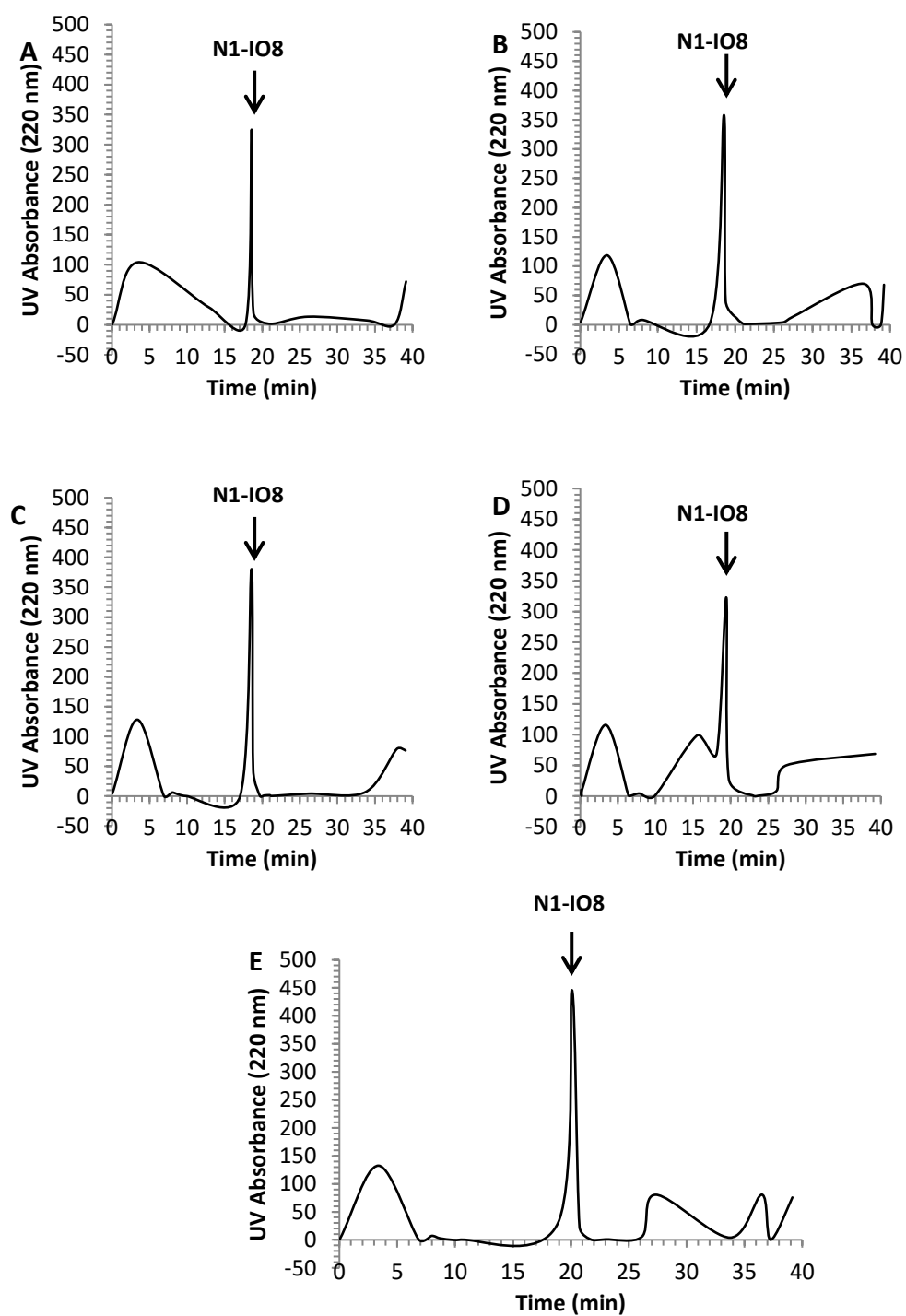


**Figure 5.2.4:** RP-HPLC profile of 100  $\mu$ M N1-IO8 and effects of proteolysis by Elastase. (A) RP-HPLC chromatographs of N1-IO8 in the absence of proteolytic enzymes. RP-HPLC chromatographs of N1-IO8 after incubation with Elastase (B) for 0 hr, (C) for 1 hr, (D) for 3 hrs, (E) for 24 hrs. Peptides were eluted with a linear gradient of 0–60% acetonitrile containing 0.01% TFA over 40 min, at a flow rate of 1 mL/min. Graphs show absorbance at 220 nm and elution time in mins.

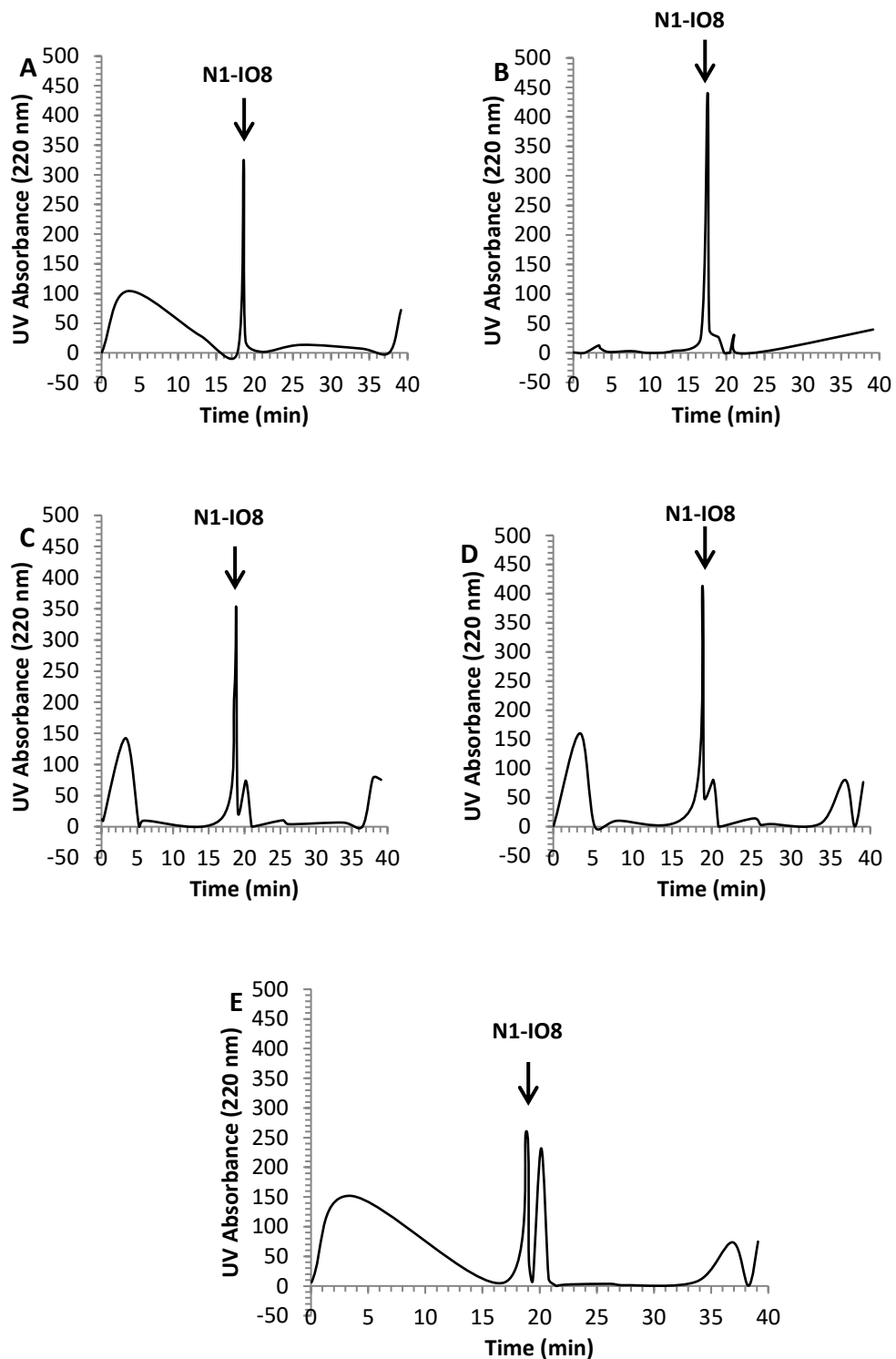


**Figure 5.2.5:** RP-HPLC profile of 100 μM N1-IO8 and effects of proteolysis by Thrombin. (A) RP-HPLC chromatographs of N1-IO8 in the absence of proteolytic enzymes. RP-HPLC chromatographs of N1-IO8 after incubation with Thrombin (B) for 0 hr, (C) for 1 hr, (D) for 3 hrs, (E) for 24 hrs. Peptides were eluted with a linear gradient of 0–60% acetonitrile containing 0.01% TFA over 40 min, at a flow rate of 1 mL/min. Graphs show absorbance at 220 nm and elution time in mins.

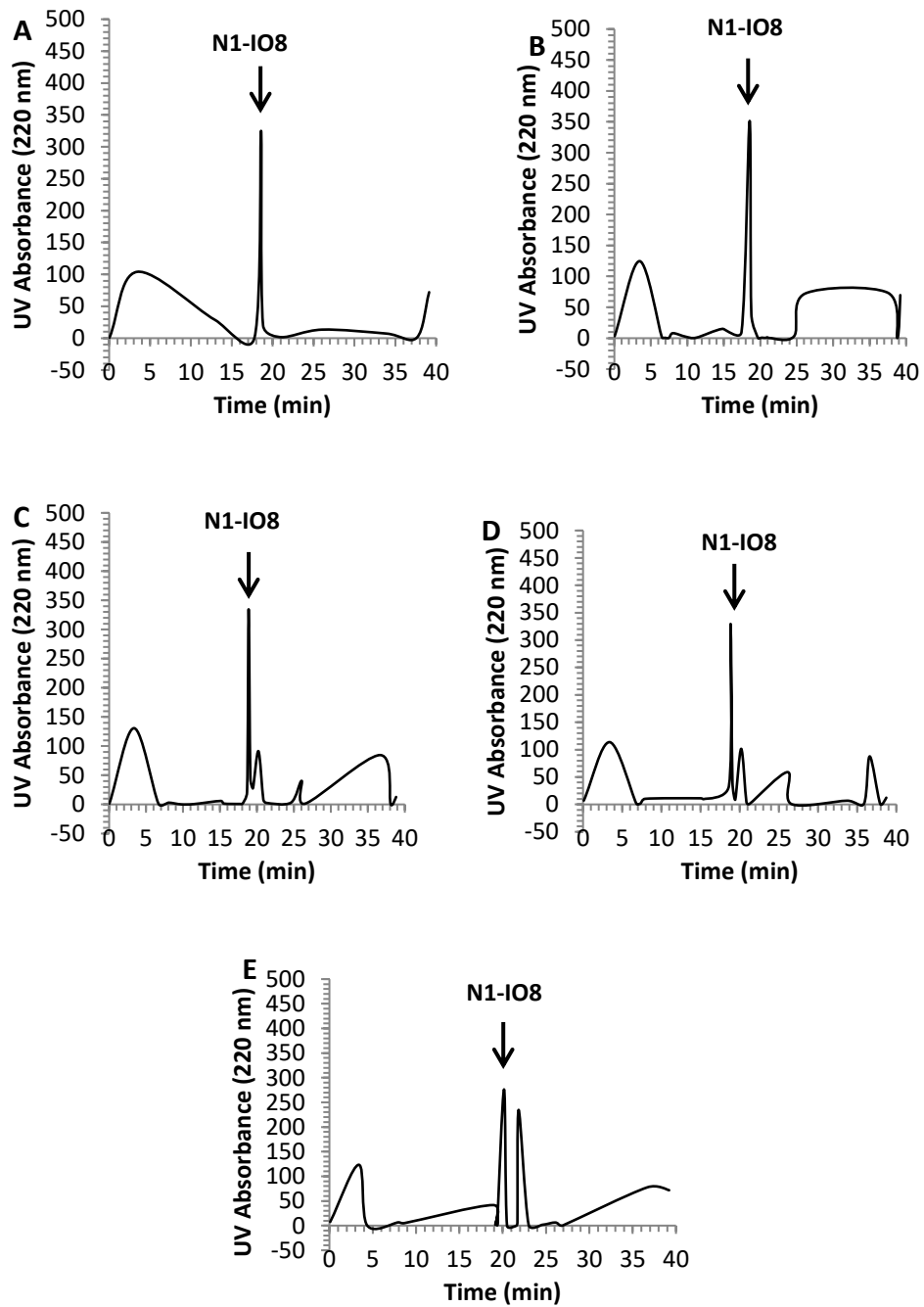


**Figure 5.2.6:** RP-HPLC profile of 100  $\mu$ M N1-IO8 and effects of proteolysis by Kallikrein. (A) RP-HPLC chromatographs of N1-IO8 in the absence of proteolytic enzymes. RP-HPLC chromatographs of N1-IO8 after incubation with Kallikrein (B) for 0 hr, (C) for 1 hr, (D) for 3 hrs, (E) for 24 hrs. Peptides were eluted with a linear gradient of 0–60% acetonitrile containing 0.01% TFA over 40 min, at a flow rate of 1 mL/min. Graphs show absorbance at 220 nm and elution time in mins.

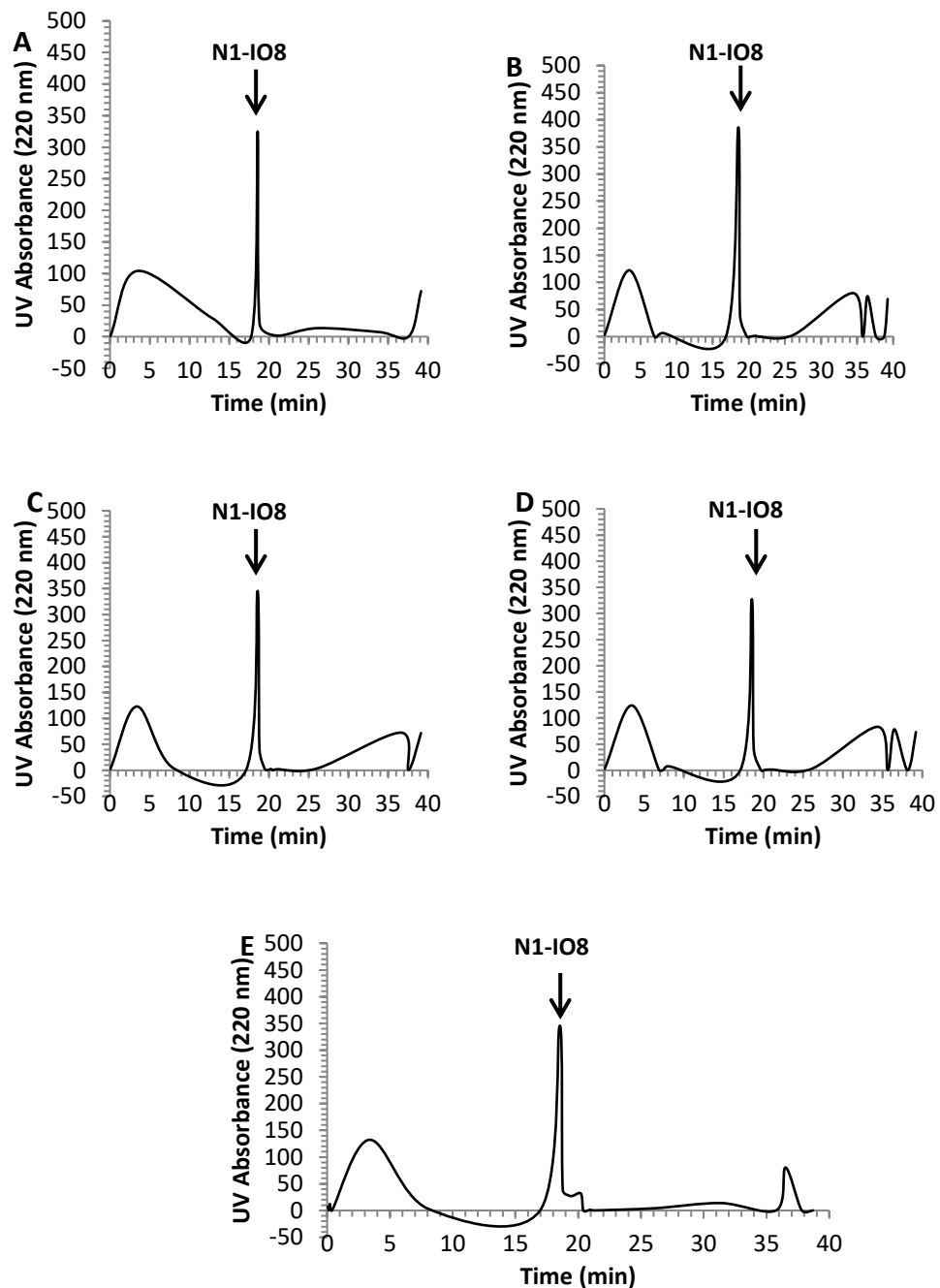


**Figure 5.2.7:** RP-HPLC profile of 100  $\mu$ M N1-IO8 and effects of proteolysis by Plasmin. (A) RP-HPLC chromatographs of N1-IO8 in the absence of proteolytic enzymes. RP-HPLC chromatographs of N1-IO8 after incubation with Plasmin (B) for 0 hr, (C) for 1 hr, (D) for 3 hrs, (E) for 24 hrs. Peptides were eluted with a linear gradient from 0–60% acetonitrile containing 0.01% TFA over 40 min, at a flow rate of 1 mL/min. Graphs show absorbance at 220 nm and elution time in mins.

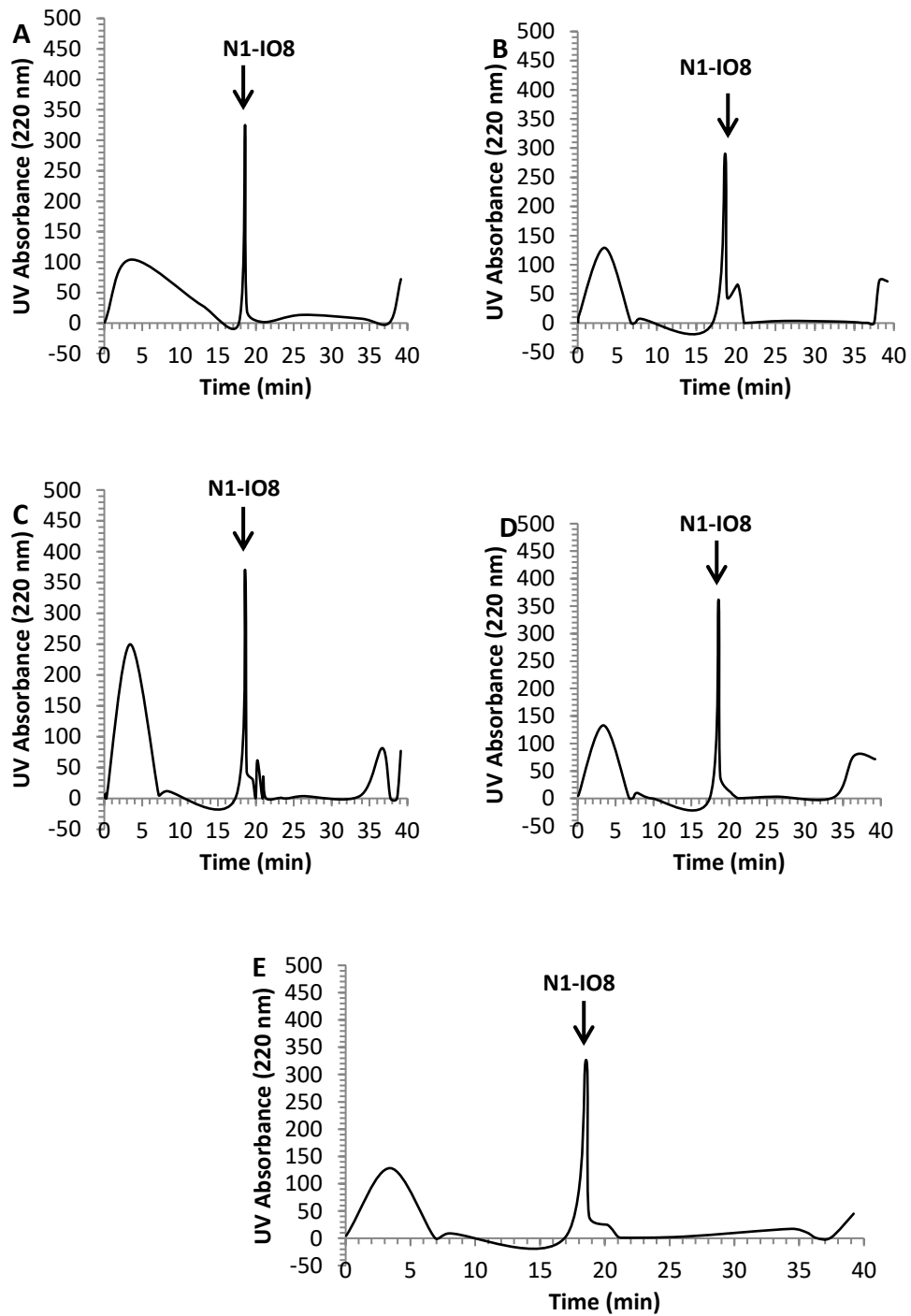


**Figure 5.2.8:** RP-HPLC profile of 100  $\mu$ M N1-IO8 and effects of proteolysis by Factor X. (A) RP-HPLC chromatographs of N1-IO8 in the absence of proteolytic enzymes. RP-HPLC chromatographs of N1-IO8 after incubation with Factor X (B) for 0 hr, (C) for 1 hr, (D) for 3 hrs, (E) for 24 hrs. Peptides were eluted with a linear gradient from 0–60% acetonitrile containing 0.01% TFA over 40 min, at a flow rate of 1 mL/min, 28 °C. Graphs show absorbance at 220 nm and elution time in mins.

### **5.3 The stability of N2-IO8 in the presence of proteolytic enzymes.**

N2-IO8 has been shown to significantly inhibit amylin aggregation. We thus assessed the stability of N2-IO8 peptide in the presence of the same proteolytic enzymes and under the same conditions as before. No apparent degradation of N2-IO8 was observed even after 24 hrs in the presence of trypsin and chymotrypsin (figure 5.3.1 B-D; figure 5.3.2 B-D). However, following 24 hrs of incubation, the chromatographic peak area of N2-IO8 was slightly decreased (figure 5.3.1 E; figure 5.3.2 E). Therefore, N2-IO8 was stable for at least for 24 hours after incubation in proteolytic enzymes. Also, cathepsin G, elastase, thrombin, kallikrein, plasmin and factor X had no effect on the chromatographic peak of N2-IO8 (figure 5.3.3- figure 5.3.8), suggesting that these enzymes did not impact on N2-IO8. Appendix A shows RP-HPLC chromatographs of these results.

<b>Protease</b>	<b>N2-IO8</b>
None	√
Chymotrypsin	√
Cathepsin G	√
Trypsin	√
Elastase	√
Thrombin	√
Kallikrein	√
Plasmin	√
Factor X	√

Table 5.3: N2-IO8 susceptibility to individual proteases. √ = Stable ; X = Degraded

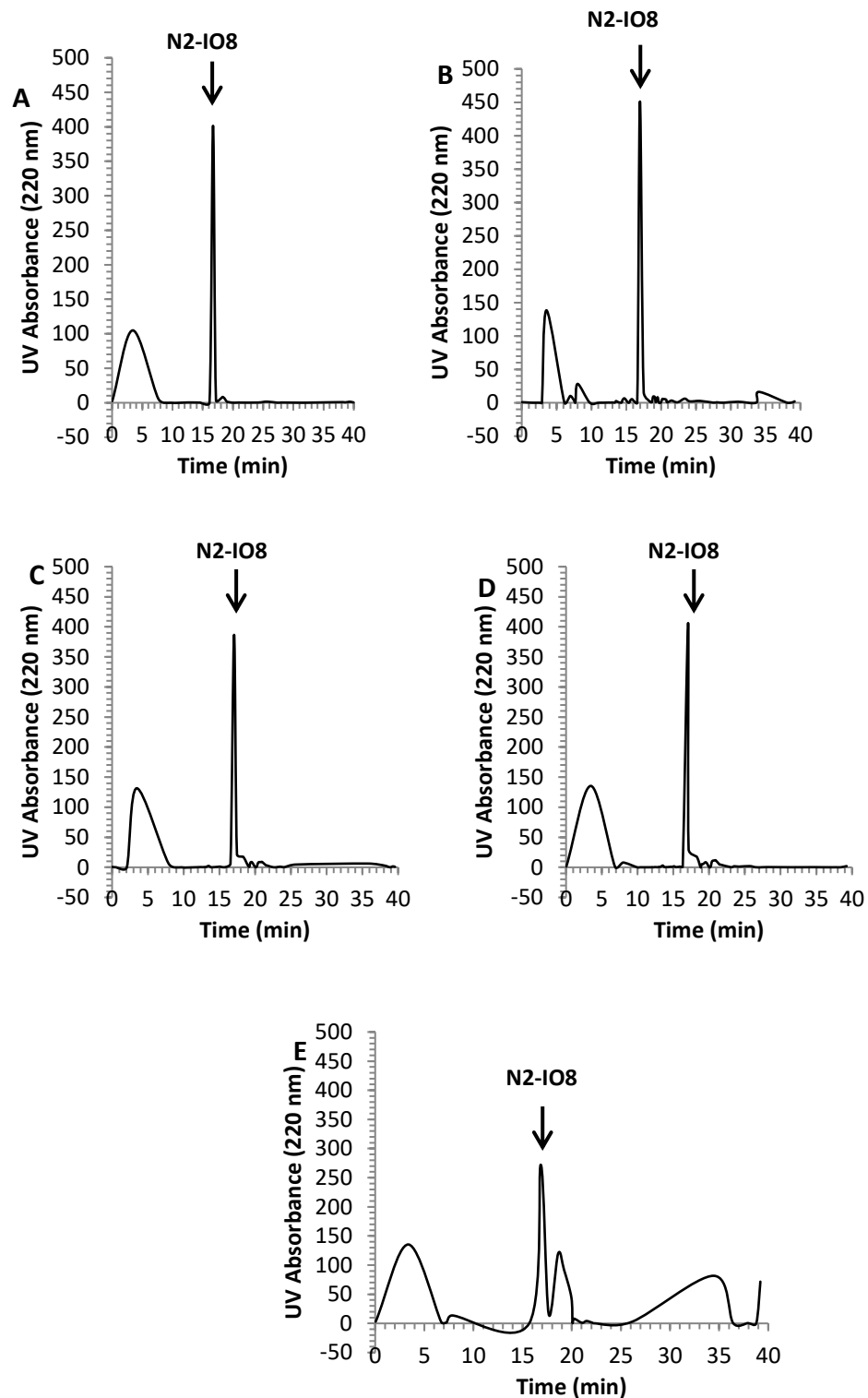


**Figure 5.3.1:** RP-HPLC profile of 100  $\mu$ M N2-IO8 and effects of proteolysis by Trypsin. (A) RP-HPLC chromatographs of N2-IO8 in the absence of proteolytic enzymes. RP-HPLC chromatographs of N2-IO8 after incubation with Trypsin (B) for 0 hr, (C) for 1 hr, (D) for 3 hrs, (E) for 24 hrs. Peptides were eluted with a linear gradient of 0–60% acetonitrile containing 0.01% TFA over 40 min, at a flow rate of 1 mL/min. Graphs show absorbance at 220 nm and elution time in mins.

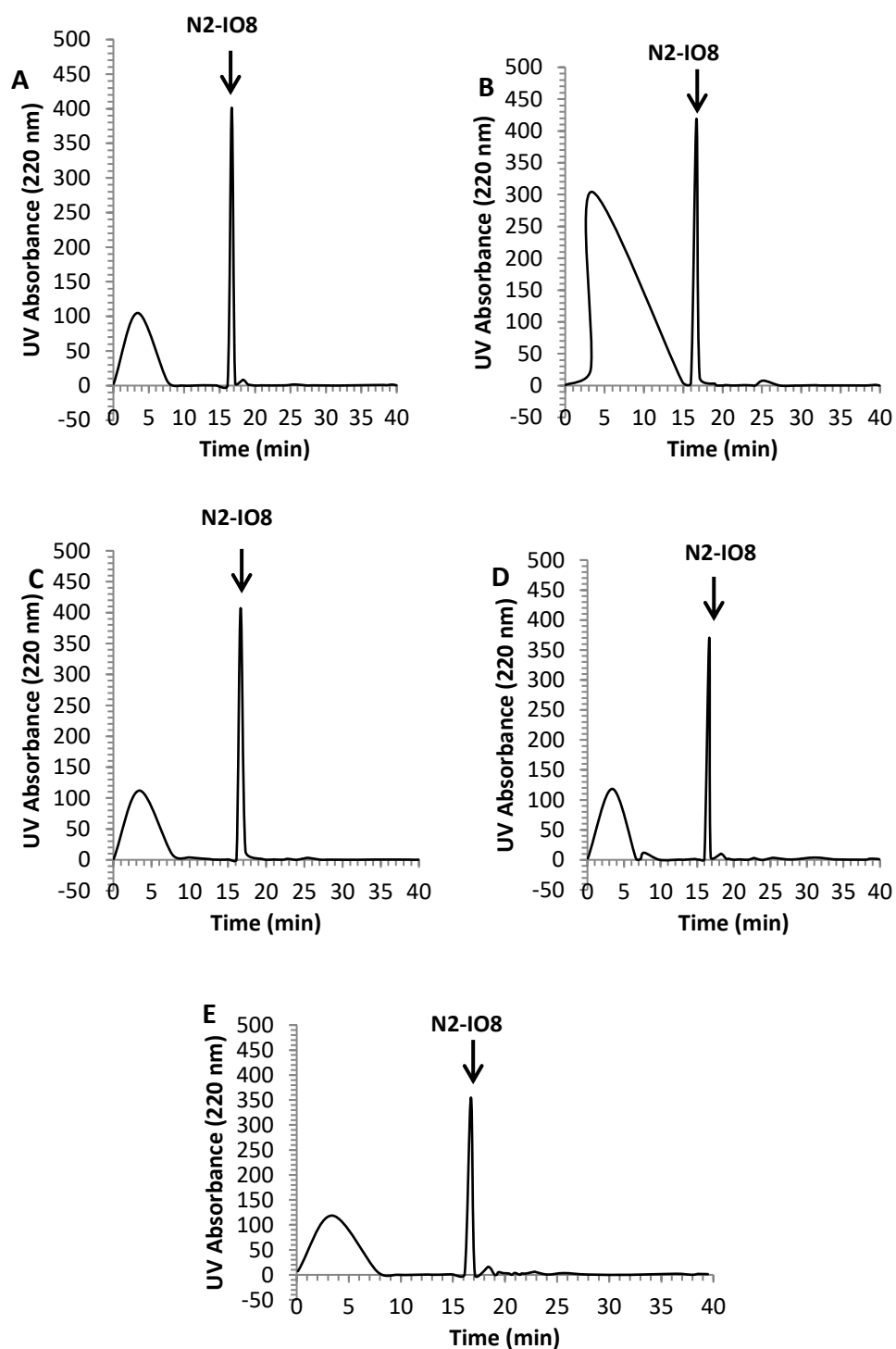


**Figure 5.3.2:** RP-HPLC profile of 100  $\mu$ M N2-IO8 and effects of proteolysis by Chymotrypsin. (A) RP-HPLC chromatographs of N2-IO8 in the absence of proteolytic enzymes. RP-HPLC chromatographs of N2-IO8 after incubation with Chymotrypsin (B) for 0 hr, (C) for 1 hr, (D) for 3 hrs, (E) for 24 hrs. Peptides were eluted with a linear gradient of 0–60% acetonitrile containing 0.01% TFA over 40 min, at a flow rate of 1 mL/min. Graphs show absorbance at 220 nm and elution time in mins.

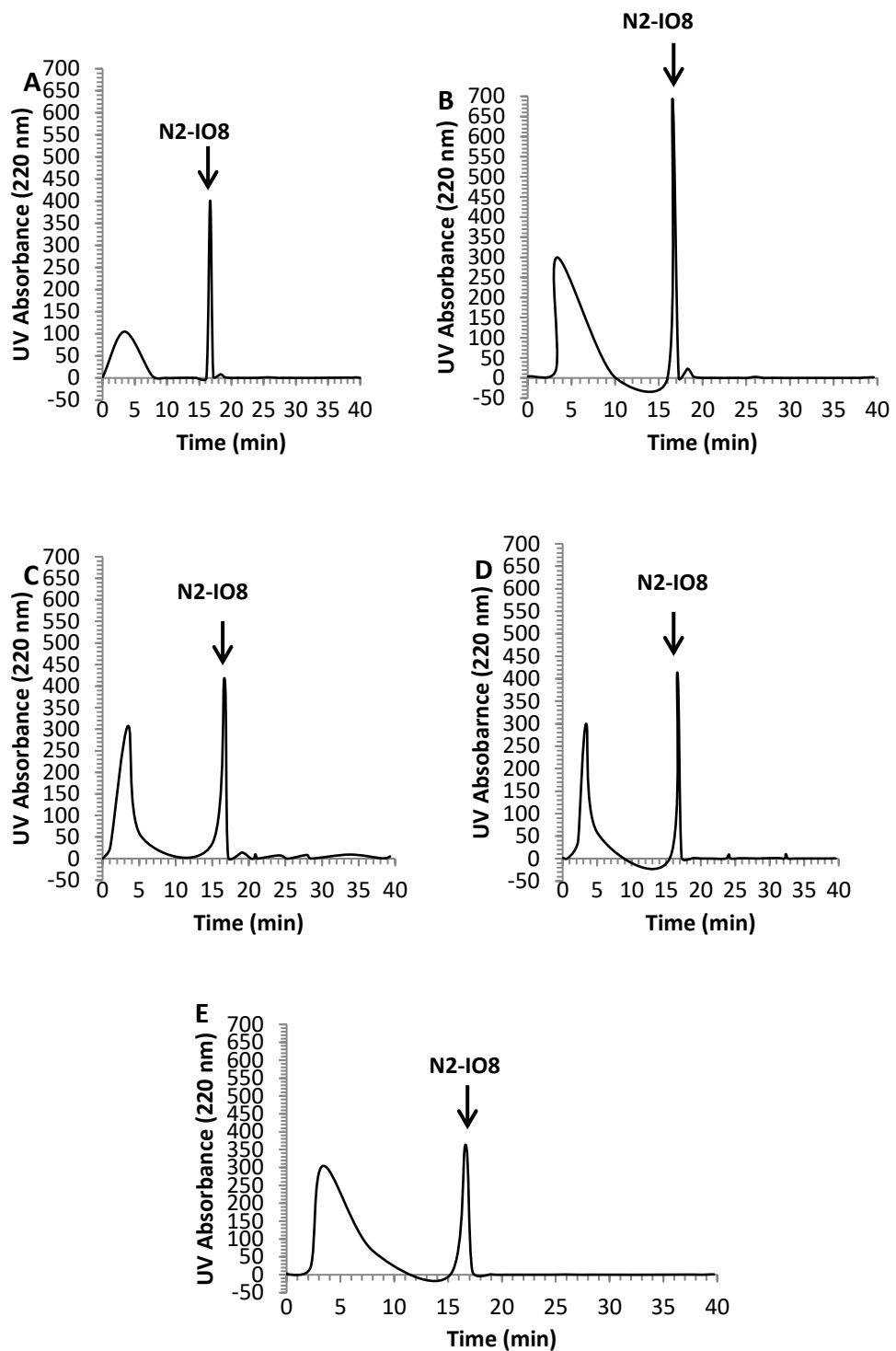


**Figure 5.3.3:** RP-HPLC profile of 100  $\mu$ M N2-IO8 and effects of proteolysis by Cathepsin G. (A) RP-HPLC chromatographs of N2-IO8 in the absence of proteolytic enzymes. RP-HPLC chromatographs of N2-IO8 after incubation with Cathepsin G (B) for 0 hr, (C) for 1 hr, (D) for 3 hrs, (E) for 24 hrs. Peptides were eluted with a linear gradient of 0–60% acetonitrile containing 0.01% TFA over 40 min, at a flow rate of 1 mL/min. Graphs show absorbance at 220 nm and elution time in mins.

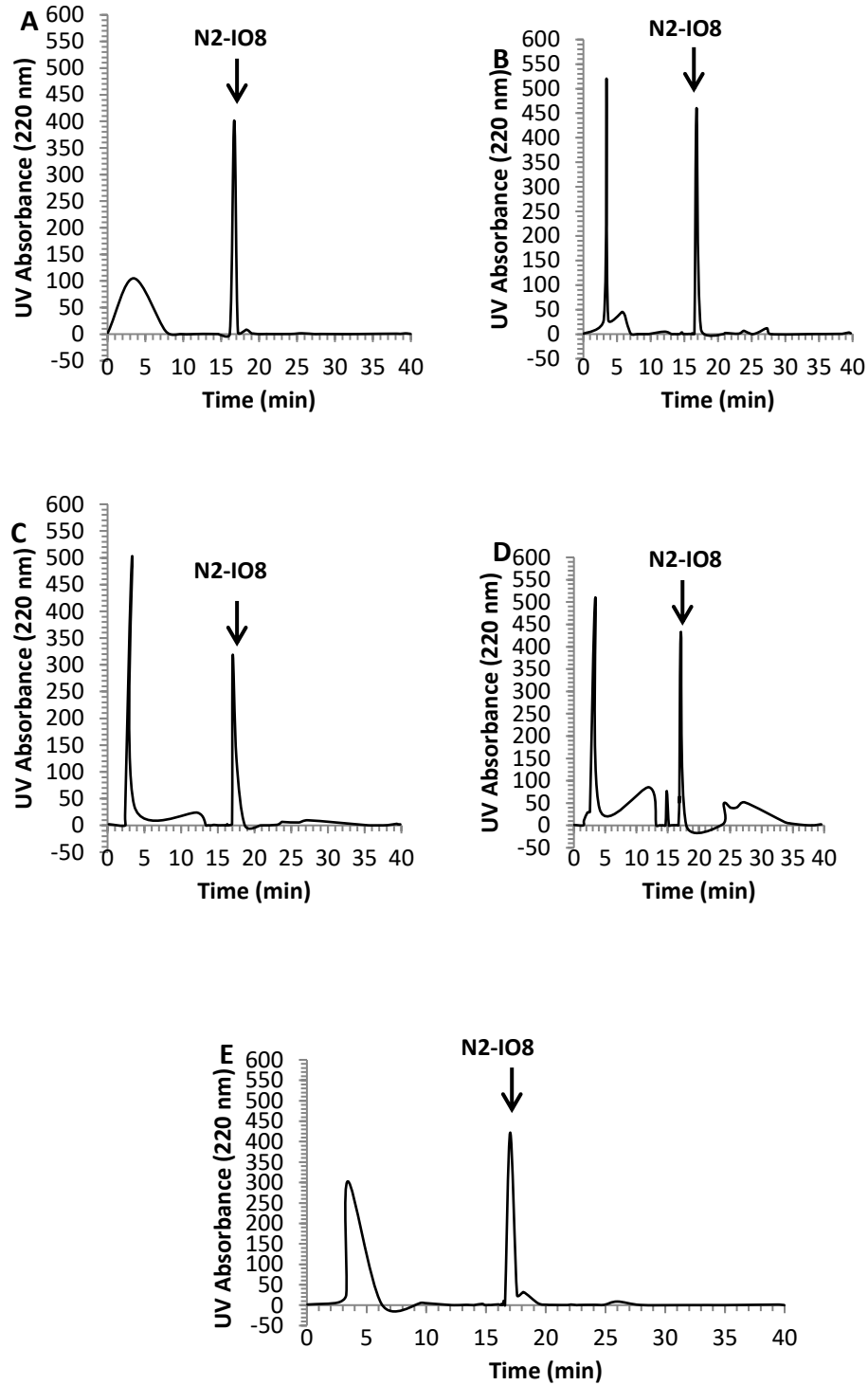


**Figure 5.3.4:** RP-HPLC profile of 100  $\mu$ M N2-IO8 and effects of proteolysis by Elastase. (A) RP-HPLC chromatographs of N2-IO8 in the absence of proteolytic enzymes. RP-HPLC chromatographs of N2-IO8 after incubation with Elastase (B) for 0 hr, (C) for 1 hr, (D) for 3 hrs, (E) for 24 hrs. Peptides were eluted with a linear gradient of 0–60% acetonitrile containing 0.01% TFA over 40 min, at a flow rate of 1 mL/min. Graphs show absorbance at 220 nm and elution time in mins.

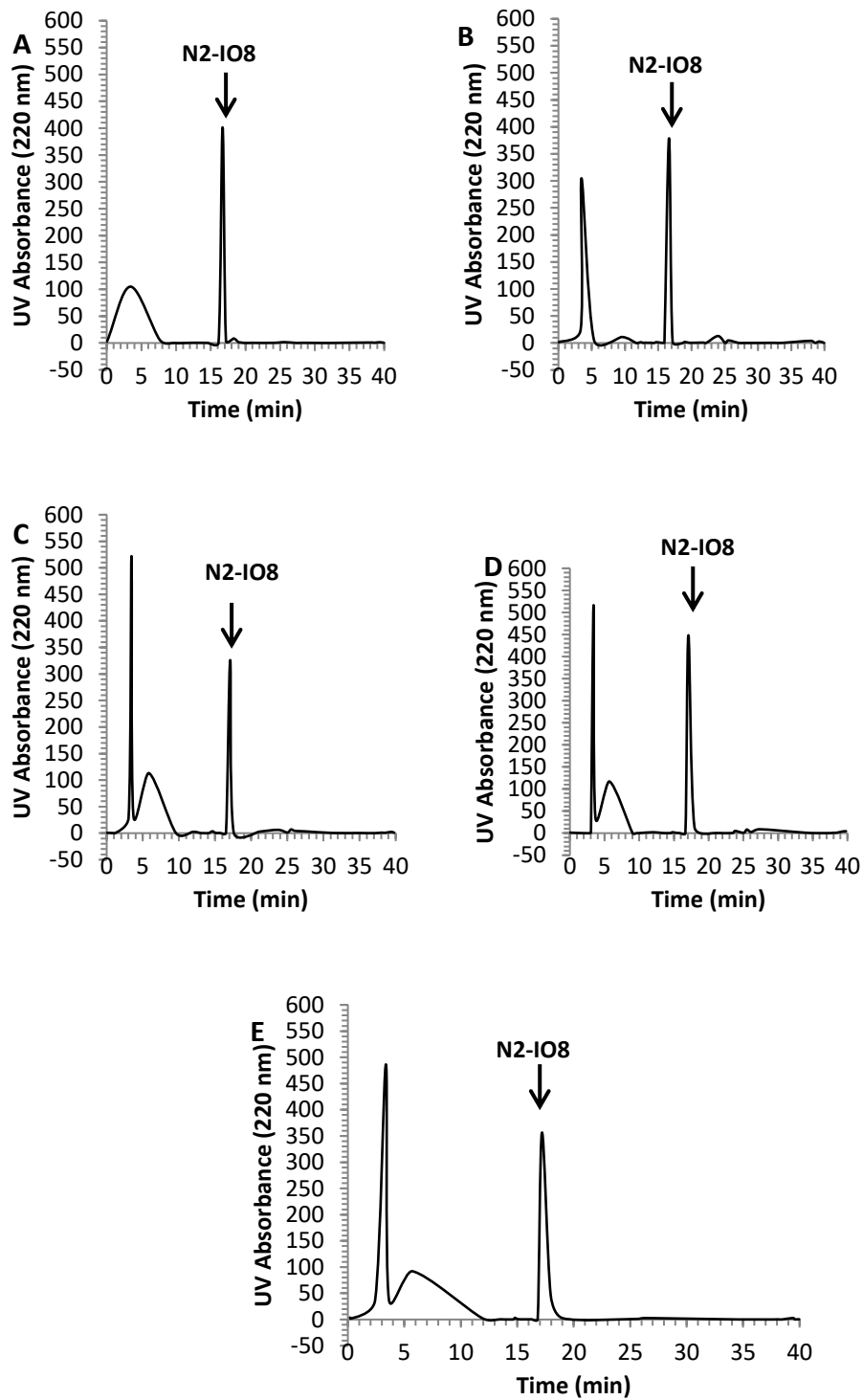


**Figure 5.3.5:** RP-HPLC profile of 100  $\mu$ M N2-IO8 and effects of proteolysis by Thrombin. (A) RP-HPLC chromatographs of N2-IO8 in the absence of proteolytic enzymes. RP-HPLC chromatographs of N2-IO8 after incubation with Thrombin (B) for 0 hr, (C) for 1 hr, (D) for 3 hrs, (E) for 24 hrs. Peptides were eluted with a linear gradient of 0–60% acetonitrile containing 0.01% TFA over 40 min, at a flow rate of 1 mL/min. Graphs show absorbance at 220 nm and elution time in mins.

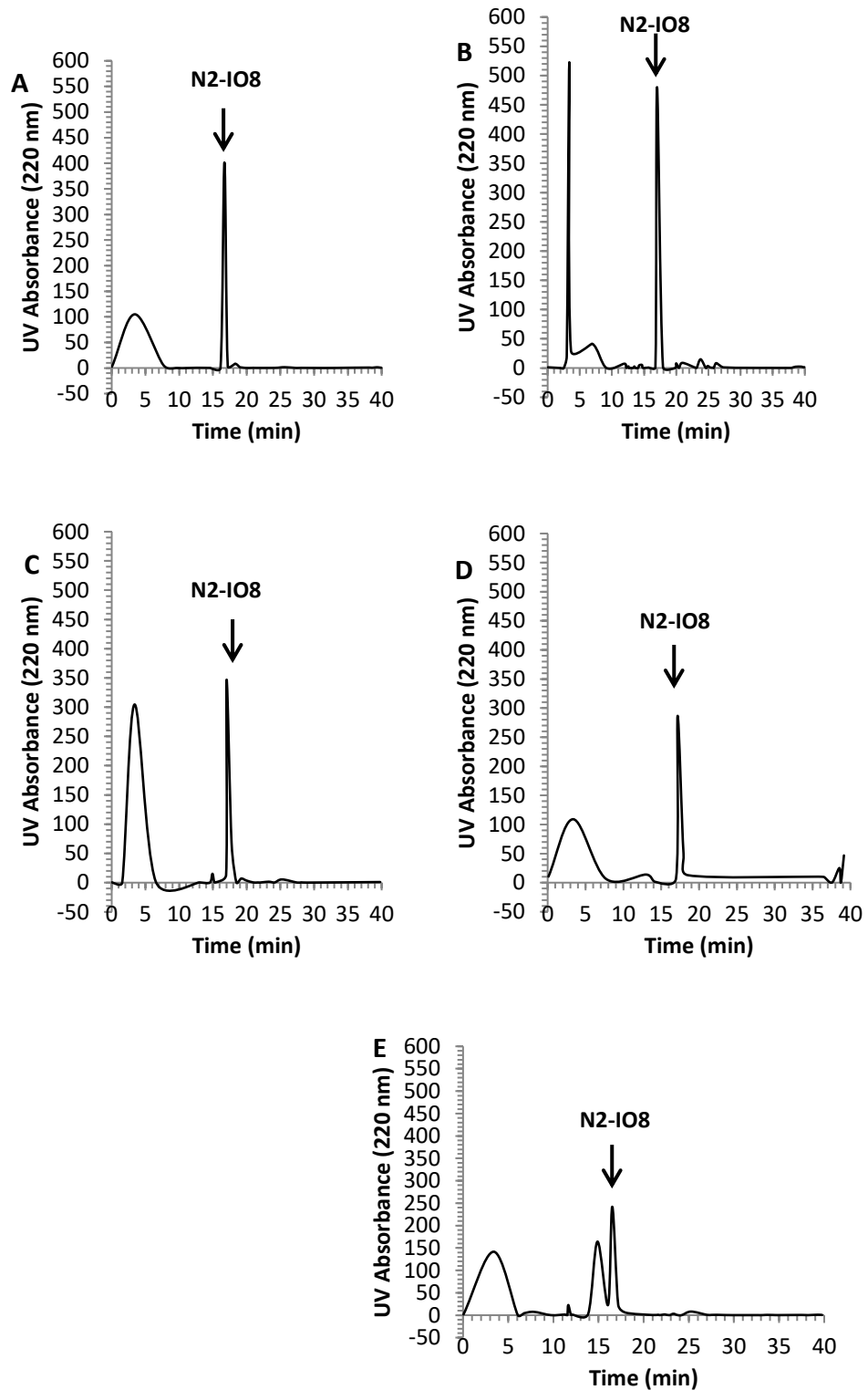


**Figure 5.3.6:** RP-HPLC profile of 100  $\mu\text{M}$  N2-IO8 and effects of proteolysis by Kallikrein. (A) RP-HPLC chromatographs of N2-IO8 in the absence of proteolytic enzymes. RP-HPLC chromatographs of N2-IO8 after incubation with Kallikrein (B) for 0 hr, (C) for 1 hr, (D) for 3 hrs, (E) for 24 hrs. Peptides were eluted with a linear gradient of 0–60% acetonitrile containing 0.01% TFA over 40 min, at a flow rate of 1 mL/min. Graphs show absorbance at 220 nm and elution time in mins.

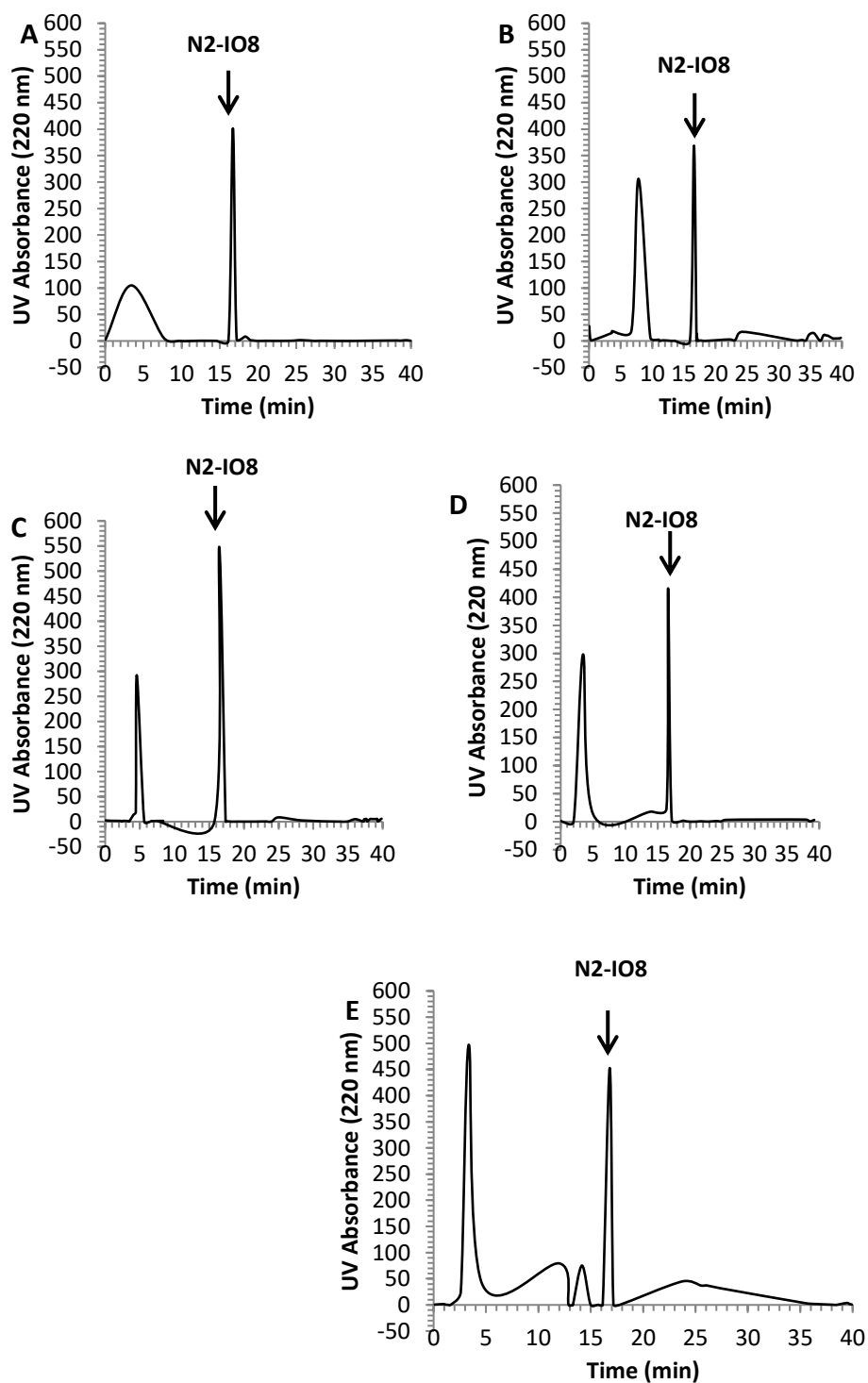


**Figure 5.3.7:** RP-HPLC profile of 100  $\mu$ M N2-IO8 and effects of proteolysis by Plasmin. (A) RP-HPLC chromatographs of N2-IO8 in the absence of proteolytic enzymes. RP-HPLC chromatographs of N2-IO8 after incubation with Plasmin (B) for 0 hr, (C) for 1 hr, (D) for 3 hrs, (E) for 24 hrs. Peptides were eluted with a linear gradient of 0–60% acetonitrile containing 0.01% TFA over 40 min, at a flow rate of 1 mL/min. Graphs show absorbance at 220 nm and elution time in mins.

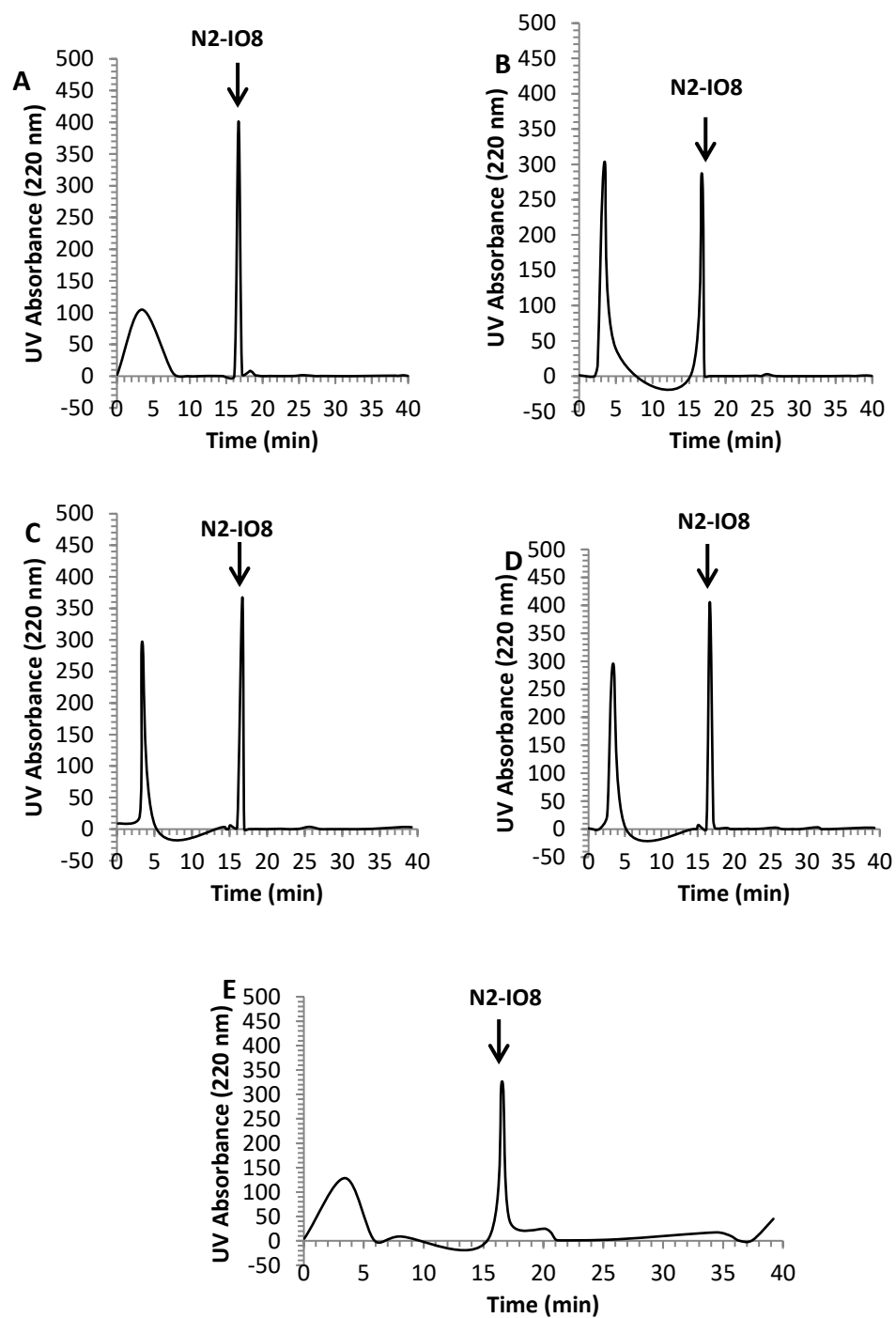


**Figure 5.3.8:** RP-HPLC profile of 100  $\mu$ M N2-IO8 and effects of proteolysis by Factor X. (A) RP-HPLC chromatographs of N2-IO8 in the absence of proteolytic enzymes. RP-HPLC chromatographs of N2-IO8 after incubation with Factor X (B) for 0 hr, (C) for 1 hr, (D) for 3 hrs, (E) for 24 hrs. Peptides were eluted with a linear gradient of 0–60% acetonitrile containing 0.01% TFA over 40 min, at a flow rate of 1 mL/min. Graphs show absorbance at 220 nm and elution time in mins.

#### **5.4 The stability of peptide inhibitors in plasma.**

After examining the effects of proteolytic enzymes on these peptides, we assessed the stability of these peptides in the presence of plasma. The stability of IO8, N1-IO8 and N2-IO8 peptides were assessed in the presence of 50% human plasma. 100  $\mu$ M of peptides in 50% plasma was incubated at varying time points of 0, 3, 24, 48 and 72 hrs at 37°C. The stability of peptides was examined by injecting 100 $\mu$ l of peptide solution onto the RP-HPLC system, with the same column and elution conditions as before. The IO8 peptide was found to be degraded in plasma, even at zero incubation time, while N1-IO8 and N2-IO8 showed negligible degradation for up to 48 hrs incubation in plasma. However, after 72 hrs of incubation, the areas of the chromatographic peaks for N1-IO8 and N2-IO8 were decreased with percentage recoveries of 7% and 19% respectively. This shows that the stability of these peptides was greatly improved, compared to that of IO8.

<b>Incubation period</b>	<b>IO8</b>	<b>N1-IO8</b>	<b>N2-IO8</b>
None	√	√	√
0 hour	X	√	√
1 hour	X	√	√
3 hours	X	√	√
24 hours	X	√	√
72 hours	X	√	√

Table 5.4: Peptide stability in plasma. √ = Stable ; X = Degraded

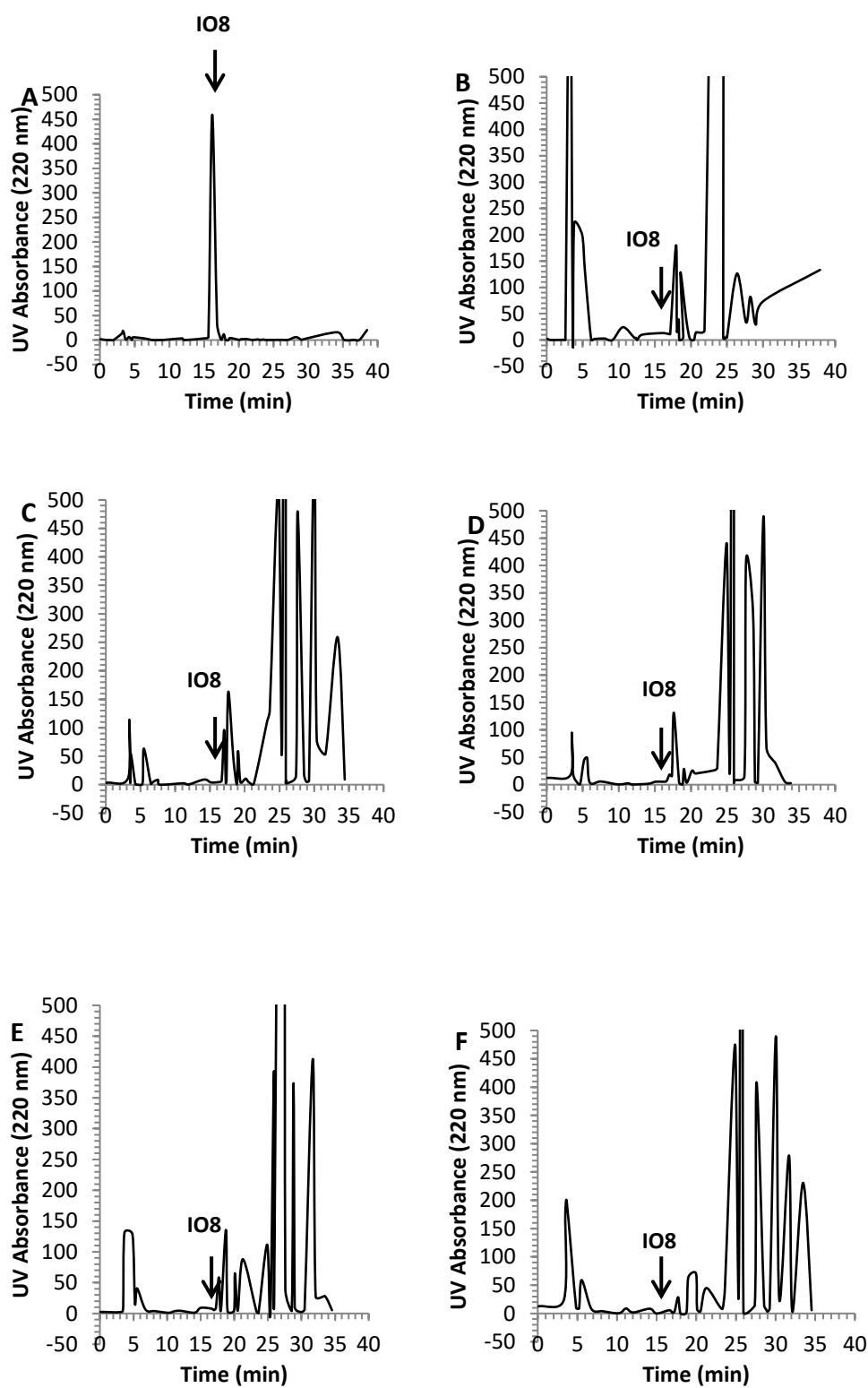


**Figure 5.4.1:** RP-HPLC profile of 100  $\mu$ M IO8 in plasma. (A) RP-HPLC chromatograph of IO8 in the absence of plasma. RP-HPLC chromatographs of IO8 after incubation with plasma (B) for 0 hr, (C) for 1 hr, (D) for 24 hrs, (E) for 48 hrs, (F) for 72 hrs. Peptides were eluted with a linear gradient of 0–60% acetonitrile containing 0.01% TFA over 40 min, at a flow rate of 1 mL/min. Graphs show absorbance at 220 nm and elution time in mins.

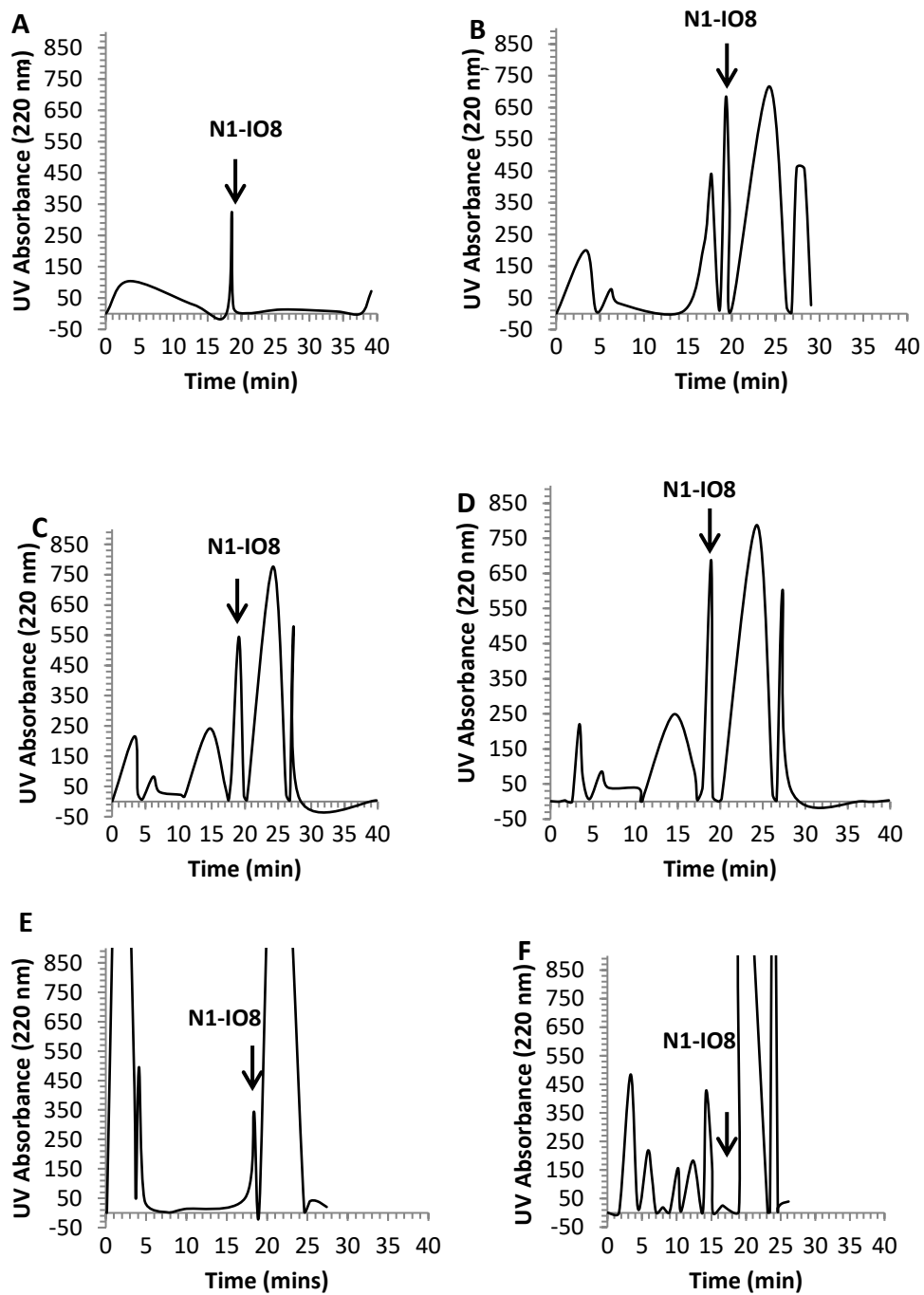


**Figure 5.4.2:** RP-HPLC profile of 100  $\mu$ M N1-IO8 in plasma. (A) RP-HPLC chromatograph of N1-IO8 in the absence of plasma. RP-HPLC chromatographs of N1-IO8 after incubation with plasma (B) for 0 hr, (C) for 1 hr, (D) for 24 hrs, (E) for 48 hrs, (F) for 72 hrs. Peptides were eluted with a linear gradient of 0-60% acetonitrile containing 0.01% TFA over 40 min, at a flow rate of 1 mL/min. Graphs show absorbance at 220 nm and elution time in mins.

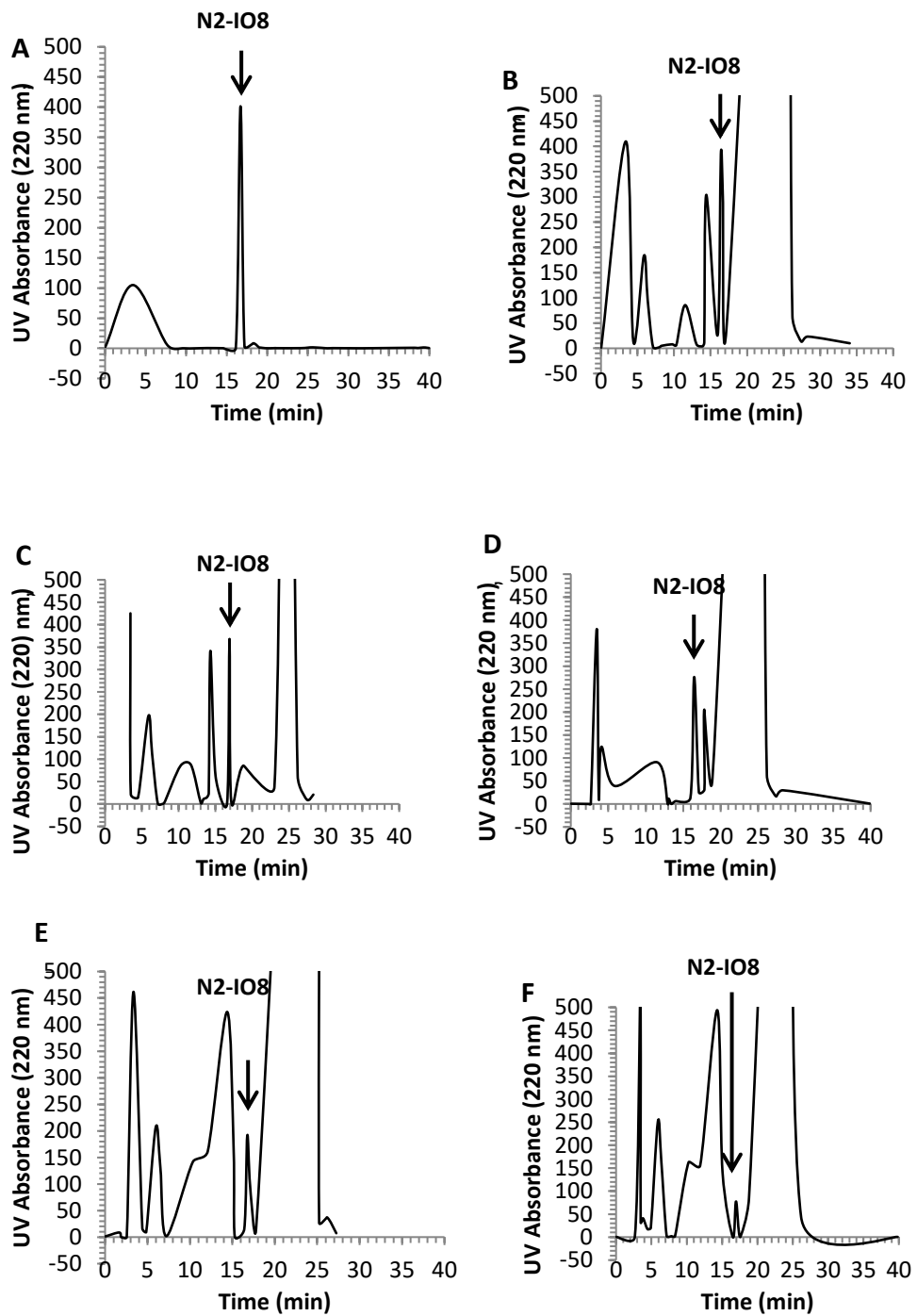


**Figure 5.4.3:** RP-HPLC profile of 100  $\mu$ M N2-IO8 in plasma. (A) RP-HPLC chromatograph of N2-IO8 in the absence of plasma. RP-HPLC chromatographs of N2-IO8 after incubation with plasma (B) for 0 hr, (C) for 1 hr, (D) for 24 hrs, (E) for 48 hrs, (F) for 72 hrs. Peptides were eluted with a linear gradient of 0–60% acetonitrile containing 0.01% TFA over 40 min, at a flow rate of 1 mL/min. Graphs show absorbance at 220 nm and elution time in mins.

## 5.5 Discussion

Peptides are excellent drug candidates as they have many therapeutic advantages over small molecules with respect to target specificity and affinity. However, due to poor bioavailability, low solubility, poor membrane permeability and most commonly poor proteolytic stability, peptides are not readily used as drugs (Giannis and Kolter 1993; McGregor 2008). The degradation of peptides and proteins by proteases is a major factor to be considered in the development of peptide-based drugs. Peptide-based drugs are easily degraded by proteolytic enzymes *in vivo* resulting in decreased pharmacokinetic properties. Previous studies have elucidated strategies for protecting peptides or proteins from proteolytic degradation. For example peptide cyclization (Hummel *et al.* 2006; Ferrie *et al.* 2013), PEGylation of peptides (Dasgupta *et al.* 2002; Werle and Bernkop-Schnurch 2006; Vlieghe *et al.*, 2010), addition of noncanonical amino acids like D-amino acids,  $\beta$ -amino acids and *N*-methylated amino acids (March *et al.*, 2012; Sani *et al.*, 2006). These approaches help in enhancing the kinetic and thermodynamic properties of peptides and proteins by rendering them proteolytically and structurally stable (Dougherty 2000; Frackenpohl *et al.* 2001). Other strategies developed to overcome proteolytic cleavage include the use of retro-inverso peptides (Fletche and Campbell, 1998), introducing peptide bond isosters (Goodman *et al.*, 2002), peptidomimetics (Giannis, 1993) and peptoids (Kessler, 1993). Although these approaches have many advantages, they can require careful configuration, which can involve difficult syntheses.

For this study, the *N*-methylation approach was used to counter the challenges of using peptides as a basis for drug development. In some previous studies,

mono-N-methylation has been applied to modify the pharmacokinetic properties of peptides (Gilon *et al.*, 2002). Multiple N-methylation has sometimes been used due to the challenges with synthesis and risk of losing activity associated with mono-N-methylation (Holladay *et al.*, 1994; Teixido *et al.*, 2005). Here, the N-methylated peptides (N1-IO8 and N2-IO8) were assessed for their stability in the presence of proteolytic enzymes and in plasma through analytical RP-HPLC compared to the unmodified peptide IO8. HPLC is a well-recognized, efficient, sensitive and reproducible approach for analyzing peptide cleavage products and reactions (Ferrie *et al.*, 2013; Hua and Huang, 2010). The degradation behaviour of IO8 was assessed in the presence of various proteolytic enzymes (table 5.1). IO8 was found to be very unstable in the presence of trypsin and chymotrypsin, and was completely degraded by these enzymes after 3 hrs of incubation. In the presence of cathepsin G, elastase, kallikrein, plasmin and thrombin, IO8 was not completely degraded after 3 hrs, although the peak area was decreased. The results obtained on the stability of IO8 suggest that this peptide-based drug must be protected from proteolytic degradation. No new peaks were seen in the chromatograms of degraded samples of IO8 (figure 5.1.1 – figure 5.1.8) suggesting that the proteolytic fragments are not resolved by this RP-HPLC system. IO8 was also completely degraded in plasma, which is not surprising since this would contain trypsin and chymotrypsin activity (Suzuki *et al.*, 1990).

Upon subjecting IO8 (H<sub>2</sub>N-RGANFLVHGR-NH<sub>2</sub>) to an ExPasy program, PeptideCutter; IO8 was cleaved at position 5 (F) by high specificity chymotrypsin and positions 5, 6, 8 (F, L, H) by low specificity chymotrypsin, while trypsin cleaves IO8 at positions 1 and 9. Other enzymes that cleave IO8 not used in this study are Arg-C proteinase, clostripain, proteinase K, pepsin and

thermolysin. These results are consistent with our RP-HPLC data and suggest that these enzymes do not have high activity for the amino acid sequence present in IO8, with the exception of trypsin and chymotrypsin. Also for confirmatory purposes, RI-IO8 (Ac-rGhvlfnGr-NH<sub>2</sub>) and HIO8 (H<sub>2</sub>N-Har-GANFLVHG-Har-NH<sub>2</sub>) were also analysed for stability using RP-HPLC. The results confirm that retro-inversion blocks recognition of this peptide by proteolytic enzymes, thus protecting it from proteolytic degradation (see data in Appendix A). The RP-HPLC results show that RI-IO8 was stable in the presence of chymotrypsin and trypsin, unlike IO8 (Appendix A). However, it should be noted that although we successfully protected IO8 from proteolytic degradation by the retro-inverso method, our retro-inverso peptide was ineffective at inhibiting the aggregation of human amylin, as described in previous chapters. Thus another approach for stabilizing IO8 was considered. RI-IO8 (Ac-rGhvlfnGr-NH<sub>2</sub>) could not be analyzed using the ExPasy PeptideCutter as this peptide is retro-inverted, with L-amino acids replaced by D- amino acids. The next step in stabilising IO8 was by targeting individual residues in the sequence and protecting them from proteolytic degradation by substituting with other amino acid analogues. Integrating non-natural amino acids to peptides is a key strategy in increasing the bioavailability of pharmacologically active peptides. Firstly, we replaced the two arginines in IO8 with Homoarginine. Our data showed that the replacement of these arginines (in IO8; H<sub>2</sub>N-RGANFLVHGR-NH<sub>2</sub>) with Homoarginine (in HIO8; H<sub>2</sub>N-HarGANFLVHGHaR-NH<sub>2</sub>) rendered HIO8 resistant to proteolytic degradation by trypsin (Appendix A). Homoarginine is an unnatural analogue of arginine, and is not recognised by trypsin (Atkinson *et al.*, 1999). The HIO8 peptide was, however, still susceptible to cleavage by

chymotrypsin (Appendix A), which selectively causes hydrolysis of peptide bonds on the C-terminal side of tyrosine, phenylalanine, tryptophan and leucine. Protection of the 'FL' residues in HIO8 would therefore be required to further develop this peptide inhibitor as a drug. A more suitable approach to protecting IO8 from proteolytic degradation was thought to be N-methylation of alternate amino acid residues, leading to the development of N1-IO8 (H<sub>2</sub>N-R-G-Am-N-Fm-L-Vm-H-G-R-NH<sub>2</sub>) which was methylated at residues A, F and V; and N2-IO8 (H<sub>2</sub>N-R-G-A-Nm-F-Lm-V-Hm-G-R-NH<sub>2</sub>), which was methylated at residues N, L and H. N-methylation, which is the methylation of nitrogen atoms, is one of the most significant chemical modifications to control biological functions. N1-IO8 (figure 5.2.1 - 5.2.8) and N2-IO8 (figure 5.3.1 - 5.3.8) were protected from proteolytic degradation by trypsin, chymotrypsin and other enzymes including cathepsin G, elastase, thrombin, kallikrein, plasmin and factor X. This confirms that N-methylation of this peptide renders it resistant to proteolytic degradation. N1-IO8 (figure 5.4.2) and N2-IO8 (figure 5.4.3) were also found to be stable in plasma for at least 48 hrs (Appendix B). The chromatographic peaks for these peptides, however, did decrease after 72 hrs. Previous studies have elucidated the impact of N-methylation on the activity, stability and structure of biologically active peptides. Research has shown that multiple N-methylation significantly improves the oral bioavailability and receptor subtype selectivity of some peptides (Biron *et al.*, 2008; Chatterjee *et al.*, 2007). Recent research has also proved that N-methylation remarkably improves the pharmacokinetic profile of drugs (Di Gioia *et al.*, 2016). This is supported by research which showed that N-methylation of a cyclopeptidic somatostatin analog cyclo (-PFwKTF-) peptide, improved the metabolic

stability, intestinal permeability and bioavailability of the peptide (Chatterjee *et al.*, 2008). Many peptides are metabolically unstable due to their short plasma half-life. The results presented here show that N- methylation can remarkably improve the plasma half-life of peptides, thus making them more metabolically stable.

#### **5.4.1 Conclusion**

This present study presents a systematic investigation of the stability of the different peptides under investigation against degradation by proteolytic enzymes and in plasma. The main aim was to develop proteolytically stable peptides which have therapeutic relevance. Five peptides were systematically characterised for their stability towards nine different proteolytic enzymes, as well as in plasma. The IO8 peptide was immediately degraded by proteases and was not stable in plasma. The substitution of the arginines with homoarginine in HIO8 led to its protection from degradation by trypsin, although HIO8 was still degraded by other proteolytic enzymes. RI-IO8, with reversal of the sequence and replacement of L-amino acids with D-amino acids, greatly improved stability towards proteases, confirming that retro-inversion of peptides can completely alter their proteolytic stability. Further investigation demonstrated that N-methylation also enhances the resistance of these peptides to degradation by proteases. NI-IO8 and N2-IO8 showed excellent stability in plasma and in the presence of proteolytic enzymes. N-methylation is an important approach for the development of peptide-based drugs, with marked improvement in their pharmacokinetic properties.

## Chapter 6

### Cell based Studies

Proteins are able to form a variety of insoluble amorphous or fibrillar aggregates. Amylin forms  $\beta$  sheet fibres (Serpell *et al.*, 2000; Luca *et al.*, 2007). A number of studies have linked the cytotoxicity of amylin with the oligomers that form during the early stages of the aggregation process, rather than the mature amyloid fibrils (Lin *et al.*, 2007; Haataja *et al.*, 2008). Therefore, the inhibition of amylin aggregation at the early stage of amyloid formation could be a promising approach to decrease islet cell disruption in T2DM as well as in other amyloidogenic diseases (Necula *et al.*, 2007). The latter would include Alzheimer's disease, where aggregated proteins of Tau and Amyloid beta ( $A\beta$ ) play key roles in disease pathogenesis; and Parkinson's disease, where aggregated  $\alpha$ -synuclein plays a key role in disease pathogenesis (Glenner *et al.*, 1984; Iwai *et al.*, 1995). This approach seems to have considerable potential as some inhibitors of  $A\beta$  and Tau aggregation have already reached clinical trials (Abian *et al.*, 2013; Lopez *et al.*, 2012; Conesa *et al.*, 2012). On the other hand, the majority of peptide-based drugs are not adequately taken up by cells and this is a major draw-back in therapeutic development. Previous Chapters of this thesis have described peptide-based inhibitors of amylin aggregation. Here, the CellTiter 96 aqueous one solution cell proliferation (MTS) and the CytoTox-ONE Homogeneous Membrane Integrity Assay also known as lactate dehydrogenase (LDH) assay (described in Methods sections 2.5.3 and 2.5.5) were used to determine the ability of these peptides to protect PANC-1 Human pancreatic 1.4E7 (ECACC 10070102) insulin-secreting cells from the toxicity of

human amylin in culture. MTS is a colorimetric technique that determines the number of viable cells by measuring NAD(P)H-dependent cellular oxidoreductase enzyme activity. The LDH enzyme is said to be stable and is found in all cell types and is quickly discharged into the cell culture medium following disruption of the plasma membrane on cell damage. The LDH released into the culture medium results in a higher fluorescent signal, indicating a greater number of nonviable cells. The ability of the inhibitory peptides to penetrate across the cell membrane was also determined by attaching the peptides to a fluorescent dye (Alexa fluor 488) and examining cells following exposure to fluorescent peptides by using confocal microscopy.

A one-way between samples ANOVA was conducted to compare the viability of human pancreatic PANC-1  $\beta$  cells in the presence of human amylin, human amylin plus (+) peptide inhibitors, no amylin, cells only and peptide only conditions. Significance was recorded at \* $P < 0.05$ , \*\* $P < 0.01$ , \*\*\* $P < 0.001$ . Post hoc comparisons using the Tukey's post hoc test indicated the significant difference between the mean cell viability between human pancreatic PANC-1  $\beta$  cells in the presence of human amylin, human amylin plus (+) peptide inhibitors, no amylin, cells only and peptide only conditions.

## **6.1 Effect of IO8 on amylin-induced toxicity in PANC-1 human pancreatic cells**

First of all, the toxic effect of freshly prepared human amylin peptide on PANC-1 human cells was determined. The ability of IO8 peptide to inhibit amylin cytotoxicity was then assessed using the MTS assay, with replicates of  $n = 6$ . Three different experiments were performed with similar results, and the data presented in figure 6.1 are from a single experiment, where results show mean  $\pm$  SEM ( $n = 6$ ). The effect of amylin alone was investigated by the addition of 20  $\mu\text{M}$  and 10  $\mu\text{M}$  of freshly prepared amylin to 96 well plates containing PANC-1 cells in media. Amylin at 20  $\mu\text{M}$  was significantly cytotoxic to untreated PANC-1 cells and reduced cell viability to 41% (figure 6.1). At 10  $\mu\text{M}$ , amylin reduced cell viability to 90 %. IO8 significantly rescued the cells from the toxic effects of amylin when present at both equimolar and 1:4 molar ratio of IO8 to amylin as compared to cells treated with amylin alone. The effect of inhibitor alone on the cells was also tested. IO8 alone at 20  $\mu\text{M}$  and 5  $\mu\text{M}$  had no significant effect on the cells. The total volume of solution in the wells was kept at 100  $\mu\text{l}$  during all of these assays.

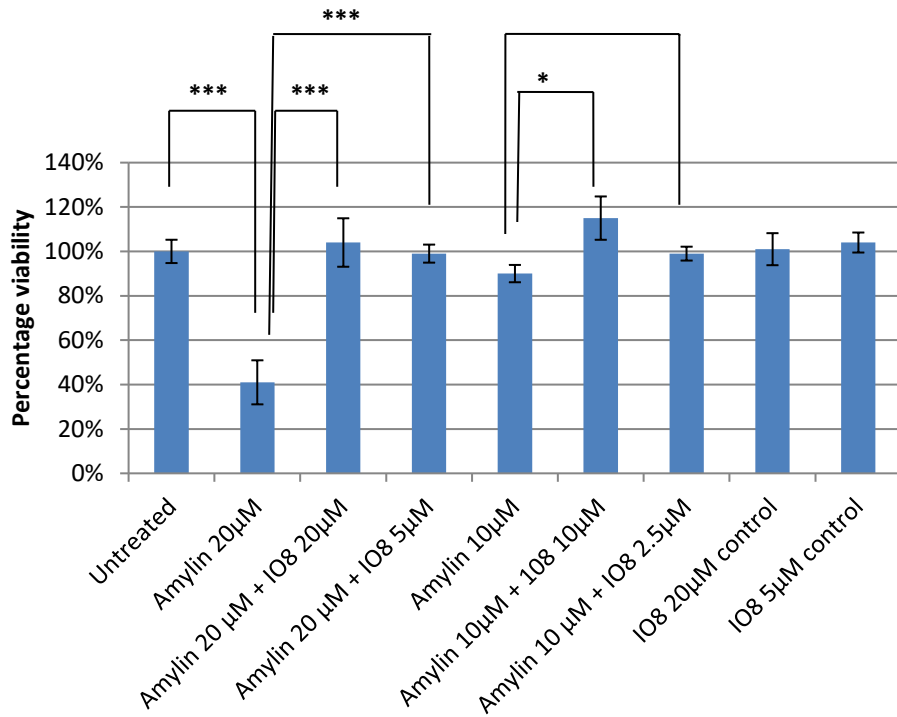


**Figure 6.1:** Cytotoxic effect of amylin in the presence or absence of IO8 peptide on PANC-1 cells. PANC-1 cells were incubated for 24 hrs with 20 µM and 10 µM human amylin in RPMI-1640 medium with or without the IO8 peptide, and viability was measured using the MTS cell proliferation assay. The results are means  $\pm$  SEM, n = 6. One-way ANOVA, Tukey's post hoc test \*P<0.05, \*\*P<0.01, \*\*\*P<0.001.

## **6.2 Effect of N1-IO8 on amylin-induced toxicity PANC-1 human pancreatic cells**

The effect of freshly prepared human amylin peptide on PANC-1 human cells was investigated, along with the ability of N1-IO8 peptide to inhibit amylin cytotoxicity, using the MTS cell proliferation assay, with the same conditions as those described previously. Three different experiments were performed with similar results, and the data presented in figure 6.2 (mean  $\pm$  SEM, n = 6) are from a single experiment. The effect of amylin alone was investigated by the addition of 20  $\mu$ M and 10  $\mu$ M of freshly prepared amylin to 96 well plates containing PANC-1 cells in media. Amylin alone at 20  $\mu$ M and 10  $\mu$ M was significantly cytotoxic to untreated PANC-1 cells and reduced cell viability to 35% (figure 6.2) and 63 % respectively. At a molar ratio of 1:1 and 1:4 of N1-IO8 peptide to amylin, N1-IO8 significantly rescued the cells from the toxic effects of amylin when compared to cells treated with amylin alone. In addition, N1-IO8 alone at 20  $\mu$ M and 5 $\mu$ M had no significant effect on untreated cells.

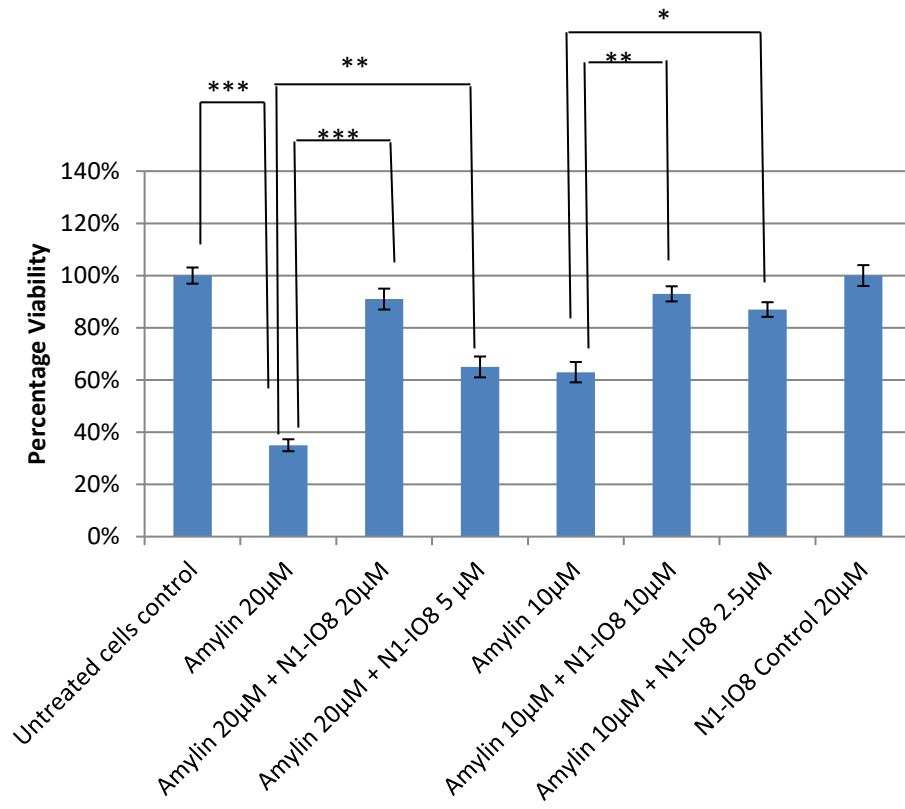


**Figure 6.2:** Cytotoxic effect of amylin in the presence or absence of N1-IO8 peptide on PANC-1 cells. PANC-1 cells were incubated for 24 hrs with 20 µM and 10 µM human amylin in RPMI-1640 medium with or without the IO8 peptide, and viability was measured using the MTS cell proliferation assay. The results are means +/- SEM, n = 6. One-way ANOVA, Tukey's post hoc test \*P<0.05, \*\*P<0.01, \*\*\*P<0.001.

### **6.3 Effect of N2-IO8 on amylin-induced toxicity PANC-1 human pancreatic cells**

The ability of N2-IO8 peptide to inhibit amylin cytotoxicity was also assessed using the MTS cell proliferation assay, with the same cells and conditions as those described previously. The experiment was performed in replicates of  $n = 6$ . The data presented in figure 6.3 are mean  $\pm$  SEM from a single experiment (where  $n = 6$ ) and are representative of 3 different experiments. Amylin at 20  $\mu\text{M}$  and 10  $\mu\text{M}$  was significantly cytotoxic to untreated PANC-1 cells and reduced cell viability to 40% and 61 % respectively. However, at a 1:1 and a 1:4 molar ratio of N2-IO8 peptide to amylin, N2-IO8 significantly rescued the cells from the toxic effects of amylin. In addition, N2-IO8 alone at 20  $\mu\text{M}$  and 5 $\mu\text{M}$  had no adverse effect on untreated cells.

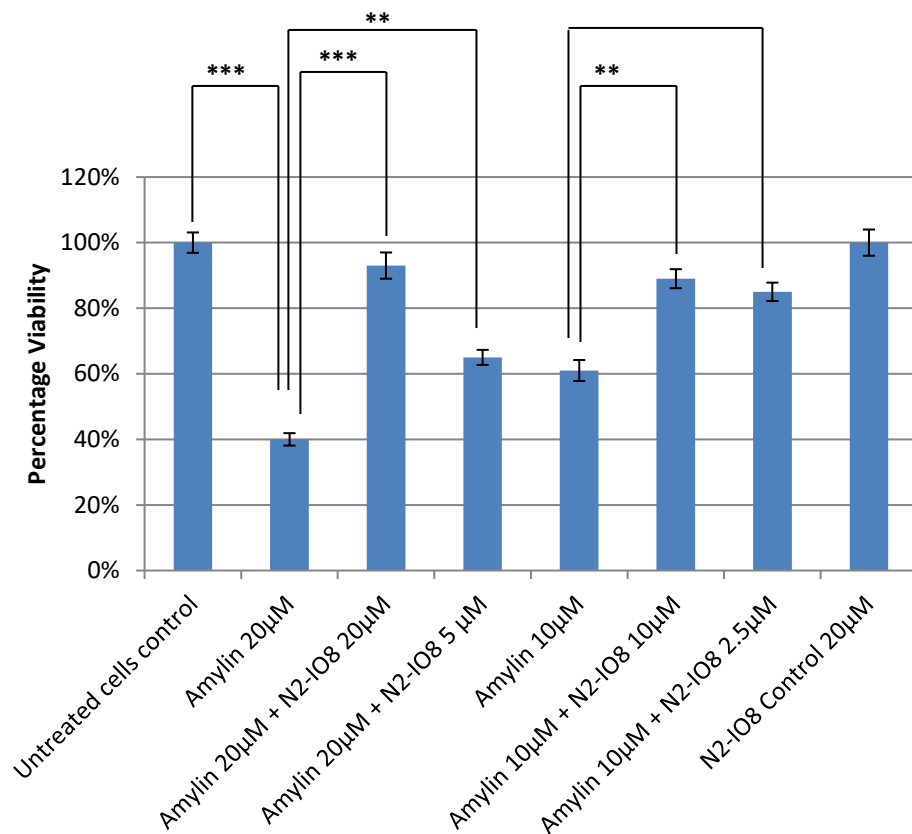


**Figure 6.3:** Cytotoxic effect of amylin in the presence or absence of N2-IO8 peptide on PANC-1 cells. PANC-1 cells were incubated for 24 hrs with 20 µM and 10 µM human amylin in RPMI-1640 medium, with or without the IO8 peptide, and viability was measured using the MTS cell proliferation assay. The results are means  $\pm$  SEM, n = 6. One-way ANOVA, Tukey's post hoc test \*P<0.05, \*\*P<0.01, \*\*\*P<0.001.

#### **6.4 LDH analysis of IO8 on amylin-induced toxicity PANC-1 human pancreatic cells**

The ability of IO8 peptide to inhibit amylin cytotoxicity was also assessed using the LDH cytotoxicity assay. Two different experiments were carried out in replicates of  $n = 6$ . The data presented in figure 6.4 are from a single experiment, where results show mean  $\pm$  SEM ( $n = 6$ ). The data show the viability of PANC1 human pancreatic cells as measured by LDH assay, after exposure to 80, 40, 20, 10, 5 and 2.5  $\mu\text{M}$  of IO8 in the presence of 20  $\mu\text{M}$  amylin. The ‘negative control’ bar is the background absorbance without cells. The ‘untreated cells control’ bar is the absorbance of cells without any intervention. The ‘LDH control’ bar indicates the absorbance of lysed cells. Amylin at 20  $\mu\text{M}$  was significantly cytotoxic to untreated PANC-1 cells and reduced cell viability as shown by a substantial increase in absorbance (figure 6.4). At concentrations of 80  $\mu\text{M}$  (4:1 molar ratio peptide to amylin to peptide), 40  $\mu\text{M}$  (2:1 molar ratio peptide to amylin), 20  $\mu\text{M}$  (1:1 molar ratio peptide to amylin), 10  $\mu\text{M}$  (1:2 molar ratio peptide to amylin), 5  $\mu\text{M}$  (1:4 molar ratio peptide to amylin) and 2.5  $\mu\text{M}$ , IO8 significantly decreased the toxic effects of human amylin.

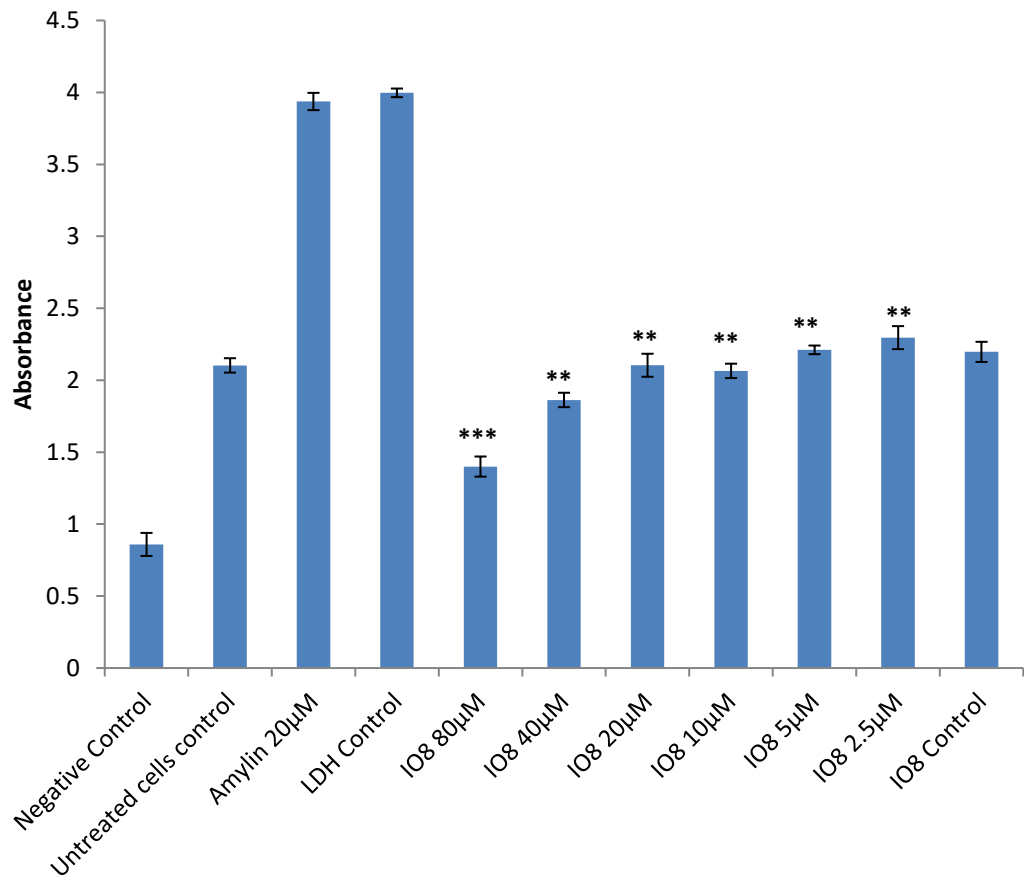


**Figure 6.4:** IO8 inhibits the toxic effects of human amylin on pancreatic islet  $\beta$  cells, as measured by LDH assay. Human amylin at 20  $\mu$ M was cytotoxic to cells. IO8 at concentrations of 80, 40, 20, 10, 5 and 2.5  $\mu$ M protected cells from amylin cytotoxicity. The “negative control” bar is the background absorbance without cells. The “untreated cells control” bar represents cell absorbance without any intervention. The “LDH control” bar represents the absorbance of lysed cells. IO8 control is 100  $\mu$ M of IO8 in cell culture. The results are means $\pm$  SEM, n =6. One-way ANOVA, Tukey's post hoc test \*P<0.05, \*\*P<0.01, \*\*\*P<0.001.

## **6.5 LDH analysis of N1-IO8 on amylin-induced toxicity PANC-1 human pancreatic cells**

The ability of N1-IO8 peptide to inhibit amylin cytotoxicity was also assessed using the LDH assay, using the same cells and conditions as described previously. The data presented in figure 6.5 are from a single experiment carried out in replicates of n=6 and are representative of two different sets of experiments. Results show means +/- SEM (n = 6). The 'negative control' bar is the background absorbance without cells. The 'untreated cells control' bar shows the absorbance of cells without treatment. The 'LDH control' bar indicates the absorbance of lysed cells. Amylin at 20  $\mu\text{M}$  was significantly cytotoxic to untreated PANC-1 cells and reduced cell viability as shown by a substantial increase in absorbance (figure 6.5). At concentrations of 80  $\mu\text{M}$  (4:1 molar ratio peptide to amylin to peptide), 40  $\mu\text{M}$  (2:1 molar ratio peptide to amylin), 20  $\mu\text{M}$  (1:1 molar ratio peptide to amylin), 10  $\mu\text{M}$  (1:2 molar ratio peptide to amylin), 5  $\mu\text{M}$  (1:4 molar ratio peptide to amylin) and 2.5  $\mu\text{M}$ , N1-IO8 significantly decreased the toxic effects of human amylin.

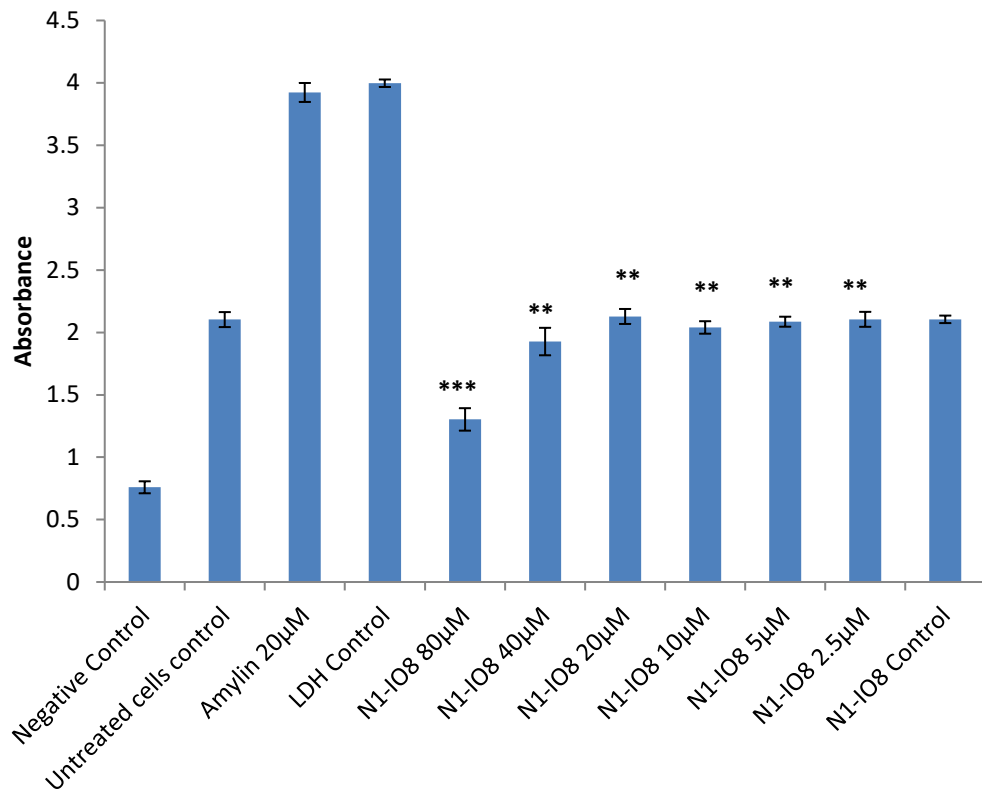


**Figure 6.5:** N1-IO8 inhibits the toxic effects of human amylin on pancreatic islet  $\beta$  cells, as measured by LDH assay. Human amylin at 20  $\mu$ M was cytotoxic to cells. N1-IO8 at concentrations of 80, 40, 20, 10, 5 and 2.5  $\mu$ M protected cells from amylin cytotoxicity. The “negative control” bar is the background absorbance without cells. The “untreated cells control” bar represents cell absorbance without any intervention. The “LDH control” bar represents the absorbance of lysed cells. N1-IO8 control is 100  $\mu$ M of IO8 in cell culture. The results are means  $\pm$  SEM, n = 6. One-way ANOVA, Tukey's post hoc test \*P<0.05, \*\*P<0.01, \*\*\*P<0.001.

## **6.6 LDH analysis of N2-IO8 on amylin-induced toxicity PANC-1 human pancreatic cells**

The ability of N2-IO8 peptide to inhibit amylin cytotoxicity was also assessed using the LDH assay, with the same conditions as above. The data presented in figure 6.6 are from a single experiment being carried out in replicates of  $n = 6$  and are representative of two separate experiments with similar results. Results show mean  $\pm$  SEM ( $n = 6$ ). The ‘negative control’ bar is the background absorbance without cells. The ‘untreated cells’ control bar is the absorbance of cells without any intervention. The ‘LDH control’ bar indicates the absorbance of lysed cells. Amylin at  $20 \mu\text{M}$  was significantly cytotoxic to PANC-1 cells and reduced cell viability (figure 6.6). At concentrations of  $80 \mu\text{M}$  (4:1 molar ratio peptide to amylin),  $40 \mu\text{M}$  (2:1 molar ratio peptide to amylin),  $20 \mu\text{M}$  (1:1 molar ratio peptide to amylin),  $10 \mu\text{M}$  (1:2 molar ratio peptide to amylin),  $5 \mu\text{M}$  (1:4 molar ratio peptide to amylin) and  $2.5 \mu\text{M}$ , N2-IO8 significantly decreased the toxic effects of human amylin.

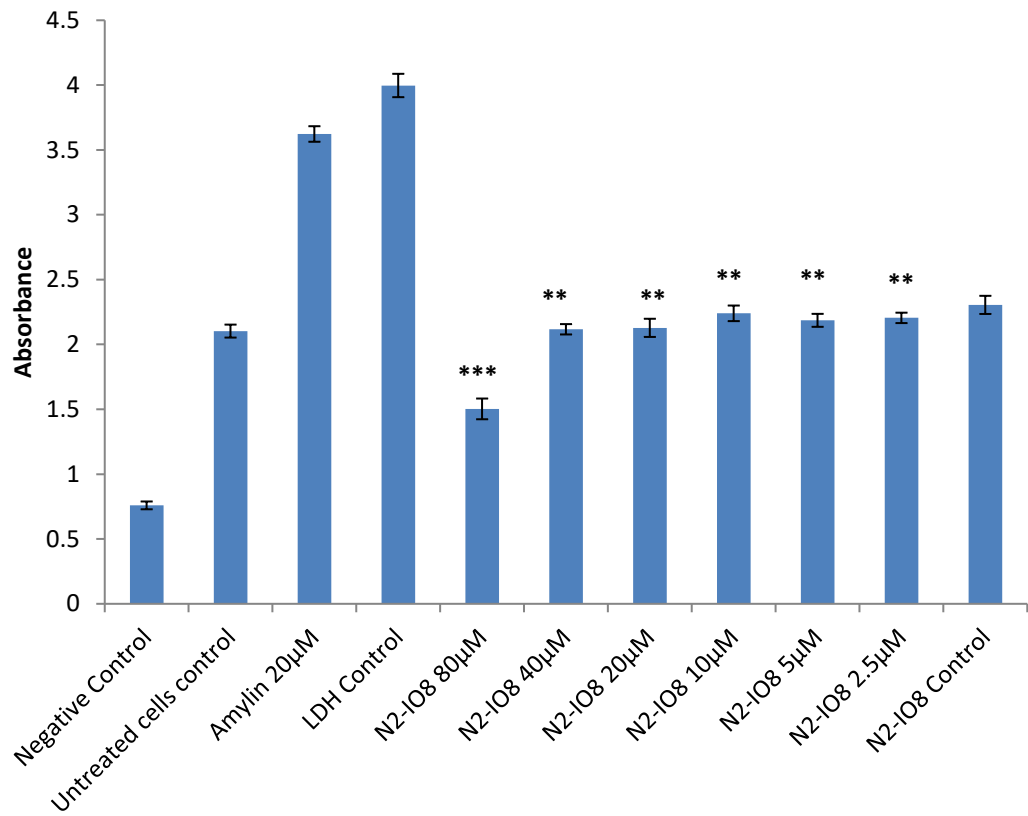


**Figure 6.6:** N2-IO8 inhibits the toxic effects of human amylin on pancreatic islet  $\beta$  cells, as measured by lactate dehydrogenase (LDH) assay. Human amylin at 20  $\mu\text{M}$  was cytotoxic to cells. N2-IO8 at concentrations of 80, 40, 20, 10, 5 and 2.5  $\mu\text{M}$  protected cells from amylin cytotoxicity. The “negative control” bar is the background absorbance without cells. The “untreated cells control” bar represents cell absorbance without any intervention. The “LDH control” bar represents the absorbance of lysed cells. N2-IO8 control is 100  $\mu\text{M}$  of IO8 in cell culture. The results are means  $\pm$  SEM,  $n = 6$ . One-way ANOVA, Tukey’s post hoc test \* $P < 0.05$ , \*\* $P < 0.01$ , \*\*\* $P < 0.001$ .

## 6.7 Peptide Cell Uptake Experiment

In the studies above, it was shown that the introduction of IO8, N1-IO8 and N2-IO8 was able to reverse the cytotoxic effects of human amylin. In this study, the ability of the most potent inhibitory peptides, IO8, N1-IO8 and N2-IO8, to penetrate into cultured cells was assessed. 10  $\mu$ M of Alexa-Fluor 488 Fluorescein-labelled versions of IO8 (Flu-IO8), N1-IO8 (Flu-N1-IO8) and N2-IO8 (Flu-N2-IO8) peptides in media were incubated with cells for 10 mins and 1 hr to assess their ability to penetrate the cell membrane. Flu-IO8, Flu-N1-IO8 and Flu-N2-IO8 all penetrated the cell membrane in as little as 10 mins, although in each case a further increase in green fluorescence was observed after incubation for 1 hr. Some auto-fluorescence was observed in all control samples. The blue stain seen in all samples is the nucleus counter-stained with DAPI. The data below are representative of three different experiments carried out under the same conditions.

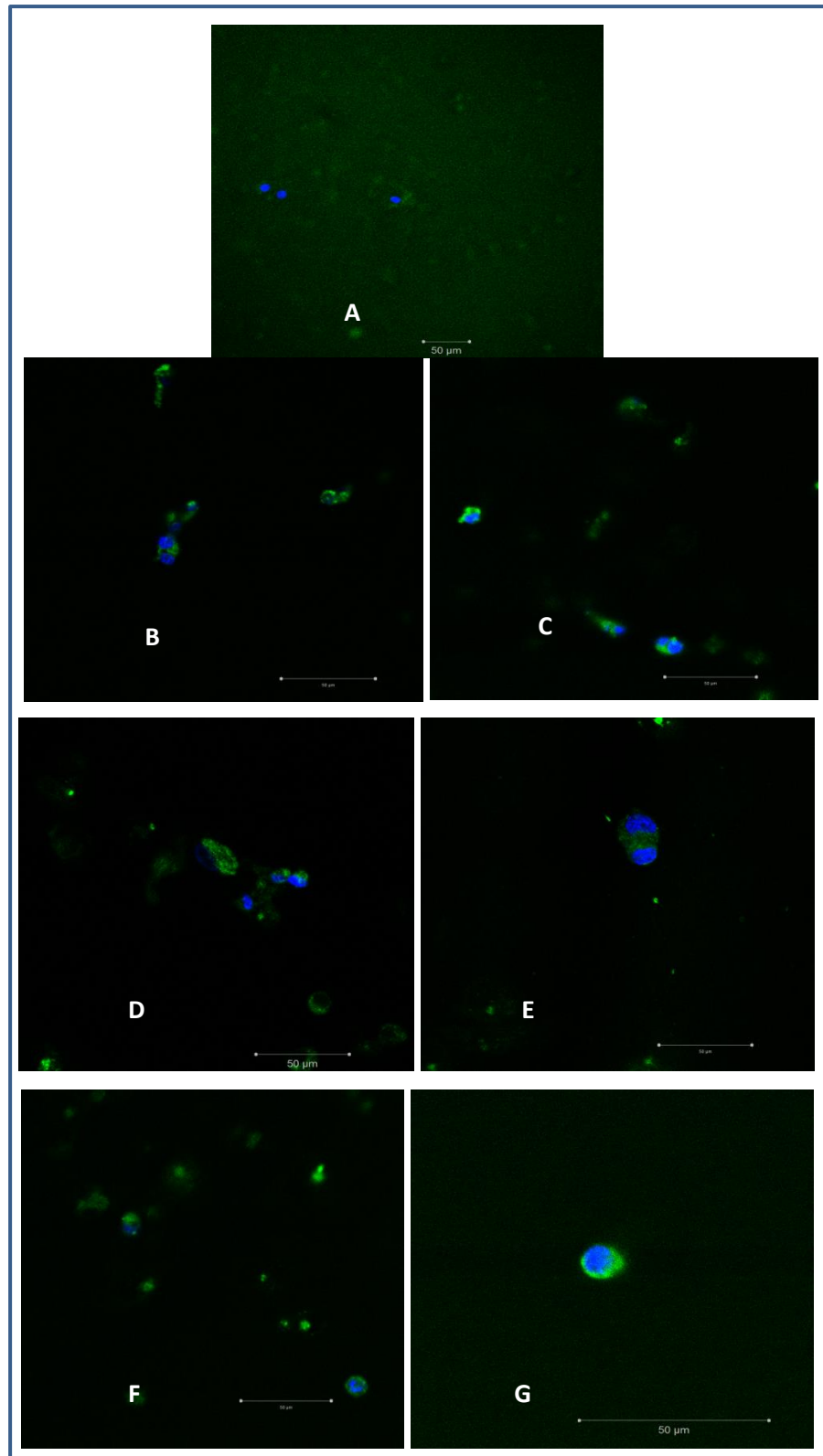


Figure 6.7: Confocal microscope images of PANC-1 cells exposed to fluorescently tagged peptides. (A) Media only, (B) 10  $\mu$ M Flu-IO8 for 10 mins, (C) 10  $\mu$ M Flu-IO8 for 1 hr, (D) 10  $\mu$ M Flu-N1-IO8 for 10 mins, (E) 10  $\mu$ M Flu-N1-IO8 for 10 mins, (F) 10  $\mu$ M Flu-N2-IO8 for 10 mins, (G) 10  $\mu$ M Flu-N2-IO8 for 1 hr. Magnification = 40X. Scale bar = 50  $\mu$ m.

## 6.8 Discussion

Given that pro-insulin and pro-amylin are processed together in the same islet secretory vesicles, an impaired processing and further hypersecretion of immature pro-amylin are likely to occur (Park and Verchere, 2001; Clark *et al.*, 1993). Elevated levels of secreted amylin and pro-amylin result in the accumulation of islet amyloid deposits which are toxic to pancreatic  $\beta$  cells leading to a decrease in  $\beta$  cell mass and subsequently  $\beta$  cell failure (Kogire *et al.*, 1991; Westermark and Grimelius, 1973).  $\beta$  cell depletion, loss of function and death are the main features of T2DM (Halban *et al.*, 2014; Ashcroft and Rorsman, 2012) and are associated with the formation of islet amyloid as well as inflammation, glucolipotoxicity and cholesterol accumulation (Poitout and Robertson, 2002; Halban *et al.*, 2014; Donath and Shoelson, 2011). The deposition of islet amyloid has also been proved to play a part in the failure of islet cell transplantation. Studies have revealed the presence of amyloid deposits in the transplanted human islets of patients with islet graft failure, and these deposits have also been shown to form quickly following islet transplantation from humans into nude mice (Westermark *et al.*, 2012; Westermark *et al.*, 2011; Udayasankar *et al.*, 2009). These findings are related to a study on mice which showed that the formation of islet amyloid precedes hyperglycaemia and is linked with the loss of  $\beta$  islet cells. Further studies have also elucidated that amylin aggregation and hyperglycaemia are contributing factors in the development of diabetes-associated cardiovascular disease (Despa *et al.*, 2014; Gilead and Gazit, 2008).

Our results are consistent with previous data and have demonstrated that amylin is cytotoxic to pancreatic  $\beta$  cells in both MTS and LDH assays. The IO8 peptide inhibited amylin cytotoxicity. In addition, N1-IO8 and N2-IO8 also impeded the cytotoxic effects of amylin on human pancreatic islet  $\beta$  cells in culture. It is possible that these peptides could be used as part of a therapeutic approach for the treatment of amyloid islet cytotoxicity in type 2 diabetic patients. The mechanism by which these peptides interact with amylin in culture is not yet known. Our results confirm the association between amylin aggregation and  $\beta$  cell death and support a previous study where human amylin decreased  $\beta$  cell viability by about 25 - 40 % (Scrocchi *et al.*, 2002), while the incubation of the peptide SNNFGA with amylin impeded amylin cell toxicity by 25 – 50 %. Although a number of protein based inhibitors have been designed for the inhibition of amyloid beta ( $A\beta$ ), less work has been done on the inhibition of amylin amyloid aggregation. In a previous study, segments of amylin sequence were inserted into the loop area of a stable IgG variable domain, leading to the inhibition of amylin amyloid formation and cytotoxicity (Ladiwala *et al.*, 2012). Studies have also shown that the calcium binding protein Nucleobindin 1 (NUCB1) inhibited amylin fibril formation and cytotoxicity (Gupta *et al.*, 2012). Progress has been made with designing inhibitors of amylin aggregation; however, more work still needs to be done to develop inhibitors of amylin amyloid formation which will also be effective in protecting cells from the cytotoxic effects of human amylin.

It has been proposed that amyloid deposition may lead to damage of  $\beta$  cell function a long time before  $\beta$  cell death (Porte and Kahn, 2001). Studies have

shown that amylin-mediated cell death is through the interaction of amylin fibrils with the cell membrane (Lorenzo *et al.*, 1994; Janson *et al.*, 1999). Another study proposed that amylin-mediated cell death is through the biochemical, morphological and structural alterations associated with apoptosis (Saafi *et al.*, 2001). Oxidative stress also plays a key role in cell degeneration upon exposure to amyloid toxic aggregates (Sochocka *et al.*, 2013; Butterfield *et al.*, 2013) and antioxidant treatments have been found to have protective properties against amylin toxicity (Zampagni *et al.*, 2012; Choi *et al.*, 2012). Studies on nerve tissue showed that ageing and oxidative stress impacts on cell viability and decrease proteasome action and expression levels (Rogers *et al.*, 2012; Keller *et al.*, 2002) leading to build-up of misfolded protein and subsequent damage by reactive oxygen species (ROS) (Fratta *et al.*, 2005). The reason behind the production of ROS following protein aggregation, for example in A $\beta$ 42 (Brunelle and Rauk, 2002), is not fully understood, although certain processes are involved. The production of hydrogen peroxide from metal ions such as Cu (I) and Fe (II) also lead to oxidative stress (Tabner, 2002; Turnbull *et al.*, 2001). Intracellular oxidative stress is typically linked to cell membrane disruptions by toxic species alongside a loss of plasma membrane protein regulation (Mattson *et al.*, 1999) and/or damage to mitochondrial function. The mitochondria play a key role in oxidative stress and apoptosis. The neurotoxicity of A $\beta$  is thought to occur through the introduction of Ca<sup>2+</sup> to the mitochondria of the neurons, resulting in increased membrane permeability (Du and Yan, 2010) and subsequent discharge of apoptotic inducers like cytochrome c. Both intracellular and extracellular amyloid toxic aggregates damages cell functions including cell signalling, synaptic communication with cell membrane

mitochondria function, which ultimately leads to apoptotic cell death and sometimes to necrosis (Bucciantini *et al.*, 2005; Ross, 2002; Morishima, 2001). Although amylin toxicity has been suggested to arise from the disruption of membrane integrity (Janson *et al.*, 1999; Trikha and Jeremic, 2011), the main cause of cell death associated with amyloid toxicity is not clear. The degree of membrane permeabilization by amylin is influenced by several factors including pH, lipid to peptide ratio, and ionic strength and increased levels of anionic lipids significantly induce amylin membrane interactions (Trikha and Jeremic, 2011). Studies are currently being carried out on amylin-induced model membrane damage. Previous studies have shown that membrane damage occurs by a detergent process; however other studies have shown that these membrane disruptions occur by pore-like mechanisms (Janson *et al.*, 1999; Bucciantini *et al.*, 2005). Further studies have indicated that the process involving fibril growth can impact on membrane damage, contrarily; some other studies suggest that  $\beta$  sheet formation do not play a role in membrane disruption (Cao *et al.*, 2013; Last *et al.*, 2011; Engel *et al.*, 2008; Anguiano *et al.*, 2002). It is likely that a combination of processes are involved and the exact mechanism involved is determined by the membrane system used (Schlamadinger and Miranker, 2014; Brender *et al.*, 2012). It is important to note that the introduction of amylin induces a number of toxic effects on a variety of related cells proposing that there are other mechanisms of cytotoxicity other than nonspecific membrane damage (Law *et al.*, 2010).

The main cause of cell death associated with amyloid toxicity is not clear, however, a number of overlapping cellular mechanisms and triggered

downstream signalling pathways result in amyloid toxicity. These comprises of both receptor-mediated and non-receptor-mediated mechanisms. Cell membrane permeabilization, oxidative stress, membrane damage, Endoplasmic reticulum (ER) stress, triggering of cell death signalling pathways and increased secretion of pro-inflammatory cytokines all play a part in amylin toxicity (Bram *et al.*, 2014; Gupta and Leahy, 2014; . Park *et al.*, 2012; Saafi *et al.*, 2001; Cooper *et al.*, 2010; Zhang *et al.*, 2003). Disputes have however arisen on the role of ER stress on amylin-induced toxicity *in vivo*. Studies on transgenic mice show that overexpressing amylin revealed the role of ER stress in mediating amylin-induced  $\beta$  cell defect. Also, inducing amylin exogenously has been shown to trigger ER stress (Gurlo *et al.*, 2010; Casas *et al.*, 2007). Further research has also proved that ER defects and ER related protein degradation induce amylin toxicity associated with  $\beta$  cell death (Westermarck *et al.*, 2011). On the contrary, a study on cultured islet cells suggested that increased physiological levels of human amylin did not trigger ER stress (Hull *et al.*, 2009). Autophagy disorders have been thought to contribute to amyloid protein toxicity. Studies have shown that the overexpression of human amylin in islet  $\beta$  cells leads to defects in autophagy (Rivera *et al.*, 2011; Gupta *et al.*, 2014). Impeding autophagy promotes amylin induced  $\beta$  cell apoptosis while triggering autophagy prevents amylin induced cytotoxicity (Rivera *et al.*, 2011; Gupta *et al.*, 2014). Another cause of amyloid toxicity could be chronic inflammation as seen in local and systemic amyloidosis. Aggregated human amylin stimulate localized inflammatory response through the activation of inflammasomes leading to  $\beta$  cell defects (Masters *et al.*, 2010; Sheedy *et al.*, 2013). Inflammasomes consist of multiproteins that dictate a wide variety of proinflammatory stimuli and

release active caspase-1, which triggers cytokines IL-1 $\beta$  and IL-18. IL-1 $\beta$  is believed to directly impact on amylin-induced  $\beta$  cell death and defects (Masters *et al.*, 2010; Sheedy *et al.*, 2013). The development of an effective therapeutic against the toxicity of amyloid will therefore involve more insight into the main characteristics of cell/tissue degeneration when they come in contact with toxic amyloid.

Regardless of the great potential of using proteins or peptides as treatments for various diseases, it is important that these molecules are capable of penetrating the cell membrane into their target cells. The results presented here show that the peptides under study were taken up by live human pancreatic PANC-1 cells when added exogenously. Fluorescently-labelled IO8, N1-IO8 and N2-IO8 were used for these experiments. Confocal images of PANC-1 cells exposed to 1  $\mu$ M of Flu-IO8, N1-Flu-IO8 or N2-Flu-IO8 for 10 mins revealed an accumulation of fluorescence inside the cells (figure 6. 3.1). Our peptides demonstrated rapid entry into cultured cells, suggesting that they possess transducing properties. The mechanism by which these cells absorb the peptide is not fully understood but it is probably by protein transduction. Cellular uptake is regulated by protein-transduction domains. Although our peptides were not attached to a peptide delivery system also known as cell-penetrating peptides (CPPs), they still transverse the cell membrane. However, an effective peptide delivery system could be necessary to enhance cellular uptake and give high cell specificity. It is pharmacologically important that efficient delivery systems are developed to allow effective uptake and accurate drug targeting (Veldhoen *et al.*, 2008; Torchilin, 2008). While great progress has been made, there is still an

apparent need for effective protein delivery systems which protect proteins from degradation, show excellent biological activity, possess excellent biosafety profile for *in vivo* therapeutic use, efficiently internalize in individual target cells, tissues and organs, and are non-cytotoxic (Heitz *et al.*, 2009). Despite the fact that the mechanism of cellular uptake by CPPs is highly disputed, they are still widely used to convey the delivery of pharmacological molecules intracellularly (Dietz *et al.*, 2004; Tamsamani and Vidal, 2004) since they are non-cytotoxic and possess excellent cell specificity (Patel *et al.*, 2007). Most biomolecules including antisense oligonucleotides (Astria-Fischer *et al.*, 2002), liposomes (Torchilin *et al.*, 2001), peptide nucleic acids (Pooga *et al.*, 1998) and nanoparticles (Lewin *et al.*, 2000) have been delivered by the protein transduction process. In addition, various proteins like HIV-1 Tat and HSV-1 VP22 have been proven to cross the cell membrane through the process of protein transduction with their biological activity conserved as they reach the nucleus (Prochiantz, 2000, Green and Loewenstein, 1998). Thus, conjugation therapeutic molecules with CPPs may be an important approach to enhance the pharmacokinetic properties of drugs.

## 6.9 Conclusion

Major advancement has been made in amylin amyloid formation research, however a lot of work is still required to understand the nature of toxic species, verify amyloid initiation sites *in vivo*, unravel the mechanism of amylin amyloid formation and  $\beta$  cell death *in vivo* and *in vitro*, which play a vital role in amylin toxicity. There are currently no clinically approved inhibitors of amylin cytotoxicity and only a few drug-like inhibitors of amylin aggregation have been published, and so more work in this area is required. The peptides under development here have been shown to penetrate into human pancreatic islet cells, and also to protect islet cells from the toxicity of human amylin; the peptides on their own were not toxic to the cells. These findings hold huge potential for the development of these inhibitors as peptide-based therapeutics and will play a key role in the development of new peptide sequences for the inhibition of amylin fibril formation.

# Chapter 7

## General Discussion and Conclusion

### 7.0 Discussion

T2DM is the most widespread endocrine disorder (Hossain *et al.*, 2007), characterised by a reduction in  $\beta$  cell mass, insulin resistance, and the presence of amyloid deposits in the pancreas, the main component being human islet amyloid polypeptide otherwise called amylin (Westermarck *et al.*, 1987). Amyloid is a particular type of protein aggregate described by characteristic fibrillar morphology, initiated by structure-specific molecular interactions in an ordered pattern (Cornwell *et al.*, 1995). Studies have shown that amyloid formation occurs through a nucleation-dependent aggregation process (Harper and Lansbury, 1997). Nucleation-dependent aggregation is different from disordered aggregation as it is initiated from the production of a defined intermediate, the aggregation nucleus, through the addition of monomeric species (Harper and Lansbury, 1997). The monomers are the smallest stable species. However, the smaller dimers and oligomers have been shown to be extremely unstable. The molecular basis of protein amyloidogenicity is not fully understood and the classification of the mechanisms that initiate the development of these pathological deposits in tissues which are the hallmark of numerous life threatening diseases are presently being investigated. A number of factors influence protein fibrillation including, electrostatic charge, protein hydrophobicity and the predisposition to form secondary structures for example,

$\alpha$ -helix and  $\beta$ -sheet (DuBay *et al.*, 2004; Chiti *et al.*, 2003), as well as pH and ionic strength (Chiti *et al.*, 2003; Tartaglia, *et al.*, 2008). In addition, fluctuations in glycosylation levels may increase the tendency of peptide aggregation (Makimattila *et al.*, 2000). Also, *in vivo* alterations in pH, changes in amylin concentration and changes in molecular binding stimulate formation of amyloid fibrils by changing the configuration of amylin from a random coil to a  $\beta$  sheet structure (Hoopener *et al.*, 1999). Partial enzymatic processing of amylin from its precursor pro-amylin have been observed in type 2 diabetes, and may possibly stimulate the “seeding” of amyloid fibrils (Higham *et al.*, 2000). Studies have shown that the overproduction of amylin in transgenic mice as well as other factors, including increased fat in mouse chow (Verchere *et al.*, 1996) or genetic traits that promote obesity and insulin resistance in mice (Soeller *et al.*, 1998; Hoppener *et al.*, 1999), increase amyloid formation. Further studies have shown that homozygous transgenic mice resulted in increased production of amylin enough for the formation of amyloid (Janson *et al.*, 1996; Hoppener *et al.*, 1999). However, other studies have shown that overproduction of amylin is not necessary for the development of amyloid in mouse models (Hoppener *et al.*, 1993; Verchere *et al.*, 1997). These studies suggest that there is a complex association between the overproduction of amylin, amyloid formation and the pathology of T2DM.

The 20-29 segment of amylin is regarded as the amyloidogenic region of the peptide and has been associated with the formation of fibrils (Moriarty and Raleigh, 1999; Westermark *et al.*, 1990). Although residues 20-29 of amylin play a crucial role in the formation of fibrils, other residues may also be

involved in fibril formation. A study suggested that the amylin 14-20 fragment forms amyloid fibrils (Sawaya *et al.*, 2007). Another study reported the role of aromatic-aromatic interactions in fibril formation (Azriel and Gazit, 2001). However, a study on 3 human amylin aromatic residues at positions 15, 23, and 37 suggested that aromatic residues are not important in the formation of amylin fibrils, as triple mutants lacking aromatic residues were seen to form fibrils *in vitro*. Moreover, this substitution reduced the rate of fibril formation and modified the propensity of amylin to aggregate. Further research reported that amylin amyloidogenic regions spans the 30-37 residues of the C-terminal region and in aqueous media, both human and rodent amylin 30-37 are likely to form amyloid fibrils (Nilsson and Raleigh, 1999). Another amyloidogenic region spanning residues 8-20 has also been reported to form  $\beta$  sheet fibrils which are structurally identical to *in vivo* amyloid (Jaikaran *et al.*, 2001). The reason for these differences is not fully understood. This is, however, likely to result from the use of dissimilar techniques in studying amyloid fibrillization.

Although several amyloidogenic regions of human amylin have been identified, this study was concerned with developing peptide inhibitors from the binding region of human amylin corresponding to amino acids 11-20 (with sequence RLANFLVHSS), and their impact on fibrillogenesis of the full-length human amylin 1–37 peptide were assessed. It has been suggested that this region is responsible for the binding of two misfolded amylin molecules, after which they begin to aggregate (Mazor *et al.*, 2002). Thus, if we are able to prevent two amylin molecules from binding, we may be able to prevent their aggregation. We initially generated 7 peptide inhibitors to target the binding region of human

amylin 1–37, and investigated the ability of each of these peptides to influence fibril formation. The peptide fragments were derived from human amylin 11-20 (IO1), as well as pentapeptides derived from human amylin 11-15 (IO2), 12-16 (IO3), 13-17 (IO4), 14-18 (IO5), 15-19 (IO6) and 16-20 (IO7). These peptides were assessed using the Th-T assay. The Th-T fluorescence assay is a key indicator of the presence of amyloid fibrils, as it interacts with the  $\beta$ -pleated sheet-containing amyloid fibrils leading to increase in Th-T fluorescence (Biancalana and Koide, 2010). IO2, IO3, IO4, IO5 and IO7 peptides showed some inhibitory effects on the aggregation of full length human amylin 1-37; however, IO1 and IO6 showed no significant effect. In addition, IO1, IO3, IO4, IO5 and IO7 significantly stimulated amylin aggregation at low concentrations (figure 3.1.1). Data from IO1, IO2, IO6 and IO7 showed unusual curves quite unlike the others, revealing a strange hump along the curve. It is likely that these peptides are not properly bound to the full length amylin sequence at the concentrations where the hump appears. It is also possible that the peptides could be insoluble to some extent at these higher concentrations (figure 3.1.1). While these peptides did not appear to completely inhibit fibril formation, it is likely that the amyloid fibrils has been inhibited but the aggregates present have been converted into another form, such as amorphous aggregates, which are still Th-T positive, but not fibrillar in nature, giving rise to the Th-T signal still observed. IO4 and IO5 showed more promising results compared to other peptides (figure 3.1.1), but they failed to reduce aggregation to less than 50%. IO4 and IO5 were thus considered for further investigation. These results are consistent with those of other studies and suggest that peptide fragments as well as human amylin derivatives are able to inhibit fibril formation *in vitro*.

However, new inhibitors are desired as many of the reported inhibitors only work when they are in molar excess (Kapoor *et al.*, 2010; Yan *et al.*, 2006; Meng, *et al.*, 2010; Saraogi *et al.*, 2010). A study on peptide fragments corresponding to human amylin residues 20-25 (SNNFGA) and human amylin residues 24-29 (GAILSS) showed strong inhibitory effect on  $\beta$ -sheet transition and amyloid aggregation. However, this inhibition was achieved at 10:1 and 20:1 molar ratios of peptide to amylin, where the peptide is in molar excess compared to amylin, and although SNNFGA significantly improved cell viability by 25%, GAILSS had no significant effect on amylin-induced cytotoxicity (Scrocchi *et al.*, 2002). Another study showed that engineered, soluble forms of the human  $\text{Ca}^{2+}$  binding protein nucleobindin 1 (NUCB1) impedes the aggregation of amylin at substoichiometric levels and disaggregates preformed fibrils, however, this anti-amyloidogenic effect was only seen in the absence of  $\text{Ca}^{2+}$  (Gupta *et al.*, 2012).

Given the encouraging results from this study, further experiments were carried out on the IO4 and IO5 peptides. The IO4 and IO5 peptides had their amino acid sequences combined to give IO8 (amino acid sequence:  ${}_{-2}\text{HN-RGANFLVHGR-NH}_2$ ). Considering that retro-inverted peptides are more stable to proteolysis, the retro-inverso form of IO8 (RI-IO8:  $\text{Ac-rGhvlfnGr-NH}_2$ ) was derived by sequence reversal and substitution of L- with D- amino acids. The Th-T assay was used to monitor the effects of IO8 and RI-IO8 on amylin aggregation. The IO8 peptide showed a strong inhibitory effect on amylin aggregation (figure 3.1.2). Also, IO8 did not appear to stimulate amylin aggregation at low concentrations. Congo red experiments also confirmed the inhibitory effect of IO8 on amylin aggregation (figure 3.2.1). The relative density and morphology

of fibrils in the presence of IO8 were also visualized using negative stain TEM. No fibrils were observed at concentrations of 100  $\mu$ M, 50  $\mu$ M and 25  $\mu$ M of IO8 (figure 4.1), relative to 25  $\mu$ M amylin. However, at a lower concentration of 5  $\mu$ M IO8, fibrils were formed but had an altered morphology; they were less compact. IO8 also disaggregated pre-existing amylin fibrils (figure 4.5.1), with a characteristic less dense fibril mesh being observed. These results support the Th-T and Congo red data, and suggest that IO8 is a strong inhibitor of amylin fibril formation. However, RP-HPLC stability analysis proved that IO8 was unstable to proteolytic degradation and in plasma (figure 5.1.1). It comes with no surprise that IO8 was completely degraded both in plasma and in the presence of proteolytic enzymes as L-analogs of peptides are quickly metabolized (Kellock *et al.*, 2016). On the other hand, RI-IO8 had no inhibitory effect on amylin aggregation, except at 100  $\mu$ M (4:1 molar ratio RI-IO8 to amylin), where the peptide reduced amylin aggregation to 77% of a non-inhibited control. At lower concentrations (figure 3.1.2) RI-IO8 significantly stimulated amylin aggregation. This finding was unexpected and suggests that RI-IO8 does not bind in the same way to human amylin as IO8, resulting in its non-inhibitory effect and facilitation of aggregation at low concentrations. The Congo red experiments also confirmed the non-inhibitory effect of RI-IO8 on amylin aggregation (figure 3.2.2). This was further supported by TEM studies where RI-IO8 greatly increased amylin fibril formation (figure 4.2). A characteristic denser fibril mesh was observed in the presence of RI-IO8. Unlike IO8, RI-IO8 did not disaggregate pre-existing amylin fibrils (figure 4.5.2). This result with RI-IO8 is contrary to a previous study, where the retro-inverso peptide RI-OR2 developed against amyloid beta ( $A\beta$ ) oligomers in Alzheimer's

disease was shown to significantly inhibit fibril formation and rescue cells from the toxic effects of A $\beta$ , and was also shown to be highly resistant to proteolysis (Taylor *et al.*, 2010). Since the retro-inverso peptide RI-IO8 did not inhibit amylin aggregation, other methods for making peptides resistant to proteolysis, such as N-methylation, were considered.

The results presented here indicate that IO8 is the most potent inhibitor of human amylin aggregation tested so far, and this is highlighted by comparison of the effects of IO8 on amylin aggregation with ANFLVH (Potter *et al.*, 2009) and NMeG24 NMeI26 (Sellin *et al.*, 2010) peptides, which have been reported to inhibit amylin fibril formation in the literature. NMeG24 NMeI26 is a modified form of amylin 22-27 fragment (NFGAIL), with N-methylation at the amide bonds G24 and I26 (Sellin *et al.*, 2010). ANFLVH could not be dissolved in aqueous solution and thus could not be used for the experiment. It is interesting to note that the peptide ANFLVH reported in the literature has a similar amino acid sequence to our IO8 peptide inhibitor (RGANFLVHGR-NH<sub>2</sub>, the similar sequence is underlined). However, our peptide possess a cationic Arginine (Arg) added at both N- and C-termini via a Glycine (Gly) spacer. The insolubility observed with the ANFLVH peptide provides further support for the rationale of placing a cationic Arg at the N- and C-termini of the peptides under study here, via a Gly spacer. The Arg and Gly residues help to facilitate the interaction between amylin and the peptide inhibitors, as well as promote the solubility of the peptides, while preventing them from self-assembly. This finding is consistent with that of Taylor *et al.* (2010) who found that Arg and Gly residues facilitate peptide solubility and prevent self-assembly. Although the ANFLVH peptide has been reported to inhibit amylin fibril formation *in*

*vitro* and to significantly increase cell viability in human islet cultures (Potter *et al.*, 2009), it should be noted that these effects were observed at equimolar and 20 fold molar excess concentrations of the peptide. In addition, at even higher concentrations of ANFLVH, incomplete inhibition of islet amyloid formation was observed, as some deposits were still seen in islets at high microscopic magnification. Furthermore, ANFLVH was reported to disaggregate pre-existing amyloid fibres and reduced amyloid load to ~33% compared to untreated cultures only when the peptide was in 10 and 20 fold molar excess of amylin (Potter *et al.*, 2009). The IO8 peptide inhibits amylin aggregation and disaggregates pre-existing amylin fibrils (figure 4.5.1) at much lower concentrations than the ANFLVH peptide. It should be noted that, for an inhibitor to be an effective drug it should be able to work at low concentrations, as high concentrations may not be biologically tolerable and may also be toxic to cells. The IO8 peptide was also assessed alongside NMeG24 NMeI26. IO8 showed strong inhibitory effects on amylin aggregation. In contrast to the study reported in the literature (Sellin *et al.*, 2010), no evidence of inhibition of amylin aggregation was observed upon addition of NMeG24 NMeI26. NMeG24 NMeI26 was also seen to significantly promote fibril formation at lower concentrations (figure 3.1.3). It is possible that NMeG24 NMeI26 was unable to bind to full length amylin and was thus incapable of exerting inhibitory effects on amylin, as it is derived from the amyloidogenic region (NFGAIL) of human amylin and not the binding region. To confirm this, we designed another peptide from the amyloidogenic region of human amylin (amyloidogenic sequence underlined: H<sub>2</sub>N-RGNNFGAILSGR-NH<sub>2</sub>). ThT studies showed that this peptide did not inhibit amylin aggregation, but rather stimulated aggregation (figure

3.1.4) at higher concentrations. This finding is in agreement with Andreasen *et al.* (2012) who showed that two human amylin derived peptides with sequence NFGAIL and SNNFGAILSS were unable to inhibit the fibrillation of human amylin, suggesting their inability to bind to existing fibril surfaces. Another finding showed that NFGAIL causes an immediate conformational alteration to  $\beta$ -sheet of amylin, suggesting that NFGAIL, rather than having inhibitory properties, promotes fibril formation (Scrocchi *et al.*, 2002). With IO8 being the most promising peptide inhibitor, it was stabilised from proteolytic degradation through N-methylation of alternate amino acid residues, to give N1-IO8 (H<sub>2</sub>N-R-G-Am-N-Fm-L-Vm-H-G-R-NH<sub>2</sub>) and N2-IO8 (H<sub>2</sub>N-R-G-A-Nm-F-Lm-V-Hm-G-R-NH<sub>2</sub>). Th-T and Congo red results showed that both N1-IO8 and N2-IO8 significantly inhibited amylin aggregation (figure 3.1.6, figure 3.2.2, figure 3.2.3). At 100  $\mu$ M, N1-IO8 and N2-IO8 decreased amylin aggregation to 15% and 12%, respectively, compared to amylin alone. TEM studies also confirmed that N1-IO8 at 100  $\mu$ M, 50  $\mu$ M and 25  $\mu$ M, completely impeded the formation of amylin fibrils, but thread-like amyloid fibrils were observed in the presence of 5  $\mu$ M N1-IO8 (figure 4.3). In addition, N2-IO8 showed completed inhibition of amylin fibrils at concentrations of 100  $\mu$ M, 50  $\mu$ M, 25  $\mu$ M, and 5  $\mu$ M (figure 4.4). N1-IO8 at 100  $\mu$ M completely disaggregated pre-existing amylin fibres and at 50  $\mu$ M (figure 4.5.3), partially disaggregated pre-existing amylin fibres, while N2-IO8 completely disaggregated pre-existing amylin fibres at both 100  $\mu$ M and 50  $\mu$ M (figure 4.5.4). N1-IO8 (figure 5.2.1- figure 5.2.8) and N2-IO8 (figure 5.3.1- figure 5.3.8) were also stable against proteolytic degradation, and in plasma, for at least 48 hrs. N-methylated (NMe) derivatives of A $\beta$  (25–35) have been reported to impede the aggregation of fibrils and prevent cytotoxicity, and

studies have suggested that analogues of amylin with amide bonds methylation do not form fibrils (Yan *et al.*, 2007; Yan *et al.*, 2006). Another peptide inhibitor designed to target the amyloidogenic region of human amylin showed ~50% decrease in amylin-induced toxicity (Scrocchi *et al.*, 2002).

Given the significant inhibitory effect of IO8 on amylin fibril formation, we investigated the effect of amylin on PANC-1 human pancreatic islet  $\beta$  cells and the ability of the IO8 peptide to inhibit amylin-induced cytotoxicity using the CellTiter 96 aqueous one solution cell proliferation (MTS) and the CytoTox-ONE Homogeneous Membrane Integrity (LDH) assays. In both experiments, externally adding human amylin to PANC-1 cells was significantly cytotoxic to the cells, resulting in decreased cell viability. However, the addition of IO8 (figure 6.1, figure 6.4), N1-IO8 (figure 6.2, figure 6.5) and N2-IO8 (figure 6.3, figure 6.6) significantly protected PANC-1 cells from the cytotoxic effects of human amylin. The toxic effect of amylin was also shown to be concentration dependent, with increased toxicity observed at a higher concentration. These findings support the idea that amylin and insulin protein levels are maintained at a molar ratio of ~1:100 of amylin to insulin in normal pancreatic  $\beta$  cells. However, in diseases, it is maintained at a molar ratio of ~1:20 of amylin to insulin (Knight *et al.*, 2008; Hull *et al.*, 2004). The increase in amylin secretion in diseased conditions may result in increases in cytotoxicity. Deposition of amyloid plaques in pancreatic  $\beta$  cells have been observed in humans with T2DM. (Chiti and Dobson, 2006). Amyloid deposits in the pancreas have been shown to result in the apoptosis of pancreatic  $\beta$  cells (Hoppener *et al.*, 2000) and the interaction of amylin with lipid membranes promote fibril formation (Engel *et al.*, 2006). Studies have shown that human amylin forms channel like pores

which penetrate the membrane and alter barrier properties (Quist *et al.*, 2005), but the non-amyloidogenic mouse amylin does not form pores in membrane (Mirzabekov *et al.*, 1996). However, studies on human neuroblastoma cells showed that the addition of oligomeric amylin to cells loaded with a fluorescent dye resulted in the cellular permeability of the dye (Demuro *et al.*, 2005). This suggests that when amylin is added to the extracellular environment, it is cytotoxic through general disruption events and not by a given ion pore. Since human amylin is situated at cellular membranes in the pancreatic islets, and is associated with alteration of the membrane structure, it is likely that the membrane may be a target for cytotoxic amylin, resulting in the death of insulin producing  $\beta$  cells (Janson *et al.*, 1999; Saafi *et al.*, 2001). This is supported by Huang *et al.* (2007) who reported that the main targets for cytotoxic amylin are the Endoplasmic Reticulum (ER) and mitochondrial membranes leading to ER stress and  $\beta$ -cell apoptosis. In addition, small human amylin aggregates have been proven to be cytotoxic in cell cultures, and these aggregates have been shown to alter the membrane structure (Janson *et al.*, 1999). Studies have shown that amylin oligomers form pores in membrane, permitting small sized molecules to pass through the membrane; however, upon maturation of the fibrils, the pores disappeared and membrane damage was minimized (Anguiano *et al.*, 2002; Porat *et al.*, 2003). Mature fibrils have been found to be less toxic to cells and they produced less membrane interruption than oligomeric amylin (Demuro *et al.*, 2005; Konarkowska *et al.*, 2006). Studies have however hypothesized that amylin-induced membrane disruption is not triggered by a given amylin specie, for example oligomers, but through the process of fibril development at the cell membrane (Knight *et al.*, 2006; Lopes *et al.*, 2007).

Research has also suggested that amylin fibril growth at cell membranes gives rise to membrane impairment. Monomeric amylin is likely to interact with membrane, as it has a high propensity to attach to phospholipid monolayers (Engel *et al.*, 2006; Knight *et al.*, 2006; Lopes *et al.*, 2007). This is supported by another study on Alzheimer's disease-related A $\beta$ , which suggest that the process of amyloid fibrillogenesis is accountable for membrane impairment and not specifically given species (Wogulis *et al.*, 2005). The exact mechanism of action by which amylin oligomers disrupts membranes is however not fully understood.

Studies are being carried out to develop molecules that inhibit amylin-induced  $\beta$ -cell death through the inhibition of amylin fibril formation. A number of these inhibitors are synthetically modified human amylin fragments which do not form fibrils, but are capable of binding to the full length human amylin and impede its fibril formation (Abedini *et al.*, 2007; Porat, *et al.*, 2004; Yan *et al.*, 2006). In our study, IO8, N1-IO8 and N2-IO8 were seen to significantly rescue PANC-1 cells from the toxic effects of human amylin both at 1:1 and 1:4 molar ratios of peptides to amylin. In addition, IO8, N1-IO8 and N2-IO8 were not toxic to normal PANC-1 cells, as no significant difference was observed between cells treated with peptides and control untreated cells. These findings are in agreement with Potter *et al.* (2009), where the addition of full length amylin resulted in 25% of cell death, but the presence of human amylin 13-18 peptide fragments appeared to reverse the toxicity formed by 12.5%, while human amylin 20-25 residues decrease amylin cytotoxicity by 25%. Furthermore, the amylin modified peptide, NF(N-Me)GA(N-Me)IL was

reported to significantly decrease amylin-induced cell damage in RIN-5fm cells (Tatarek-Nossol *et al.*, 2005). Modified full length amylin with N-methylation at positions 24 and 26 has been shown to impede amylin-induced cytotoxicity in RIN-5fm cells (Yan *et al.*, 2006). This is supported by another study which showed that human amylin derived peptides containing residues 20-25 decreased amylin toxicity by 25%, while the peptide containing residues 24-29 did not (Scrocchi *et al.*, 2002). A study reported that dehydrophenylalanine containing peptides inhibit human amylin fibrillization and protects  $\beta$  cells from amylin-induced toxicity (Mishra *et al.*, 2009). Another recent study also showed that the polyphenol, 1,2,3,4,6-penta-O-galloyl-beta-D-glucose (PGG) is a potent inhibitor of amylin aggregation and was found to inhibit amylin aggregation in a 1:1 molar ratio, it was also shown to protect PC12 rat cells from the toxic effects of human amylin, and has been shown to have anti-cancer and anti-diabetic properties (Bruno *et al.*, 2013). Also, a study on two salen derivatives with established antioxidants properties, EUK-8 and EUK-134, significantly impeded amyloid formation at 1:1 and 5:1 drug to protein molar ratios (Bahramikia and Yazdanparast, 2013), with greater inhibitory effect at the 5:1 drug to protein molar ratio. In a recent study, benzbromarone, quercetin, and folic acid exerted inhibitory effects on amylin aggregation. However, benzbromarone and folic acid were cytotoxic to RIN-m5F cells, while quercetin partially protected the cells from the cytotoxic effects of human amylin (López *et al.*, 2016). However, another study reported that quercetin did not inhibit amylin aggregation, whereas Morin, a closely linked flavonoid to quercetin, was reported to inhibit amylin aggregation and also disintegrate preformed aggregates (Noor *et al.*, 2012). These contradictions could be a result of the

varied experimental conditions used. In addition, a human amylin derived peptide marketed as pramlintide, with proline substitutions at positions 25, 28 and 29, has been reported to have undergone clinical trials (Kong *et al.*, 1998; Maggs *et al.*, 2004; Thompson *et al.*, 1998) and administered alongside insulin for management of T2DM. It is important to note that this peptide has not been assessed as an inhibitor of human amylin aggregation or its associated cytotoxicity. Furthermore, the effects of Metformin and Rosiglitazone on amylin aggregation have been studied *in vivo* (Hull *et al.*, 2005). These therapeutic agents of diabetes significantly decreased amyloid deposit formation in the pancreas of amylin transgenic mice (Hull *et al.*, 2005). However, these interventions are only able to manage the disease and not cure the disease. This emphasises the need for developing inhibitors of amylin aggregation, particularly short peptides, as the full length human amylin sequence is hard to synthesize.

Due to the fact that the interaction of amylin and membranes in non-diabetic individuals do not usually cause  $\beta$  cell death (Jaikaran *et al.*, 2001), it is interesting to consider that certain conditions associated with T2DM trigger amylin-induced membrane damage. In insulin resistance, the level of amylin which is co-secreted with insulin is increased; this increase could set off amylin fibril formation. Changes in the ratio of insulin to amylin secretion, as seen in diabetic individuals, may possibly result in a reduced inhibitory effect of insulin on amylin amyloid fibril formation (Jaikaran *et al.*, 2001). Our peptides IO8, N1-IO8 and N2-IO8 significantly decreases amylin aggregation even at a very low molar concentrations of 1:10 (peptide to amylin), suggesting that they are

highly potent in inhibiting amylin-related fibrillogenesis. IO8, N1-IO8 and N2-IO8 also showed significant inhibition of amylin aggregation as observed under the TEM, with N2-IO8 showing even greater inhibitory effect and the only one of the three most potent peptides that completely disaggregates pre-formed amylin fibrils. IO8, N1-IO8 and N2-IO8 also protected PANC-1 cells from the toxic effects of human amylin. The mechanism by which these peptides prevents aggregation of full length human amylin is probably by direct binding of the peptides to full-length amylin to prevent its self-assembly. It is likely that this interaction occurs at the initial stage of protein folding, by making contact with the random coil conformation which would impede amyloidogenic  $\beta$ -sheet formation. Interactions at this stage would prevent amylin aggregation as observed in our study.

## **7.1 Conclusion**

Despite the therapeutic agents of T2DM available in the market, there is still a huge unmet medical need, as the current therapeutics are not able to treat or cure diabetes, but are only able manage the disease. These therapeutics are also not able to prevent diabetes associated complications. Studies to find inhibitors of amylin aggregation and associated cytotoxicity are currently advancing. However, for these peptides to be developed as therapeutics, novel techniques that provide affordable and quick screening of potential drugs for T2DM are required. The data presented here clearly demonstrate that IO8, and the N-methylated peptides, N1-IO8 and N2-IO8, are effective inhibitors of amylin amyloid formation and also protect cells from the toxic effects of human amylin

in cell culture. N1-IO8 and N2-IO8 were found to be stable to proteolytic degradation and in plasma and while N1-IO8 partially disaggregated pre-existing fibrils, N2-IO8 completely disaggregated already-formed amylin fibrils. N2-IO8 demonstrates inhibitory effects on amylin aggregation even at substoichiometric ratios, and possibly binds to amylin oligomeric species, and has been shown to completely disaggregate amyloid formation when added to the lag phase of the amyloid formation pathway. It thus holds huge potential for treating individuals already presented with amyloid formation in their pancreas. N-methylation has been shown to improve the pharmacokinetic properties of peptides, protecting them from proteolysis (Chatterjee *et al.*, 2008), thus increasing their potential to be used as drugs. The inhibition of amylin amyloid formation is therefore an important therapeutic strategy for treating T2DM.

## 7.2 Limitations of study and future experimental plans

### 7.2.1 Limitations of study

This study was limited to the use of Th-T and Congo red assays to monitor amylin fibril formation as well as the CellTiter 96 aqueous one solution (MTS) cell proliferation assay (Promega) and the CytoTox-ONE homogeneous membrane integrity (LDH) assay (Promega). This study is also limited to the use of Reverse Phase High Performance Liquid Chromatography (RP-HPLC) to assess the stability of our peptides in plasma and proteolytic enzymes. The Th-T and Congo red assays are excellent techniques that are often used to measure the formation and inhibition of amyloid fibrils in the presence of anti-amyloidogenic agents (Hudson *et al.*, 2009; Klunk *et al.*, 1999). However, biases can arise when using the Th-T assay, as there can be a direct interaction between Th-T and other agents as well as a competitive binding for amyloid fibrils with Th-T (Hudson *et al.*, 2009). In addition, studies have reported that Congo red is an inhibitor of amyloid aggregation (Bartolini *et al.*, 2007; Podlisny *et al.*, 1998; Hong *et al.*, 2009) and this inhibitory effect is sometimes equivalent to that observed with small molecule inhibitors (Yang, *et al.*, 2005; Podlisny *et al.*, 1998), and so this raises concerns when using Congo red as a reporter dye in amyloid inhibition studies. Thus, transmission electron microscopy (TEM) was used to monitor amylin amyloid fibril assembly as a confirmatory test for the results obtained from the Th-T and Congo red studies. Although these dye-binding assays have been used to indicate potential interactions between peptide inhibitors and amylin, these techniques do not reveal the binding affinity of

these peptides for exact conformations. In order to test direct binding of the peptides to amylin, other techniques such as NMR studies or surface plasmon resonance (SPR) are needed and these can also determine the affinity of the peptide inhibitors for amylin.

### **7.2.2 Future Research**

Further research is required to verify the interactions and binding affinity of the peptide inhibitors to amylin, for example using solid-state NMR spectroscopy, which is a nuclear magnetic resonance (NMR) spectroscopy to characterize and study molecular interactions. Magic angle spinning recoupling  $^1\text{H}$ - $^1\text{H}$  NMR experiments can be used to examine atomic-level characterization of the non-fibrillar aggregation products of the amylin peptide and the detection of specific oligomers which are believed to play a key role in amyloid pathology. This provides especially useful structural details not observed by other biophysical measurements. Another technique known as NMR relaxation enhancement by paramagnetic metals gives excellent information on the three-dimensional structures of proteins in solution, and can be used alongside cross-polarization magic-angle spinning (CP-MAS) solid-state NMR to study the interaction of amylin with peptide-based inhibitors. Also, considering the fact that medical history and blood sugar tests do not take into account the long preclinical features of the disease, and pancreatic islet damage precedes disease symptoms, a biomarker for improved diagnosis of T2DM is therefore highly required. A future study would be to use Dynamic light scattering (DLS) as a laser scattering

technique to provide objective quantitative analysis of amyloid aggregation. DLS can be used in addition to Th-T assay because not only can it detect fibrils, it can also detect non-fibrillar intermediates which the Th-T fluorescence assay cannot (Hill *et al.*, 2009; Lomakin *et al.*, 1996). An additional study would be the use of Circular dichroism (CD) spectroscopy. CD provides extensive information on the conformation and secondary structure of proteins/peptides and can be used to study how protein conformation and secondary structure changes when they interact with other macromolecules. Also, to improve selectivity and specificity of our peptide for target cells/organ, a future approach will be conjugating our peptide with a cell penetrating homing peptide and with liposomes. This is a useful approach to improve intracellular drug delivery. Furthermore, a future study would be to carry out *in vivo* experiments on the impact of our peptides on the levels of soluble amylin oligomers and on glucose tolerance in transgenic amylin overexpressed mice.

## References

- Abedini, A. and Raleigh, D. P. (2005). The role of His-18 in amyloid formation by human islet amyloid polypeptide. *Biochemistry*. 44:16284-16291.
- Abedini, A. and Raleigh, D. P. (2006). Destabilization of human IAPP amyloid fibrils by proline mutations outside of the putative amyloidogenic domain: is there a critical amyloidogenic domain in human IAPP. *Journal of Molecular Biology*. 355: 274-281.
- Abedini, A. and Raleigh, D. P. (2009). A role for helical intermediates in amyloid formation by natively unfolded polypeptides. *Physical Biology*. 6: 015005.
- Abedini, A., Meng, F. L. and Raleigh, D. P. (2007). A single-point mutation converts the highly amyloidogenic human islet amyloid polypeptide into a potent fibrillization inhibitor. *Journal of the American Chemical Society*. 129(37):11300-11301.
- Abian, O., Vega, S., Sancho, J. and Velazquez-Campoy, A. (2013). Allosteric inhibitors of the NS3 protease from the hepatitis c virus. *PLoS ONE*. 8:e69773.
- Abreu, J. R. F. and Roep, B. O. (2013). Immune Monitoring of Islet and Pancreas Transplant Recipients. *Current Diabetes Report*. 13:704-712.
- Adler, J., Scheidt, H. A., Krüger, M. *et al.* (2014). Local interactions influence the fibrillation kinetics, structure and dynamics of A $\beta$  (1–40) but leave the general fibril structure unchanged. *Physical Chemistry Chemical Physics*.16:7461-7471.
- Aguilar, M. I. and Hearn, M. T. (1996). High-resolution reversed-phase high-performance liquid chromatography of peptides and proteins. *Methods in Enzymology*. 270:3-26.
- Ahmad, E., Ahmad, A., Singh, S., Arshad, M. *et al.*, (2011). A mechanistic approach for islet amyloid polypeptide aggregation to develop anti-amyloidogenic agents for type-2 diabetes, *Biochimie*. 93(5):793-805.
- Ahrén, B. Oosterwijk, C. Lips, C. J. M., and Höppener, J. W. M. (1998). Transgenic overexpression of human islet amyloid polypeptide inhibits insulin secretion and glucose elimination after gastric glucose gavage in mice. *Diabetologia*. 41(11):1374.
- Ahrén, B., Simonsson, E., Scheurink, A. J. W. H. *et al.* (1997). Dissociated insulinotropic sensitivity to glucose and carbachol in high-fat diet-induced insulin resistance in C57 BL/6J mice. *Metabolism*. 46(1):97.
- Aitken, J. F., Loomes, K. M., Konarkowska, B. and Cooper, G. J. (2003) Suppression by polycyclic compounds of the conversion of human amylin into insoluble amyloid, *Biochemical Journal*. 374:779-784.
- Aitken, J. F., Loomes, K. M., Scott, D. W. *et al.* (2010). Tetracycline treatment retards the onset and slows the progression of diabetes in human amylin/islet amyloid polypeptide transgenic mice. *Diabetes*. 59 (1): 161-171.
- Akter, R., Cao, P., Noor, H. *et al.* (2015). Islet Amyloid Polypeptide: Structure, Function, and Pathophysiology. *Journal of Diabetes Research*. 2016: 2798269.
- Ali, O. (2013). Genetics of type 2 diabetes. *World Journal of Diabetes*. 4 (4):114-23.

- Amaro, M., Birch, D. J. S. and Rolinski, O. J. (2011) Beta-amyloid oligomerization monitored by intrinsic tyrosin fluorescence. *Physical Chemistry Chemical Physics*. 13:6434-6441.
- Andreasen, M., Nielsen, S. B., Mittag, T., Bjerring, M. *et al.* (2012). Modulation of fibrillation of hIAPP core fragments by chemical modification of the peptide backbone. *Biochimica et Biophysica Acta*. 1824 (2): 274-285.
- Anguiano, M., Nowak, R. J. and Lansbury Jr., T. T. (2002). Protofibrillar islet amyloid polypeptide permeabilizes synthetic vesicles by a pore-like mechanism that may be relevant to type II diabetes. *Biochemistry*. 41(38):11338-11343.
- Anguiano, M., Nowak, R. J. and Lansbury P. T. (2002). Protofibrillar islet amyloid polypeptide permeabilizes synthetic vesicles by a pore-like mechanism that may be relevant to type II diabetes. *Biochemistry*. 41 (38). 11338-11343.
- Anguiano, M., Nowak, R. J. and Lansbury P. T. (2002). Protofibrillar islet amyloid polypeptide permeabilizes synthetic vesicles by a pore-like mechanism that may be relevant to type II diabetes. *Biochemistry*. 41 (38). 11338-11343.
- Arnelo, U., Permert, J., Adrian, T. E. and Larsson, J. (1996). Chronic infusion of islet amyloid polypeptide causes anorexia in rats. *American Journal of Physiology*. 271: R1654-R1659.
- ASD, (2007). Amputee Statistical Database for the United Kingdom Lower limb amputations. [Online]. Available at: [http://www.cot.co.uk/sites/default/files/commissioning\\_ot/public/Lower-Limb-Evidence-Fact-sheet.pdf](http://www.cot.co.uk/sites/default/files/commissioning_ot/public/Lower-Limb-Evidence-Fact-sheet.pdf). (Accessed 17<sup>th</sup> July, 2013).
- Ashcroft, F. M. and Rorsman, P. (2012). Diabetes mellitus and the  $\beta$  cell: the last ten years. *Cell*. 148(6):1160-1171.
- Astriab-Fischer, A., Sergueev, D., Fischer, M. *et al.* (2002). Conjugates of Antisense Oligonucleotides with the Tat and Antennapedia Cell-Penetrating Peptides: Effects on Cellular Uptake, Binding to Target Sequences, and Biologic Actions. *Pharmaceutical Research*. 19(6):744-754.
- Atkinson, R. N., Moore, L., Tobin, J. and King, S. B. (1999). Asymmetric Synthesis of Conformationally Restricted L-Arginine Analogues as Active Site Probes of Nitric Oxide Synthase. *Journal of Organic Chemistry*. 64(10):3467-3475.
- Azriel, R., and Gazit, E. (2001). Analysis of the minimal amyloidforming fragment of the islet amyloid polypeptide—an experimental support for the key role of the phenylalanine residue in amyloid formation,” *Journal of Biological Chemistry*. 276 (36). 34156-34161.
- Bahramikia, S. and Yazdanparast, R. (2013). Inhibition of human islet amyloid polypeptide or amylin aggregation by two manganese-salen derivatives. *European Journal of Pharmacology*. 707 (1-3): 17-25.
- Barth, S. W., Riediger, T., Lutz, T. A. and Rechkemmer, G. (2003). Differential effects of amylin and salmon calcitonin on neuropeptide gene expression in the lateral hypothalamic area and the arcuate nucleus of the rat. *Neuroscience Letters*. 341 (2):131-134.
- Bartolini, M., Naldi, M., Fiori, J., Valle, F. *et al.* (2011). Kinetic characterization of amyloid-beta 1–42 aggregation with a multimethodological approach. *Analytical Biochemistry*. 414(2):215-225.
- Bartolini, M., Bertucci, C., Bolognesi, M. L. *et al.* (2007). Insight into the kinetics of amyloid  $\beta$  (1–42) peptide self-aggregation: elucidation of inhibitors’ mechanism of action. *ChemBioChem*. 8: 2152-2161.

Bell, E. T. (1959). Hyalinization of the islets of Langerhans in nondiabetic individuals. *American Journal of Pathology*. 35: 801-805.

Bellin, M. D., Barton, F. B., Heitman, A. *et al.* (2012). Potent induction immunotherapy promotes long-term insulin independence after islet transplantation in type 1 diabetes. *American Journal of Transplantation*. 12:1576-1583.

Betsholtz, C., Svensson, V., Rorsman, F., Engström, U. *et al.* (1989). Islet amyloid polypeptide (IAPP): cDNA cloning and identification of an amyloidogenic region associated with species-specific occurrence of age-related diabetes mellitus. *Experimental Cell Research*. 183: 484-493.

Biancalana, M., Koide, S. (2010). Molecular Mechanism of Thioflavin-T Binding to Amyloid Fibrils. *Biochemica et Biophysica Acta*. 1804 (7): 1405-1412.

Biron, E., Chatterjee, J., Ovadia, O. *et al.* (2008). Improving oral bioavailability of peptides by multiple N-methylation: somatostatin analogs *Angewandte. Chemie International Edition*. 47:2595-2599.

Brain, S. D., Wimalawansa, S., MacIntyre, I. and Williams, T. J. (1990). The demonstration of vasodilator activity of pancreatic amylin amide in the rabbit. *American Journal of Pathology*. 136: 487-490.

Bram, Y., Frydman-Marom, A., Yanai, I. *et al.* (2014). Apoptosis induced by islet amyloid polypeptide soluble oligomers is neutralized by diabetes-associated specific antibodies. *Scientific Reports*. 4:4267.

Brender, J. R. Krishnamoorthy, J. Messina G. M. L *et al.* (2013). Zinc stabilization of prefibrillar oligomers of human islet amyloid polypeptide. *Chemical Communications*. 49(32): 3339-3341.

Brender, J. R., Salamekh, S. and Ramamoorthy, A. (2012). Membrane disruption and early events in the aggregation of the diabetes related peptide IAPP from a molecular perspective. *Accounts of Chemical Research*. 45(3):454-462.

Bretherton-Watt, D., Gilbey, S. G., Ghatei, M. A., Beacham, J. *et al.* (1992). Very high concentrations of islet amyloid polypeptide are necessary to alter the insulin response to intravenous glucose in man. *Journal of Clinical Endocrinology and Metabolism*. 74(5):1032-1035.

Breyer, M. D., Bottinger, E., Brosius, F. C. *et al.* (2005). Diabetic nephropathy: of mice and men. *Advances in Chronic Kidney Disease*. 12:128-145.

Broderick, C. L., Brooke, G. S., DiMarchi, R. D. and Gold, G. (1991). Human and rat amylin have no effects on insulin secretion in isolated rat pancreatic islets. *Biochemical and Biophysical Research Communications*. 177 (3): 932-938.

Brosius, F. C. III., Alpers, C. E., Bottinger, E. P. *et al.* (2009). Mouse models of diabetic nephropathy. *Journal of American Society of Nephrology*. 20:2503-2512.

Brown, K. and Mastrianni, J. A. (2010). The prion diseases. *Journal of Geriatric Psychiatry and Neurology*. 23 (4): 277-298.

Brunelle, P. and Rauk, A. (2002). The radical model of Alzheimer's disease: Specific recognition of Gly29 and Gly33 by Met35 in a beta-sheet model of Aβ: An ONIOM study. *Journal of Alzheimers Disease*. 4(4): 283-289.

Bruno E., Pereira, C., Roman, K. P., Takiguchi, M. *et al.* (2013). IAPP aggregation and cellular toxicity are inhibited by 1,2,3,4,6-penta-O-galloyl-β-D-glucose. *Amyloid Journal of Protein Folding Disorders*. 20(1): 34-38.

- Bucciantini, M., Rigacci, S., Berti, A. *et al.* (2005). Patterns of cell death triggered in two different cell lines by HypF-N pre-fibrillar aggregates *FASEB Journal*. 19(3):437-439.
- Buell, A. K., Dobson, C. M., Knowles, T. P. J. and Welland, M. E. (2010). Interactions between amyloidophilic dyes and their relevance to studies of amyloid inhibitors. *Biophysical Journal*. 99(10):3492-3497.
- Butterfield, D.A., Swomley, A. M. and Sultana, R. (2013). Amyloid  $\beta$ -peptide (1–42)-induced oxidative stress in Alzheimer disease: Importance in disease pathogenesis and progression. *Antioxidants and Redox Signalling*. 19(8):823-835.
- Calloni, G., Lendel, C., Campioni, S., Giannini, S. *et al.* (2008). Structure and dynamics of a partially folded protein are decoupled from its mechanism of aggregation. *Journal of American Chemical Society*. 130 (9): 13040-13050.
- Cao, P, Meng, F., Abedini, A. and Raleigh, D. P. (2010). The ability of rodent islet amyloid polypeptide to inhibit amyloid formation by human islet amyloid polypeptide has important implications for the mechanism of amyloid formation and the design of inhibitors. *Biochemistry*. 49: 872–881.
- Cao, P., Abedini, A., Wang, H. *et al.* (2013). Islet amyloid polypeptide toxicity and membrane interactions,” *Proceedings of the National Academy of Sciences of the United States of America*. 110(48):19279-19284.
- Cao, P., Marek, P., Noor, H., Patsalo, V. *et al.* (2013). Islet amyloid: From fundamental biophysics to mechanisms of cytotoxicity. *FEBS letters*. 587 (8): 1106-1118.
- Casas, S., Gomis, R., Gribble, F. M. *et al.* (2007). Impairment of the ubiquitin-proteasome pathway is a Downstream endoplasmic reticulum stress response induced by extracellular human islet amyloid polypeptide and contributes to pancreatic  $\beta$ -cell apoptosis. *Diabetes*. 56(9):2284-2294.
- Cauchi ,S., Meyre, D., Dina, C., *et al.* (2006). Transcription factor TCF7L2 genetic study in the French population: expression in human beta-cells and adipose tissue and strong association with type 2 diabetes. *Diabetes*. 55 (10):2903-8.
- Caughey, B. and Lansbury, P. T. (2003). Protofibrils, pores, fibrils, and neurodegeneration: separating the responsible protein aggregates from the innocent bystanders. *Annual Review of Neuroscience*. 26:267-298.
- Chang, W., Chen, L. and Hatch, G. W. (2015). Berberine as a therapy for type 2 diabetes and its complications: From mechanism of action to clinical studies. *Biochemistry and Cell Biology*. 93(5):479-86.
- Chapman, I., Parker, B., Doran, S., Feinle-Bisset C. *et al.* (2007). Low-dose pramlintide reduced food intake and meal duration in healthy, normal-weight subjects. *Obesity* 15 (5):1179-1186.
- Charge, S.B.P., de Koning, E.J.P. and Clark, A. (1995). Effect of pH and insulin on fibrillogenesis of islet amyloid polypeptide *in vitro*. *Biochemistry*. 34:14588-14593.
- Chatterjee, J., Gilon, C., Hoffman, A. and Kessler, H. (2008). N-methylation of peptides: a new perspective in medicinal chemistry. *Accounts of Chemical Research*. 41(10):1331-1342.

- Chatterjee, J., Ovadia, O., Zahn, G. *et al.* (2007). Multiple N-methylation by a designed approach enhances receptor selectivity. *Journal of Medicinal Chemistry*. 50(24): 5878-5881.
- Chatterjee, J., Rechenmacher, F. and Kessler, H. (2013). N-Methylation of Peptides and Proteins: An Important Element for Modulating Biological Functions. *Angewandte. Chemie International Edition*. 52: 254-269.
- Cheng, B. A., Liu, X. R., Gong, H. *et al.* (2011). Coffee components inhibit amyloid formation of human islet amyloid polypeptide in vitro: Possible link between coffee consumption and diabetes mellitus. *Journal of Agricultural and Food Chemistry*. 59(24):13147-13155.
- Cheng, A. C., Coleman, R. G., Smyth, K. T. *et al.* (2007). Structure-based maximal affinity model predicts small-molecule druggability. *Nature Biotechnology*. 25:71-75.
- Child & Family Research Institute (CFRI). (2016). Scientists engineer immune cells to protect organs from transplant rejection: Findings could also lead to new treatments for autoimmune disorders. *ScienceDaily*. [Online]. Available at: [www.sciencedaily.com/releases/2016/04/160401130831.htm](http://www.sciencedaily.com/releases/2016/04/160401130831.htm). (Accessed 26 April 2016).
- Chiti, F. and Dobson, C. M. (2006). Protein misfolding, functional amyloid, and human disease. *Annual Review of Biochemistry*. 75: 333 -366.
- Cho, W. J., Trikha, S., and Jeremic, A. M. (2009). Cholesterol regulates assembly of human islet amyloid polypeptide on model membranes. *Journal of Molecular Biology*. 393(3): 765-775.
- Choi, D. Y., Lee, Y. J., Hong, J. T. and Lee, H. J. (2012). Antioxidant properties of natural polyphenols and their therapeutic potentials for Alzheimer's disease. *Brain Research Bulletin*. 87(2-3):144-153.
- Christmansson, L., Rorsman, F., Stenman, G., Westermark, P., and Betsholtz, C. (1990). The human islet amyloid polypeptide (IAPP) gene. Organization, chromosomal localization and functional identification of a promoter region. *FEBS Letters*. 267 (1): 160-166.
- Christopoulos, G., Paxinos, G., Huang, X. F., Beaumont, K. *et al.* (1995). Comparative distribution of receptors for amylin and the related peptides calcitonin gene related peptide and calcitonin in rat and monkey brain. *Canadian Journal of Physiology and Pharmacology* 73 (7):1037-1041.
- Clark, A., Wells, C. A., Buley, I. D. *et al.* (1988). Islet amyloid, increased A-cells, reduced B-cells and exocrine fibrosis: quantitative changes in the pancreas in type 2 diabetes. *Diabetes Research*. 9(4): 151-159.
- Clark, T. D., Buriak, J. M., Kobayashi, K. *et al.* (1998). Cylindrical  $\beta$  sheet peptide assemblies. *Journal of the American Chemical Society*. 120(35). 8949-8962.
- Clodi, M., Thomaseth, K. and Pacini, G. (1998). Distribution and kinetics of amylin in humans. *American Journal of Physiology*. 274(5 Pt 1)E903-E908.
- Cohen, S. I., Linse, S., Luheshi, L. M. *et al.* (2013). Proliferation of amyloid- $\beta$ 42 aggregates occurs through a secondary nucleation mechanism. *Proceedings of the National Academy of Sciences United States of America*. 110(24):9758-9763.
- Colhoun, H. M., Betteridge, D. J., Durrington, P. N. *et al.* (2004). Primary prevention of cardiovascular disease with atorvastatin in Type 2 diabetes in the Collaborative Atorvastatin Diabetes Study (CARDS): multicentre randomised placebo-controlled trial. *Lancet*. 364 (9435): 685-696.

- Conesa, C., Doss, M. X., Antzelevitch, C. *et al.* (2012). Identification of specific pluripotent stem cell death-inducing small molecules by chemical screening. *Stem Cell Review*. 8:116-127.
- Cooper, G. J. S., Aitken, J. F. and Zhang, S. (2010). Is type 2 diabetes an amyloidosis and does it really matter to patients? *Diabetologia*. 53(6):1011-1016.
- Cooper, G. J.S. (1994). Amylin Compared with Calcitonin Gene-Related Peptide: Structure, Biology, and Relevance to Metabolic Disease. *Endocrine Reviews*. 15(2):163-201.
- Cooper, G. J. S., Leighton, B., Dimitriadis, G. D., Parry-Billings, M. *et al.* (1988). Amylin found in amyloid deposits in human type 2 diabetes mellitus may be a hormone that regulates glycogen metabolism in skeletal muscle. *Proceedings of the National Academy of Sciences USA*. 85 (20): 7763-7767.
- Cooper, G. J. S., Willis, A. C., Clark, A. Turner, R. C. *et al.* (1987). Turner RC, Sim RB, Reid KBM: Purification and characterization of a peptide from amyloid-rich pancreases of type 2 diabetic patients. *Proceedings of the National Academy of Sciences of the United States of America*. 84(23):8628-8632.
- Coppieters, K. T., Dotta, F., Amirian, N., Campbell, P. D. *et al.* (2012). Demonstration of islet-autoreactive CD8 T cells in insulitic lesions from recent onset and long-term type 1 diabetes patients. *Journal of Experimental Medicine*. 209 (1): 51-60.
- Cornwell G. C., Johnson, K. H. and Westermark, P. (1995). The age related amyloids: a growing family of unique biochemical substances. *Journal of Clinical Pathology*. 48 (11): 984-989.
- Cui, W., Ma, J. W., Lei, P. and Wu, W. H. *et al.* (2009). Insulin is a kinetic but not a thermodynamic inhibitor of amylin aggregation. *FEBS Journal*. 276 (12): 3365-3371.
- D'Amour K. A. Bang, A. G., Eliazer, S. *et al.* (2006). Production of pancreatic hormone-expressing endocrine cells from human embryonic stem cells. *Nature Biotechnology*. 24(11):1392-401.
- D'Este, L., Casini, A., Wimalawansa, S. J. and Renda, T. G. (2000). Immunohistochemical localization of amylin in rat brainstem. *Peptides*. 21 (11): 1743-1749.
- D'Este, L., Wimalawansa, S. J., Renda, T. G. (2001). Distribution of amylin-immunoreactive neurons in the monkey hypothalamus and their relationships with the histaminergic system. *Archives of Histology and Cytology*. 64 (3): 295-303.
- da Silva Xavier, G., Loder, M. K., McDonald, A. *et al.* (2009). TCF7L2 regulates late events in insulin secretion from pancreatic islet beta-cells. *Diabetes*. 58(4):894-905.
- Dasgupta, P., Singh, A. and Mukherjee, R. (2002). N-terminal acylation of somatostatin analog with long chain fatty acids enhances its stability and anti-proliferative activity in human breast adenocarcinoma cells. *Biological and Pharmaceutical Bulletin*. 25(1):29-36.
- Davidson, H. W. and Hutton, J. C. (1987). The insulin-secretory-granule carboxypeptidase H. Purification and demonstration of involvement in proinsulin processing. *Biochemical Journal*. 245 (2): 575-582.
- Day, R., Lazure, C., Basak, A. *et al.* (1998) Prodynorphin processing by proprotein convertase 2. *Journal of Biological Chemistry*. 273: 829-836.

de Koning, E. J. P., Clark, A., Bodkin, N. and Hansen, B. C. (1993). Diabetes mellitus in *Macaca mulatta* monkeys is characterised by islet amyloidosis and reduction in beta-cell population. *Diabetologia*. 36(5):378-384.

De Strooper, B. (2010). Proteases and proteolysis in Alzheimer disease: a multifactorial view on the disease process. *Physiological Reviews*. 90(2): 465-494.

Deeds M. C., Anderson, J. M., Armstrong ,A. S., *et al.* (2011). Single dose streptozotocin-induced diabetes: considerations for study design in islet transplantation models. *Laboratory Animals*. 45(3):131-140.

Deems, R. O., Deacon, R. W. and Young, D. A. (1991). Amylin activates glycogen phosphorylase and inactivates glycogen synthase via a cAMP-independent mechanism. *Biochemical and Biophysical Research Communications*. 174(2): 716-720.

DeFronzo, R. A. (2004). Pathogenesis of type 2 diabetes mellitus. *Medical Clinics of North America*. 88 (4): 787-835.

Degano, P., Silvestre, R. A. Salas, M. Peiro, E. and Marco, J. (1993). Amylin inhibits glucose-induced insulin secretion in a dose dependent manner. Study in the perfused rat pancreas. *Regulatory Peptides*. 43(1-2):91-96.

Demuro, A., Mina, E., Kaye, R., Milton, S. C. *et al.* (2005). Calcium dysregulation and membrane disruption as a ubiquitous neurotoxic mechanism of soluble amyloid oligomers. *Journal of Biological Chemistry*. 280 (17): 17294-17300.

Despa, S., Sharma, S., Harris, T. R. *et al.* (2014). Cardioprotection by controlling hyperamylinemia in a 'humanized' diabetic rat model. *Journal of the American Heart Association*. 3(4): e001015.

Di Gioia, M. L., Leggio, A., Malagrino, F. *et al.* (2016). N-Methylated  $\alpha$ -Amino Acids And Peptides: Synthesis And Biological Activity. *Mini Reviews in Medicinal Chemistry*. 16(9):683-90.

Diabetes UK. (2015). Key statistics on Diabetes. [online]. Available at: <http://www.diabetes.org.uk>. (Accessed 17<sup>th</sup> August 2015).

Diabetes UK. (2016). Key statistics on Diabetes. [online]. Available at: <http://www.diabetes.org.uk>. (Accessed 17<sup>th</sup> March 2016).

Dietz, G.P. and Bahr, M. (2004). Delivery of bioactive molecules into the cell: the Trojan horse approach. *Molecular and Cellular Neuroscience*. 27(2):85-131.

Dillin, A. and Cohen, E. (2011). Ageing and protein aggregation mediated disorders: from invertebrates to mammals. *Philosophical Transactions of the Royal Society B: Biological Sciences*. 366 (1561): 94-98.

Dobolyi, A. (2009). Central amylin expression and its induction in rat dams. *Journal of Neurochemistry*. 111 (6): 1490-1500.

Dobson, C. M. (1999). Protein misfolding, evolution and disease. *Trends in Biochemical Sciences*. 24(9):329-332.

Donath, M. Y. and Shoelson, S. E. (2011). Type 2 diabetes as an inflammatory disease. *Nature Reviews Immunology*. 11(2):98-107.

Dor, Y. and Melton, D. A. (2004). How important are adult stem cells for tissue maintenance? *Cell Cycle*. 3:1104-1106.

Doria, A., Patti, M. E., Kahn, C. R. (2008). The emerging genetic architecture of type 2 diabetes. *Cell Metabolism*. 8(3):186-200.

Dougherty, D. A. (2000). Unnatural amino acids as probes of protein structure and function. *Current Opinion in Chemical Biology*. 4(6):645-652.

Du, H. and Yan, S. S. (2010). Mitochondrial permeability transition pore in Alzheimer's disease: Cyclophilin D and amyloid beta. *Biochimica et Biophysica Acta*. 1802(1):198-204.

DuBay, K. F. Pawar, A. P., Chiti, F., Zurdo, J. *et al.* (2004). Prediction of the absolute aggregation rates of amyloidogenic polypeptide chains. *Journal of Molecular Biology*. 341 (5): 1317-1326.

Ehtisham, S., Barrett, T. G. and Shaw, N. J. (2000). Type 2 diabetes mellitus in UK children: an emerging problem. *Diabetic Medicine*. 17 (12): 867-871.

Eisert, R., Felau, L. and Brown, L. R. (2006). Methods for enhancing the accuracy and reproducibility of Congo red and thiolavin T assays. *Analytical Biochemistry*. 353(1):144-146.

Elgersma, R. C., Meijneke, T. Posthuma, G. *et al.* (2006). Self-assembly of amylin (20-29) amide-bond derivatives into helical ribbons and peptide nanotubes rather than fibrils. *Chemistry*.3;12(14):3714-3725.

Engel, M. F., Khemtémourian, L., Kleijer, C. C., Meeldijk, H. J. *et al.* (2008). Membrane damage by human islet amyloid polypeptide through fibril growth at the membrane. *Proceedings of the National Academy of Sciences USA*. 105 (16): 6033-6038.

Engel, M. F., Yigittop, H., Elgersma, R. C., Rijkers, T. D. *et al.* (2006). Islet amyloid polypeptide inserts into phospholipid monolayers as monomer. *Journal of Molecular Biology*. 356 (3): 783-789.

EuroStemCell. (2016). <http://www.eurostemcell.org/factsheet/diabetes-how-could-stem-cells-help>. Online. Accessed 7 April 2016.

Fan, L., Westermark, G., Chan, S. J. and Steiner, D. F. (1994). Altered gene structure and tissue expression on islet amyloid polypeptide in the chicken. *Molecular Endocrinology*. 8 (6): 713-721.

Fauchere, J. L. and Pliska, V. (1983). Hydrophobic parameters of amino acid side chains from the partitioning of N-acetyl-amino-acid amides. *European Journal of Medicinal Chemistry*. 18(4):369-375.

Ferrie, J. J., Gruskos, J. J. and Goldwasser. A. L. (2013). A comparative protease stability study of synthetic macrocyclic peptides that mimic two endocrine hormones. *Bioorganic Medicinal Chemistry Letters*. 23(4):989-995.

Findeis, M. A., (2000). Approaches to discovery and characterization of inhibitors of amyloid  $\beta$ -peptide polymerization. *Biochimica Biophysica Acta*. 1502:76-84.

- Fletcher, M. D. and Campbell, M. M. (1998). Partially modified retro-inverso peptides: Development, synthesis, and conformational behavior. *Chemical Reviews*. 98(2):763-795.
- Florez, J. C., Jablonski, K. A., Bayley, N. *et al.* (2006). TCF7L2 polymorphisms and progression to diabetes in the Diabetes Prevention Program. *New England Journal of Medicine*. 355(3):241-50.
- Fox, A. Snollaerts, T. Errecart Casanova, C. *et al.* (2010). Selection for nonamyloidogenic mutants of islet Amyloid Polypeptide (IAPP) identifies an extended region for amyloidogenicity. *Biochemistry*. 49(36) 7783-7789.
- Frackenpohl, J., Arvidsson, P. I., Schreiber, J. V. and Seebach, D. (2001). The outstanding biological stability of  $\beta$ - and  $\gamma$ -peptides toward proteolytic enzymes: an in vitro investigation with fifteen peptidases. *ChemBioChem*. 2(6):445-455.
- Fratta, P., Engel, W. K., McFerrin, J. *et al.* (2005). Proteasome inhibition and aggresome formation in sporadic inclusion-body myositis and in amyloid-beta precursor protein-overexpressing cultured human muscle fibers. *American Journal Pathology*. 167(2):517-526.
- Gautier, A., Roussel, R., Lange, C. *et al.* (2011). Effects of genetic susceptibility for type 2 diabetes on the evolution of glucose homeostasis traits before and after diabetes diagnosis: data from the D.E.S.I.R. Study. *Diabetes*. 60(10):2654-63.
- Gebre-Medhin, S., Mulder, H., Zhang, Y., Sundler, F. *et al.* (1998). Reduced nociceptive behavior in islet amyloid polypeptide (amylin) knockout mice. *Brain Research*. 63(1): 180-183.
- Gella, A., and Durany, N. (2009). Oxidative stress in Alzheimer disease. *Cell Adhesion and Migration*. 3(1):88-93.
- German, M. S., Moss, L. G., Wang, J., Rutter, W. J. *et al.* (1992). The insulin and islet amyloid polypeptide genes contain similar cell-specific promoter elements that bind identical beta-cell nuclear complexes. *Molecular and Cellular Biology*. 12 (4): 1777-1788.
- German, M., Ashcroft, S., Docherty, K., Edlund, H. *et al.* (1995). The insulin gene promoter. A simplified nomenclature. *Diabetes*. 44 (8): 1002-1004.
- Gestwicki, J. E., Crabtree, G. R. and Graef, I. A. (2004). Harnessing chaperones to generate small-molecule inhibitors of amyloid beta aggregation. *Science*. 306:865-869.
- Giannis, A. (1993). Peptidomimetics for receptor ligands discovery, development, and medical perspectives. *Angewandte. Chemie International Edition*. 32(9):1244-1267.
- Gibson, T. J. and Murphy, R. M. (2005). Design of peptidyl compounds that affect beta-amyloid aggregation: importance of surface tension and context. *Biochemistry*. 44:8898-8907.
- Gilead, S. and Gazit, E. (2008). The role of the 14–20 domain of the islet amyloid polypeptide in amyloid formation. *Experimental Diabetes Research*. 2008:256954.
- Gjesing, A. P., Kjems, L. L., Vestmar, M. A., Grarup, N. *et al.* (2011). Carriers of the TCF7L2 rs7903146 TT genotype have elevated levels of plasma glucose, serum proinsulin and plasma gastric inhibitory polypeptide (GIP) during a meal test. *Diabetologia*. 54(1):103-10.
- Glabe, C. G. (2008). Structural classification of toxic amyloid oligomers. *Journal of Biological Chemistry*. 283: 29639-29643.
- Glennner, G. G. and Wong, C. W. (1984). Alzheimer's disease and down's syndrome: Sharing of a unique cerebrovascular amyloid fibril protein. *Biochemical and Biophysical Research Communications*. 122(3):1131-1135.

- Glenner, G. G., Eanes, E. D. and Wiley, C. A. (1988). Amyloid fibrils formed from a segment of the pancreatic-islet amyloid protein. *Biochemical and Biophysical Research Communications*. 155(2):608-614.
- Goldsbury, C., Goldie, K., Pellaud, J. *et al.* (2000). Amyloid Fibril Formation from Full-Length and Fragments of Amylin. *Journal of Structural Biology*. 130(2-3):352-362.
- Goodman, M. and Chorev, M. (1979). Concept of linear modified retro-peptide structures. *Accounts of Chemical Research*. 12: 1-7.
- Goodman, M., Felix, A., Moroder, L. *et al.* (2000) *Houben-Weyl Methods of Organic Chemistry*. Eds.; Georg Thieme Verlag: Stuttgart, Germany. E22c: Chapter 10: 213-633.
- Green, M. and Loewenstein, P. M. (1988). Autonomous functional domains of chemically synthesized human immunodeficiency virus tat trans-activator protein. *Cell*. 55(6):1179-1188.
- Groenning, M. (2010). Binding mode of Thioflavin T and other molecular probes in the context of amyloid fibrils—current status. *Journal of Chemical Biology*. 3(1): 1-18.
- Gupta R., Kapoor, N., Raleigh, D. P. and Sakmar T. P. (2012). Nucleobindin 1 Caps Human Islet Amyloid Polypeptide Protofibrils to Prevent Amyloid Fibril Formation. *Journal of Molecular Biology*. 421 (2-3):378-789.
- Gupta, D. and Leahy, J. L. (2014). Islet amyloid and type 2 diabetes: overproduction or inadequate clearance and detoxification? *The Journal of Clinical Investigation*. 124(8):3292-3294.
- Gurlo, T., Ryazantsev, S., Huang, C. J. *et al.* (2010). Evidence for proteotoxicity in  $\beta$  cells in type 2 diabetes: toxic islet amyloid polypeptide oligomers form intracellularly in the secretory pathway. *The American Journal of Pathology*. 176(2):861-869.
- Haataja, L., Gurlo, T., Huang, C. J. and Butler, P.C. (2008). Islet amyloid in type 2 diabetes, and the toxic oligomer hypothesis. *Endocrine Reviews*. 29(3):303-316.
- Habener, J. F., Kemp, D. M., Thomas, M. K. (2005). Minireview: transcriptional regulation in pancreatic development. *Endocrinology*. 146:1025-1034.
- Hajduk, P. J. and Burns, D. J. (2002). Integration of NMR and high-throughput screening. *Combinatorial Chemistry and High Throughput Screening*. 5:613-621.
- Halban, P. A., Polonsky, K. S., Bowden, D. W. *et al.* (2014).  $\beta$ -cell failure in type 2 diabetes: postulated mechanisms and prospects for prevention and treatment. *The Journal of Clinical Endocrinology and Metabolism*. 99(6):1983-1992.
- Hanna, J., Wernig, M., Markoulaki, S. *et al.* (2007). Treatment of sickle cell anemia mouse model with iPS cells generated from autologous skin. *Science*. 318:1920-1923.
- Hara, M., Wang, X., Kawamura, T. *et al.* (2003). Transgenic mice with green fluorescent protein-labeled pancreatic  $\beta$ -cells. *American Journal of Physiology - Endocrinology and Metabolism*. 284(1):E177-E183.
- Hardy, J. and Selkoe, D. J. (2002). The Amyloid Hypothesis of Alzheimer's Disease: Progress and Problems on the Road to Therapeutics. *Science*. 353-356.

Harper, J. D. and Lansbury P. T. (1997). Models of amyloid seeding in Alzheimer's disease and scrapie: mechanistic truths and physiological consequences of the time-dependent solubility of amyloid proteins. *Annual Review of Biochemistry*. 66: 385-407.

Hauner, H. (2010). Obesity and Diabetes, in Textbook of Diabetes, Fourth Edition (eds R. I. G. Holt, C. S. Cockram, A. Flyvbjerg and B. J. Goldstein), Wiley-Blackwell, Oxford, UK.

Hawe, A., Sutter, M. and Jiskoot, W. (2008). Extrinsic fluorescent dyes as tools for protein characterization. *Pharmaceutical Research*. 25:1487-1499.

Heitz, F., Morris, M. C. and Divita, G. (2009). Twenty years of cell-penetrating peptides: from molecular mechanisms to therapeutics. *British Journal of Pharmacology*. 157(2):195-206.

Henry, M. (1991). Design requirements of silica-based matrices for biopolymer chromatography. *Journal of Chromatography*. 544:413-443.

Hiddinga, H. J. and Eberhardt, N. L. (1999). Intracellular amyloidogenesis by human islet amyloid polypeptide induces apoptosis in COS-1 cells. *American Journal of Pathology*. 154(4): 1077-1088.

Higham, C. E., Hull, R. L., Lawrie, L. *et al.* (2000). Processing of synthetic pro-islet amyloid polypeptide (proIAPP) "amylin" by recombinant prohormone convertase enzymes, PC2 and PC3, *in vitro*. *European Journal of Biochemistry*. 267(16): 4998-5004.

Hill, S. E., Robinson, J., Matthews, G. and Muschol, M. (2009). Amyloid Protofibrils of Lysozyme Nucleate and Grow Via Oligomer Fusion. *Biophysical Journal*. 96:3781-3790.

Hirsch, I. B. (1999). Type 1 diabetes mellitus and the use of flexible insulin regimens. *American Family Physician*. 60:2343-2356.

Holladay, M. W., Kopecka, H., Miller, T. R. *et al.* (1994). Tetrapeptide CCK-a agonists - Effect of backbone N-methylations on *in-vitro* and *in-vivo* CCK activity. *Journal of Medicinal Chemistry*. 37(5):630-635.

Hölscher, C. (2014). Drugs developed for treatment of diabetes show protective effects in Alzheimer's and Parkinson's diseases. *Acta Physiologica Sinica*. 66(5):497-510.

Hong, H. S., Rana, S. and Barrigan, L. (2009). Inhibition of Alzheimer's amyloid toxicity with a tricyclic pyrone molecule *in vitro* and *in vivo*. *Journal of Neurochemistry*. 108:1097-1108.

Höppener J. W. M., Oosterwijk C., Nieuwenhuis, M. G. *et al.* (1999). Extensive islet amyloid formation is induced by development of type II diabetes mellitus and contributes to its progression: pathogenesis of diabetes in a mouse model. *Diabetologia*. 42(4):427.

Höppener, J. W. Ahren, B. and Lips, C. J. (2000). Islet amyloid and type 2 diabetes mellitus. *New England Journal of Medicine*. 343: 411-419.

Höppener, J. W. M., Jacobs, H. M., Wierup, N. *et al.* (2008). Human Islet Amyloid Polypeptide Transgenic Mice: *In Vivo* and *Ex Vivo* Models for the Role of hIAPP in Type 2 Diabetes Mellitus. *Experimental Diabetes Research*. 2008(8):697035.

Höppener, J. W. M., Verbeek, J. S., de Koning, E. J. P. *et al.* (1993). Chronic overproduction of islet amyloid polypeptide/amylin in transgenic mice: lysosomal localization of human islet

- amyloid polypeptide and lack of marked hyperglycaemia or hyperinsulinaemia. *Diabetologia*. 36(12):1258.
- Hori, Y. *et al.* (2002). Growth inhibitors promote differentiation of insulinproducing tissue from embryonic stem cells. *Proceedings of the National Academy of Sciences of the United States of America*. 99(25):16105-16110.
- Hossain, P., Kavar, B., and Nahas. M. E. (2007). Obesity and diabetes in the developing world--a growing challenge. *New England Journal of Medicine*. 356 (3): 213-235.
- HSCI. (2016). <http://hsci.harvard.edu/diabetes-0> 2016. Online. Accessed 15 March 2016.
- Hua, J., Huang, K. L. (2010). A reversed phase HPLC method for the analysis of nucleotides to determine 5'-PDE enzyme activity. *Bulletin of the Chemical Society of Ethiopia*. 24(2):167-174.
- Huang, C. J., Lin, C. Y., Haataja, L. *et al.* (2007). High expression rates of human islet amyloid polypeptide induce endoplasmic reticulum stress-mediated  $\beta$ -cell apoptosis, a characteristic of humans with type 2 but not type 1 diabetes. *Diabetes*. 56 (8): 2016-2027.
- Hudson, S. A., Ecroyd, H., Kee, T. W. and Carver, J. A. (2009). The thioflavin T fluorescence assay for amyloid fibril detection can be biased by the presence of exogenous compounds. *The FEBS journal*. 276(20):5960-5972.
- Hughes, E., Burke, R. M. and Doig A. J. (2000). Inhibition of toxicity in the  $\beta$ -amyloid peptide fragment  $\beta$ -(25-35) using N-methylated derivatives. *Journal of Biological Chemistry*. 275(33): 25109-25115.
- Hull, R. L., Zraika, S., Udayasankar, J. *et al.* (2009). Amyloid formation in human IAPP transgenic mouse islets and pancreas, and human pancreas, is not associated with endoplasmic reticulum stress. *Diabetologia*. 52(6):1102-1111.
- Hull, R. L., Shen, Z. P., Watts, M. R. Kodama, K. *et al.* (2005). Long-term treatment with rosiglitazone and metformin reduces the extent of, but does not prevent, islet amyloid deposition in mice expressing the gene for human islet amyloid polypeptide. *Diabetes*. 54 (7): 2235-2244.
- Hull, R. L., Westermark, G. T., Westermark., P. and Kahn, S. E. (2004). Islet amyloid: a critical entity in the pathogenesis of type 2 diabetes. *Journal of Clinical Endocrinology and Metabolism*. 89 (8): 3629-3643.
- Hummel, G., Reineke, U. and Reimer, U. (2006) Translating peptides into small molecules. *Molecular BioSystems*. 2(10):499-508.
- Humpel, C. (2011). Identifying and validating biomarkers for Alzheimer's disease, *Trends in Biotechnology*. 29 (1): 26-32.
- IDF (2015). International Diabetes Federation. [Online]. Available at: <http://www.idf.org/>. (Accessed 15<sup>th</sup> October, 2015).
- IDF, (2012). International diabetic Federation. [online]. Available at: <http://www.idf.org/worlddiabetesday/toolkit/gp/facts-figures> (Accessed 16th September 2013).
- Inkster, M. E., Fahey, T. P., Donnan, P. T *et al.* (2006). Poor glycated haemoglobin control and adverse pregnancy outcomes in type 1 and type 2 diabetes mellitus: systematic review of observational studies. *BMC Pregnancy and Childbirth*. 6: 30.
- Iwai, A., Masliah, E., Yoshimoto, M. *et al.* ( 1995). The precursor protein of non-A<sub>β</sub> component of Alzheimer's disease amyloid is a presynaptic protein of the central nervous system. *Neuron*.14:467-475.

- Jaikaran, E. T. A. S., Nilsson, M. R., and Clark, A. (2004). Pancreatic  $\beta$ -cell granule peptides form heteromolecular complexes which inhibit islet amyloid polypeptide fibril formation. *Biochemical Journal*. 377:709-716.
- Jaikaran, E. T., Higham, A. S., Serpell, C. E., L. Zurdo, L. C. *et al.* (2001). Identification of a novel human islet amyloid polypeptide b-sheet domain and factors influencing fibrillogenesis. *Journal of Molecular Biology*. 308 (3): 515-525.
- Jaikaran, E. T., Nilsson, M. R. and Clark, A. (2004). Pancreatic beta cell granule peptides form heteromolecular complexes which inhibit islet amyloid polypeptide fibril formation. *Biochemical Journal*. 377: 709-716.
- Janciauskiene, S., Eriksson, S., Carlemalm, E. and Ahren, B. (1997). b cell granule peptides affect human islet amyloid polypeptide (IAPP) fibril formation in vitro. *Biochemical and Biophysical Research Communications*. 236(3):580-585.
- Janson, J., Ashley, R. H., Harrison, D. *et al.* (1999). The mechanism of islet amyloid polypeptide toxicity is membrane disruption by intermediate-sized toxic amyloid particles. *Diabetes*. 48(3):491-498.
- Janson, J., Soeller, W. C., Roche, P. C., Nelson, R. T. *et al.* (1996). Spontaneous diabetes mellitus in transgenic mice expressing human islet amyloid polypeptide. *Proceedings of the National Academy of Sciences, USA*. 93 (14): 7283-7288.
- Jarrett, P.T. Lansbury Jr. (1993). Seeding one-dimensional crystallization of amyloid: a pathogenic mechanism in Alzheimer's disease and scrapie? *Cell*. 73:1055-1058.
- Jean, L. C., Lee C, Shaw, M. and Vaux, D. J. (2010). Competing discrete interfacial effects are critical for amyloidogenesis. *FASEB Journal*. 24: 309-317.
- JGRF. (2016) <https://jdrf.org.uk/our-research/about-our-research/cure/immune-therapies/> . Online. Accessed 20 April 2016
- Jha, S. Snell, J. M. Sheftic S. R. *et al.* (2014). PH dependence of amylin fibrillization. *Biochemistry*. 53(2)300-310.
- Johnson, K. H., O'Brien, T. D., Jordan, K. H., Betsholtz, C. *et al.* (1990). The putative hormone islet amyloid polypeptide (IAPP) induces impaired glucose tolerance in cats. *Biochemical and Biophysical Research Communications*. 167(2): 507-513.
- Junod, A., Lambert, A. E., Stauffacher, W. and Renold, A. E. (1969). Diabetogenic action of streptozotocin: relationship of dose to metabolic response. *Journal of Clinical Investigation*. 48(11):2129-2139.
- Jurgens, C. A., Toukatly, M. N., Fligner, C. L. *et al.* (2011). Beta-cell loss and beta-cell apoptosis in human type 2 diabetes are related to islet amyloid deposition. *American Journal of Pathology*. 178(6):2632-2640.
- Kahn, C. R. (2003b). Knockout mice challenge our concepts of glucose homeostasis and the pathogenesis of diabetes. *Experimental Diabetes Research*. 4:169-182.
- Kahn, S. E. (2000). The importance of the beta cell in the pathogenesis of type 2 diabetes. *American Journal of Medicine*. 108: 2S-8S.
- Kahn, S. E. (2003a). The relative contributions of insulin resistance and beta-cell dysfunction to the pathophysiology of Type 2 diabetes. *Diabetologia* 46 (1): 3-19.

- Kahn, S. E., Andrikopoulos, S. and Verchere, C. B. (1999). Islet amyloid, a long-recognized but underappreciated pathological feature of type 2 diabetes. *Diabetes*. 48 (2): 241-253.
- Kahn, S. E., Fujimoto, W. Y., D'Alessio, D. A., Ensinck, J. W. *et al.* (1991). Glucose stimulates and potentiates islet amyloid polypeptide secretion by the B-cell. *Hormone and Metabolic Research* 23 (12): 577-580.
- Kahn, S. E., Verchere, C. B., Andrikopoulos, S. *et al.* (1998). Reduced amylin release is a characteristic of impaired glucose tolerance and type 2 diabetes in Japanese Americans. *Diabetes*. 47:640-645.
- Kahn, S. E., Zraika, S., Utzschneider, K. M. and Hull, R. L. (2009). The beta cell lesion in type 2 diabetes: there has to be a primary functional abnormality. *Diabetologia*. 52: 1003-1012.
- Kapoor, N., Gupta, R., Menon, S. T., Folta-Stogniew, E. *et al.* (2010). Nucleobindin 1 is a calcium-regulated guanine nucleotide dissociation inhibitor of G $\alpha$ i1. *Journal of Biological Chemistry*. 285 (41): 31647-31660.
- Kapurniotu, A., Schmauder, A. and Tenidis, K. (2002). Structure-based design and study of non-amyloidogenic double N-methylated IAPP amyloid core sequence of IAPP amyloid formation and cytotoxicity. *Journal of Molecular Biology*. 315(3): 339-350.
- Kapurniotu, A. (2001). Amyloidogenicity and cytotoxicity of islet amyloid polypeptide. *Biopolymers*. 60 (6): 438-459.
- Kapurniotu, A., Bernhagen, J., Greenfield N. *et al.* (1998). Contribution of advanced glycosylation to the amyloidogenicity of islet and amyloid polypeptide. *European Journal of Biochemistry*. 251(1-2).208-216.
- Karunanyake, E. H., Hearse, D. J. and Mellows, G. (1974). The synthesis of C<sup>14</sup> Streptozotocin and its distribution and excretion in the rat. *Biochemical Journal*.142:673-683.
- Kautzky-Willer, A., Thomaseth, K., Pacini, G. *et al.* (1994). Role of islet amyloid polypeptide secretion in insulin-resistant humans. *Diabetologia*. 37:188-194.
- Kawahara, M., Kuroda, Y., Arispe, N. and Rojas, E. (2000). Alzheimer's beta-amyloid, human islet amylin, and prion protein fragment evoke intracellular free calcium elevations by a common mechanism in a hypothalamic GnRH neuronal cell line. *Journal of Biological Chemistry*. 275 (19): 14077-14083.
- Kayed, R., Bernhagen, J., Greenfield, N. *et al.* (1999). Conformational transitions of islet amyloid polypeptide (IAPP) in amyloid formation in vitro. *Journal of molecular Biology*. 287(4):781-796.
- Kayed, R., Head, E., Thompson, J. L. McIntire, T. M. *et al.* (2003). Common structure of soluble amyloid oligomers implies common mechanism of pathogenesis. *Science*. 300 (5618): 486-489.
- Kayed, R., Pensalfini, A., Margol, L., Sokolov, Y. *et al.* (2009). Annular protofibrils are a structurally and functionally distinct type of amyloid oligomer. *Journal of Biological Chemistry*. 284: 4230-4237.
- Keirstead, H. S., Nistor, G., Bernal. G. *et al.* (2005). Human embryonic stem cell-derived oligodendrocyte progenitor cell transplants remyelinate and restore locomotion after spinal cord injury. *Journal of Neuroscience*. 25:4694-4705.

- Keller, J. N., Huang, F. F. and Markesbery, W. R. (2002). Decreased levels of proteasome activity and proteasome expression in aging spinal cord. *Neuroscience*.98(1): 149-156.
- Kellock, J., Hopping, G., Caughet, B. and Daggetti, V. (2016). Peptides Composed of Alternating L- and D-Amino Acids Inhibit Amyloidogenesis in Three Distinct Amyloid Systems Independent of Sequence. *Journal of Molecular Biology*. 428:2317-2328.
- Keskin, O., Gursoy, A., Ma, B. and Nussinov, R. (2008). Principles of protein-protein interactions: what are the preferred ways for proteins to interact. *Chemical Reviews*. 108:1225-44.
- Kessler, H. (1993). Peptoids-a new approach to the development of pharmaceuticals *Angewandte. Chemie International Edition*. 32(4):543-544.
- Khemtémourian, L., Killian, J. A., Höppener, J. M. and Engel, M. M. (2008). Recent insights in islet amyloid polypeptide-induced membrane disruption and its role in beta cell death in type 2 diabetes mellitus. *Experimental Diabetes Research*. 2008: 1-9.
- Khurana, R., Coleman, C., Ionescu-Zanetti, C., Carter, S. *et al.* (2005). Mechanism of thioflavin T binding to amyloid fibrils. *Journal of Structural Biology*. 151(3): 229-238.
- Klaus, A., Birchmeier, W. (2008). Wnt signalling and its impact on development and cancer. *Nature Reviews Cancer*. 8(5):387-98.
- Klunk, W. E., Jacob, R. F. and Mason, R. P. (1999). Quantifying amyloid  $\beta$ -peptide (A $\beta$ ) aggregation using the Congo red-A $\beta$  (CR-A $\beta$ ) spectrophotometric assay. *Analytical Biochemistry*. 266(1):66-76.
- Knight, J. D., Hebda, J. A. and Miranker, A. D. (2006). Conserved and cooperative assembly of membrane-bound  $\alpha$ -helical states of islet amyloid polypeptide. *Biochemistry*. 45 (31): 9496-9508.
- Knight, J. D., Williamson, J. A. and Miranker, A. D. (2008). Interaction of membrane-bound islet amyloid polypeptide with soluble and crystalline insulin. *Protein Science*. 17 (10): 1850-1860.
- Knip, M., Veijola, R., Virtanen, S. M. *et al.* (2005). Environmental Triggers and Determinants of Type 1 Diabetes. *Diabetes*. 54(2): S125-S136.
- Knudsen, L. B. (2010). Liraglutide: the therapeutic promise from animal models. *International Journal of Clinical Practice*. 64: 4-11.
- Kodali, R. and Wetzel, R. (2007). Polymorphism in the intermediates and products of amyloid assembly. *Current Opinion in Structural Biology*. 17(1): 48-57.
- Kogire, M., Ishizuka, J., Thompson, J. C. and Greeley, G. J. (1991). Inhibitory action of islet amyloid polypeptide and calcitonin gene-related peptide on release of insulin from the isolated perfused rat pancreas. *Pancreas*. 6:459-463.
- Konarkowska, B., Aitken, J. F., Kistler, J., Zhang, S. and Cooper, G. J. S. (2006), The aggregation potential of human amylin determines its cytotoxicity towards islet  $\beta$ -cells. *FEBS Journal*. 273(15):3614-3624.
- Kong, M. F., Stubbs, T. A. King P., Macdonald I. A. *et al.* (1998). The effect of single doses of pramlintide on gastric emptying of two meals in men with IDDM. *Diabetologia*. 41 ( 5). 577-583.

- Koo, B. W. and Miranker, A. D. (2005). Contribution of the intrinsic disulfide to the assembly mechanism of islet amyloid. *Protein Science*. 14(1):231-239.
- Kumar, S., Vasudeva, N. and Sharma, S. (2012). GC-MS analysis and screening of antidiabetic, antioxidant and hypolipidemic potential of Cinnamomum tamala oil in streptozotocin induced diabetes mellitus in rats. *Cardiovascular Diabetology*. 11:95.
- Landchild, M. J., Knowles, N. G., Yao, Q. *et al.* (2000). Increased  $\beta$ -cell secretory demand is not the simple explanation for inefficient proinsulin processing and islet amyloid formation in type 2 diabetes. *Journal of Investigative Medicine*. 48:21A.
- Larson, J. L. and Miranker, A. D. (2004). The mechanism of insulin action on islet amyloid polypeptide fiber formation. *Journal of Molecular Biology*. 335: 221-231.
- Last, N. B., Rhoades, E. and Miranker, A. D. (2011). Islet amyloid polypeptide demonstrates a persistent capacity to disrupt membrane integrity. *Proceedings of the National Academy of Sciences of the United States of America*. 108(23):9460-9465.
- Law, E., Lu, S., Kieffer, T. J. *et al.* (2010). Differences between amyloid toxicity in alpha and beta cells in human and mouse islets and the role of caspase-3. *Diabetologia*. 53(7):1415-1427.
- Lee, S. J. C., Choi, T. S., Lee, J. W., Lee, H. J. *et al.* (2016). Structure and assembly mechanisms of toxic human islet amyloid polypeptide oligomers associated with copper. *Chemical Science*. 7:5398-5406.
- Lee, S. J., Lim, H. M., Masliah, E. and Lee, H. J. (2011). Protein aggregate spreading in neurodegenerative diseases: problems and perspectives, *Neuroscience Research*. 70 (4): 339-348.
- Leiter, E. H. (2009). Selecting the 'right' mouse model for metabolic syndrome and type 2 diabetes research. *Methods in Molecular Biology*. 560:1-17.
- Lenzen, S. (2008). The mechanisms of alloxan and streptozotocin-induced diabetes. *Diabetologia*. 51(2):216-226.
- Lesné, S., Koh, M. T., Kotilinek, L., Kaye, R. *et al.* (2006). A specific amyloid-beta protein assembly in the brain impairs memory. *Nature*. 440: 352-357.
- Levine, H. III. (1993). Thioflavine T interaction with synthetic Alzheimer's disease  $\beta$ -amyloid peptides: Detection of amyloid aggregation in solution. *Protein Science*. 2(3):404-410.
- Lewin, M., Carlesso, N., Tung, C. H. *et al.* (2000). Tat peptide-derivatized magnetic nanoparticles allow in vivo tracking and recovery of progenitor cells. *Nature Biotechnology*. 18(4):410-414.
- Lin, C. Y., Gurlo, T., Kaye, R. *et al.* (2007). Toxic human islet amyloid polypeptide (H-IAPP) oligomers are intracellular, and vaccination to induce anti-toxic oligomer antibodies does not prevent h-iapp-induced  $\beta$ -cell apoptosis in H-IAPP transgenic mice. *Diabetes*. 56(5):1324-1332.
- Lindberg, D. J., Wrann, M. S. Gatty, M. G. *et al.* (2015). Steady-state and time-resolved Thioflavin-T fluorescence can report on morphological differences in amyloid fibrils formed by A $\beta$ (1-40) and A $\beta$ (1-42). *Biochemical and Biophysical Research Communications*. 458(2):418-423.
- Liu, R., Su, R., Liang, M. *et al.* (2012). Physicochemical Strategies for Inhibition of Amyloid Fibril Formation: An Overview of Recent Advances. *Current Medicinal Chemistry*. 19: 4157-4174.
- Lolicato, F., Raudino, A., Milardi, D. and La Rosa, C. (2015) Resveratrol interferes with the aggregation of membrane-bound human-IAPP: a molecular dynamics study. *European Journal of Medicinal Chemistry*. 92: 876-881.

- Lomakin, A., Chung, D. S., Benedek, G. B. *et al.* (1996). On the nucleation and growth of amyloid beta-protein fibrils: detection of nuclei and quantitation of rate constants. *Proceedings of the National Academy of Sciences*. 93: 1125-1129.
- Lonskaya, I., Hebron, M., Chen, W. *et al.* (2014). Tau deletion impairs intra cellular  $\beta$ -amyloid-42 clearance and leads to more extracellular plaque deposition in gene transfer models. *Molecular Neurodegeneration*.9:46.
- Lopes, D. H., Meister, A., Gohlke, A., Hauser, A. *et al.* (2007). Mechanism of islet amyloid polypeptide fibrillation at lipid interfaces studied by infrared reflection absorption spectroscopy. *Biophysical Journal*. 93 (9). 3132-3141.
- Lopez, L. C., Dos-Reis, S., Espargaro, A. *et al.* (2012). Discovery of novel inhibitors of amyloid  $\beta$ -peptide 1-42 aggregation. *Journal of Medicinal Chemistry*. 55:9521-9530.
- Lopez, L. C., Varea, O., Navarro, S. *et al.* (2016). Benzbromarone, Quercetin, and Folic Acid Inhibit Amylin Aggregation. *International Journal of Molecular Sciences*. 17(6):964.
- Lorenzo, A, Razzaboni , Weir, B. G. C. and Yankner, B. A. (1994). Pancreatic islet cell toxicity of amylin associated with type-2 diabetes mellitus. *Nature*. 368:756-760.
- Lorenzo, A. and Yankner, B. A. (1994).  $\beta$ -Amyloid neurotoxicity requires fibril formation and is inhibited by Congo red. *Proceedings of the National Academy of Sciences USA*. 91:12243-12247.
- Lorenzo, A. and Yankner, B. A. (1996). Amyloid fibril toxicity in Alzheimer's disease and diabetes. *Annals of New York Academy of Sciences*. 777:89-95.
- Lowe, T. L., Strzelec, A., Kiessling, L. L and Murphy, R. M. (2001). Structure-function relationships for inhibitors of beta-amyloid toxicity containing the recognition sequence KLVFF. *Biochemistry*. 40: 7882-7889.
- Luca, S., Yau, W. M., Leapman, R. and Tycko, R. (2007). Peptide conformation and supramolecular organization in amylin fibrils: Constraints from solid-state NMR. *Biochemistry*. 46: 13505-13522.
- Luchsinger, J. A., Tang, M. S. Shea, S. and Mayeux, R. (2014). Hyperinsulinemia and risk of Alzheimer disease. *Neurology*. 63(7):1187-1192.
- Lukinius, A., Wilander, E., Westermark, G. T. *et al.* (1989). Co-localization of islet amyloid polypeptide and insulin in the B cell secretory granules of the human pancreatic islets. *Diabetologia*. 32:240-244.
- Lumelsky, N. *et al.* (2001). Differentiation of embryonic stem cells to insulin-secreting structures similar to pancreatic islets. *Science*. 292(5520):1389-1394.
- Lutz, T. A. (2006). Amylinergic control of food intake. *Physiology and Behaviour*. 89(4):465-471.
- Lysenko, V., Lupi, R., Marchetti, P. *et al.* (2007). Mechanisms by which common variants in the TCF7L2 gene increase risk of type 2 diabetes. *Journal of Clinical Investigation*. 117(8):2155-63.
- MacIntyre, I. (1989). Amylinamide, bone conservation, and pancreatic beta cells. *Lancet*. 2 (8670): 1026-1027.
- Maezawa, I., Hong, H.-S., Liu, R., Wu, C.-Y. *et al.* (2008) Congo red and thioflavin-T analogues detect A $\beta$  oligomers. *Journal of Neurochemistry*. 104(2):457-468.

Maggs, D. G., Fineman, M., Kornstein, J., Burrell, T. *et al.* (2004). Pramlintide reduces postprandial glucose excursions when added to insulin lispro in subjects with type 2 diabetes: a dose-timing study. *Diabetes/Metabolism Research and Reviews*. 20 (1): 55-60.

Makimattila, S., Fineman, M. S. and Yki-Jarvinen, H. (2000). Deficiency of total and nonglycosylated amylin in plasma characterizes subjects with impaired glucose tolerance and type 2 diabetes. *Journal of Clinical Endocrinology and Metabolism*. 85 (8): 2822-2827.

Manavalan, P. and Momany, F. A. (1980). Conformational energy studies on N-methylated analogs of thyrotropin releasing hormone, enkephalin, and luteinizing hormone-releasing hormone. *Biopolymers*. 19(11): 1943-1973.

Mant, C. T. and Hodges, R. S. (1996) Analysis of peptides by high performance liquid chromatography. *Methods in Enzymology*. 271:3-50.

March, T. L., Johnston, M. R., Duggan, P. J. and Gardiner, J. (2012). Synthesis, structure, and biological applications of  $\alpha$ -fluorinated  $\beta$ -amino acids and derivatives. *Chemistry and Biodiversity*. 9(11):2410-2441.

Marchesi, V.T. (2011). Alzheimer's dementia begins as a disease of small blood vessels, damaged by oxidative-induced inflammation and dysregulated amyloid metabolism: implications for early detection and therapy. *FASEB Journal*. 25 (1):5-13.

Martínez-Álvarez, R. M., Volkoff, H., Munoz Cueto, J. A. and Delgado, M. J. (2008). Molecular characterization of calcitonin gene-related peptide (CGRP) related peptides (CGRP, amylin, adrenomedullin and adrenomedullin-2/intermedin) in goldfish (*Carassius auratus*): cloning and distribution. *Peptides*. 29 (9): 1534-1543.

Marzban, L., Trigo-Gonzalez, G., Zhu, X., Rhodes, C. J. *et al.* (2004). Role of beta-cell prohormone convertase (PC)1/3 in processing of pro-islet amyloid polypeptide. *Diabetes*. 53 (1): 141-148.

Masaki, T., Takiya, T., Tsunasawa, S. *et al.* (1994). Hydrolysis of S-2 aminoethylcysteinyl peptide bond by achromobacter protease I. *Bioscience, Biotechnology and Biochemistry*. 58(1):215-216.

Masters, S. L., Dunne, A., Subramanian, S. L., Hull, R. L. *et al.* (2010). Activation of the NLRP3 inflammasome by islet amyloid polypeptide provides a mechanism for enhanced IL-1 $\beta$  in type 2 diabetes. *Nature Immunology*. 11(10): 897-904.

Mata-Cantero, L., Cid, C., Gomez-Lorenzo, M. G. *et al.* (2015). Development of two novel high-throughput assays to quantify ubiquitinated proteins in cell lysates: application to screening of new anti-malarials. *Malaria Journal*. 14:200.

Matsuda, M., Kawasaki, F., Mikami, Y. *et al.* (2002). Rescue of beta-cell exhaustion by diazoxide after the development of diabetes mellitus in rats with streptozotocin-induced diabetes. *European Journal of Pharmacology*. 53(1):141-148.

Mattson, M. P. (1999). Impairment of membrane transport and signal transduction systems by amyloidogenic proteins. *Methods Enzymology*. 309:733-768.

Mazor, Y., Gilead, S., Benhar, I., and Gazit, E. (2002). Identification and characterization of a novel molecular-recognition and self-assembly domain within the islet amyloid polypeptide. *Journal of Molecular Biology*. 322 (5). 1013-1024.

- McClellan, P. L and Hölscher, C. (2014). Lixisenatide, a drug developed to treat type 2 diabetes, shows neuroprotective effects in a mouse model of Alzheimer's disease. *Neuropharmacology*. 86:241-58.
- McGregor, D. P. (2008). Discovering and improving novel peptide therapeutics. *Current Opinion in Pharmacology*. 8:616-619.
- Meier, D. T., Tu, L. H., Zraika, S. *et al.* (2015). Matrix Metalloproteinase-9 Protects Islets from Amyloid induced Toxicity. *Journal of Biological Chemistry*. 290(51): 30475-30485.
- Meng ,F. L., Marek, P., Potter, K. J. *et al.* (2008). Rifampicin does not prevent amyloid fibril formation by human islet amyloid polypeptide but does inhibit fibril thioflavin-T interactions: Implications for mechanistic studies beta-cell death. *Biochemistry*. 47(22):6016-6024.
- Meng, F., Abedini, A., Plesner, A. *et al.* (2010). The sulfated triphenyl methane derivative acid fuchsin is a potent inhibitor of amyloid formation by human islet amyloid polypeptide and protects against the toxic effects of amyloid formation. *Journal of Molecular Biology*. 400(3):555-566.
- Merlini, G. and Westermark, P. (2004). The systemic amyloidosis: clearer understanding of the molecular mechanisms offer hope for more effective therapies. *Journal of Intern Medicine*. 255: 159-178.
- Middleton, C. T., Marek, P., Cao, P., Chiu, C-c. *et al.* (2012) Two-dimensional infrared spectroscopy reveals the complex behaviour of an amyloid fibril inhibitor. *Nature Chemistry*. 4(5):355-360.
- Milton, R.C. de L., Milton, S.C.F. and Adams, P.A. (1990). Prediction of difficult sequences in solid phase peptide synthesis. *Journal of the American Chemical Society*. 112(16):6039-6046.
- Mirzabekov, T. A. Lin, M. C. and Kagan, B. L. (1996). Pore formation by the cytotoxic islet amyloid peptide amylin. *Journal of Biological Chemistry*. 271(4): 1988-1992.
- Mishra, R., Sellin, D., Radovan, D., Gohlke, A. *et al.* (2009). Inhibiting islet amyloid polypeptide fibril formation by the red wine compound resveratrol. *ChemBioChem*. 10 (3): 445-449.
- Miyazato, M., Nakazato, M., Shiomi, K., Aburaya, J. (1991). Identification and characterization of islet amyloid polypeptide in mammalian gastrointestinal tract. *Biochemical and Biophysical Research Communications*. 181(1): 293-300.
- Miyazato, M., Nakazato, M., Shiomi, K., Aburaya, J. *et al.* (1992). Molecular forms of islet amyloid polypeptide (IAPP/amylin) in four mammals. *Diabetes Research and Clinical Practiice*. 15 (1): 31-36.
- Moriarty, D. F. and Raleigh, D. P. (1999). Effects of sequential proline substitutions on amyloid formation by human amylin 20–29. *Biochemistry*. 38(6):1811-1818.
- Morishima, Y., Gotoh, Y., Zieg, J. *et al.* (2001). Beta-amyloid induces neuronal apoptosis via a mechanism that involves the c-Jun N-terminal kinase pathway and the induction of Fas ligand. *Journal of Neuroscience*. 21(19):7551-7560.

- Morrish, N. J. Wang, S. L., Stevens, L. K., Fuller, J. H. *et al* (2001). Mortality and causes of death in the WHO multinational study of vascular disease in diabetes. *Diabetologia*. 44 (2): s14-s21.
- Mosselman, S., Höppener, J. W. Lips, C. J. and Jansz, H. S. (1989). The complete islet amyloid polypeptide precursor is encoded by two exons. *FEBS Letters*. 247 (1):154-158.
- Mulder, H., Ahrén, B. and Sundler, F. (1995). Differential expression of islet amyloid polypeptide (amylin) and insulin in experimental diabetes in rodents. *Molecular and Cellular Endocrinology*. 114: 101-109.
- Mulder, H., Ahrén, B. and Sundler, F. (1996). Islet amyloid polypeptide and insulin gene expression are regulated in parallel by glucose in vivo in rats. *American Journal of Physiology*. 271: E1008-E1014.
- Mulder, H., Lindh, A. C., Ekblad, E., Westermark, P. *et al*. (1994). Islet amyloid polypeptide is expressed in endocrine cells of the gastric mucosa in the rat and mouse. *Gastroenterology*. 107: 712-719.
- Nanga, R. P., Brender, J. R., Xu, J., Hartman, K. *et al*. (2009). Three dimensional structure and orientation of rat islet amyloid polypeptide protein in a membrane environment by solution NMR spectroscopy. *Journal of American Chemical Society*. 131(23):8252-8261.
- Naot, D. and Cornish, J. (2008). The role of peptides and receptors of the calcitonin family in the regulation of bone metabolism. *Bone*. 43 (5): 813-818.
- Necula, M., Kayed, R., Milton, S. and Glabe, C. G.(2007). Small molecule inhibitors of aggregation indicate that amyloid\_ oligomerization and fibrillization pathways are independent and distinct. *Journal of Biological Chemistry*. 282:10311-10324.
- NHS UK (2015). [Online]. Available at: <http://www.nhs.uk/Conditions/Diabetes/Pages/Diabetes.aspx>. Accessed 19<sup>th</sup> November 2015).
- NIDDK (2014). National Institute of Diabetes and Digestive and Kidney Disease. [Online]. Available at: <https://www.niddk.nih.gov/health-information/diabetes>. (Accessed 22<sup>nd</sup> March 2014).
- Nie, Q., Du, X. and Geng, M. (2011). Small molecule inhibitors of amyloid  $\beta$  peptide aggregation as a potential therapeutic strategy for Alzheimer's disease. *Acta Pharmacologica Sinica*. 32: 545-551.
- Nilsson, M. R. (2004). Techniques to study amyloid fibril formation *in vitro*. *Methods*. 34(1):151-160.
- Nilsson, M. R. and Raleigh, D. P. (1999). Analysis of amylin cleavage products provides new insights into the amyloidogenic region of human amylin. *Journal of Molecular Biology*. 294 (5): 1375-1385.
- Nishi, M., Sanke, T., Seino, S. and Eddy, R. L. (1989). Human islet amyloid polypeptide gene: complete nucleotide sequence, chromosomal localization, and evolutionary history. *Molecular Endocrinology*. 3 (11): 1775-1781.
- Nolan, C., Margoliash, E., Peterson, J. D. and Steiner, D. F. (1971). The structure of bovine proinsulin. *Journal of Biological Chemistry*. 246 (6):2780-2795.
- Noor, H., Cao, P. and Raleigh, D. P. (2012). Morin hydrate inhibits amyloid formation by islet amyloid polypeptide and disaggregates amyloid fibers. *Protein Science*. 21: 373-382.

- NSF (2013). National service framework for diabetes. [Online]. Available at: <https://www.gov.uk/government/publications/national-service-framework-diabetes>. (Accessed 5th August 2013).
- O'Brien, T., Westermark, P. and Johnson, K. H. (1991). Islet amyloid polypeptide and insulin secretion from isolated perfused pancreas of fed, fasted, glucose-treated, and dexamethasone-treated rats. *Diabetes*. 40 (12): 1701-1706.
- O'Brien, T. D., Westermark, P. and Johnson, K. H. (1990). Islet amyloid polypeptide (IAPP) does not inhibit glucose-stimulated insulin secretion from isolated perfused rat pancreas. *Biochemical and Biophysical Research Communications*. 170 (3): 1223-1228.
- Ono, K., Yoshiike, Y., Takashima, A. *et al.* (2003). Potent anti-amyloidogenic and fibril-destabilizing effects of polyphenols in vitro: implications for the prevention and therapeutics of Alzheimer's disease. *Journal of Neurochemistry*. 87:172-181.
- Oroszlan, P., Wicar, S. and Teshima, G. (1992). Conformational effects in the reversed phase chromatographic behaviour of recombinant human growth hormone (rhGH) and N-methionyl recombinant human growth hormone (met-hGH). *Analytical Chemistry*. 64:1623-1631.
- Park, K. and Verchere, C. B. (2001). Identification of a heparin binding domain in the N-terminal cleavage site of pro-islet amyloid polypeptide. *Journal of Biological Chemistry*. 276(20):16611-16616.
- Park, Y. J., Lee, S., Kieffer, T. J. *et al.* (2012). Deletion of Fas protects islet beta cells from cytotoxic effects of human islet amyloid polypeptide. *Diabetologia*. 55(4):1035-1047.
- Patel, L. N., Zaro, J. L. and Shen, W. C. (2007). Cell Penetrating Peptides: Intracellular Pathways and Pharmaceutical Perspectives. *Pharmaceutical Research*. 24(11):1977-1992.
- Patil, M. A., Suryanarayana, P., Putcha, U. K. *et al.* (2014). Evaluation of neonatal streptozotocin induced diabetic rat model for the development of cataract. *Oxidative Medicine and Cellular Longevity*. 2014(10):463264.
- Patil, S. M., Xu, S., Sheftic, S. R. and Alexandrescu, A. T. (2009). Dynamic  $\alpha$ -helix structure of micellebound human amylin. *Journal of Biological Chemistry*. 284(18):11982-11991.
- Paulsson, J. F., Andersson, A., Westermark, P. and Westermark, G. T. (2006). Intracellular amyloid-like deposits contain unprocessed pro islet amyloid polypeptide (proIAPP) in beta-cells of transgenic mice overexpressing human IAPP and transplanted human islets. *Diabetologia*. 49(6): 1237-1246.
- Pearse, A. E., Ewen, S. W. and Polak, J. M. (1972). The genesis of apudamyloid in endocrine polypeptide tumours: histochemical distinction from immunamyloid. *Virchows Archives B Cell pathology*. 10: 93-107.
- Pepys, M. B. (2006). Amyloidosis. *Annual Reviews of Medicine*. 57: 223-241.
- Pettersson, M., Ahrén, B. (1990). Failure of islet amyloid polypeptide to inhibit basal and glucose-stimulated insulin secretion in model experiments in mice and rats. *Acta Physiologica Scandinavica*. 138: 389-394.
- Pimplikar, S. W., Nixon, R. A., Robakis, N. K. *et al.* (2010). Amyloid-independent mechanisms in Alzheimer's disease pathogenesis. *The Journal of neuroscience : the official journal of the Society for Neuroscience*. 30(45): 14946-14954.

- Podlisny, M. B., Walsh, D. M., Amarante, P. et al. (1998). Oligomerization of endogenous and synthetic amyloid  $\beta$ -protein at nanomolar levels in cell culture and stabilization of monomer by Congo red. *Biochemistry*. 37:3602-3611.
- Poitout, V. and Robertson, R. P. (2002). Minireview: secondary  $\beta$ -cell failure in type 2 diabetes--a convergence of glucotoxicity and lipotoxicity. *Endocrinology*.143(2):339-342.
- Pooga, M., Soomets, U., Hallbrink, M. et al. (1998). Cell penetrating PNA constructs regulate galanin receptor levels and modify pain transmission in vivo. *Nature Biotechnology*. 16(9):857-861.
- Porat, Y. Kolusheva, S., Jelinek, R. and Gazit, E. (2003). The human islet amyloid polypeptide forms transient membrane-active prefibrillar assemblies. *Biochemistry*. 42 (37): 10971-10977.
- Porat, Y., Mazor, Y., Efrat, S. and Gazit, E. (2004). Inhibition of islet amyloid polypeptide fibril formation: a potential role for heteroaromatic interactions. *Biochemistry*. 43 (45): 14454-14462.
- Porte, D. and Kahn, S. E. (2001).  $\beta$ -cell dysfunction and failure in type 2 diabetes. *Diabetes*, 50, S160-S163.
- Porte, D. Jr. (1991). Banting lecture 1990. Beta-cells in type II diabetes mellitus. *Diabetes*. 40(2):166-180.
- Porte, D. Jr. and Kahn, S. E. (1991). Mechanisms for hyperglycemia in type II diabetes mellitus: therapeutic implications for sulfonylurea treatment--an update. *American Journal of Medicine*. 90(6A):8S-14S.
- Portha, B., Blondel O, Serradas P, et al. (1989). The rat models of non-insulin dependent diabetes induced by neonatal streptozotocin. *Diabetes and Metabolism*. 15(2):61-75.
- Potes, C. S. and Lutz, T. A. (2010). Brainstem mechanisms of amylin-induced anorexia. *Physiology and Behavior*. 100(5):511-518.
- Potter, K. J., Scrocchi, L. A., Warnock, G. L., Ao, Z. et al. (2009). Amyloid inhibitors enhance survival of cultured human islets. *Biochimica et Biophysica Acta* 1790: 566-574.
- Prochiantz, A. (2000). Messenger proteins: homeoproteins, TAT and others. *Current Opinion in Cell Biology*. 12(4):400-406.
- Promega (2012). CellTiter 96 aqueous one solution proliferation assay. Technique bulletin. I-6.
- Qi, D., Cai, K., Wang, O. and Li, Z. (2010). Fatty acids induce amylin expression and secretion by pancreatic beta-cells. *American Journal of physiology: Endocrinology and Metabolism*. 298: E99-E107.
- Quist, A., Doudevski, I., Lin, H., Azimova, R. et al. (2005). Amyloid ion channels: a common structural link for protein-misfolding disease. *Proceedings of the National Academy of Sciences, USA*. 102 (30): 10427-10432.
- Quist, A., Doudevski, I., Lin, H., Azimova, R. et al. (2005). Amyloid ion channels: a common structural link for protein-misfolding disease. *Proceedings of the National Academy of Sciences, USA*. 102(30): 10427-10432.
- Rakieten, N., Rakieten, M. L. and Nadkarni, M. R. (1963). Studies on the diabetogenic action of streptozotocin (NSC-37917). *Cancer Chemotherapy Reports*. 29:91-98.

- Ramírez-Alvarado, M., Blanco, F. J. and Serrano, L. (1996). De novo design and structural analysis of a model beta-hairpin peptide system. *Nature Structural and Molecular Biology*. 3:(1996) 604-612.
- Reidelberger, R. D., Arnelo, U., Granqvist, L. and Permert, J. (2001). Comparative effects of amylin and cholecystokinin on food intake and gastric emptying in rats. *American Journal of Physiology: Regulatory Integrative and Comparative Physiology*. 280: R605-R611.
- Reinke, A. A. and Gestwicki, J. E. (2011). Insight into amyloid structure using chemical probes. *Chemical Biology and Drug Design*. 77:399-411.
- Reixach, N., Crooks, E., Ostresh, J. M. *et al.* (2000). Inhibition of  $\beta$ -amyloid-induced neurotoxicity by imidazopyridoindoles derived from a synthetic combinatorial library. *Journal of Structural Biology*. 130:247-258.
- Rerup, C. C. (1970). Drugs producing diabetes through damage of the insulin secreting cells. *Pharmacological Reviews*. 22(4):485-518.
- Richards, K. L., Aguilar, M. I., and Hearn, M. T. W. (1994). The effect of protein conformation on experimental bandwidths in RP-HPLC. *Journal of Chromatography*. 676:33-41.
- Ritzel, R. A., Meier, J. J., Lin, C. Y., Veldhuis, J. D. *et al.* (2007). Human islet amyloid polypeptide oligomers disrupt cell coupling, induce apoptosis, and impair insulin secretion in isolated human islets. *Diabetes*. 56 (1): 65-71.
- Rivera, J. F., Gurlo, T., Daval, M. *et al.* (2011). Human-IAPPdisrupts the autophagy/lysosomal pathway in pancreatic B-cells: protective role of p62-positive cytoplasmic inclusions. *Cell Death and Differentiation*. 18(3):415-426.
- Rochet, J. C. and Lansbury, P. T. (2000). Amyloid fibrillogenesis: themes and variations. *Current Opinion in Structural Biology*. 10: 60-68.
- Rogers, I., Kerr, F., Martinez, P. *et al.* (2012). Ageing increases vulnerability to A $\beta$ 242 toxicity in Drosophila. *PLoS One*.7(7): e40569.
- Roh, J., Chang, C. L., Bhalla, A., Klein, C. *et al.* (2004). Intermedin is a calcitonin/calcitonin gene-related peptide family peptide acting through the calcitonin receptor-like receptor/receptor activity-modifying protein receptor complexes. *Journal of Biological Chemistry*. 279 (8): 7264-7274.
- Ross, C.A. (2002). Polyglutamine pathogenesis: Emergence of unifying mechanisms for Huntington's disease and related disorders. *Neuron*. 35(5): 819-822.
- Rusnak, F., Zhou, J. and Hathaway, G. M. (2002). Identification of phosphorylated and glycosylated sites in peptides by chemically targeted proteolysis. *Journal of Biomolecular Techniques*. 13(4):228-237.
- Ryan, D. A., Narrow, W. C., Federoff, H. J. and Bowers, W. J. (2010). An improved method for generating consistent soluble amyloid-beta oligomers preparations for *in vitro* neurotoxicity studies. *Journal of Neuroscience Methods*. 190(2):171-179.
- Saafi, E. L., Konarkowska, B., Zhang, S. *et al.* (2001). Ultrastructural evidence that apoptosis is the mechanism by which human amylin evokes death in RINm5F pancreatic islet beta-cells. *Cell Biology International*. 25(4):339-350.
- Sale, M. M., Smith, S. G., Mychaleckyj, J. C., *et al.* (2007). Variants of the transcription factor 7-like 2 (TCF7L2) gene are associated with type 2 diabetes in an African-American population enriched for nephropathy. *Diabetes*. 56(10):2638-42.

- Sandler, S. and Stridsberg, M. (1994). Chronic exposure of cultured rat pancreatic islets to elevated concentrations of islet amyloid polypeptide (IAPP) causes a decrease in islet DNA content and medium insulin accumulation. *Regulatory Peptides*. 53(2): 103-109.
- Sandler, S. and Swenne, I. (1983). Streptozotocin, but not alloxan, induces DNA repair synthesis in mouse pancreatic islets in vitro. *Diabetologia*. 25:444-447.
- Sani, M., Sinisi, R. and Viani, F. (2006). Peptidyl fluoro-ketones as proteolytic enzyme inhibitors. *Current Topics in Medicinal Chemistry*. 6(14):1545-1566.
- Sanke, T., Bell, G. I., Sample, C., Rubenstein, A. H. *et al.* (1988). An islet amyloid peptide is derived from an 89-amino acid precursor by proteolytic processing. *Journal of Biological Chemistry*. 263 (33): 17243-17246.
- Saraogi, I., Hebda, J. A., Becerril, J., Estroff, L. A. *et al.* (2010). Synthetic alpha-helix mimetics as agonists and antagonists of islet amyloid polypeptide aggregation. *Angewandte Chemie (International Edition England)*. 49 (4): 736-739.
- Sarwar, N., Gao, P., Seshasai, S. R., Gobin, R. *et al.* (2010). Emerging Risk Factors Collaboration Diabetes mellitus, fasting blood glucose concentration, and risk of vascular disease: a collaborative meta-analysis of 102 prospective studies. *Lancet*. 375 (9733): 2215-2222.
- Sawaya, M. R., Sambashivan, S., Nelson, R. *et al.* (2007). Atomic structures of amyloid cross- $\beta$  spines reveal varied steric zippers. *Nature*. 447 (7143): 453-457.
- Schafer, S. A., Tschritter, O., Machicao, F. *et al.* (2007). Impaired glucagon-like peptide-1-induced insulin secretion in carriers of transcription factor 7-like 2 (TCF7L2) gene polymorphisms. *Diabetologia*. 50(12):2443-50.
- Schlamadinger, D. and Miranker, A. (2014). Fiber-dependent and -independent toxicity of islet amyloid polypeptide. *Biophysical Journal*. 107(11):2559-2566.
- Schofield, C. J., Libby, G., Brennan, G. M., MacAlpine, R. R. *et al.* (2006). Mortality and hospitalization in patients, after amputation: a comparison between patients with and without diabetes. *Diabetes Care*. 29 (10): 2252-2256.
- Scott, L. J., Bonnycastle, L. L., Willer, C. J. *et al.* (2006). Association of transcription factor 7-like 2 (TCF7L2) variants with type 2 diabetes in a Finnish sample. *Diabetes*. 55 (9):2649-53.
- Scrocchi, L. A., Chen, Y., Waschuk, S. *et al.* (2002). Design of Peptide-based Inhibitors of Human Islet Amyloid Polypeptide Fibrillogenesis. *Journal of Molecular Biology*. 318(3):697-706.
- Sellin, D., Yan, L., Kapurniotu, A. and Winter, R. (2010). Suppression of IAPP fibrillation at anionic lipid membranes via IAPP-derived amyloid inhibitors and insulin. *Biophysical Chemistry*. 150 (1-3): 73-79.
- Serpell, L. C., Sunde, M., Benson, M. D. *et al.* (2000). The protofilament substructure of amyloid fibrils. *Journal of molecular Biology*. 300(5):1033-1039.
- Shapiro, A. M., Lakey, J. R., Ryan, E. A. *et al.* (2000). Islet transplantation in seven patients with type 1 diabetes mellitus using a glucocorticoid-free immunosuppressive regimen. *New England Journal of Medicine*. 343:230-238.
- Shapiro, A. M., Ricordi, C., Hering, B. J. *et al.* (2006). International trial of the Edmonton protocol for islet transplantation. *New England Journal of Medicine*. 355:1318-1330.

- Sharadrao, M. P. and Andrei, T. A. (2015). Charge-Based Inhibitors of Amylin Fibrillization and Toxicity. *Journal of Diabetes Research*. 2015(13).
- Sheedy, F. J., Grebe, A., Rayner, K. J. *et al.* (2013). CD36 coordinates NLRP3 inflammasome activation by facilitating intracellular nucleation of soluble ligands into particulate ligands in sterile inflammation. *Nature Immunology*. 14(8):812-820.
- Shiba, Y., Fernandes, S., Zhu, W. Z. *et al.* (2012). Human ES-cell-derived cardiomyocytes electrically couple and suppress arrhythmias in injured hearts. *Nature*. 489:322-325.
- Shu, L., Sauter, N. S., Schulthess, F. T. *et al.* (2008). Transcription factor 7-like 2 regulates beta-cell survival and function in human pancreatic islets. *Diabetes*. 57(3):645-53.
- Silbernagel, G., Renner, W., Grammer, T. B. *et al.* (2011). Association of TCF7L2 SNPs with age at onset of type 2 diabetes and proinsulin/insulin ratio but not with glucagon-like peptide 1. *Diabetes Metabolism Research and Reviews*. 27(5):499-505.
- Silvestre, R. A., Rodríguez-Gallardo, J., Gutiérrez, E. and Marco, J. (1997). Influence of glucose concentration on the inhibitory effect of amylin on insulin secretion. Study in the perfused rat pancreas. *Regulatory Peptides*. 68 (1): 31-35.
- Sinha, S., Lopes, D., Du, Z. *et al.* (2011). Lysine-specific molecular tweezers are broad-spectrum inhibitors of assembly and toxicity of amyloid proteins. *Journal of American Chemical Society*. 133(42):16958-16969.
- Sivanesam, K., Shu, I., Huggins, K. N. *et al.* (2016). Peptide Inhibitors of the amyloidogenesis of IAPP: verification of the hairpin-binding geometry hypothesis. *FEBS Letters*. 590:2575-2583.
- Skofitsch, G., Wimalawansa, S. J., Jacobowitz, D. M. and Gubisch, W. (1995). Comparative immuno histochemical distribution of amylin-like and calcitonin gene related peptide like immunoreactivity in the rat central nervous system. *Canadian Journal of Physiology and Pharmacology*. 73 (7): 945-956.
- Skovso, S. (2014). Modeling type 2 diabetes in rats using high fat diet and streptozotocin. *Journal of Diabetes Investigation*. 5(4):349-358.
- Smeeckens, S. P., Montag, A., Thomas, G., Albiges-Rizo, C. *et al.* (1992). Proinsulin processing by the subtilisin-related proprotein convertases furin, PC2, and PC3. *Proceedings of the National Academy of Sciences, USA*. 89 (18): 8822-8826.
- Smith, P. S., Brender, J. R. and Ramamoorthy, A. (2009). Induction of negative curvature as a mechanism of cell toxicity by amyloidogenic peptides: the case of islet amyloid polypeptide. *Journal of American Chemical Society*. 131(12): 4470-4478.
- Smith, R. D., Hu, L., Falkner, J. A. *et al.* (2006). Exploring protein-ligand recognition with Binding MOAD. *Journal of Molecular Graphics and Modelling*. 24:414-425.
- Sochocka, M., Koutsouraki, E. S., Gąsiorowski, K. and Leszek, J. (2013). Vascular oxidative stress and mitochondrial failure in the pathobiology of Alzheimer's disease: New approach to therapy. *CNS and Neurological Disorders Drug Targets*. 12(6):870-881.
- Soeller, W. C., Janson, J., Hark, S. E., Parker, J. C. (1998). Islet amyloid associated diabetes in obese A(vy)/a mice expressing human islet amyloid polypeptide. *Diabetes*. 47 (5): 43-750.
- Soria, B. *et al.* (2000). Insulin-secreting cells derived from embryonic stem cells normalize glycemia in streptozotocin-induced diabetic mice. *Diabetes*. 49(2):157-162.

Soto, C., Kindy, M. S., Baumann, M., Frangione, B. (1996). Inhibition of Alzheimer's amyloidosis by peptides that prevent beta-sheet conformation. *Biochemical and Biophysical Research Communications*. 226(3):672-680.

Soto, E. M., Sigurdsson, L. Morelli, R.A. *et al.* (1998).  $\beta$ -Sheet breaker peptides inhibit fibrillogenesis in rat brain model of amyloidosis: implications for Alzheimer's therapy. *Nature Medicine*. 4:822-826.

Spellman, C. W. (2010). Pathophysiology of Type 2 Diabetes: Targeting Islet Cell Dysfunction. *Journal of American Osteopathic Association*. 110 (3): S2-S7.

Srinivasan, K., Viswanad, B., Asrat, L. *et al.* (2005). Combination of high-fat diet-fed and low-dose streptozotocin-treated rat: a model for type 2 diabetes and pharmacological screening. *Pharmacological Research*. 52(4):313-320.

Stefani, M. and Rigacci, S. (2013). Protein Folding and Aggregation into Amyloid: The Interference by Natural Phenolic Compounds. *International Journal of Molecular Science*. 14(6): 12411-12457.

Stridsberg, M., Tjälve, H. and Wilander, E. (1993). Whole-body autoradiography of <sup>123</sup>I-labelled islet amyloid polypeptide (IAPP). Accumulation in the lung parenchyma and in the villi of the intestinal mucosa in rats. *Acta Oncologica*. 32(2):155-159.

Sullivan, K. A., Hayes, J. M., Wiggin, T. D. *et al.* (2007). Mouse models of diabetic neuropathy. *Neurobiology of Disease*. 28:276-285.

Sun, X. and Lorenzi, G. P. (1994). On the stacking of  $\beta$ -rings: the solution self-association behaviour of two partially N-methylated cyclo (hexaleucines). *Helvetica Chimica Acta*. 77(6):1520-1526.

Sunde, M., Serpell, L. C., Bartlam, M. *et al.* (1997). Common core structure of amyloid fibrils by synchrotron X-ray diffraction. *Journal of Molecular Biology*. 273(3):729-739.

Surwit, R. S. Kuhn, C. M. Cochrane C. *et al.* (1988). Diet-induced type II diabetes in C57BL/6J mice. *Diabetes*. 37(9):1163.

Suzuki, Y., Yoshida, K., Ichimiya, T. *et al.* (1990). Trypsin inhibitors in guinea pig plasma: isolation and characterization of contrapsin and two isoforms of alpha-1-antitrypsin and acute phase response of four major trypsin inhibitors. *Journal of Biochemistry*. 107(2):173-9.

Szkudelski, T. (2001). The mechanism of alloxan and streptozotocin action in B cells of the rat pancreas. *Physiological Research*. 50(6):537-546.

Szkudelski, T. (2012). Streptozotocin- nicotinamide-induced diabetes in the rat. Characteristics of the experimental model. *Experimental Biology and Medicine*. 237(5):481-490.

Tabner, B. J., Turnbull, S., El-Agnaf, O. M. and Allsop, D. (2002). Formation of hydrogen peroxide and hydroxyl radicals from A $\beta$  and  $\alpha$ -synuclein as a possible mechanism of cell death in Alzheimer's disease and Parkinson's disease. *Free Radical Biology and Medicine*. 32(11):1076-1083.

Taniguchi, C. M., Emanuelli, B. and Kahn, C. R. (2006). Critical nodes in signalling pathways: insights into insulin action. *Nature Reviews: Molecular Cell Biology*. 7: 85-96.

Tartaglia, G. G., Pawar, A. P., Campioni, S., Dobson, C. M. *et al.* (2008). Prediction of aggregation-prone regions in structured proteins. *Journal of Molecular Biology*. 380 (2): 425-436.

- Tatarek-Nossol, M., Yan, L. M., Schmauder, A. *et al.* (2005). Inhibition of hIAPP amyloid-fibril formation and apoptotic cell death by a designed hIAPP amyloid- core-containing hexapeptide. *Chemistry and Biology*. 12(7):797-809.
- Taylor, M., Moore, S., Mayes, J., Parkin, E. *et al.* (2010). Development of a Proteolytically Stable Retro-Inverso Peptide Inhibitor of  $\beta$ -Amyloid Oligomerization as a Potential Novel Treatment for Alzheimer's Disease. *Biochemistry*. 49 (15): 3261-3272.
- Teich, A. F. and Arancio, O. (2012). Is the amyloid hypothesis of Alzheimer's disease therapeutically relevant? *The Biochemical journal*. 446(2): 165-177.
- Teichmann, S. A. (2002). Principles of protein-protein interactions. *Bioinformatics*. 18:S249.
- Teixido, M., Albericio, F. and Giralt, E. (2005). Solid-phase synthesis and characterization of N-methyl-rich peptides. *Journal of Peptide Research*. 65(2):153-166.
- Temsamani, J. and Vidal, P. (2004). The use of cell-penetrating peptides for drug delivery. *Drug Discovery Today*. 9(23):1012-1019.
- Tenidis, K., Waldner, M., Bernhagen, J. Fischle, W. *et al.* (2000). Identification of a penta- and hexapeptide of islet amyloid polypeptide (IAPP) with amyloidogenic and cytotoxic properties. *Journal of Molecular Biology*. 295 (4): 1055-1071.
- Thompson, R. G., Pearson, L., Schoenfeld, S. L. and Kolterman, O. G. (1998). Pramlintide, a synthetic analog of human amylin, improves the metabolic profile of patients with type 2 diabetes using insulin. The Pramlintide in Type 2 Diabetes Group. *Diabetes Care*. 21 (6): 987-993.
- Thorn, D.C., Ecroyd, H., Sunde, M. *et al.* (2008). Amyloid Fibril Formation by Bovine Milk  $\kappa$ S2-Casein Occurs under Physiological Conditions Yet Is Prevented by Its Natural Counterpart,  $\kappa$ S1-Casein. *Biochemistry*. 47(12):3926-3936.
- Tjemberg, L. O., Lilliehook, C., Callaway, D. J. E. *et al.* (1997). Controlling amyloid  $\beta$ -peptide fibril formation with protease-stable ligands. *Journal of Biological Chemistry*. 272(19): 12601-12605.
- Tomic, J. L., Pensalfini, A., Head, E. and Glabe, C. G. (2009). Soluble fibrillar oligomer levels are elevated in Alzheimer's disease brain and correlate with cognitive dysfunction. *Neurobiology of Disease*. 35: 352-358.
- Torchilin, V. P. (2008). Cell penetrating peptide-modified pharmaceutical nanocarriers for intracellular drug and gene delivery. *Biopolymers*. 90:604-610.
- Torchilin, V. P., Rammohan, R., Weissig, V. and Levchenko T. S. (2001). TAT peptide on the surface of liposomes affords their efficient intracellular delivery even at low temperature and in the presence of metabolic inhibitors. *Proceedings of the National Academy of Sciences U. S. A*. 98(15):8786-8791.
- Toshimori, H., Narita, R., Nakazato, M., Asai, J. *et al.* (1990). Islet amyloid polypeptide (IAPP) in the gastrointestinal tract and pancreas of man and rat. *Cell Tissue Research*. 262:401-406.
- Trikha, S. and Jeremic, A. M. (2011). Clustering and internalization of toxic amylin oligomers in pancreatic cells require plasma membrane cholesterol, *The Journal of Biological Chemistry*. 286(41):36086-36097.
- Turnbull, S., Tabner, B. J., El-Agnaf, O.M.A. *et al.* (2001).  $\alpha$ -Synuclein implicated in Parkinson's disease catalyzes the formation of hydrogen peroxide *in vitro*. *Free Radical Biology and Medicine*. 30(10):1163-1170.

Udayasankar, J., Kodama, K., Hull, R. L. *et al.* (2009). Amyloid formation results in recurrence of hyperglycaemia following transplantation of human IAPP transgenic mouse islets. *Diabetologia*. 52(1):145-153.

Vaxillaire, M. and Froguel, P. (2010). The genetics of Type 2 diabetes: from candidate gene biology to genome-wide studies, in Holt RIG, Cockram CS, Flyvbjerg A *et al.* (ed.) Textbook of diabetes, 4th edition. Oxford: Wiley-Blackwell.

Veldhoen S., Laufer S.D. and Restle, T. (2008). Recent developments in Peptide-based nucleic Acid delivery. *International Journal of Molecular Science*. 9:1276-1320.

Verchere, C. B., D'Alessio, D. A., Wang, S., Andrikopoulos, S. *et al.* (1997). Transgenic overproduction of islet amyloid polypeptide (amylin) is not sufficient for islet amyloid formation. *Hormone and Metabolic Research*. 29 (6): 311-316.

Verchere, C. B., D'Alessio, D. A., Palmiter, R. D., Weir, G. C. *et al.* (1996). Islet amyloid formation associated with hyperglycemia in transgenic mice with pancreatic beta cell expression of human islet amyloid polypeptide. *Proceedings of the National Academy of Sciences, USA*. 93: 492-3496.

Vitoux, B., Aubry, A., Thong, C. and Marraud, M. (1986). N-methyl peptides. VII. Conformational perturbations induced by N-methylation of model dipeptides. *Journal of Peptide Research*. 27(6):617-532.

Vlieghe, P., Lisowski, V., Martinez, J. and Khrestchatsky, M. (2010). Synthetic therapeutic peptides: science and market. *Drug Discovery Today*. 15:40-56.

Wakabayashi, M. and Matsuzaki, K. (2009). Ganglioside-induced amyloid formation by human islet amyloid polypeptide in lipid rafts. *FEBS Letters*. 583(17): 2854-2858.

Walsh, P., Simonetti, K., and Sharpe, S. (2009). Core Structure of Amyloid Fibrils Formed by Residues 106-126 of the Human Prion Protein. *Structure*. 17(3):417-426.

Wang, J., Xu, J., Finnerty, J., Furuta, M. *et al.* (2001). Steiner DF, Verchere CB. The prohormone convertase enzyme 2 (PC2) is essential for processing pro-islet amyloid polypeptide at the NH<sub>2</sub>-terminal cleavage site. *Diabetes*. 50 (3): 534-539.

Wang, Q, Jin. T. (2009). The role of insulin signaling in the development of beta-cell dysfunction and diabetes. *Islets*. 1(2):95-101.

Wang, Q., Ning, L., Niu, Y., Liu, H. and Yao, X. (2015). Molecular mechanism of the inhibition and remodelling of human islet amyloid polypeptide (hIAPP(1-37) oligomer by resveratrol from molecular dynamics simulation. *Journal of Physical Chemistry B*. 119: 15-24.

Watada, H., Kajimoto, Y., Kaneto, H. Matsuoka, T. *et al.* (1996). Involvement of the homeodomain-containing transcription factor PDX-1 in islet amyloid. *Biochemical and Biophysical research communications*. 229 (3): 745-751.

Weiss, W. A. (2007). *et al.* Recognizing and exploiting differences between RNAi and small-molecule inhibitors. *Nature Chemical Biology*. 3(12):739-44.

Wells, J. A. and McClendon, C. L. (2007). Reaching for high-hanging fruit in drug discovery at protein-protein interfaces. *Nature*. 450:1001-1009.

Werle, M. and Bernkop-Schnürch, A. (2006). Strategies to improve plasma half life time of peptide and protein drugs. *Amino Acids*. 30(4):351-367.

- Westermarck, G. T., Davalli, A. M., Secchi, A. *et al.* (2012). Further evidence for amyloid deposition in clinical pancreatic islet grafts. *Transplantation*. 93(2):219-223.
- Westermarck, G. T., Falkmer, S., Steiner, D. F., Chan, S. J. *et al.* (2002). Islet amyloid polypeptide is expressed in the pancreatic islet parenchyma of the teleostean fish. *Myoxocephalus (Cottus) scorpius*. *Comparative Biochemistry and Physiology*. 133: 119-125.
- Westermarck, G. T., Leckström, A., Zhi, M. and Westermarck, P. (1998). Increased release of IAPP in response to long-term high fat intake in mice. *Hormone and Metabolic Research*. 30 (5): 256-258.
- Westermarck, P and Grimelius, L. (1973). The pancreatic islet cells in insular amyloidosis in human diabetic and non-diabetic adults. *Acta pathologica et microbiologica Scandinavica*. 81: 291-300.
- Westermarck, P. Andersson, A. and Westermarck, G. T. (2011). Islet amyloid polypeptide, islet amyloid, and diabetes mellitus. *Physiological Reviews*. 91(3):795-826.
- Westermarck, P. (1972). Quantitative studies on amyloid in the islets of Langerhans. *Upsala Journal of Medical Science*. 77(2): 91-94.
- Westermarck, P. (2005). Aspects on human amyloid forms and their fibril polypeptides. *FEBS Letters*. 272 (23): 5942-5949.
- Westermarck, P. (2011). Amyloid in the islets of Langerhans: thoughts and some historical aspects. *Upsala Journal of Medical Sciences*. 116 (2): 81-89.
- Westermarck, P. and Grimelius, L. (1973). The pancreatic islet cell in insular amyloidosis in human diabetic and non-diabetic islets. *Acta Pathologica et Microbiologica Scandinavica, section A*. 81(3):291-300.
- Westermarck, P. and Wilander, E. (1978). The influence of amyloid deposits on the islet volume in maturity onset diabetes mellitus. *Diabetologia*. 15: 417-421.
- Westermarck, P., Benson, M. D., Buxbaum, J. N. *et al.* (2007). A primer of amyloid nomenclature. *Amyloid*. 14 (3): 179-183.
- Westermarck, P., Engstrom, U., Johnson, K. H. *et al.* (1990). Islet amyloid polypeptide - pinpointing amino-acidresidues linked to amyloid fibril formation. *Proceedings of the National Academy of Sciences of the United States of America*. 87(13): 5036-5040.
- Westermarck, P., Johnson, K. H., O'Brien, T. D. and Betsholtz, C. (1992). Islet amyloid polypeptide: a novel controversy in diabetes research. *Diabetologia*. 35: 297-303.
- Westermarck, P., Li, Z. C., Westermarck, G. T., Leckström, A. *et al.* (1996). Effects of beta cell granule components on human islet amyloid polypeptide fibril formation. *FEBS Letters*. 379 (3): 203-206.
- Westermarck, P., Wernstedt, C., Wilander, E., Hayden, D. W. *et al.* (1987). Amyloid fibrils in human insulinoma and islets of Langerhans of the diabetic cat are derived from a neuropeptide-like protein also present in normal islet cells. *Proceedings of the National Academy of Science, USA*. 84 (11): 3881-3885.
- Westermarck, U. P., Engström, K., Johnson, H., Westermarck, G. T. *et al.* (1990). Islet amyloid polypeptide: pinpointing amino acid residues linked to amyloid fibril formation. *Proceedings of the National Academy of Sciences, USA*. 87 (13): 5036-5040.

- Whitty, A. and Kumaravel, G. (2006). Between a rock and a hard place. *Nature Chemical Biology*. 2:112-118.
- WHO (2016). World Health Organisation. Diabetes. [Online]. Available at: <http://www.who.int/diabetes/en/> . (Accessed 12<sup>th</sup> January 2016).
- Willcox, A. R., Bone, A. J., Foulis, A. K. and Morgan, N. G. (2009). Analysis of islet inflammation in human type 1 diabetes. *Clinical and Experimental Immunology*. 155 (2): 173-181.
- Wilson, M. R., Yerbury, J. J. and Poon, S. (2008). Potential roles of abundant extracellular chaperones in the control of amyloid formation and toxicity. *Molecular BioSystems*. 4(1):42-52.
- Wiltzius, J. J., Sievers, S. A., Sawaya, M. R. *et al.* (2008). Atomic structure of the cross-beta spine of islet amyloid polypeptide (amylin). *Protein Science*. 17(9):1467-1474.
- Wimalawansa, S. J. (1997). Amylin, calcitonin gene-related peptide, calcitonin, and adrenomedullin: a paptide superfamily. *Critical Reviews in Neurobiology*. 11(2-3): 167-239.
- Woerle, H. J., Albrecht, M., Linke, R., Zschau, S. *et al.* (2008). Impaired hyperglycemia-induced delay in gastric emptying in patients with type 1 diabetes deficient for islet amyloid polypeptide. *Diabetes Care*. 31 (12): 2325-2331.
- Wogulis, M., Wright, S., Cunningham, D., Chilcote, T. *et al.* (2005). Nucleation-dependent polymerization is an essential component of amyloid-mediated neuronal cell death. *Journal of Neuroscience*. 25 (5): 1071-1080.
- Wolfe, L. S., Calabrese, M. F., Nath, A. *et al.* (2010). Protein-induced photophysical changes to the amyloid indicator dye thioflavin T. *Proceedings of the National Academy of Sciences United States of America*. 107(39):16863-16868.
- Wookey, P. J., Tikellis, C., Du, H. C., Qin, H. F. *et al.* (1996). Amylin binding in rat renal cortex, stimulation of adenylyl cyclase, and activation of plasma renin. *American Journal of Physiology*. 270(2): F289-F294.
- Wu, J and Yan L J. (2015). Streptozotocin-induced type 1 diabetes in rodents as a model for studying mitochondrial mechanisms of diabetic  $\beta$  cell glucotoxicity. *Diabetes, Metabolic Syndrome and Obesity*. 8:181-188.
- Wu, M. S., Liang, J. T., Lin, Y. D. *et al.* (2008). Aminoguanidine prevents the impairment of cardiac pumping mechanics in rats with streptozotocin and nicotinamide-induced type 2 diabetes. *British Journal of Pharmacology*. 154(4):758-764.
- Yan, L. M., Velkova, A., Taterek-Nossol, M., Andreetto, E. *et al.* (2007). IAPP mimic blocks Abeta cytotoxic self-assembly: cross-suppression of amyloid toxicity of Abeta and IAPP suggests a molecular link between Alzheimer's disease and type II diabetes. *Angewandte Chemie International Edition*. 46 (8): 1246-1252.
- Yan, L., Taterek-Nossol, M., Velkova, A. *et al.* (2006). Design of a mimic of nonamyloidogenic and bioactive human islet amyloid polypeptide (IAPP) as nanomolar affinity inhibitor of IAPP cytotoxic fibrillogenesis. *Proceedings of the National Academy of Sciences USA*. 103(7):2046-2051.
- Yang, F., Lim, G. P., Begum, A. N. *et al.* (2005). Curcumin inhibits formation of amyloid  $\beta$  oligomers and fibrils, binds plaques, and reduces amyloid *in vivo*. *Journal of Biological Chemistry*. 280:5892-5901.

- Yankner, B. A., Dawes, L. R., Fisher, S., Villa-Komaroff, L. *et al.* (1989). Neurotoxicity of a fragment of the amyloid precursor associated with Alzheimer's disease. *Science*. 245:417-420.
- Yankner, B. A., Duffy, L. K. and Kirschner, D. A. (1990). Neurotrophic and neurotoxic effects of amyloid beta protein: reversal by tachykinin neuropeptides. *Science*. 250(4978):279-282.
- Yin, D., Tao, J., Lee, D. D. *et al.* (2006). Recovery of islet beta-cell function in streptozotocin-induced diabetic mice: an indirect role for the spleen. *Diabetes*. 55(12):3256-3263.
- Zaidi, M., Datta, H. K., Bevis, P. J., Wimalawansa, S. J. *et al.* (1990). Amylin-amide: a new bone-conserving peptide from the pancreas. *Experimental Physiology*. 75: 529-536.
- Zampagni, M., Wright, D., Cascella, R. *et al.* (2012). Novel S-acyl glutathione derivatives prevent amyloid oxidative stress and cholinergic dysfunction in Alzheimer disease models. *Free Radical Biology and Medicine*. 52(8):1362-1371.
- Zhang, S., Liu, J., Dragunow, M. and Cooper, C. J. S. (2003). Fibrillogenic amylin evokes islet  $\beta$ -cell apoptosis through linked activation of a caspase cascade and JNK1. *The Journal of Biological Chemistry*. 278: 52810-52819.
- Zhang, Y., Ranta, F., Tang, C., Shumilina, E. *et al.* (2009). Sphingomyelinase dependent apoptosis following treatment of pancreatic beta-cells with amyloid peptides A $\beta$ (1-42) or IAPP. *Apoptosis*. 14 (7): 878-889.
- Zhou, Q., Law, A. C., Rajagopal, J. *et al.* (2007). A multipotent progenitor domain guides pancreatic organogenesis. *Developmental Cell*. 13:103-114.
- Zierath, J. R., Galuska, D., Engström, A., Johnson K. H. *et al.* (1992). Human islet amyloid polypeptide at pharmacological levels inhibits insulin and phorbol ester-stimulated glucose transport in in vitro incubated human muscle strips. *Diabetologia* 35: 26-31.
- Zraika, S., Hull, R. L., Verchere, C. B., Clark, A. *et al.* (2010). Toxic oligomers and islet beta cell death: guilty by association or convicted by circumstantial evidence? *Diabetologia*. 53 (6): 1046-1056.

# APPENDICES

## APPENDIX A

### Reversed-Phase High-Performance Liquid Chromatography of IO8, N1-IO8 and N2-IO8

This appendix shows the stability of data of IO8, N1-IO8 and N2-IO8 peptides in the presence of varying proteolytic enzymes and plasma performed using Reversed-Phase High-Performance Liquid Chromatography (RP-HPLC). Chromatographs from these studies are outlined below.

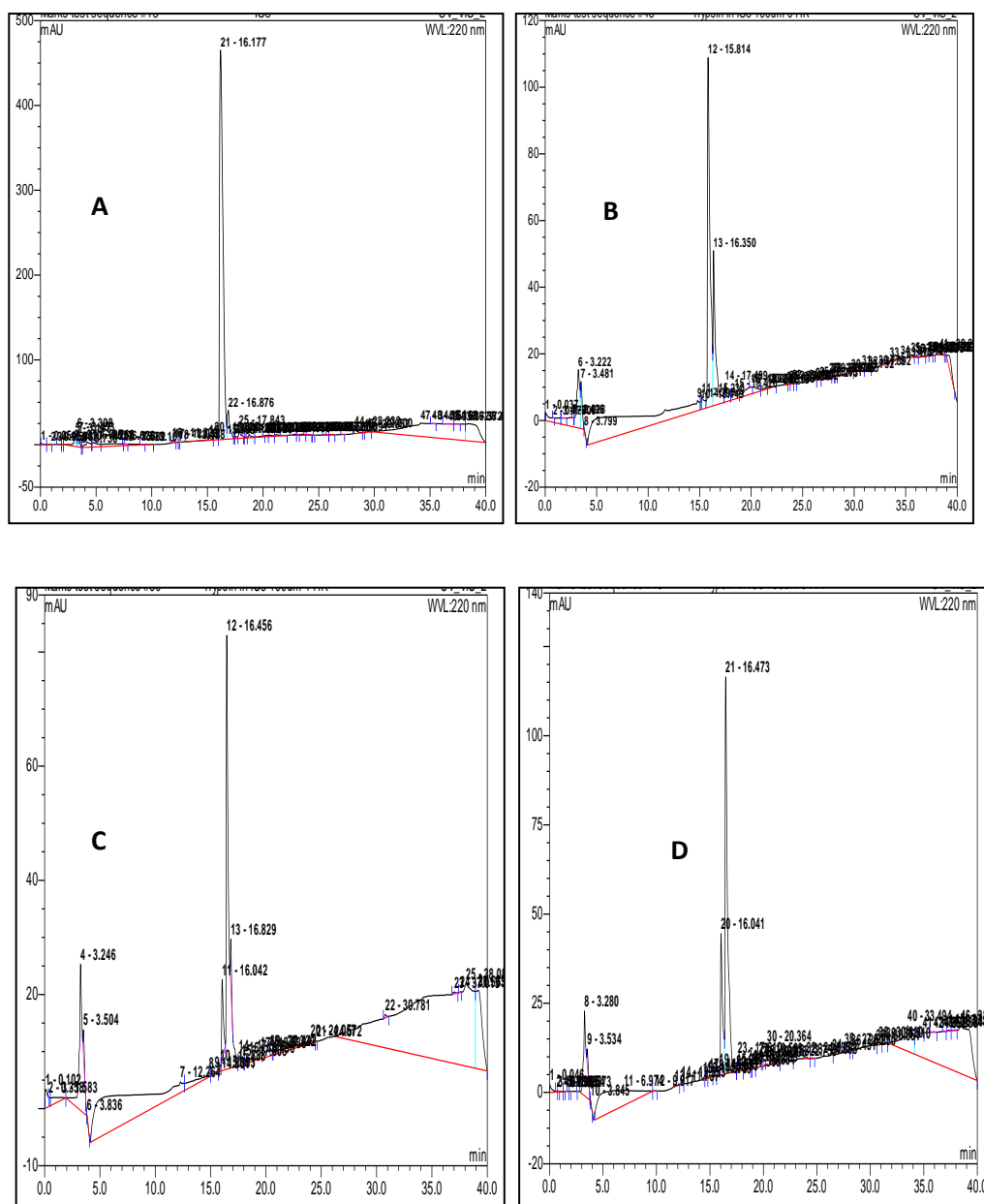


Figure A1.1: Relative Resistance of IO8 to proteolysis. (A) RP-HPLC chromatographs of IO8 before incubation in proteolytic enzymes. RP-HPLC chromatographs of IO8 after incubation in Trypsin (B) 0 hr (C) 1 hr (D) 3 hrs. Conditions, linear gradient from 0–60% acetonitrile with 0.1% TFA over 40 min, at a flow rate of 1 mL/min, 28 °C. Absorbance at 220 nm and elution time in minutes

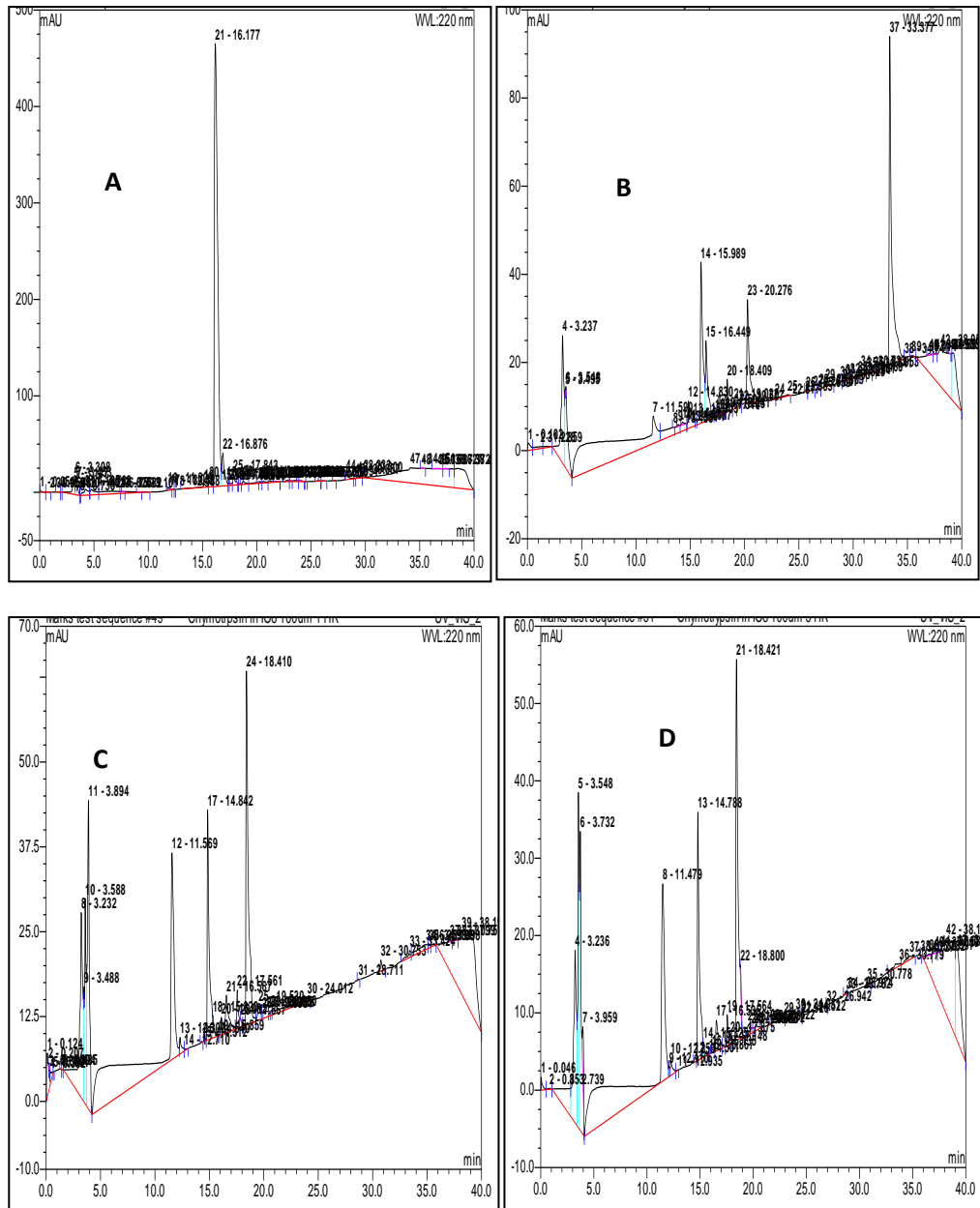


Figure A.1.2: Relative Resistance of IO8 to proteolysis. (A) RP-HPLC chromatographs of IO8 before incubation in proteolytic enzymes. RP-HPLC chromatographs of IO8 after incubation in Chymotrypsin (B) 0 hr (C) 1 hr (D) 3 hrs. Conditions, linear gradient from 0–60% acetonitrile with 0.1% TFA over 40 min, at a flow rate of 1 mL/min, 28 °C. Absorbance at 220 nm and elution time in minutes

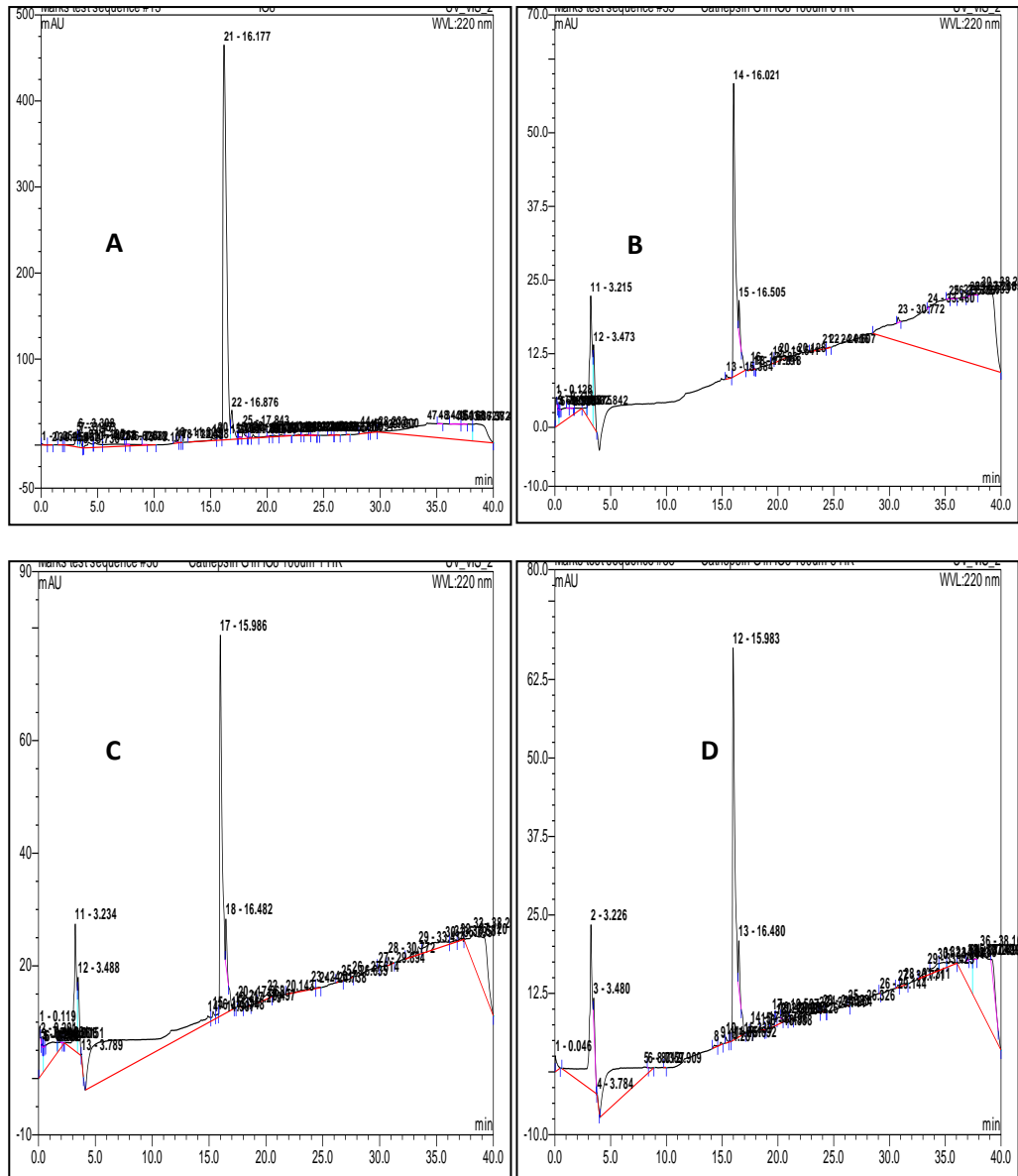


Figure A1.3: Relative Resistance of IO8 to proteolysis. (A) RP-HPLC chromatographs of IO8 before incubation in proteolytic enzymes. RP-HPLC chromatographs of IO8 after incubation in Cathepsin G (B) 0 hr (C) 1 hr (D) 3 hrs. Conditions, linear gradient from 0–60% acetonitrile with 0.1% TFA over 40 min, at a flow rate of 1 mL/min, 28 °C. Absorbance at 220 nm and elution time in minutes

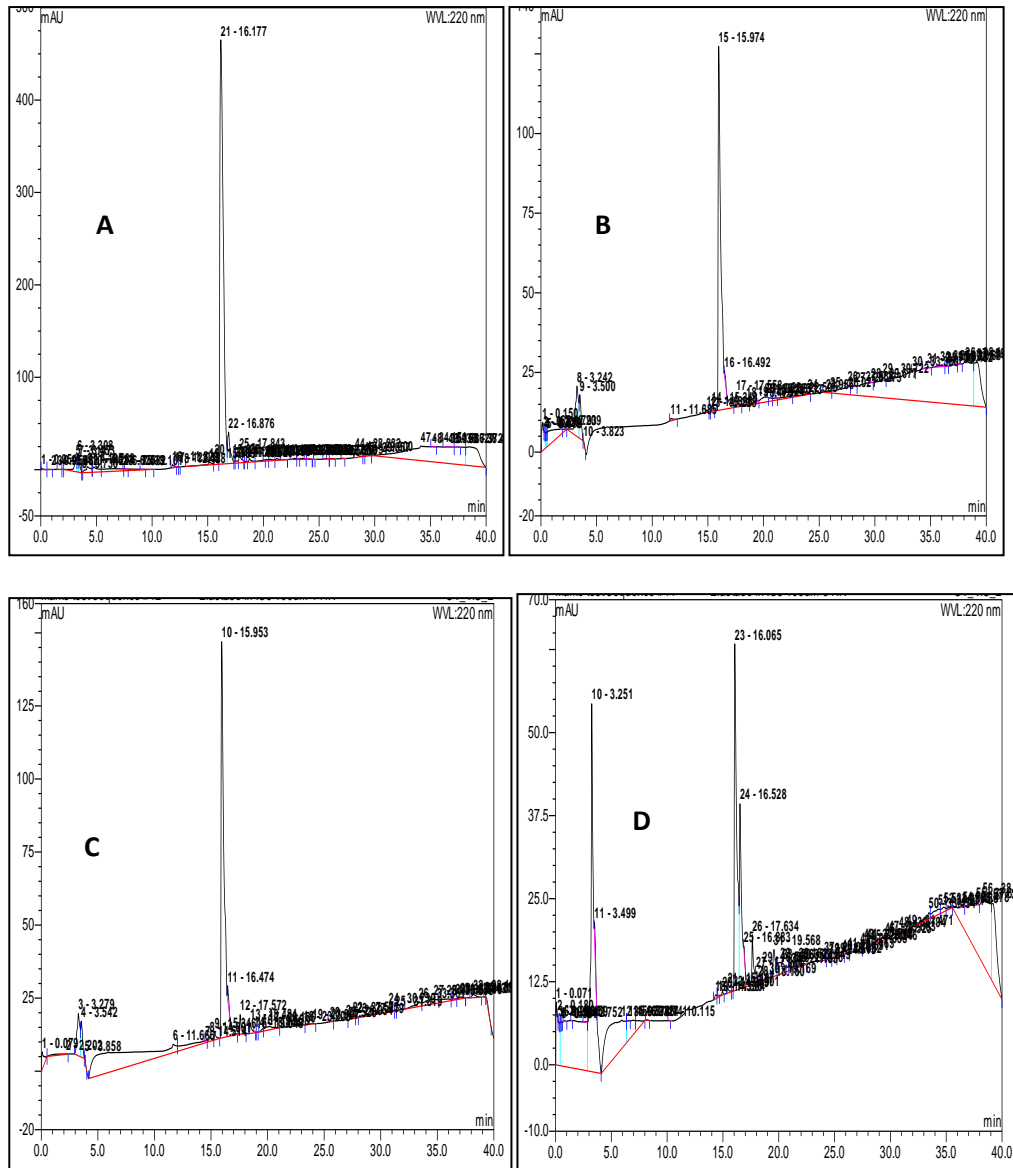


Figure A1.4: Relative Resistance of IO8 to proteolysis. (A) RP-HPLC chromatographs of IO8 before incubation in proteolytic enzymes. RP-HPLC chromatographs of IO8 after incubation in Elastase (B) 0 hr (C) 1 hr (D) 3 hrs. Conditions, linear gradient from 0–60% acetonitrile with 0.1% TFA over 40 min, at a flow rate of 1 mL/min, 28 °C. Absorbance at 220 nm and elution time in minutes

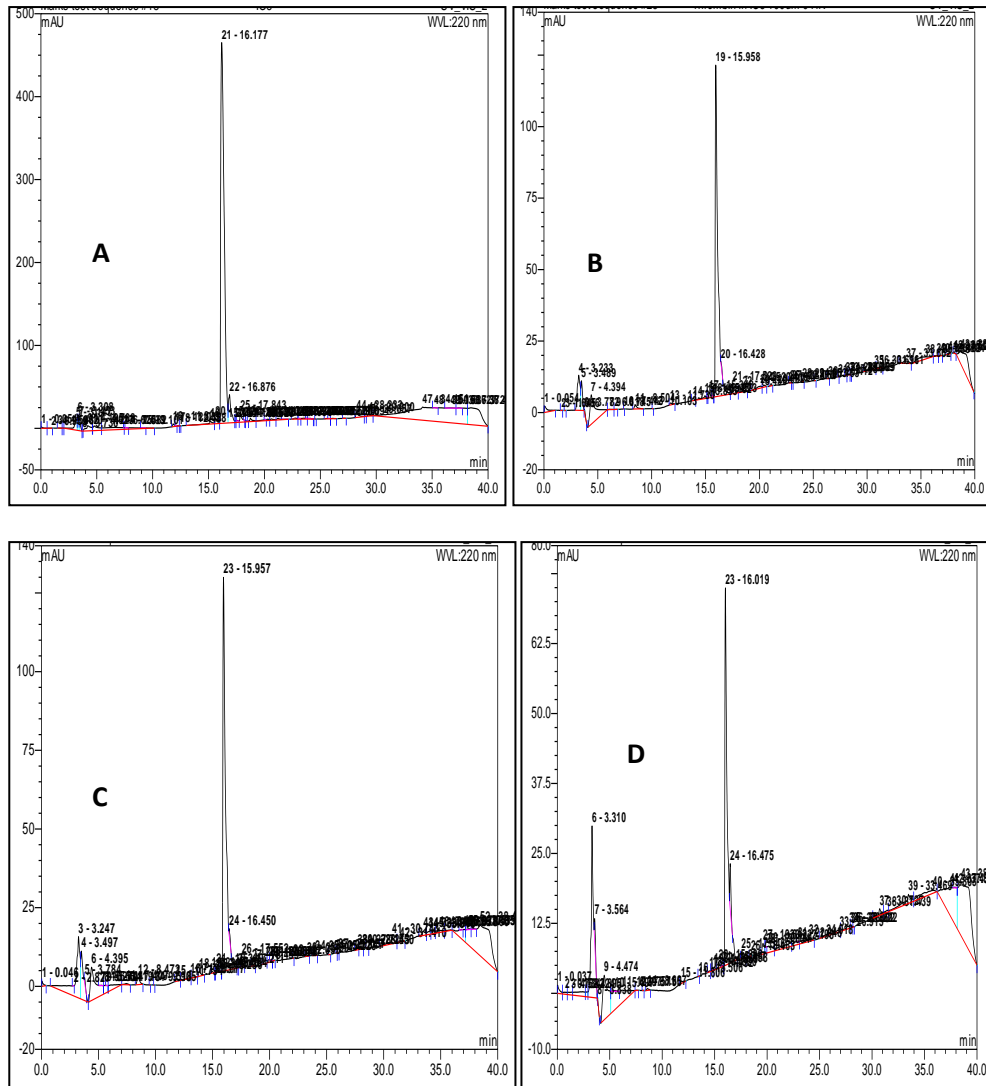


Figure A1.5: Relative Resistance of IO8 to proteolysis. (A) RP-HPLC chromatographs of IO8 before incubation in proteolytic enzymes. RP-HPLC chromatographs of IO8 after incubation in Thrombin, (B) 0 hr (C) 1 hr (D) 3 hrs. Conditions, linear gradient from 0–60% acetonitrile with 0.1% TFA over 40 min, at a flow rate of 1 mL/min, 28 °C. Absorbance at 220 nm and elution time in minutes

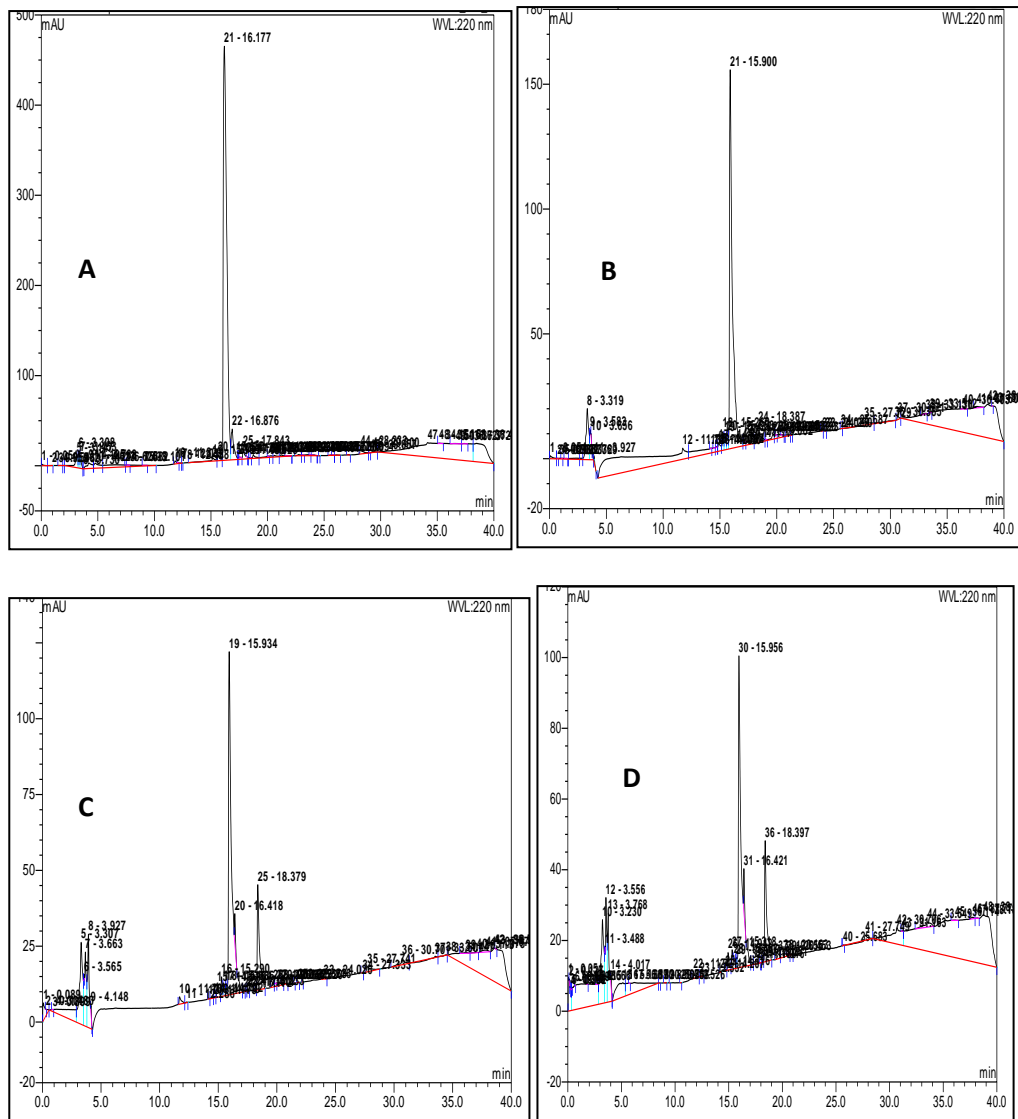


Figure A.1.6: Relative Resistance of IO8 to proteolysis. (A) RP-HPLC chromatographs of IO8 before incubation in proteolytic enzymes. RP-HPLC chromatographs of IO8 after incubation in Kallikrein, (B) 0 hr (C) 1 hr (D) 3 hrs. Conditions, linear gradient from 0–60% acetonitrile with 0.1% TFA over 40 min, at a flow rate of 1 mL/min, 28 °C. Absorbance at 220 nm and elution time in minutes

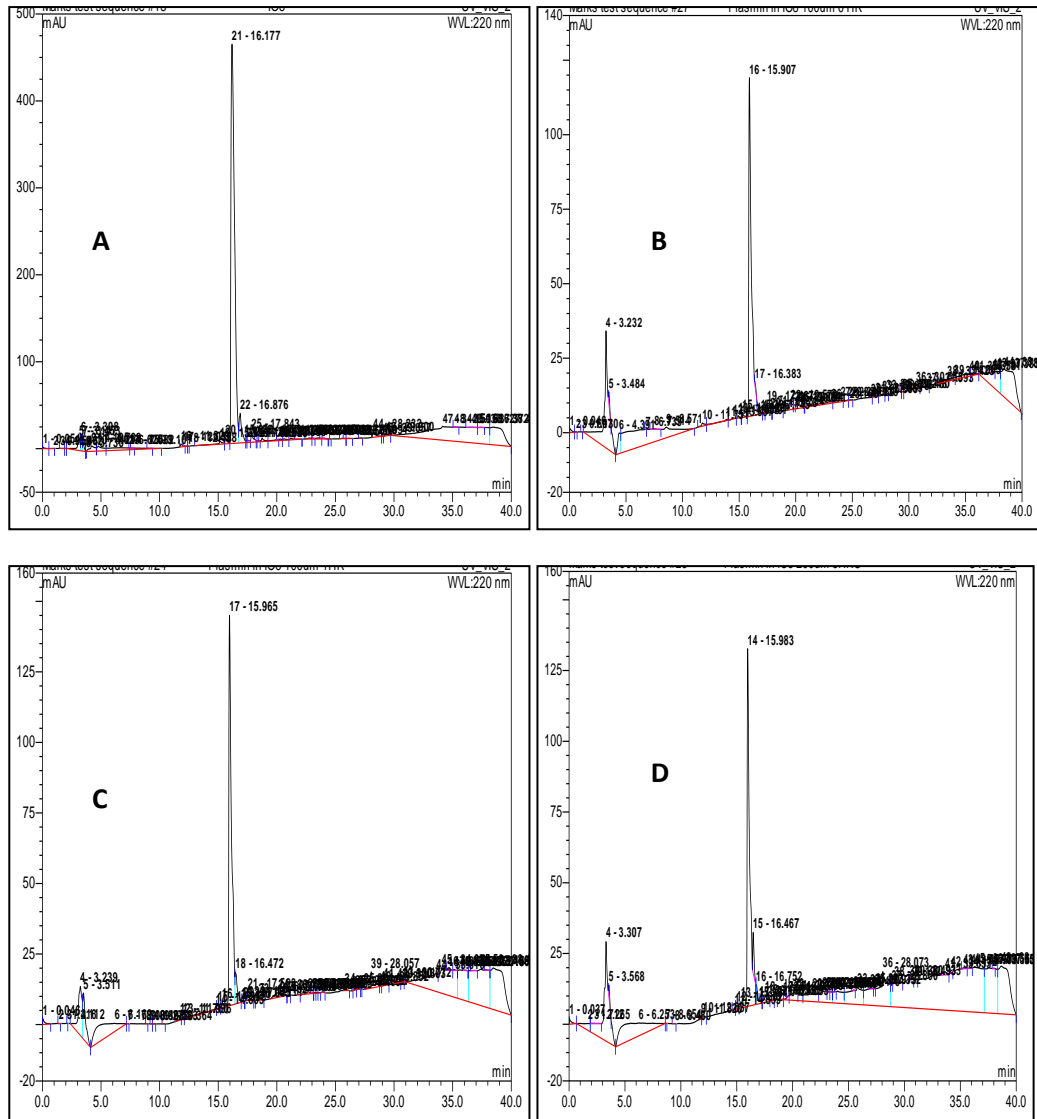


Figure A1.7: Relative Resistance of IO8 to proteolysis. (A) RP-HPLC chromatographs of IO8 before incubation in peoteolytic enzymes. RP-HPLC chromatographs of IO8 after incubation in Plasmin (B) 0 hr (C) 1 hr (D) 3 hrs. Conditions, linear gradient from 0–60% acetonitrile with 0.1% TFA over 40 min, at a flow rate of 1 mL/min, 28 °C. Absorbance at 220 nm and elution time in minutes

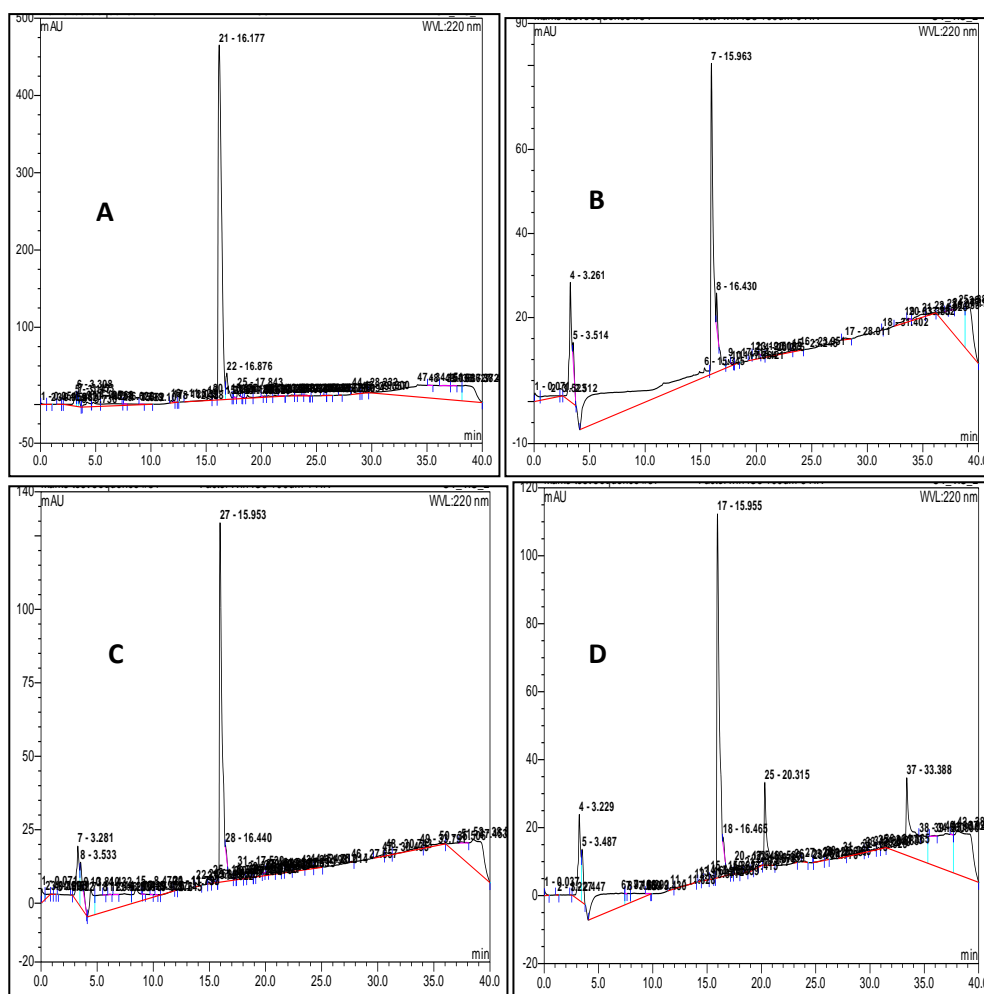


Figure A1.8: Relative Resistance of IO8 to proteolysis. (A) RP-HPLC chromatographs of IO8 before incubation in pteolytic enzymes. RP-HPLC chromatographs of IO8 after incubation in Factor X (B) 0 hr (C) 1 hr (D) 3 hrs. Conditions, linear gradient from 0–60% acetonitrile with 0.1%TFA over 40 min, at a flow rate of 1 mL/min, 28 °C. Absorbance at 220 nm and elution time in minutes

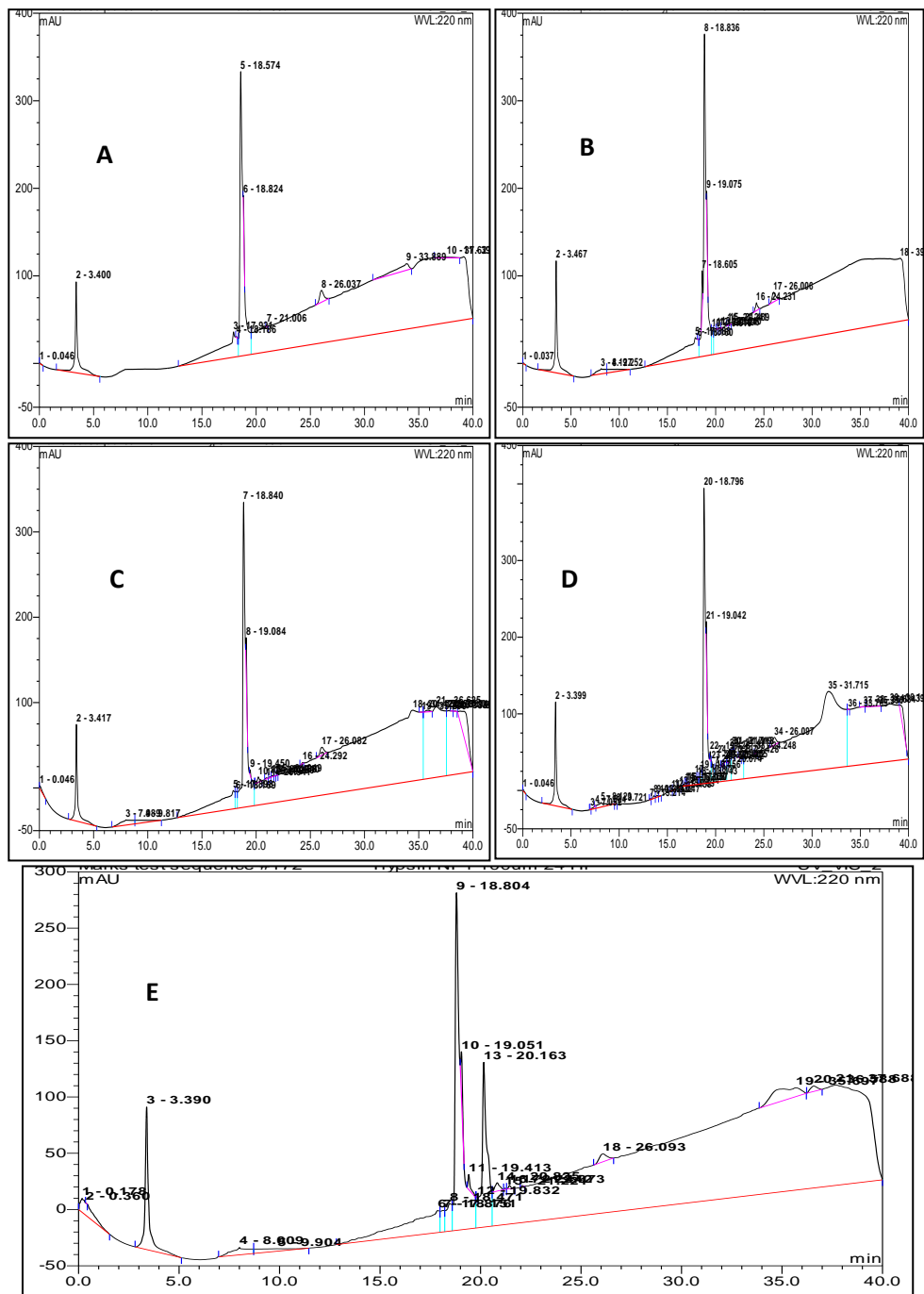


Figure A2.1: Relative Resistance of N1-IO8 to proteolysis. (A) RP-HPLC chromatographs of N1-IO8 before incubation in proteolytic enzymes. RP-HPLC chromatographs of N1-IO8 after incubation in Trypsin (B) 0 hr (C) 1 hr (D) 3 hrs (E) 24 hrs. Conditions, linear gradient from 0–60% acetonitrile with 0.1%TFA over 40 min, at a flow rate of 1 mL/min, 28 °C. Absorbance at 220 nm and elution time in minutes

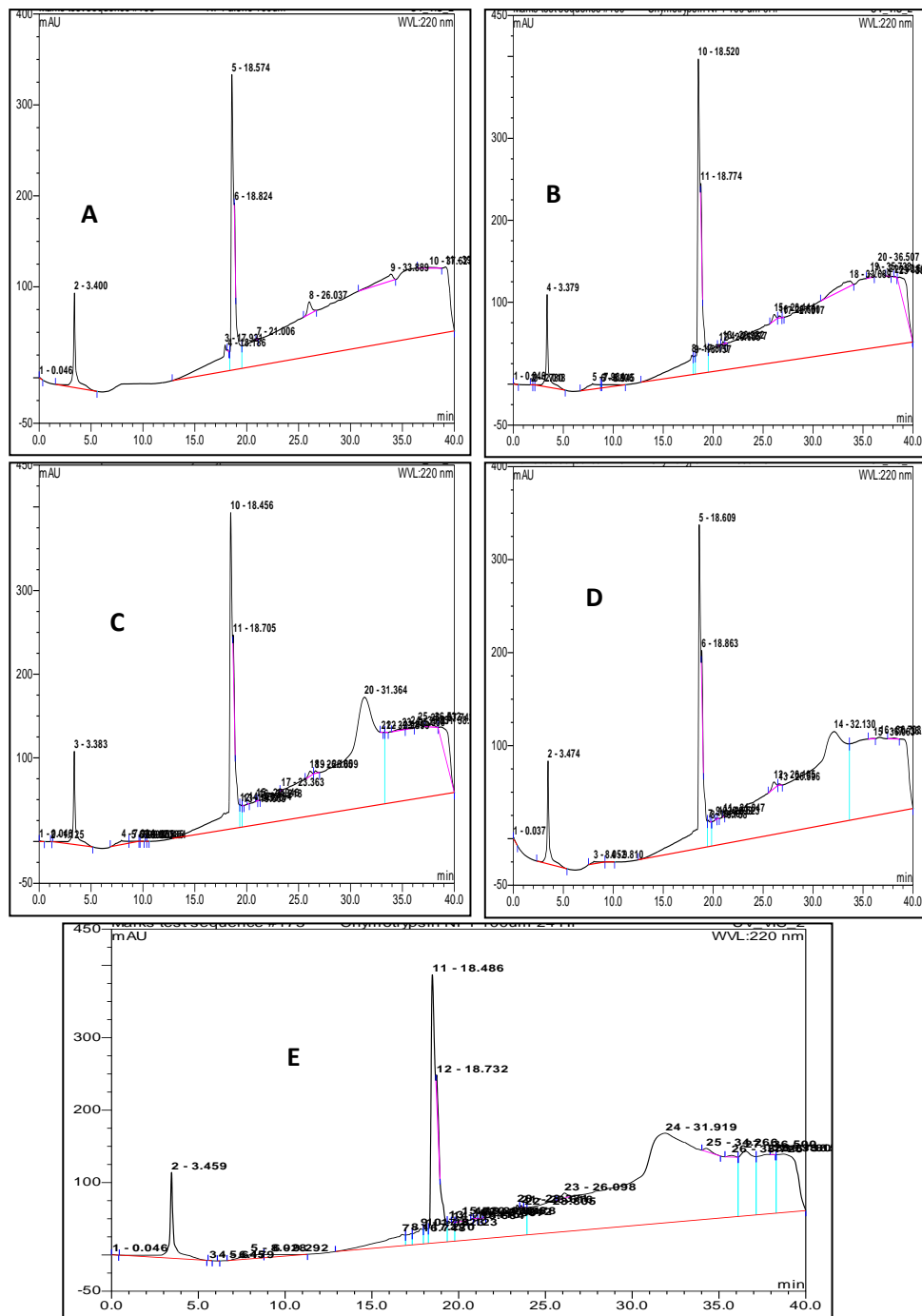


Figure A2.2: Relative Resistance of N1-IO8 to proteolysis. (A) RP-HPLC chromatographs of N1-IO8 before incubation in proteolytic enzymes. RP-HPLC chromatographs of N1-IO8 after incubation in Chymotrypsin (B) 0 hr (C) 1 hr (D) 3 hrs (E) 24 hrs. Conditions, linear gradient from 0–60% acetonitrile with 0.1% TFA over 40 min, at a flow rate of 1 mL/min, 28 °C. Absorbance at 220 nm and elution time in minutes

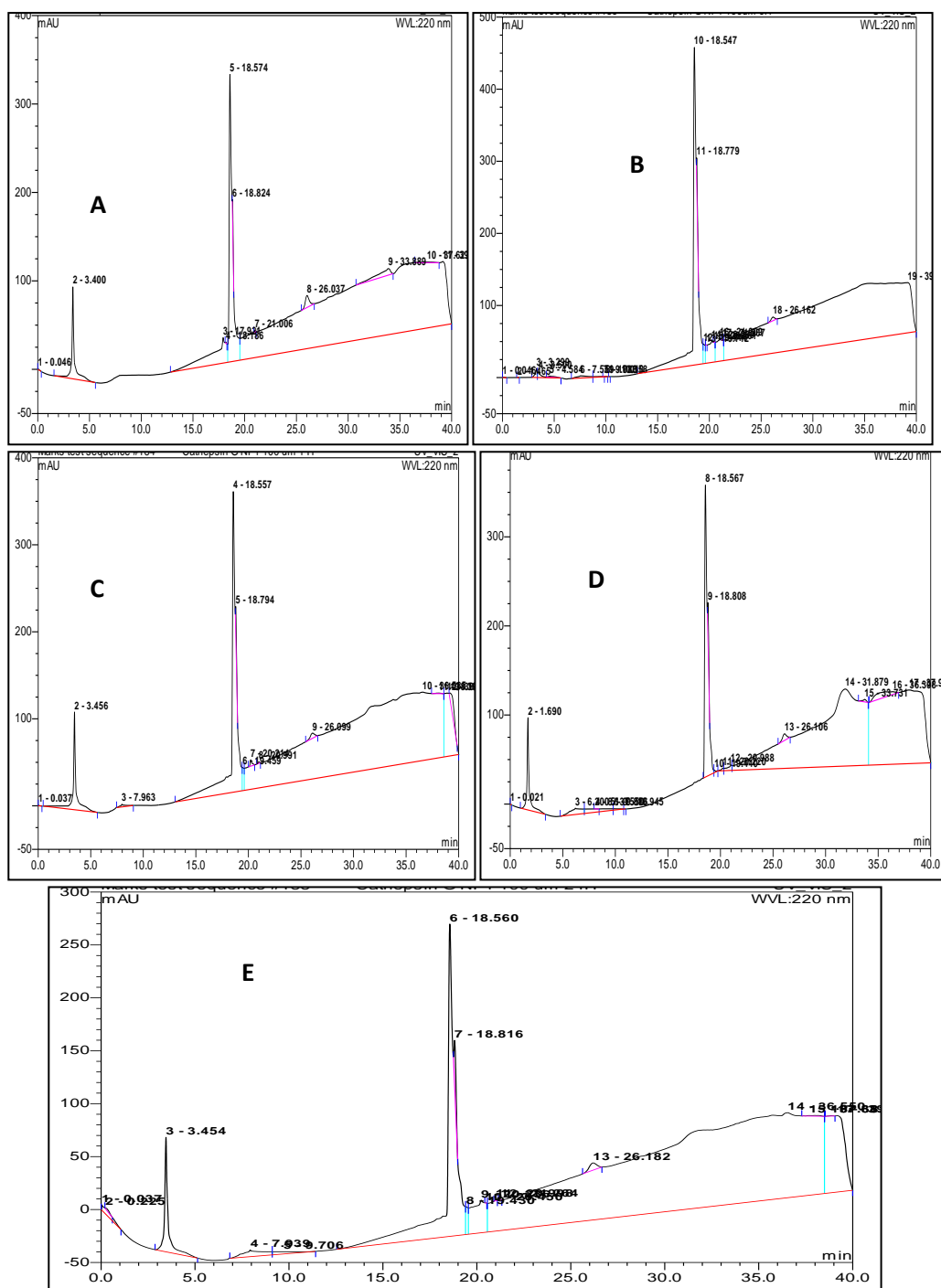


Figure A2.3: Relative Resistance of N1-IO8 to proteolysis. (A) RP-HPLC chromatographs of N1-IO8 before incubation in proteolytic enzymes. RP-HPLC chromatographs of N1-IO8 after incubation in Cathepsin G (B) 0 hr (C) 1 hr (D) 3 hrs (E) 24 hrs. Conditions, linear gradient from 0–60% acetonitrile with 0.1% TFA over 40 min, at a flow rate of 1 mL/min, 28 °C. Absorbance at 220 nm and elution time in minutes.

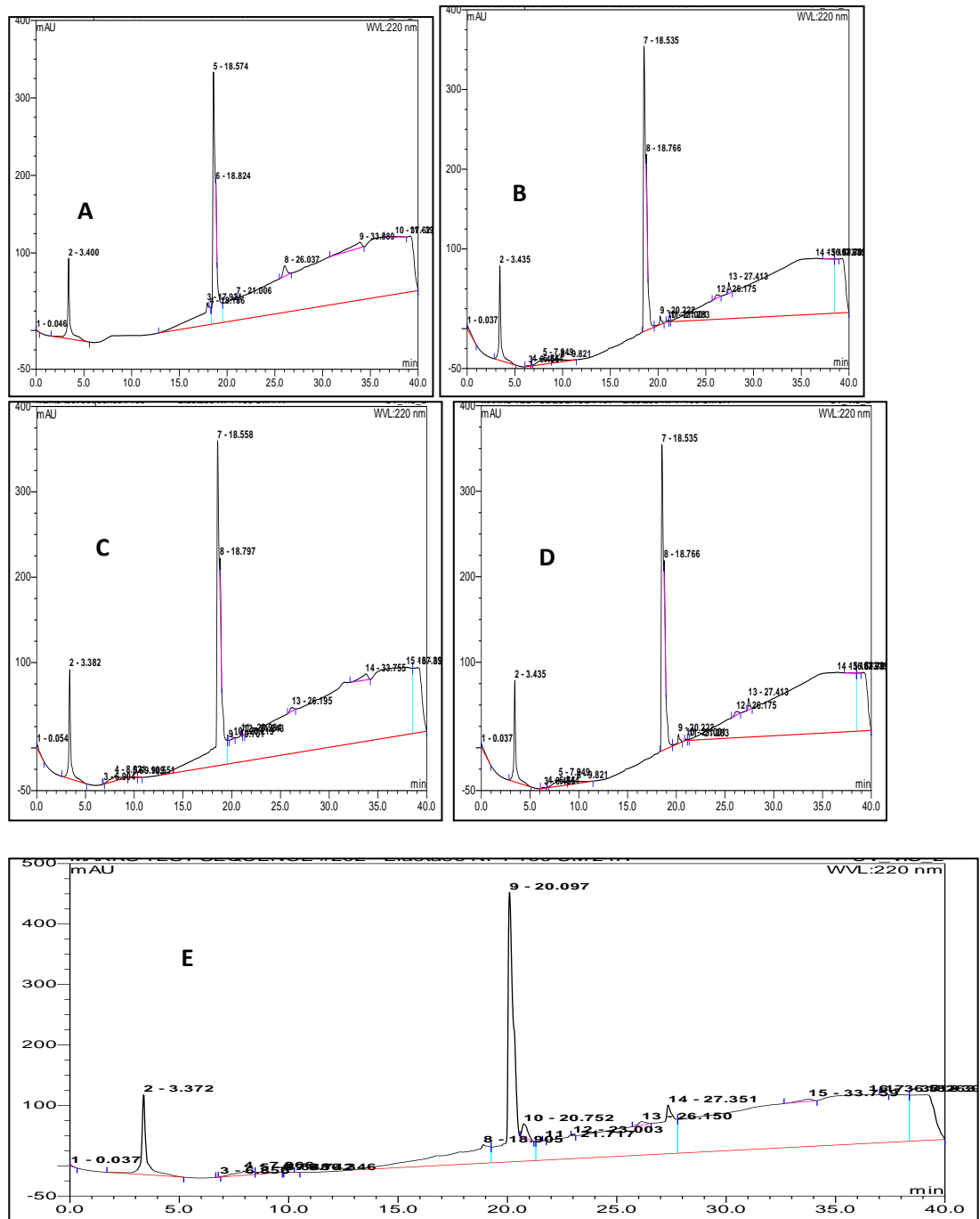


Figure A2.4: Relative Resistance of N1-IO8 to proteolysis. (A) RP-HPLC chromatographs of N1-IO8 before incubation in proteolytic enzymes. RP-HPLC chromatographs of N1-IO8 after incubation in Elastase (B) 0 hr (C) 1 hr (D) 3 hrs (E) 24 hrs. Conditions, linear gradient from 0–60% acetonitrile with 0.1% TFA over 40 min, at a flow rate of 1 mL/min, 28 °C. Absorbance at 220 nm and elution time in minutes.

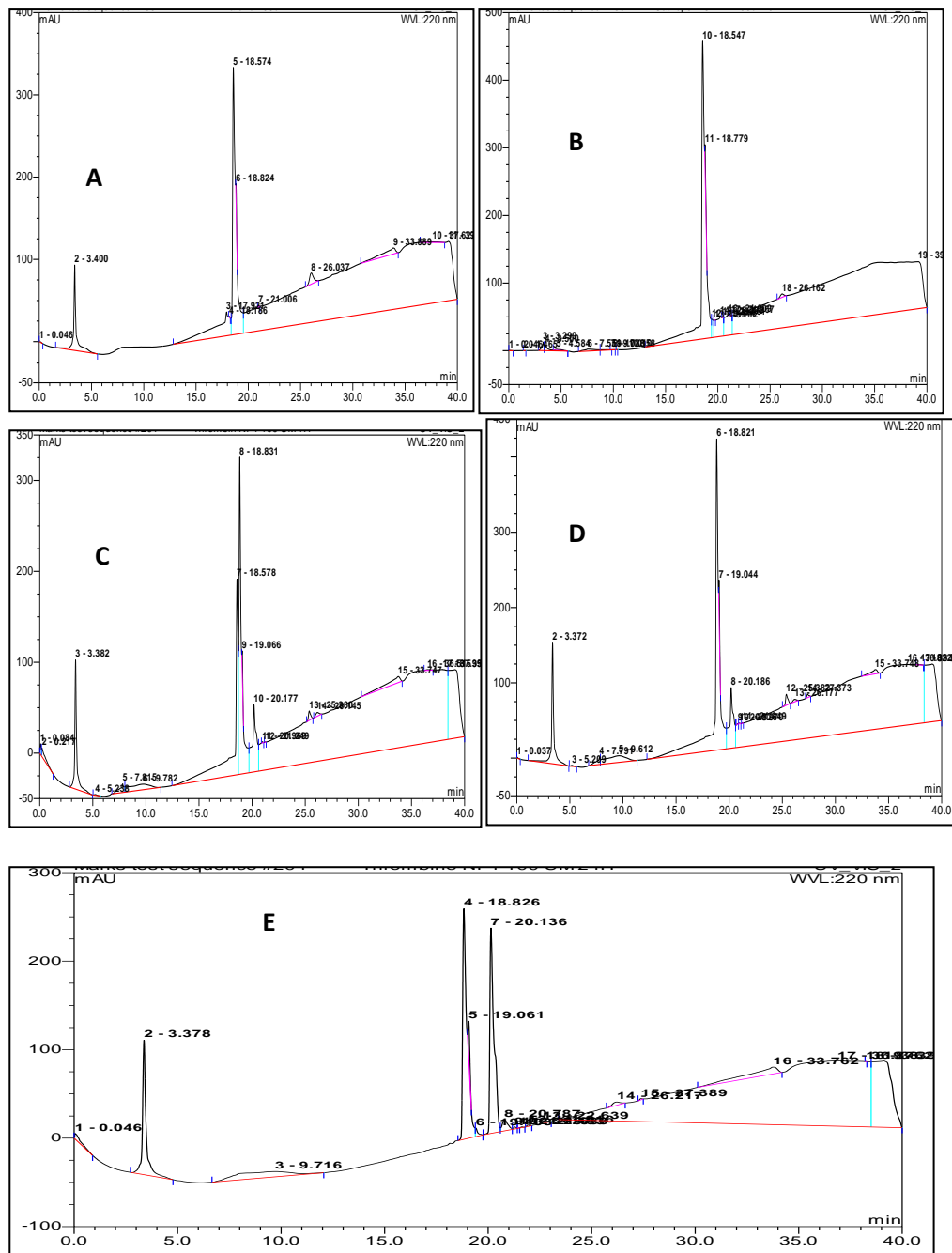


Figure A2.5: Relative Resistance of N1-IO8 to proteolysis. (A) RP-HPLC chromatographs of N1-IO8 before incubation in proteolytic enzymes. RP-HPLC chromatographs of N1-IO8 after incubation in Thrombin, (B) 0 hr (C) 1 hr (D) 3 hrs (E) 24 hrs. Conditions, linear gradient from 0–60% acetonitrile with 0.1% TFA over 40 min, at a flow rate of 1 mL/min, 28 °C. Absorbance at 220 nm and elution time in minutes.

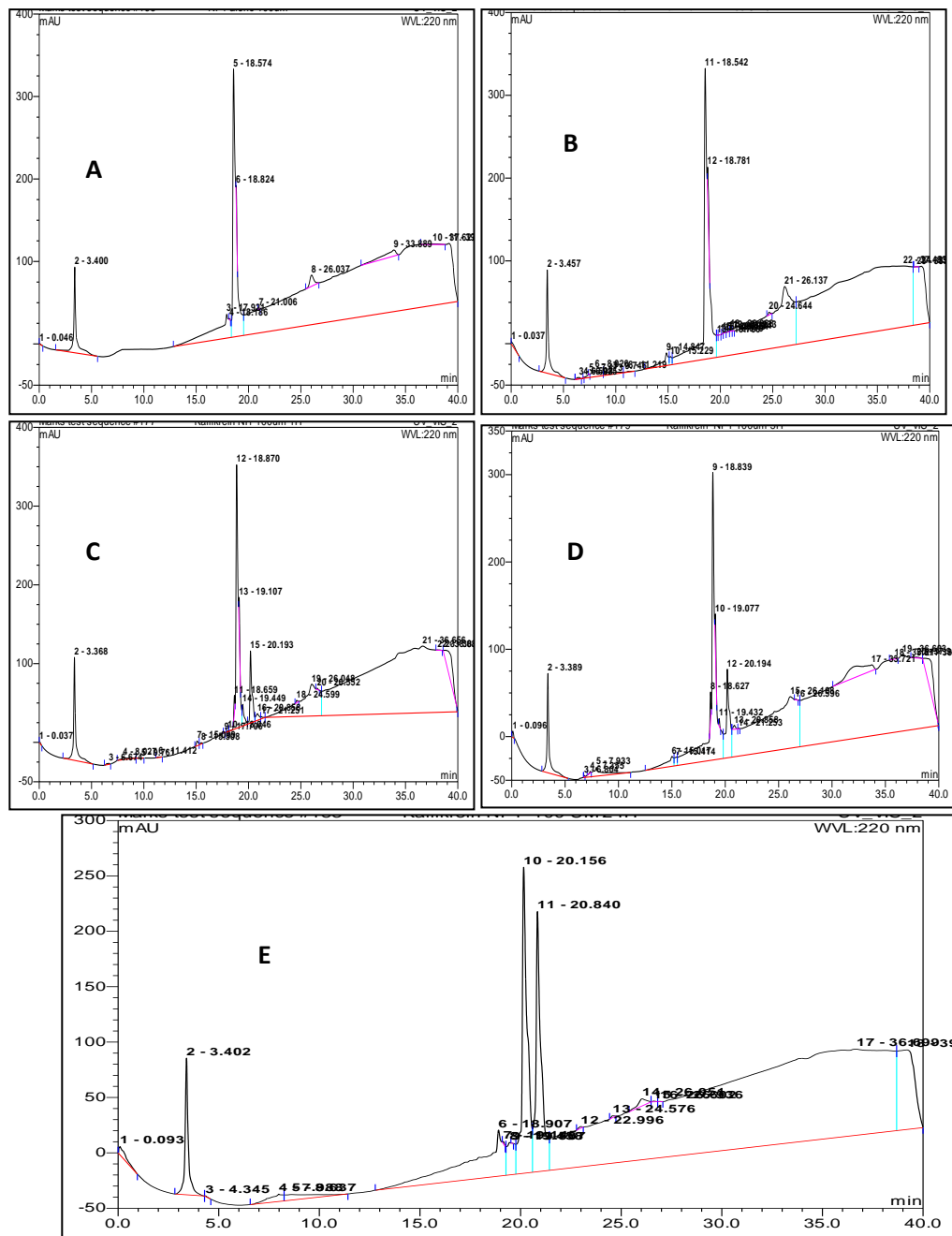


Figure A2.6: Relative Resistance of N1-IO8 to proteolysis. (A) RP-HPLC chromatographs of N1-IO8 before incubation in proteolytic enzymes. RP-HPLC chromatographs of N1-IO8 after incubation in Kallikrein, (B) 0 hr (C) 1 hr (D) 3 hrs (E) 24 hrs. Conditions, linear gradient from 0–60% acetonitrile with 0.1% TFA over 40 min, at a flow rate of 1 mL/min, 28 °C. Absorbance at 220 nm and elution time in minutes.

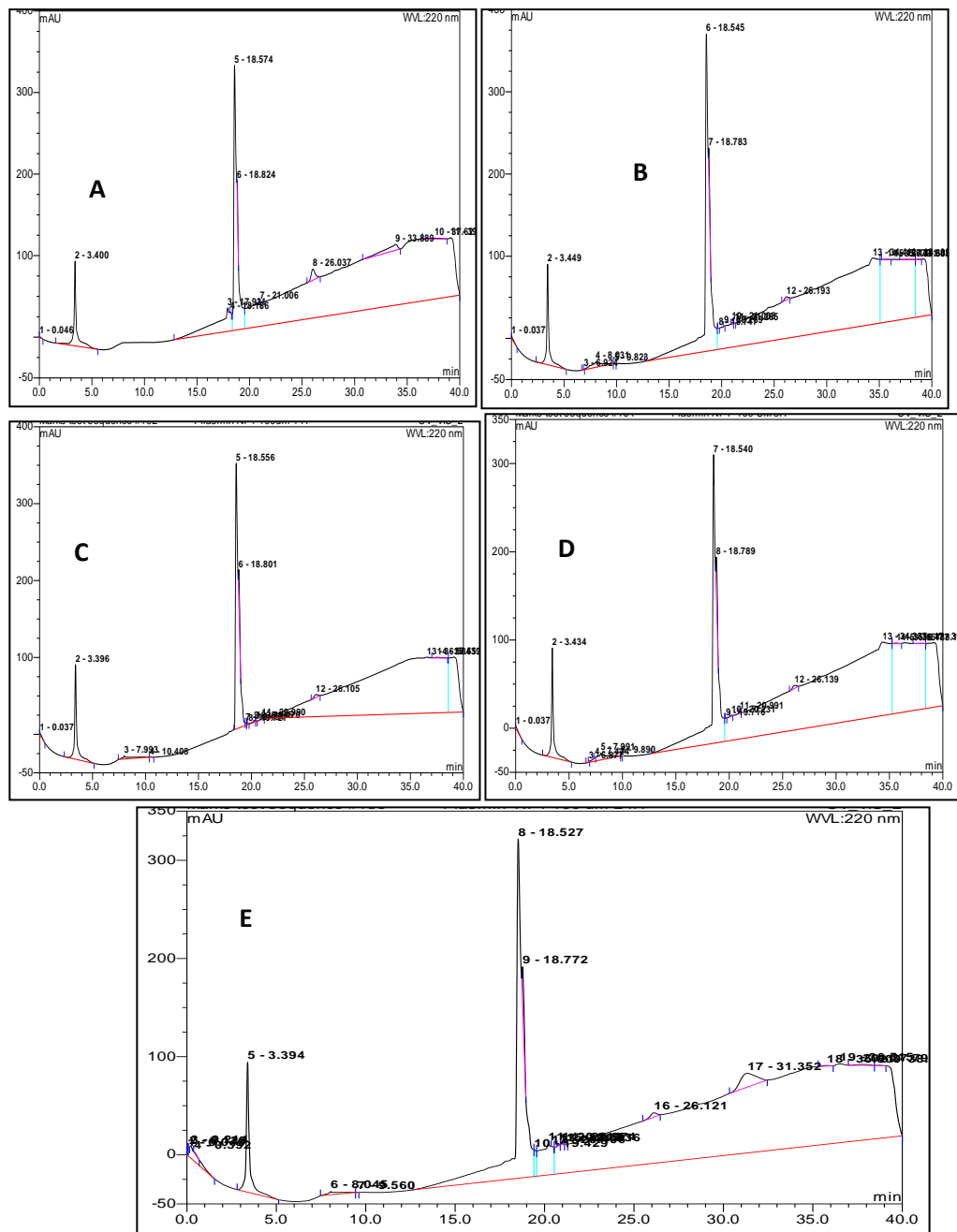


Figure A2.7: Relative Resistance of N1-IO8 to proteolysis. (A) RP-HPLC chromatographs of N1-IO8 before incubation in proteolytic enzymes. RP-HPLC chromatographs of N1-IO8 after incubation in Plasmin (B) 0 hr (C) 1 hr (D) 3 hrs (E) 24 hrs. Conditions, linear gradient from 0–60% acetonitrile with 0.1% TFA over 40 min, at a flow rate of 1 mL/min, 28 °C. Absorbance at 220 nm and elution time in minutes

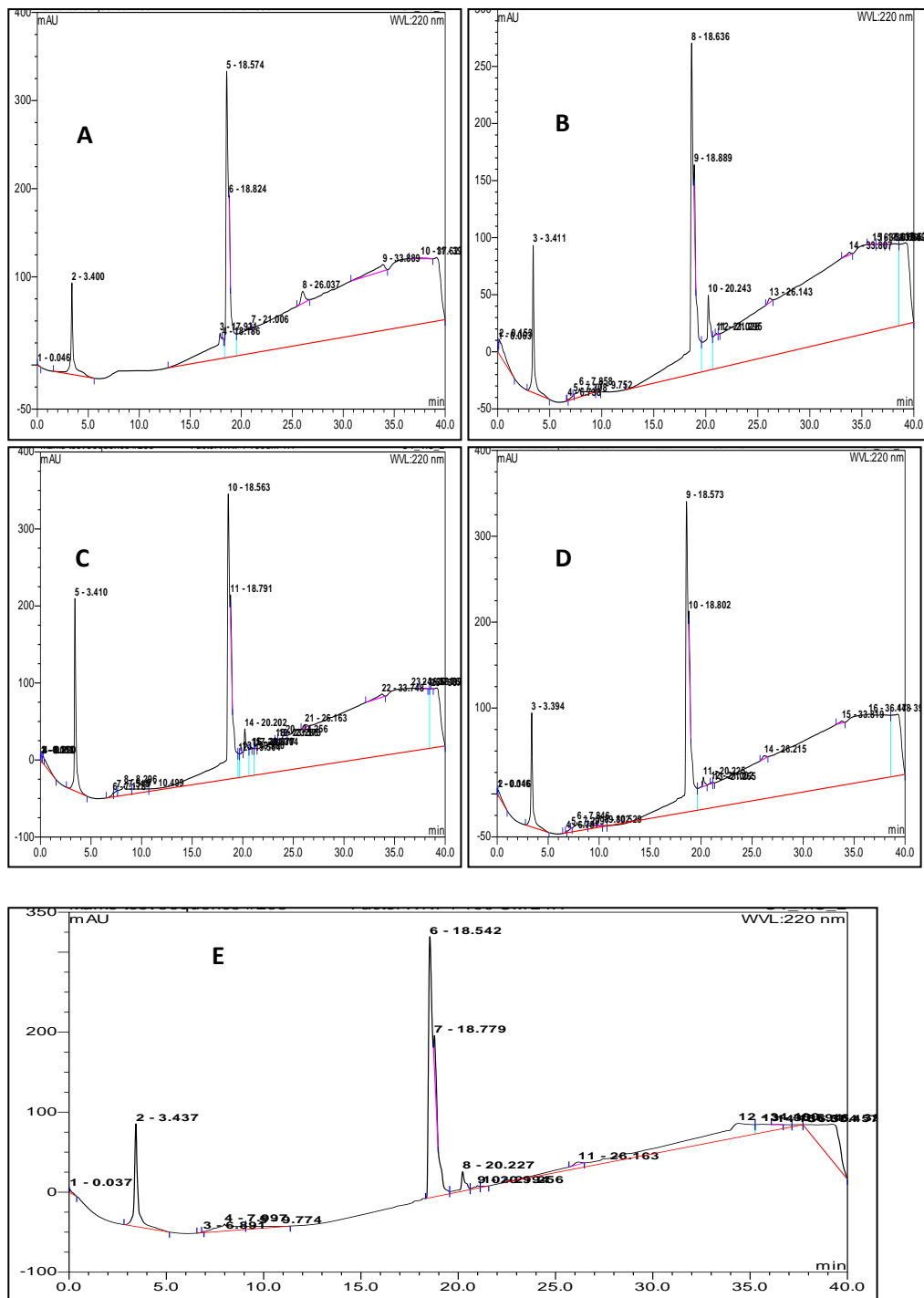


Figure A2.8: Relative Resistance of N1-IO8 to proteolysis. (A) RP-HPLC chromatographs of N1-IO8 before incubation in proteolytic enzymes. RP-HPLC chromatographs of N1-IO8 after incubation in Factor X (B) 0 hr (C) 1 hr (D) 3 hrs (E) 24 hrs. Conditions, linear gradient from 0–60% acetonitrile with 0.1%TFA over 40 min, at a flow rate of 1 mL/min, 28 °C. Absorbance at 220 nm and elution time in minutes.

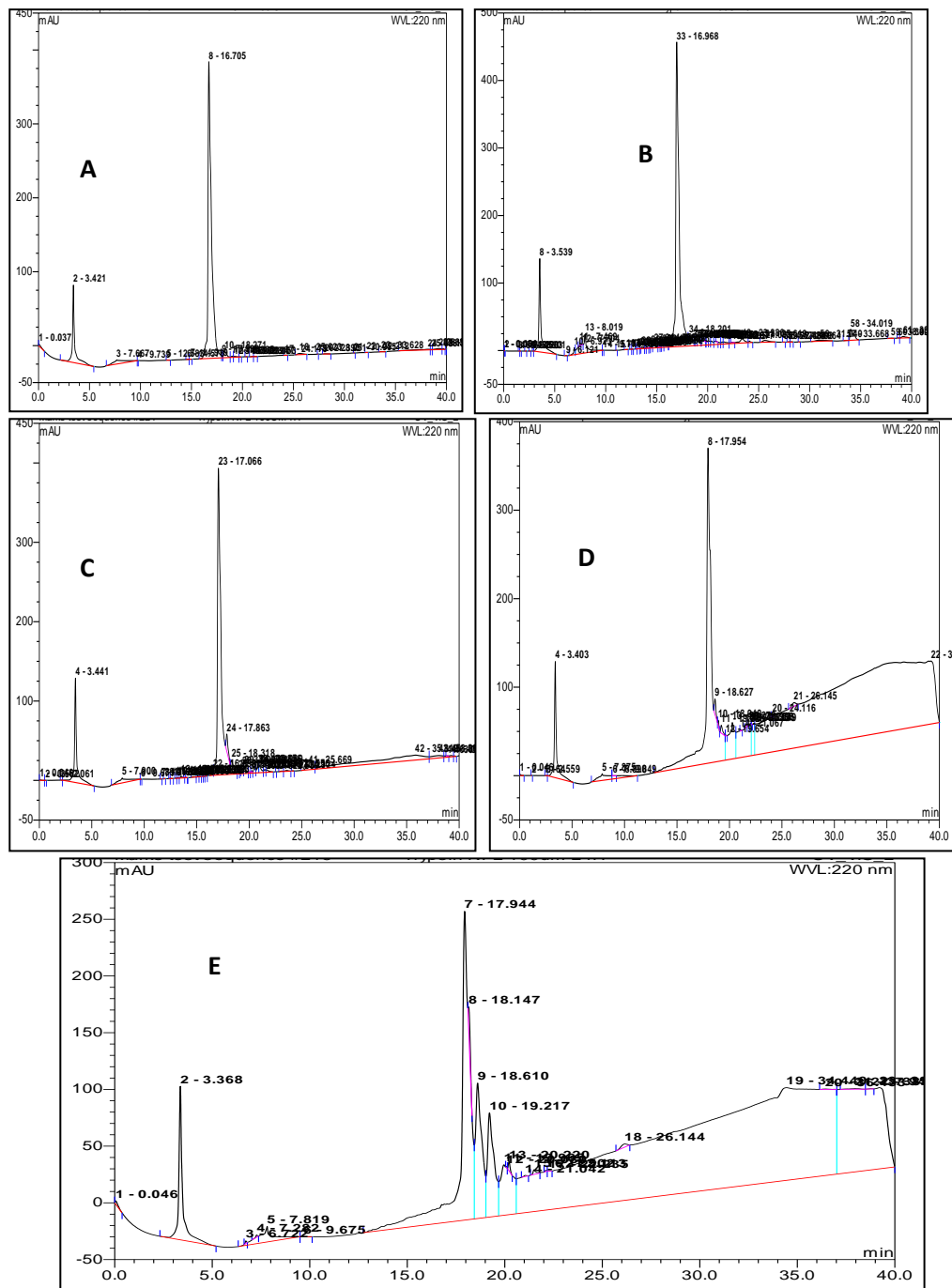


Figure A3.1: Relative Resistance of N2-IO8 to proteolysis. (A) RP-HPLC chromatographs of N2-IO8 before incubation in proteolytic enzymes. RP-HPLC chromatographs of N2-IO8 after incubation in Trypsin (B) 0 hr (C) 1 hr (D) 3 hrs (E) 24 hrs. Conditions, linear gradient from 0–60% acetonitrile with 0.1% TFA over 40 min, at a flow rate of 1 mL/min, 28 °C. Absorbance at 220 nm and elution time in minutes

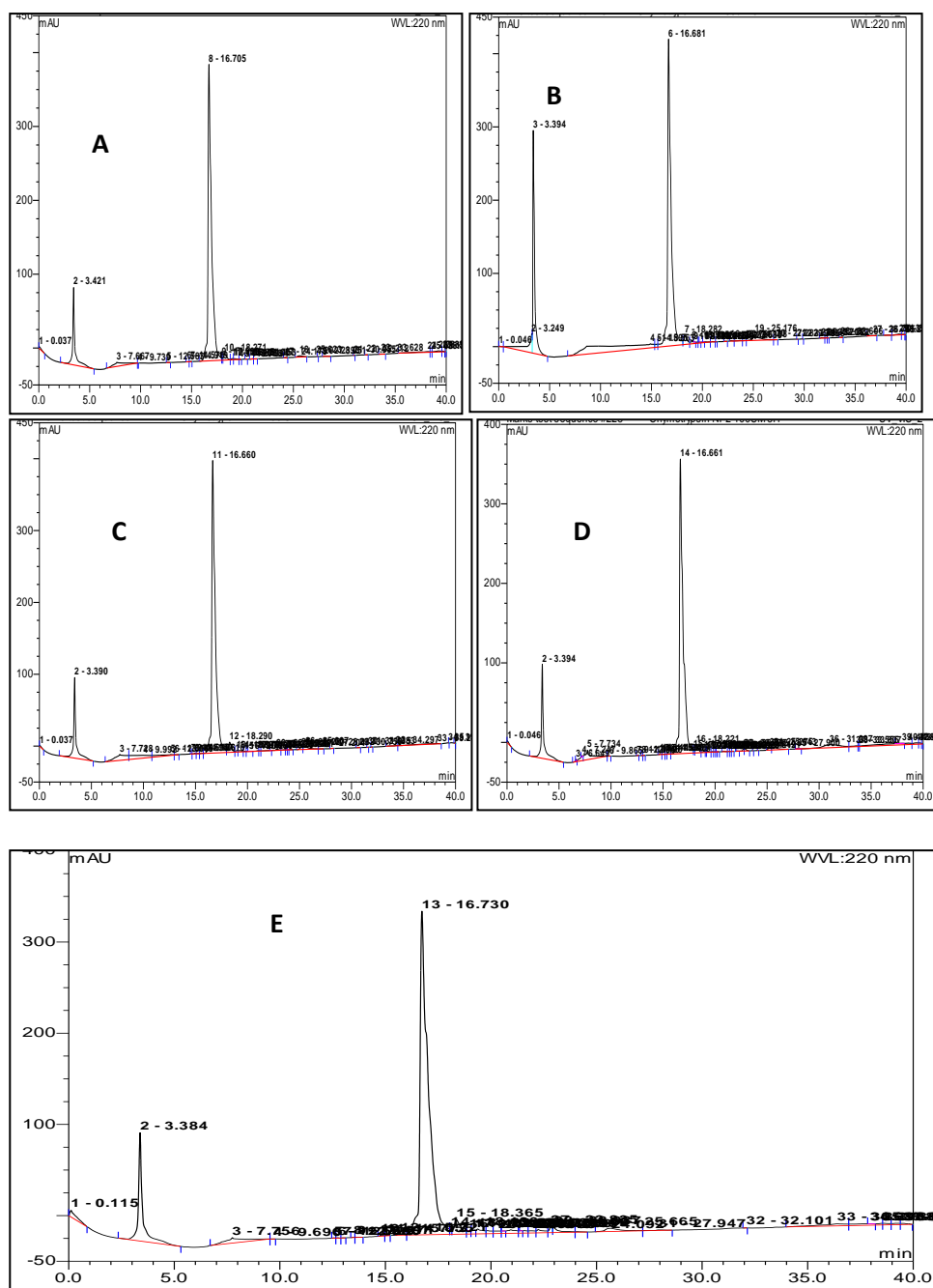


Figure A3.2: Relative Resistance of N2-IO8 to proteolysis. (A) RP-HPLC chromatographs of N2-IO8 before incubation in proteolytic enzymes. RP-HPLC chromatographs of N2-IO8 after incubation in Chymotrypsin (B) 0 hr (C) 1 hr (D) 3 hrs (E) 24 hrs. Conditions, linear gradient from 0–60% acetonitrile with 0.1% TFA over 40 min, at a flow rate of 1 mL/min, 28 °C. Absorbance at 220 nm and elution time in minutes.

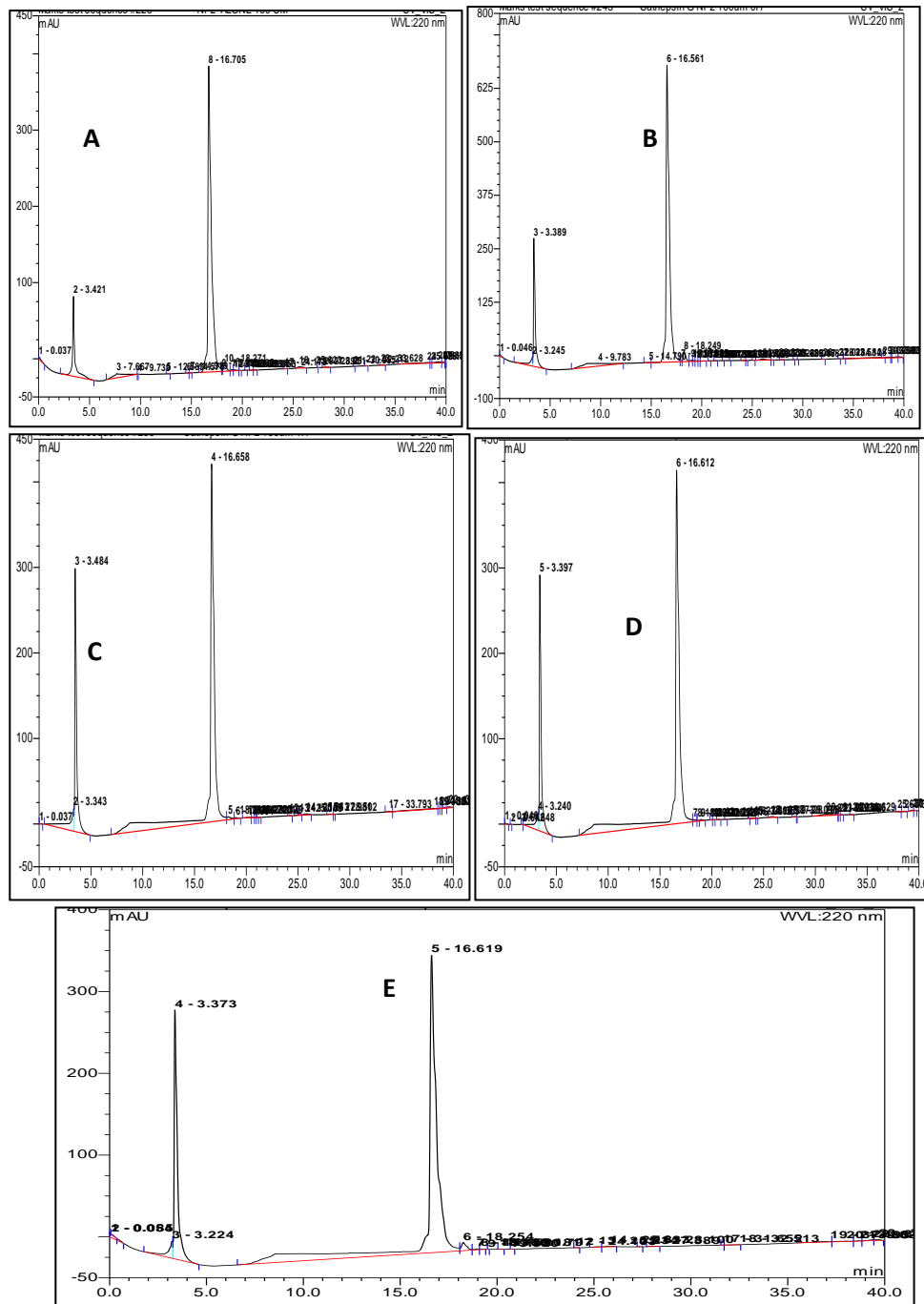


Figure A2.3: Relative Resistance of N2-IO8 to proteolysis. (A) RP-HPLC chromatographs of N2-IO8 before incubation in proteolytic enzymes. RP-HPLC chromatographs of N2-IO8 after incubation in Cathepsin G (B) 0 hr (C) 1 hr (D) 3 hrs (E) 24 hrs. Conditions, linear gradient from 0–60% acetonitrile with 0.1% TFA over 40 min, at a flow rate of 1 mL/min, 28 °C. Absorbance at 220 nm and elution time in minutes

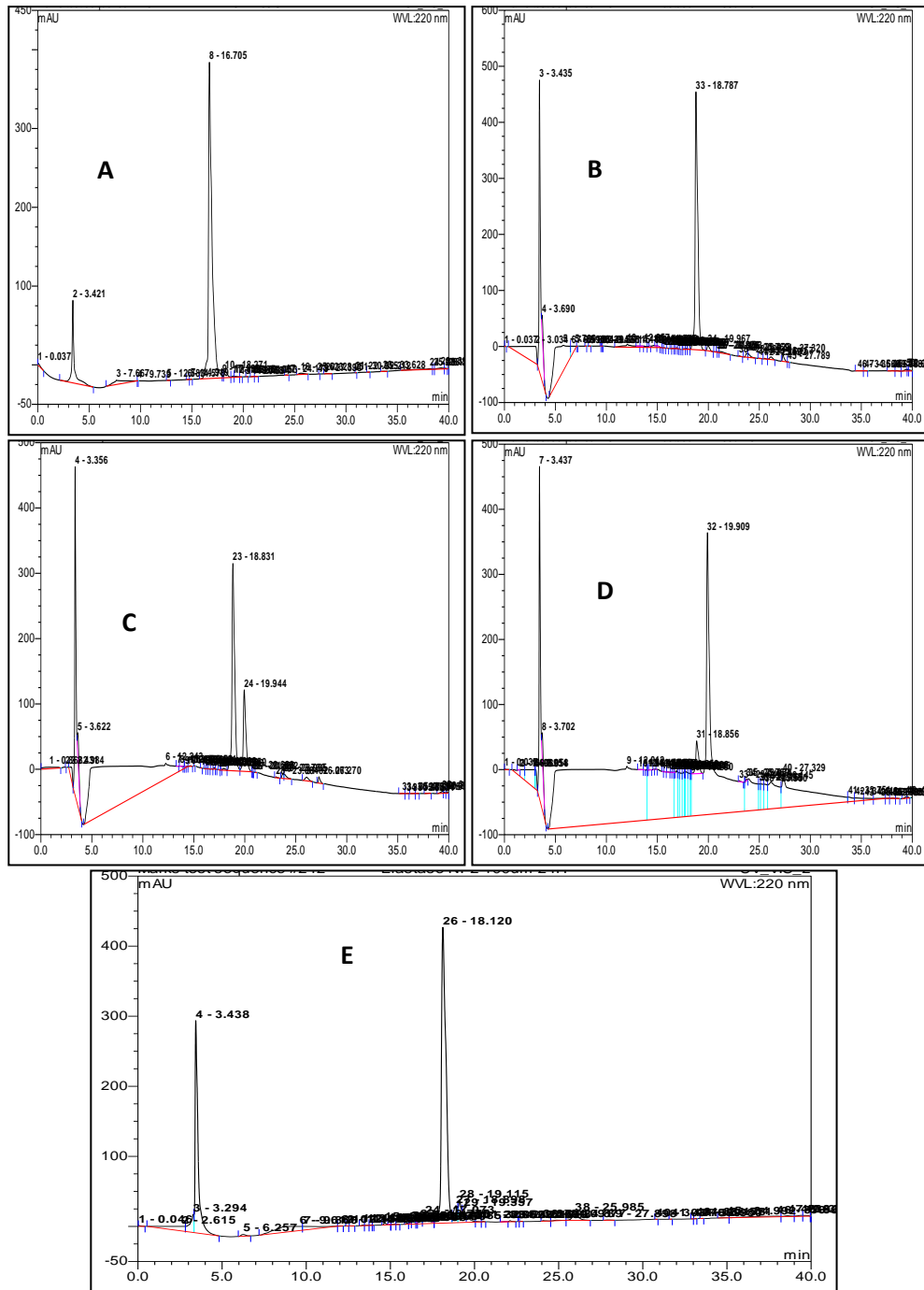


Figure A3.4: Relative Resistance of N2-IO8 to proteolysis. (A) RP-HPLC chromatographs of N2-IO8 before incubation in proteolytic enzymes. RP-HPLC chromatographs of N2-IO8 after incubation in Elastase (B) 0 hr (C) 1 hr (D) 3 hrs (E) 24 hrs. Conditions, linear gradient from 0–60% acetonitrile with 0.1% TFA over 40 min, at a flow rate of 1 mL/min, 28 °C. Absorbance at 220 nm and elution time in minutes.

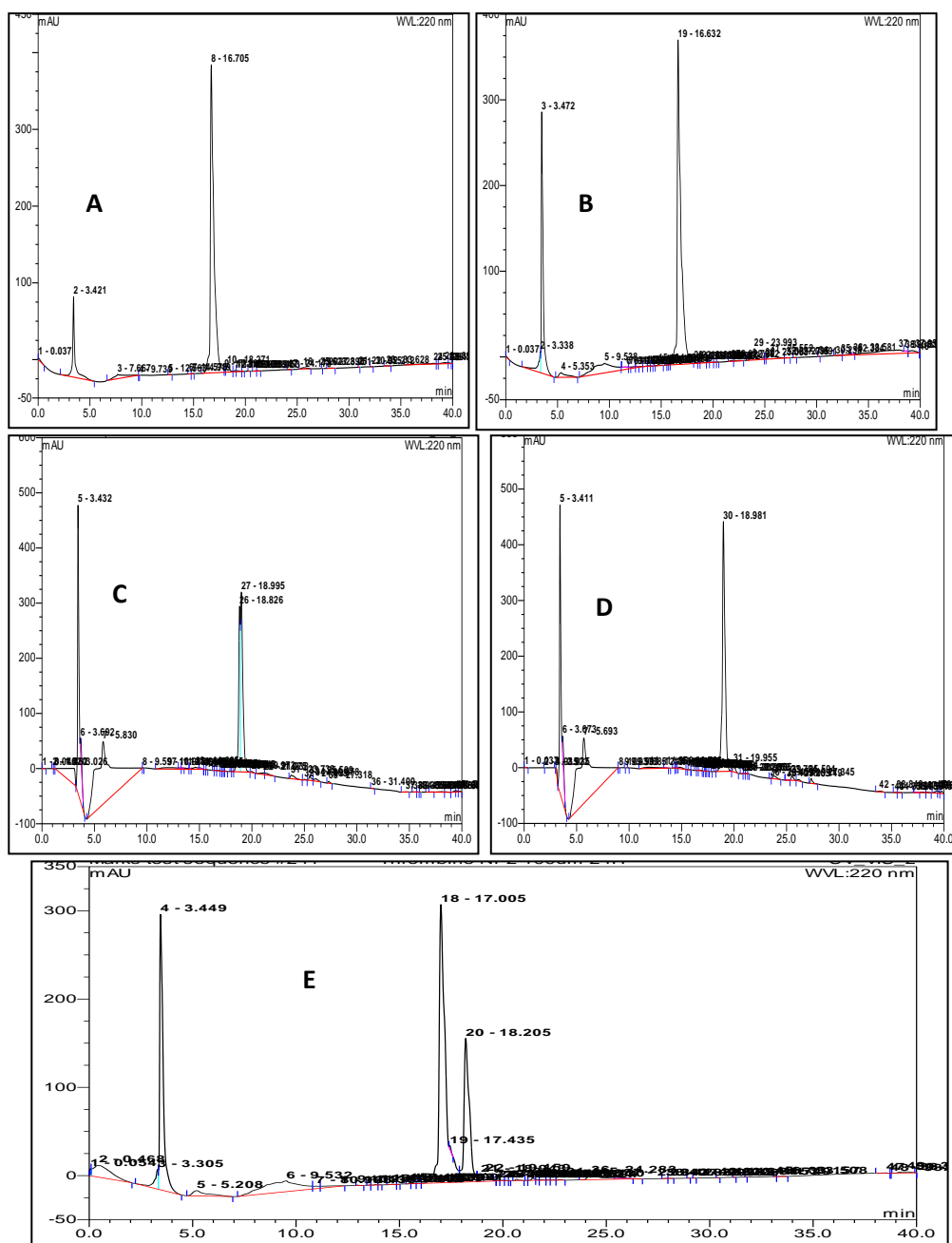


Figure A3.5: Relative Resistance of IO8 to proteolysis. (A) RP-HPLC chromatographs of IO8 before incubation in proteolytic enzymes. RP-HPLC chromatographs of IO8 after incubation in Thrombin, (B) 0 hr (C) 1 hr (D) 3 hrs (E) 24 hrs. Conditions, linear gradient from 0–60% acetonitrile with 0.1% TFA over 40 min, at a flow rate of 1 mL/min, 28 °C. Absorbance at 220 nm and elution time in minutes.

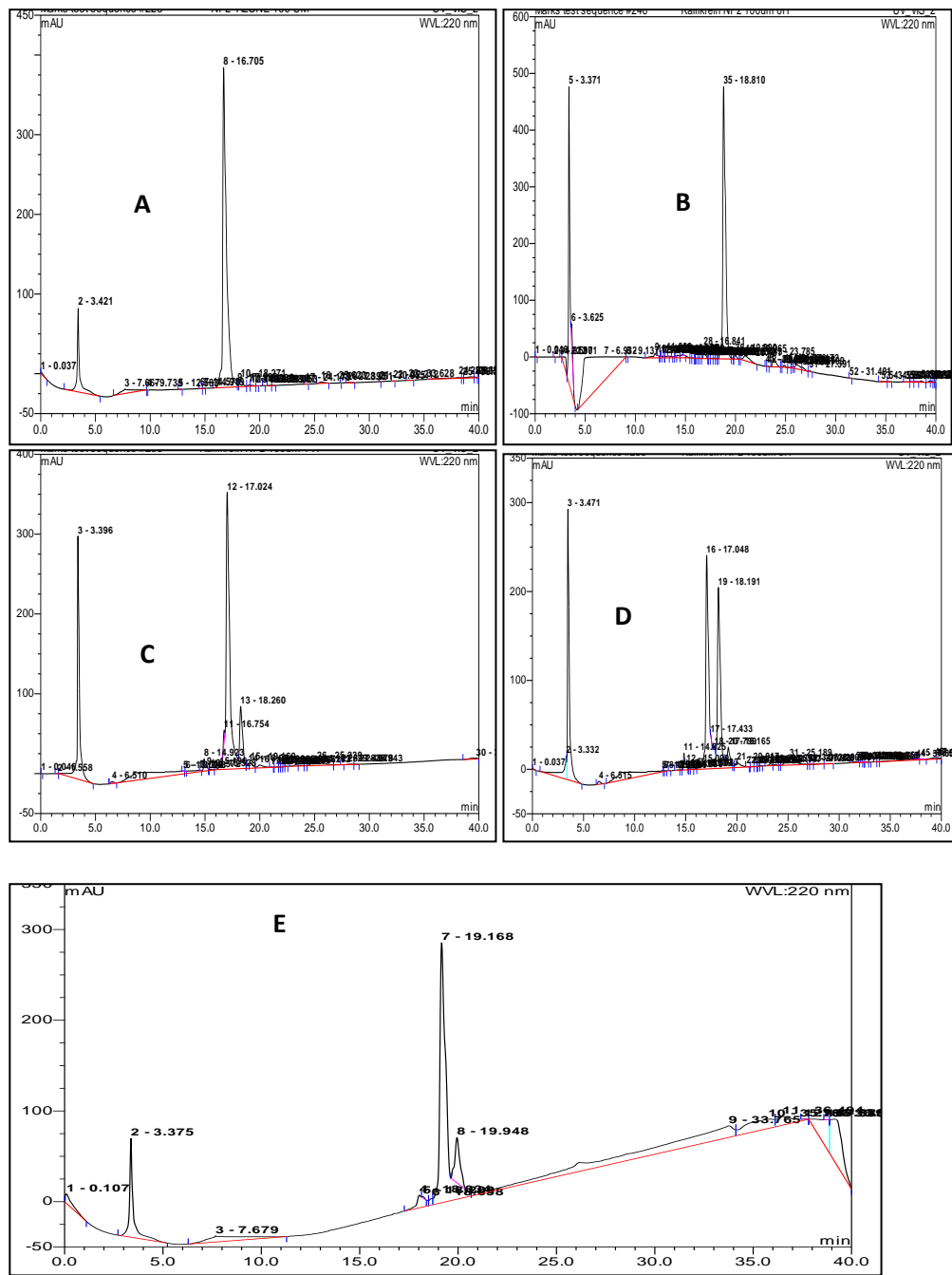


Figure A3.6: Relative Resistance of N2-IO8 to proteolysis. (A) RP-HPLC chromatographs of N2-IO8 before incubation in proteolytic enzymes. RP-HPLC chromatographs of N2-IO8 after incubation in Kallikrein, (B) 0 hr (C) 1 hr (D) 3 hrs (E) 24 hrs. Conditions, linear gradient from 0–60% acetonitrile with 0.1% TFA over 40 min, at a flow rate of 1 mL/min, 28 °C. Absorbance at 220 nm and elution time in minutes.

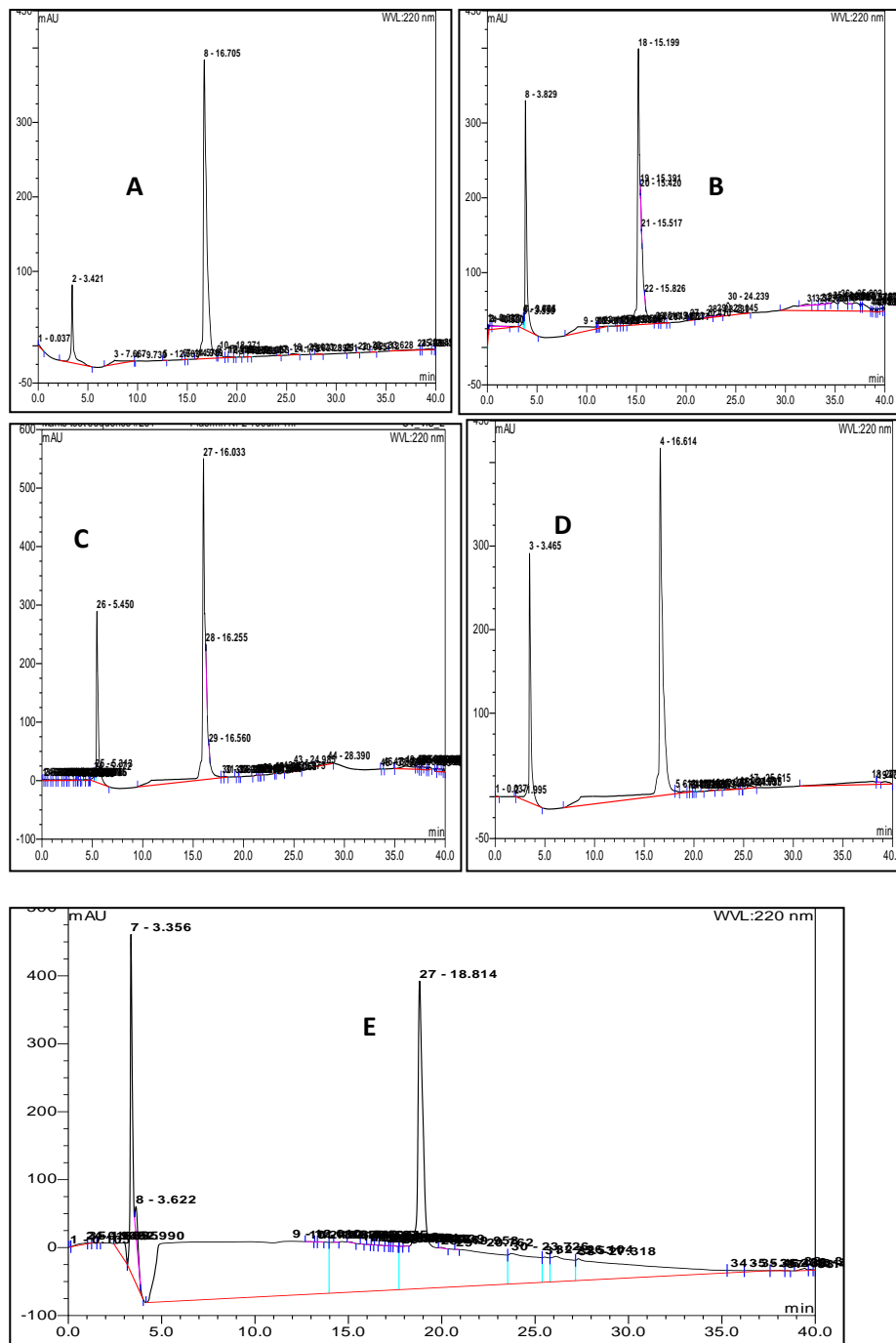


Figure A3.7: Relative Resistance of N2-IO8 to proteolysis. (A) RP-HPLC chromatographs of N2-IO8 before incubation in proteolytic enzymes. RP-HPLC chromatographs of N2-IO8 after incubation in Plasmin (B) 0 hr (C) 1 hr (D) 3 hrs (E) 24 hrs. Conditions, linear gradient from 0–60% acetonitrile with 0.1% TFA over 40 min, at a flow rate of 1 mL/min, 28 °C. Absorbance at 220 nm and elution time in minutes

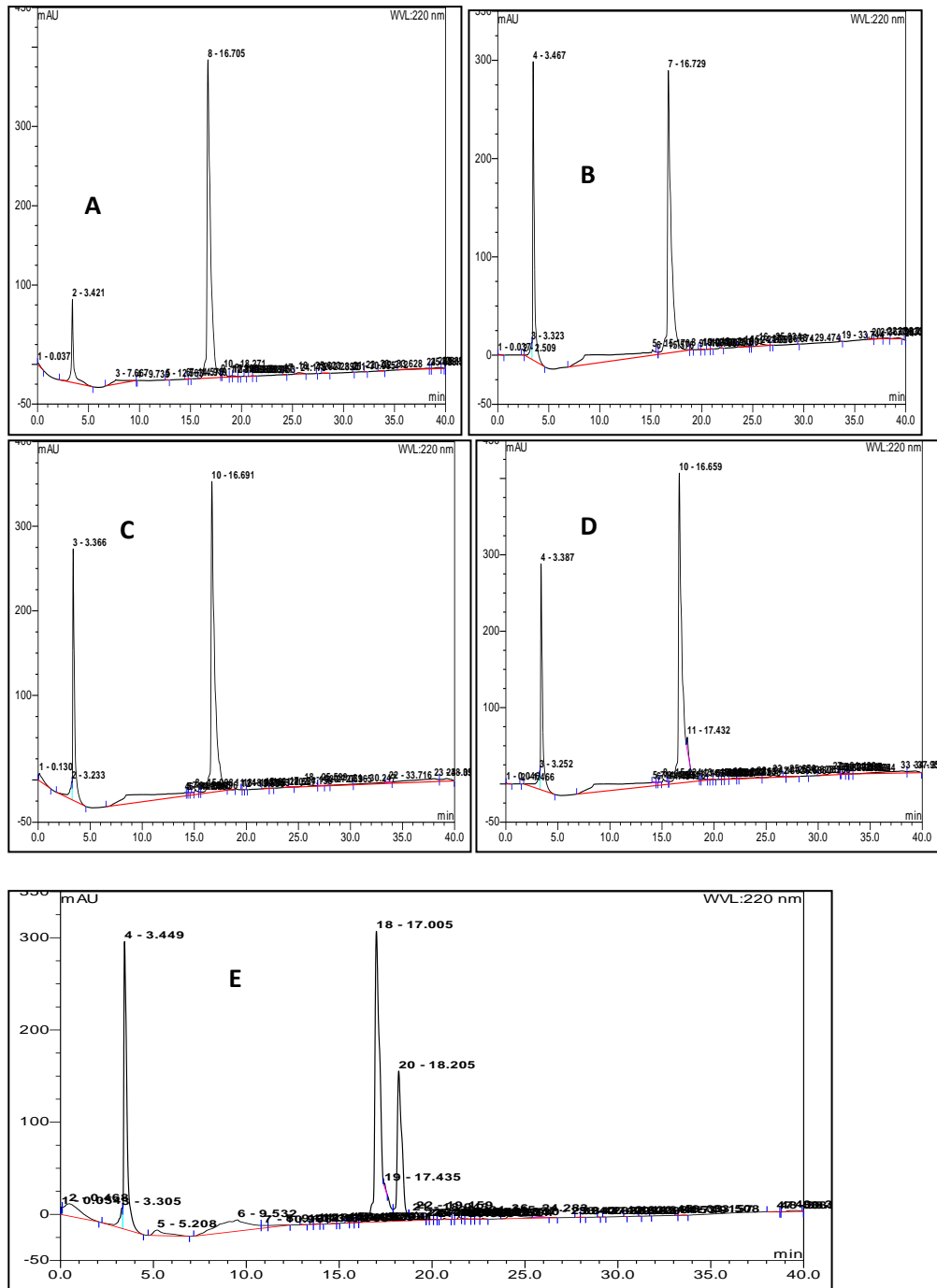


Figure A3.8: Relative Resistance of N2-IO8 to proteolysis. (A) RP-HPLC chromatographs of N2-IO8 before incubation in peoteolytic enzymes. RP-HPLC chromatographs of N2-IO8 after incubation in Factor X (B) 0 hr (C) 1 hr (D) 3 hrs (E) 24 hrs. Conditions, linear gradient from 0–60% acetonitrile with 0.1% TFA over 40 min, at a flow rate of 1 mL/min, 28 °C. Absorbance at 220 nm and elution time in minutes

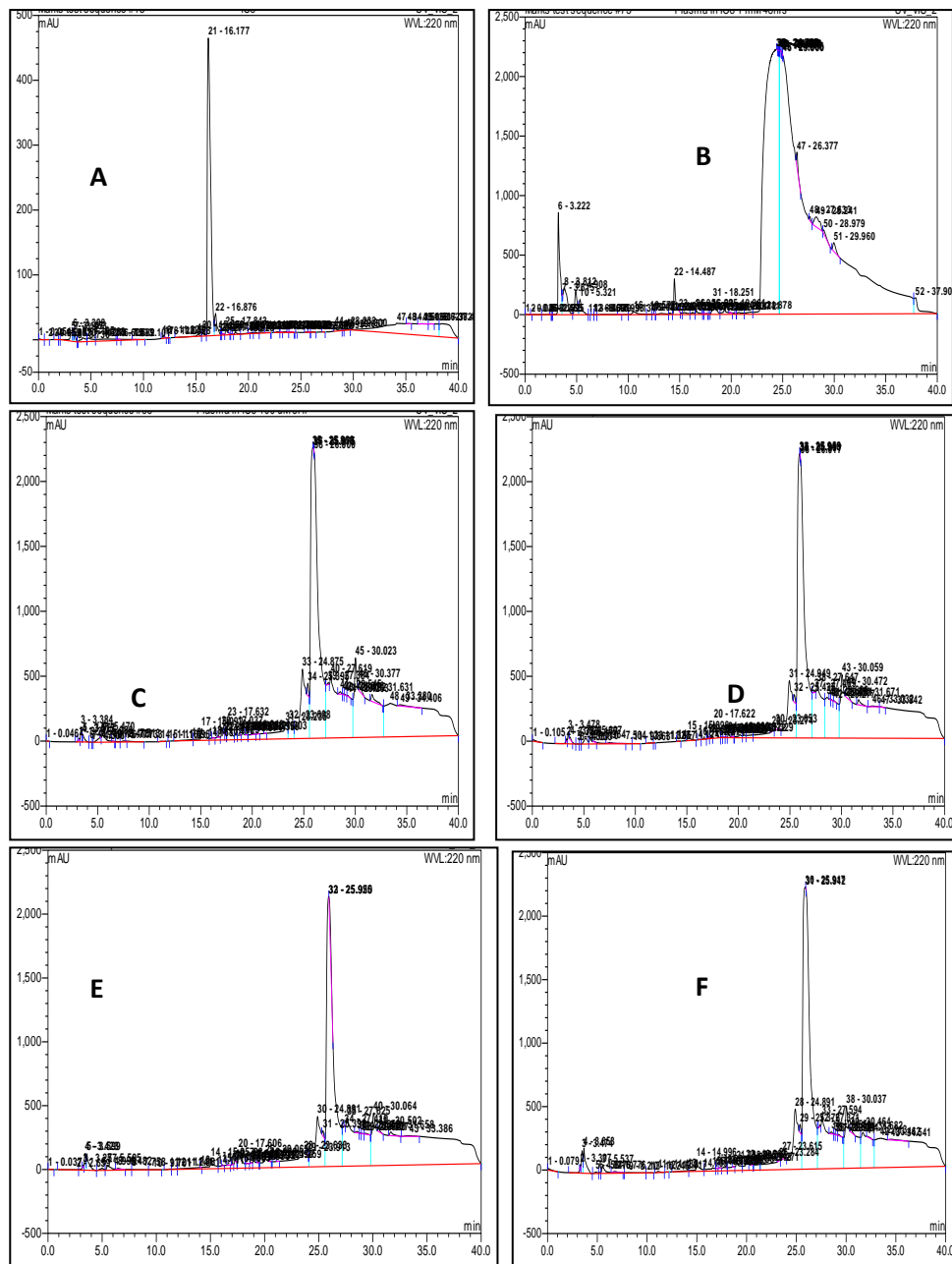


Figure A4.1: Plasma stability of IO8 peptide. (A) RP-HPLC chromatographs of IO8 before incubation in plasma. RP-HPLC chromatographs of IO8 after incubation in plasma at (B) 0 hr (C) 1 hr (D) 3 hrs (E) 24 hrs. (F) 72 hrs. Conditions, linear gradient from 0–60% acetonitrile with 0.1%TFA over 40 min, at a flow rate of 1 mL/min, 28 °C. Absorbance at 220 nm and elution time in minutes

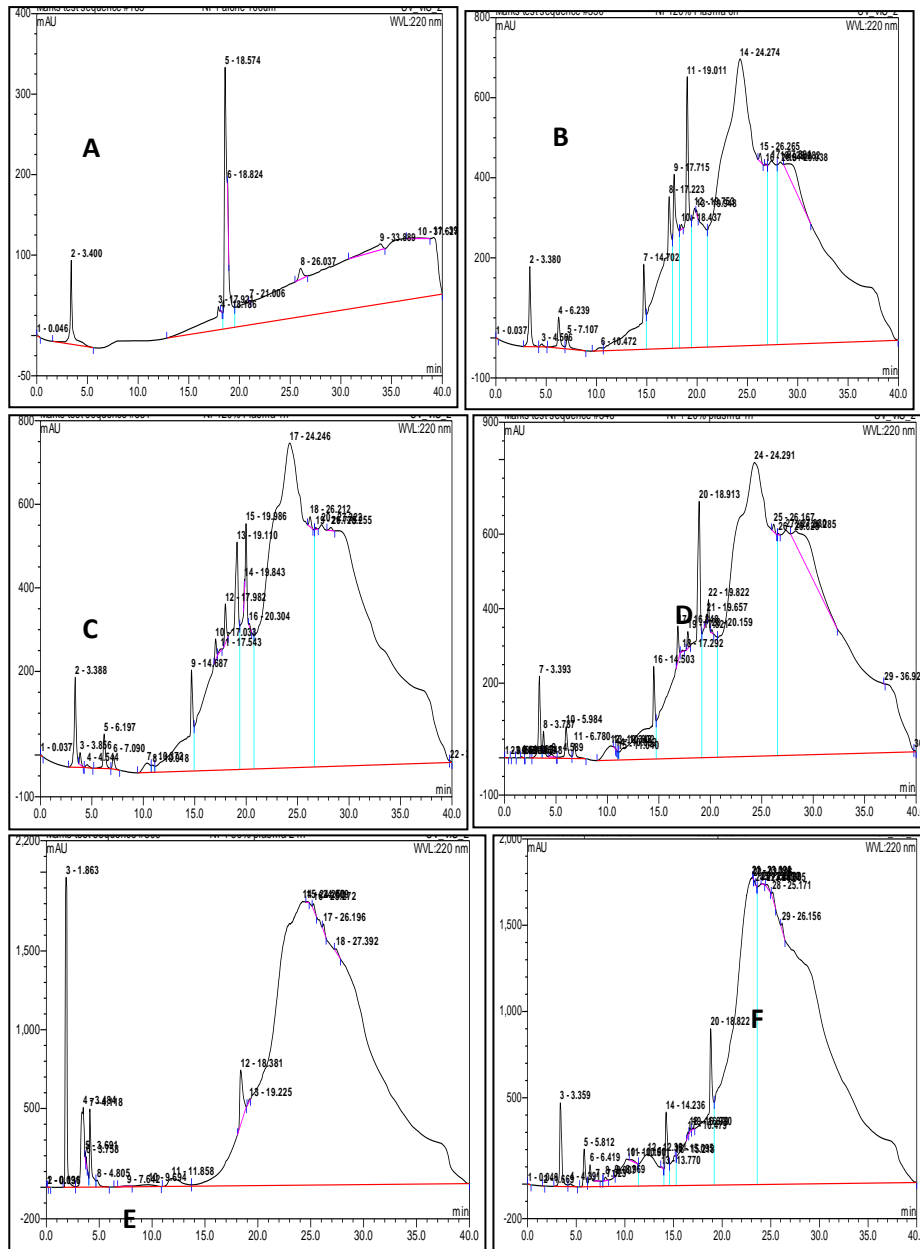


Figure A4.2: Plasma stability of N1-IO8 peptide. (A) RP-HPLC chromatographs of N1-IO8 before incubation in plasma. RP-HPLC chromatographs of N1-IO8 after incubation in plasma at (B) 0 hr (C) 1 hr (D) 3 hrs (E) 24 hrs (F) 72 hrs. Conditions, linear gradient from 0–60% acetonitrile with 0.1%TFA over 40 min, at a flow rate of 1 mL/min, 28 °C. Absorbance at 220 nm and elution time in minutes.

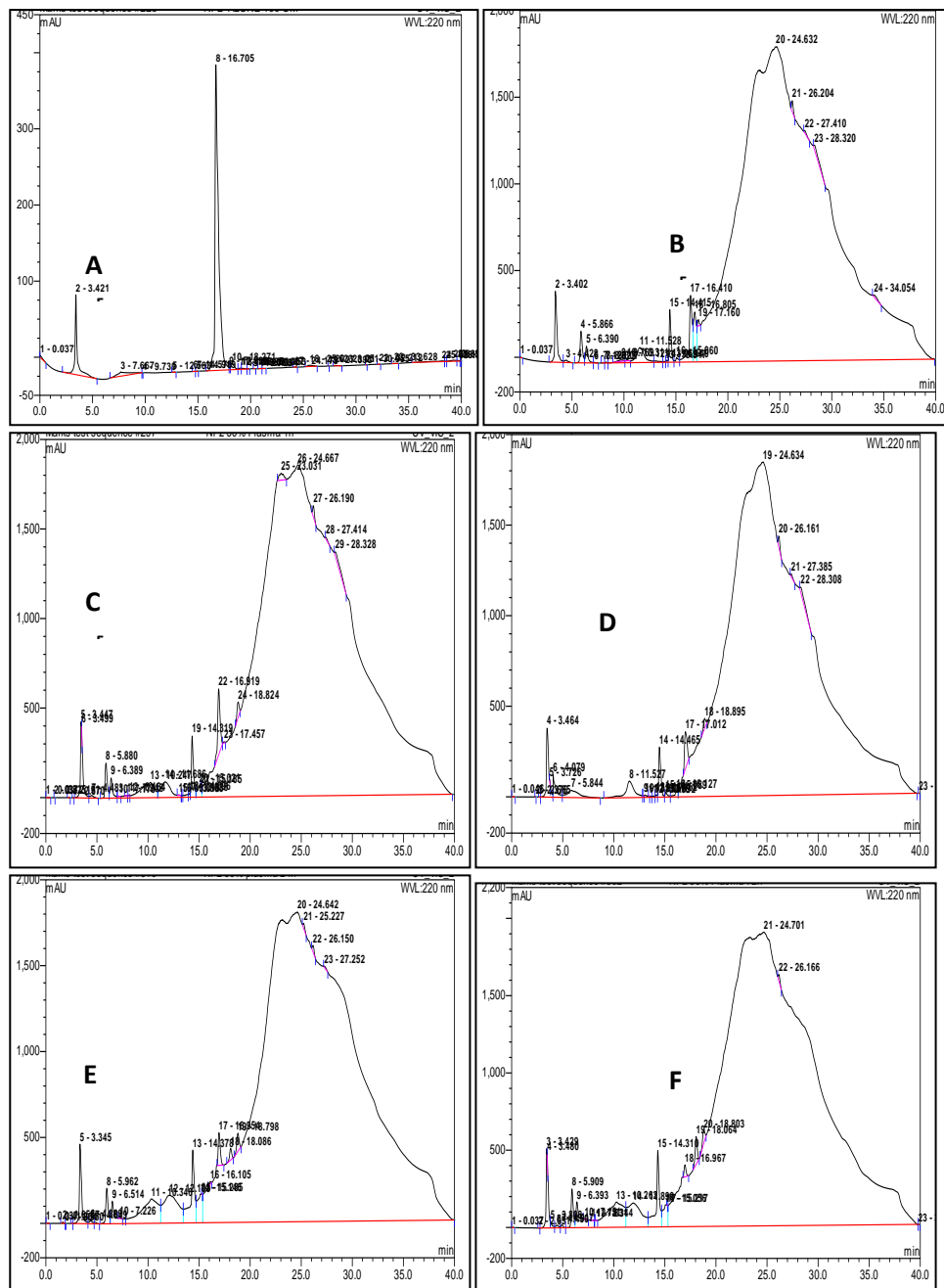


Figure A4.3: Plasma stability of N2-IO8 peptide. (A) RP-HPLC chromatographs of N2-IO8 before incubation in plasma. RP-HPLC chromatographs of N2-IO8 after incubation in plasma at (B) 0 hr (C) 1 hr (D) 3 hrs (E) 24 hrs (F) 72 hrs. Conditions, linear gradient from 0–60% acetonitrile with 0.1% TFA over 40 min, at a flow rate of 1 mL/min, 28 °C. Absorbance at 220 nm and elution time in minutes.

## APPENDIX B

### Reversed-Phase High-Performance Liquid Chromatography of RIO8 and HIO8

This appendix shows the stability of data of RI-IO8 and HIO8 peptides in the presence of varying proteolytic enzymes performed using Reversed-Phase High-Performance Liquid Chromatography (RP-HPLC). Chromatographs from these studies are outlined below. Although our study showed that RI-IO8 had no inhibitory effect on human amylin aggregation, experiments on RI-IO8 was carried out to prove its stability in proteolytic enzymes, particularly trypsin and chymotrypsin in which IO8 was readily degraded (figure A1.1- A1.8). The stability of our RI-IO8 peptide proves that our retro-inverso approach aimed at making IO8 proteolytically stable was successful. The HIO8 peptide was designed by replacing the arginine residue in IO8 (**R**GANFLVHGR-NH<sub>2</sub>) with homoarginin (**Har**GANFLVHGR-NH<sub>2</sub>) with the aim of protecting the peptide against proteolytic degradation by trypsin.

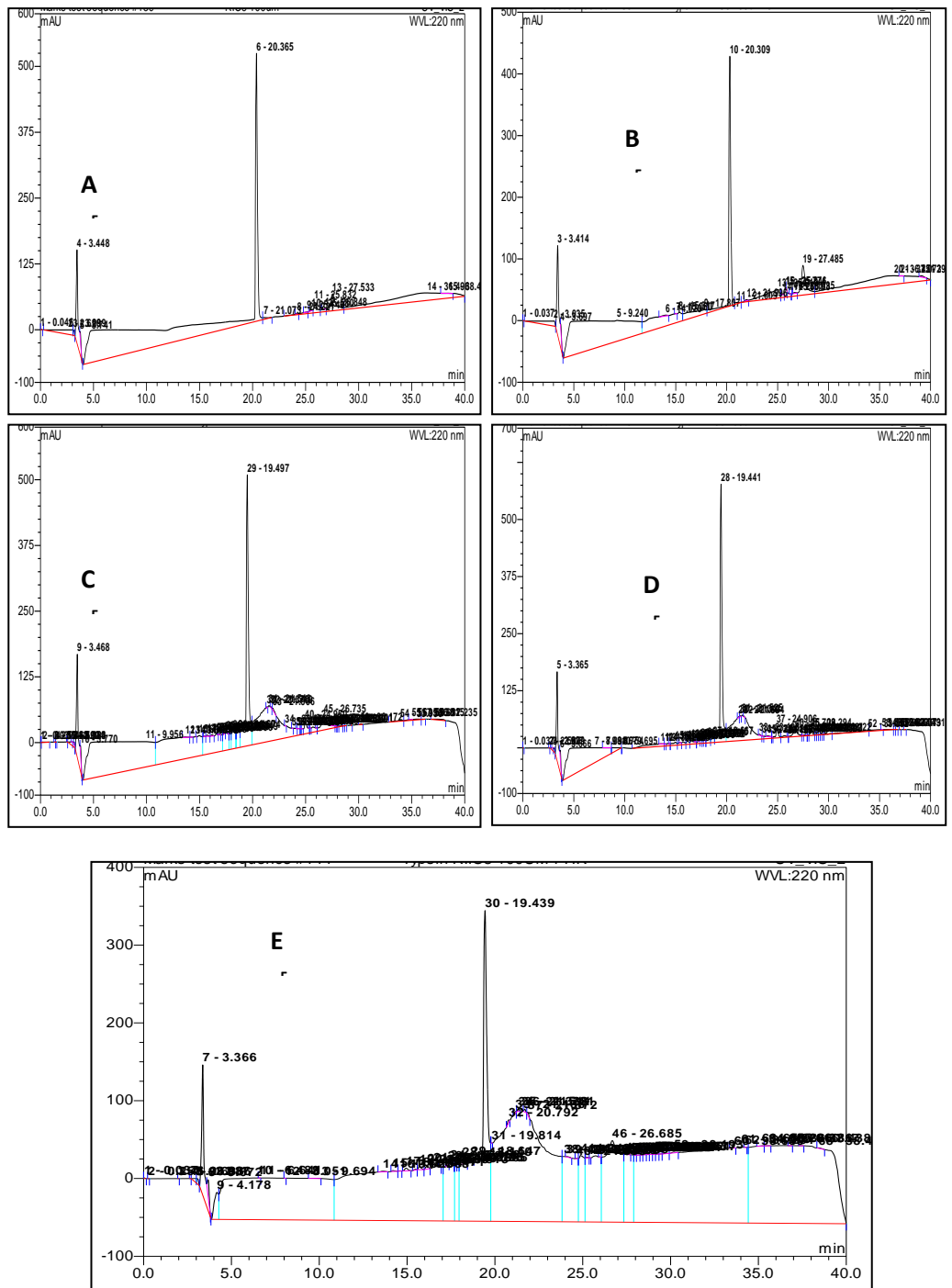


Figure B1.1: Relative Resistance of RI-IO8 to proteolysis. (A) RP-HPLC chromatographs of RI-IO8 before incubation in proteolytic enzymes. RP-HPLC chromatographs of RI-IO8 after incubation in Trypsin, (B) 0 hr (C) 1 hr (D) 3 hrs (E) 24 hrs. Conditions, linear gradient from 0–60% acetonitrile with 0.1% TFA over 40 min, at a flow rate of 1 mL/min, 28 °C. Absorbance at 220 nm and elution time in minutes.

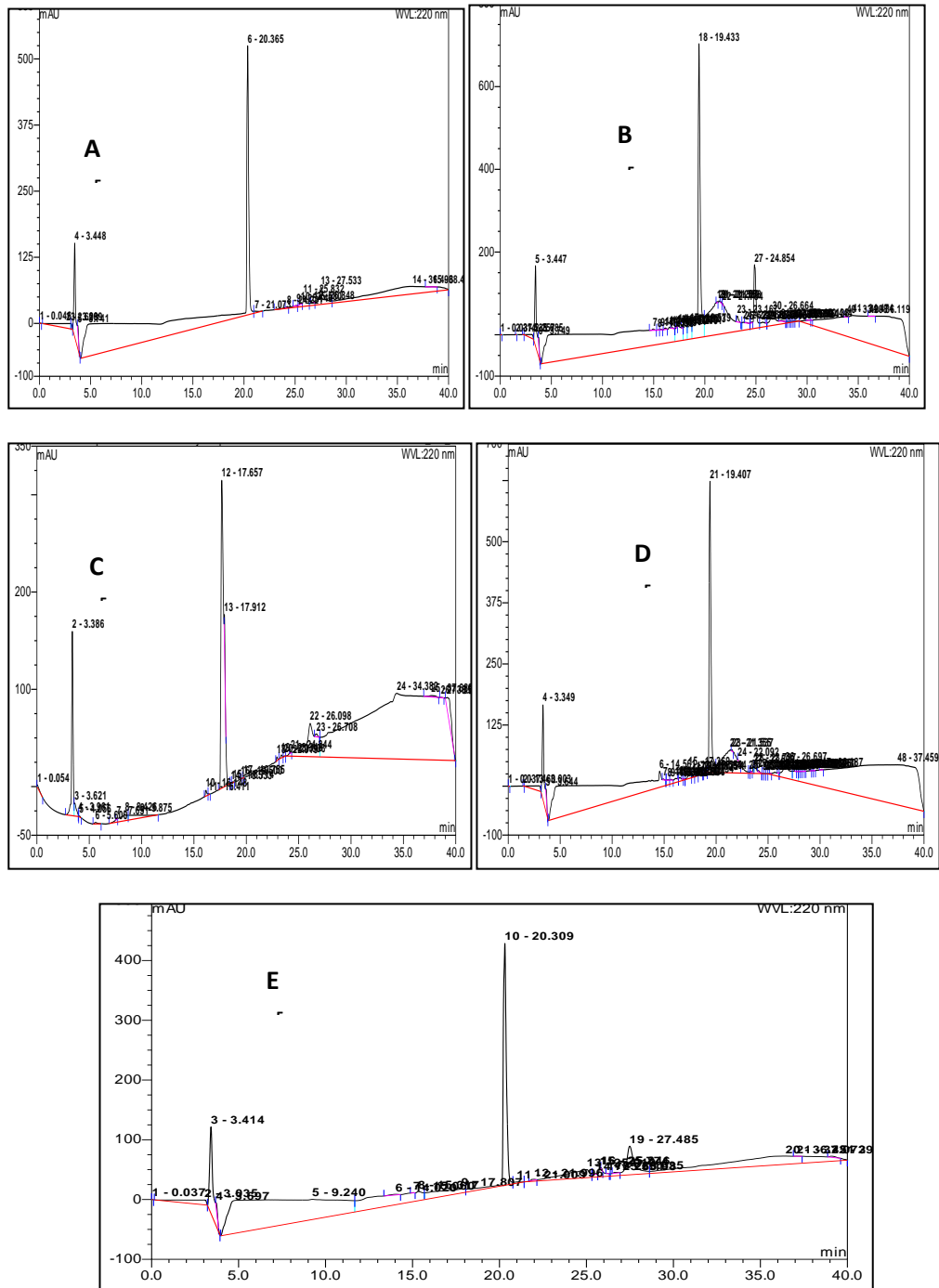


Figure B1.2: Relative Resistance of RI-IO8 to proteolysis. (A) RP-HPLC chromatographs of RI-IO8 before incubation in proteolytic enzymes. RP-HPLC chromatographs of RI-IO8 after incubation in Chymotrypsin, (B) 0 hr (C) 1 hr (D) 3 hrs (E) 24 hrs. Conditions, linear gradient from 0–60% acetonitrile with 0.1% TFA over 40 min, at a flow rate of 1 mL/min, 28 °C. Absorbance at 220 nm and elution time in minutes.

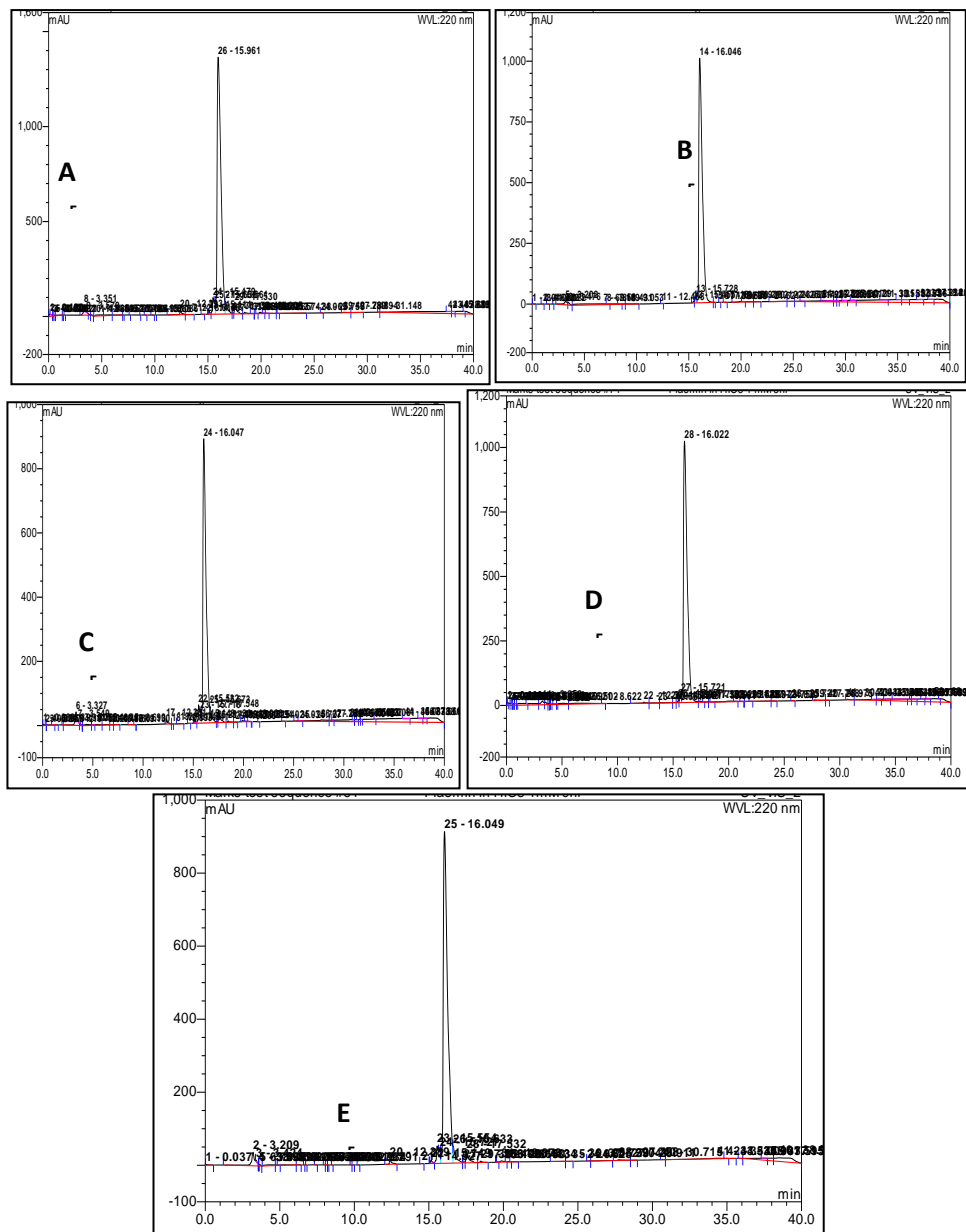


Figure B1.3: Relative Resistance of HIO8 to proteolysis. (A) RP-HPLC chromatographs of HIO8 before incubation in proteolytic enzymes. RP-HPLC chromatographs of HIO8 after incubation in Trypsin, (B) 0 hr (C) 1 hr (D) 3 hrs (E) 24 hrs. Conditions, linear gradient from 0–60% acetonitrile with 0.1%TFA over 40 min, at a flow rate of 1 mL/min, 28 °C. Absorbance at 220 nm and elution time in minutes.

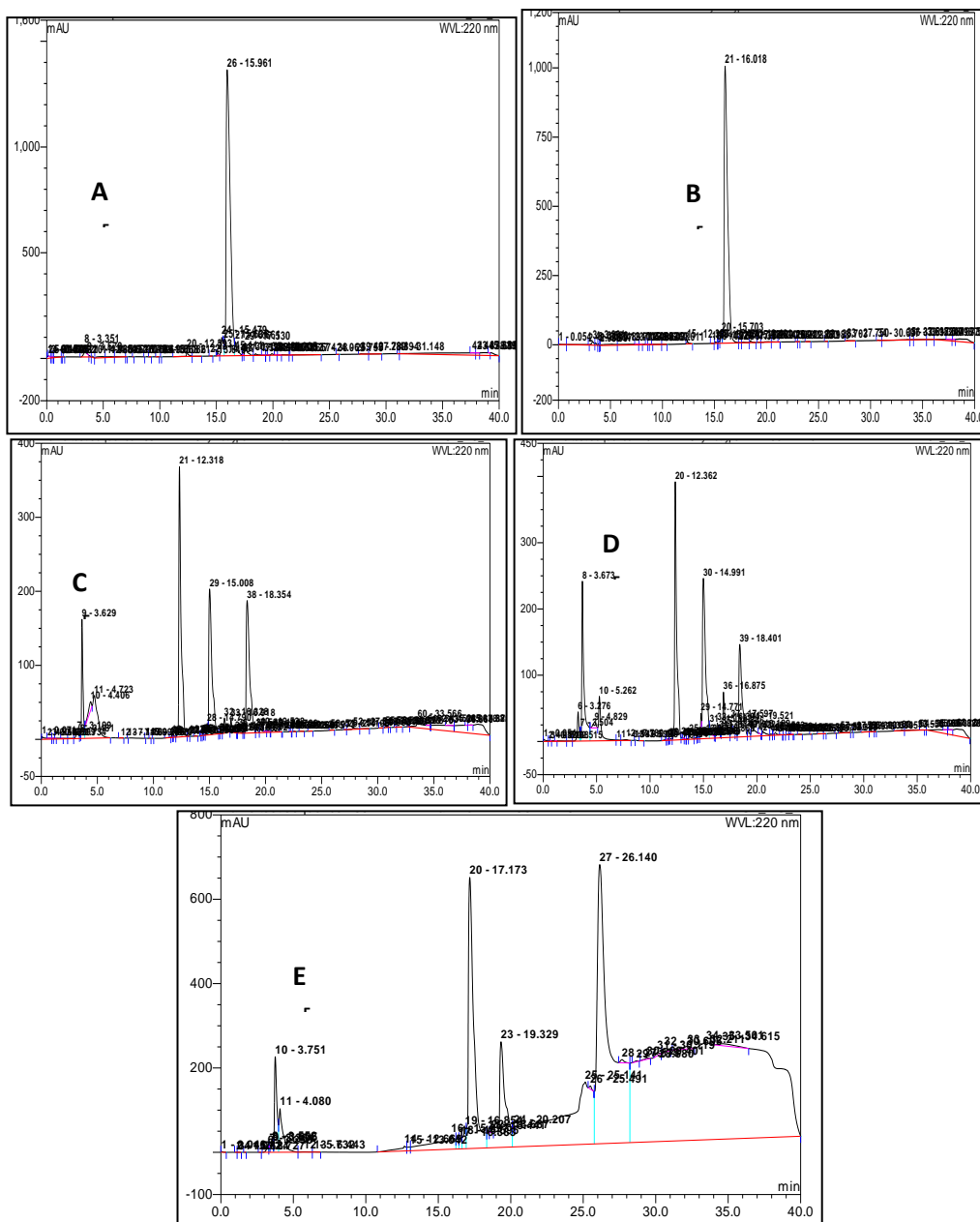


Figure B1.4: Relative Resistance of HIO8 to proteolysis. (A) RP-HPLC chromatographs of HIO8 before incubation in proteolytic enzymes. RP-HPLC chromatographs of HIO8 after incubation in Chymotrypsin, (B) 0 hr (C) 1 hr (D) 3 hrs (E) 24 hrs. Conditions, linear gradient from 0–60% acetonitrile with 0.1% TFA over 40 min, at a flow rate of 1 mL/min, 28 °C. Absorbance at 220 nm and elution time in minutes.

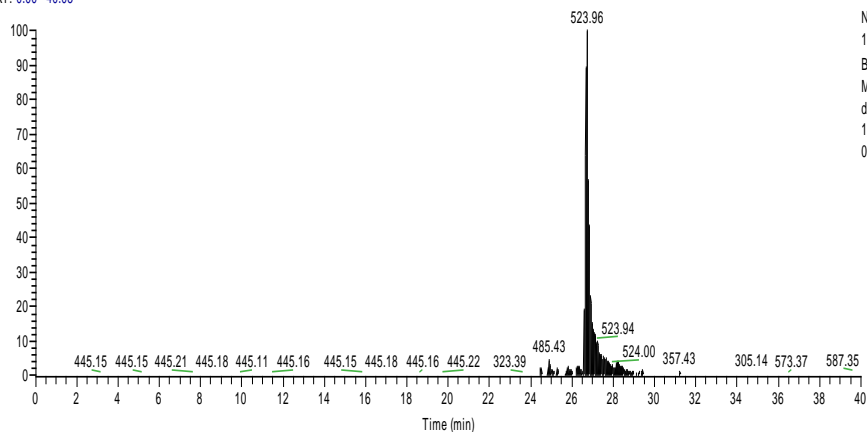
## APPENDIX C

### HPLC-MS data for China-made peptides

C:\Xcalibur\data\da-101-1\_13050810

5/8/2013 10:26:17 AM

RT: 0.00 - 40.03



NL:  
1.84E8  
Base Peak  
MS  
da-101-  
1\_1305081  
02617

da-101-1\_130508102617 #7824-7954 RT: 26.58-27.01 AV: 44 NL: 7.12E7  
T: ITMS + c NSI Full ms [300.00-1800.00]

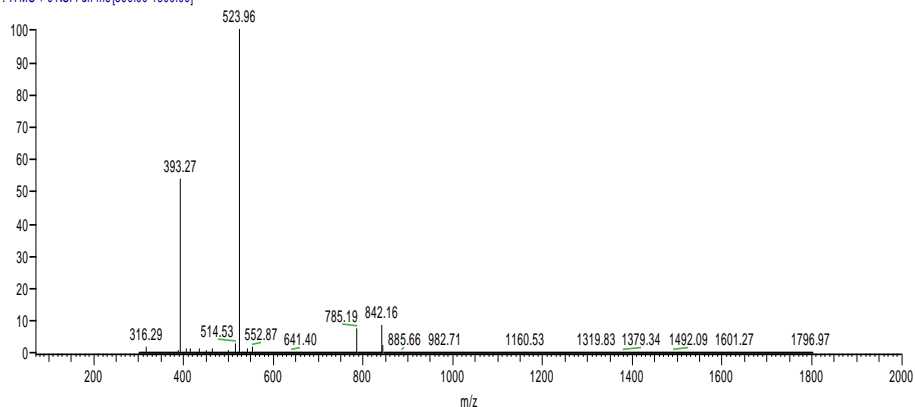
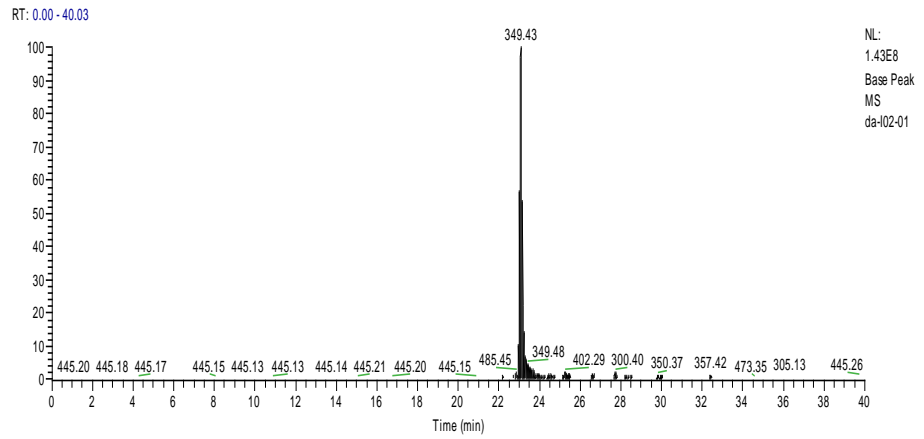


Figure C1: HPLC-MS data for IO1 peptide (R G R L A N F L V H S S G R-NH<sub>2</sub>)



da-I02-01 #6607-6710 RT: 22.85-23.18 AV: 35 NL: 5.25E7  
T: ITMS + c NSI Full ms [300.00-1800.00]

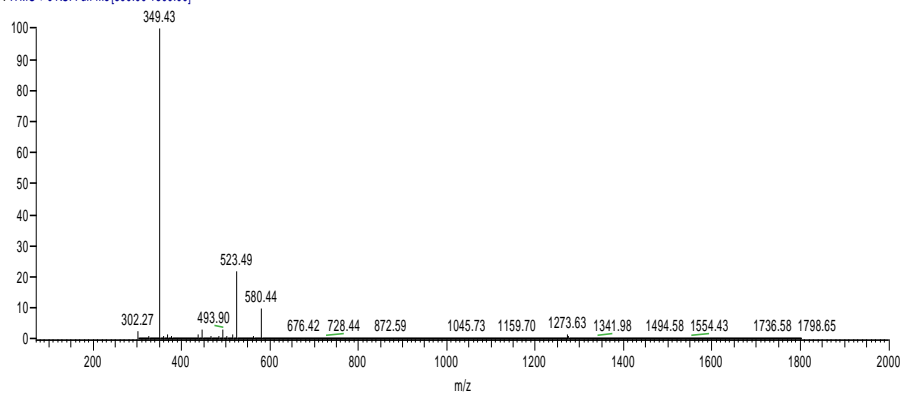


Figure C2: HPLC-MS data for IO2 peptide (R G R L A N F G R-NH<sub>2</sub>)

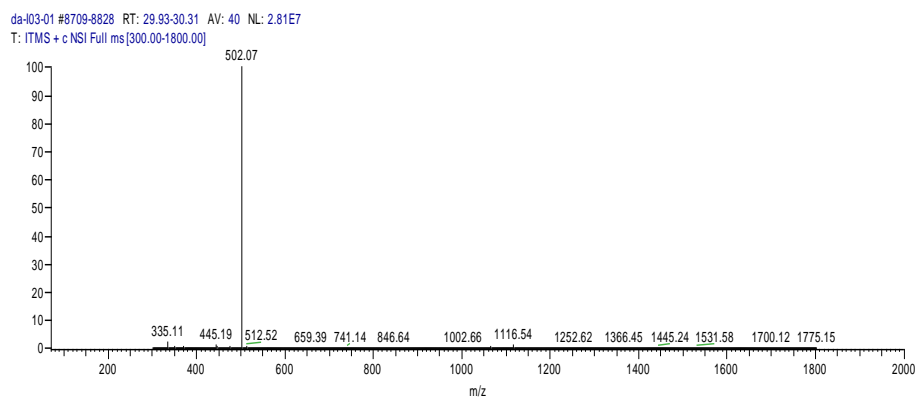
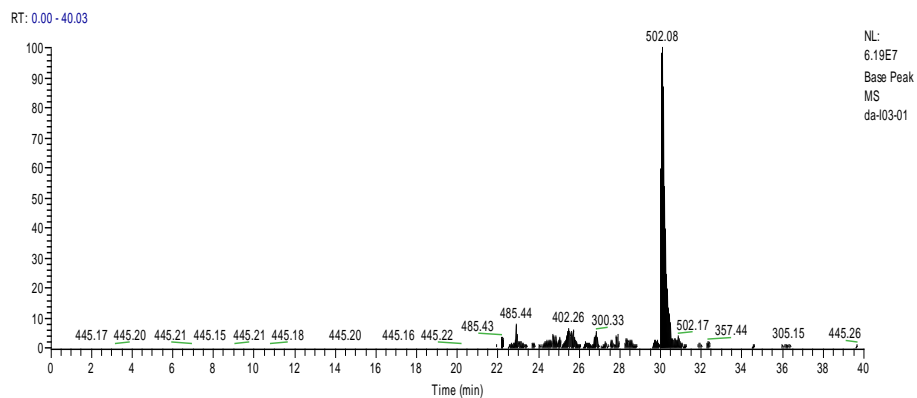


Figure C3: HPLC-MS data for IO3 peptide (H<sub>2</sub>N.R G L A N F L G R-NH<sub>2</sub>)

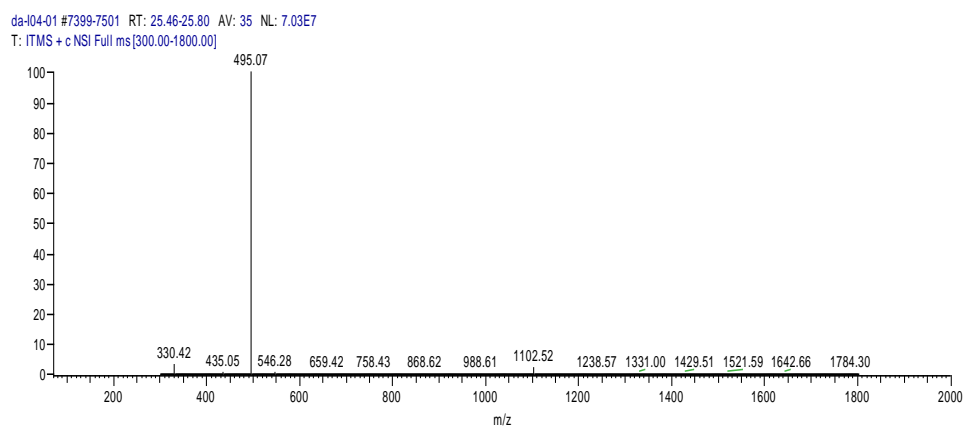
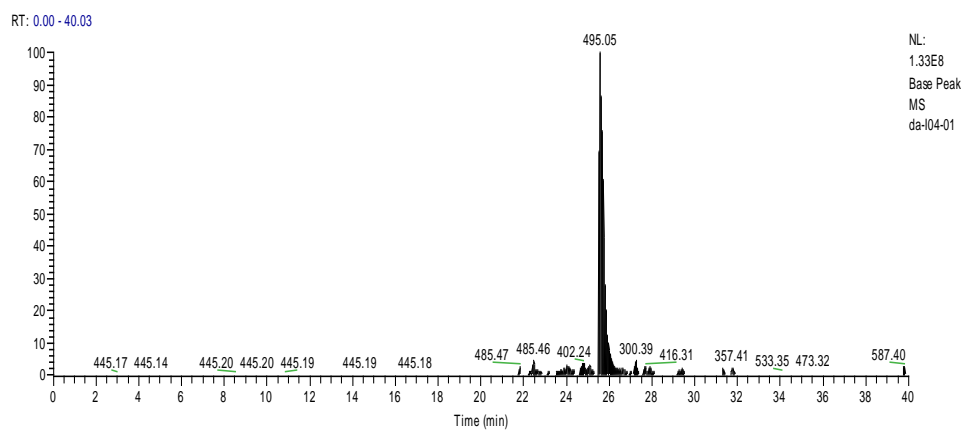


Figure C4: HPLC-MS data for IO4 peptide (R G A N F L V G R-NH<sub>2</sub>)

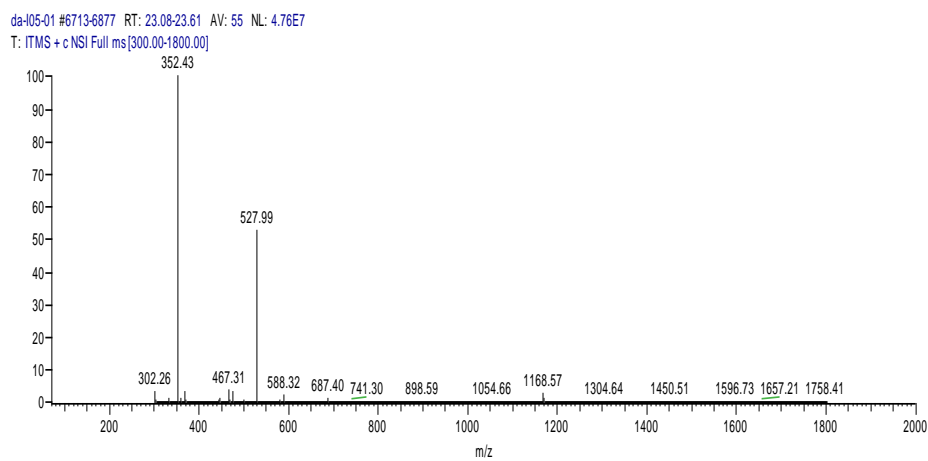
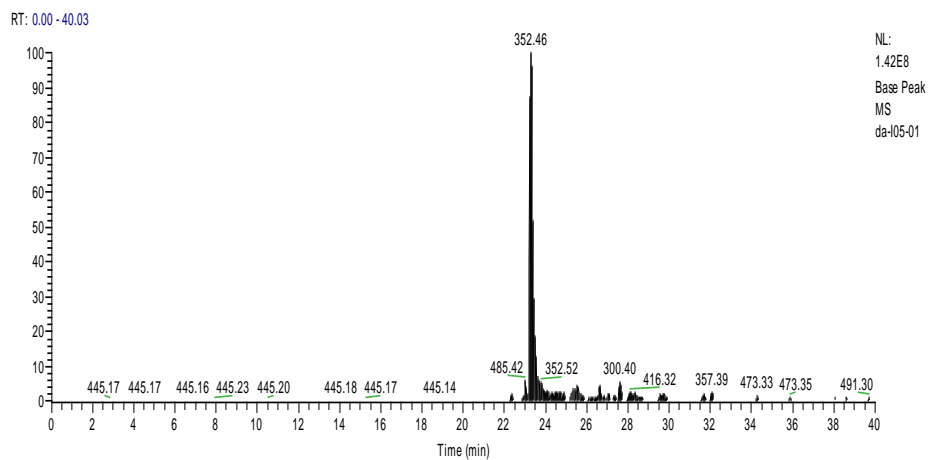
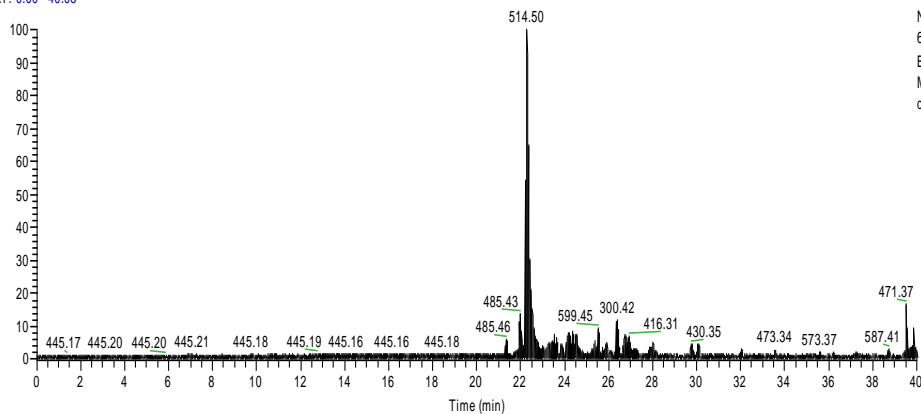


Figure C5: HPLC-MS data for IO5 peptide (R G N F L V H G R-NH<sub>2</sub>)

RT: 0.00 - 40.03



NL:  
6.63E7  
Base Peak  
MS  
da-106-01

da-106-01 #6627-6777 RT: 22.06-22.54 AV: 50 NL: 2.00E7  
T: ITMS + c NSI Full ms[300.00-1800.00]

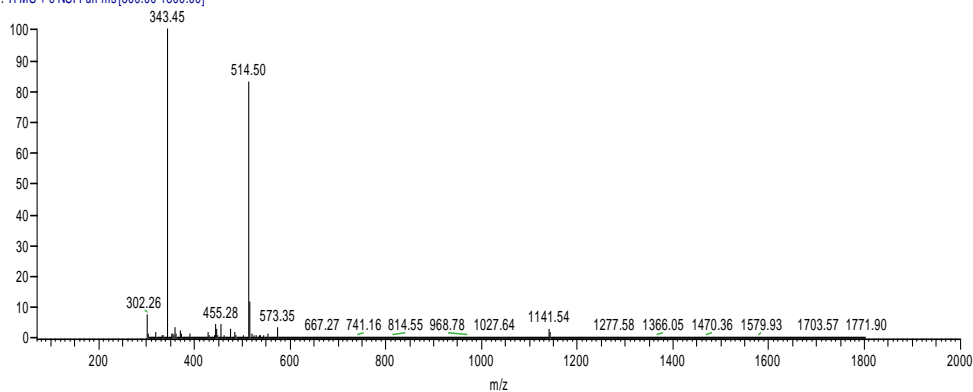
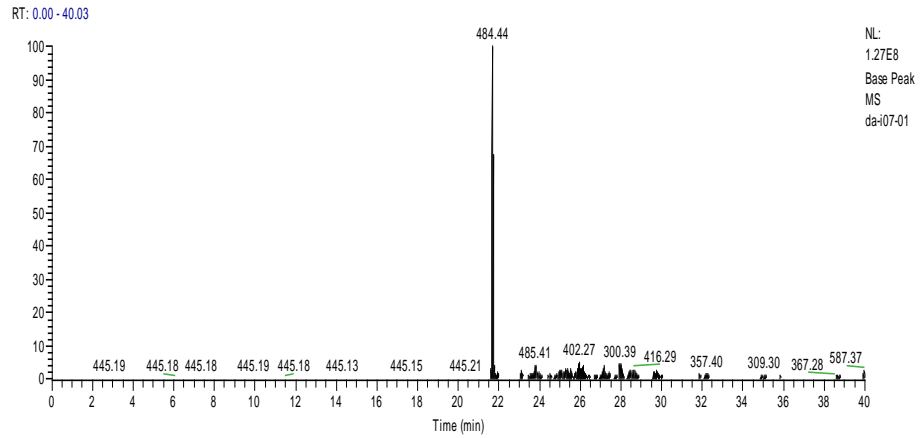


Figure C6: HPLC-MS data for IO6 peptide (R G F L V H S G R-NH<sub>2</sub>)



da-i07-01 #6364-6483 RT: 21.47-21.85 AV: 40 NL: 2.69E7  
T: ITMS + c NSI Full ms [300.00-1800.00]

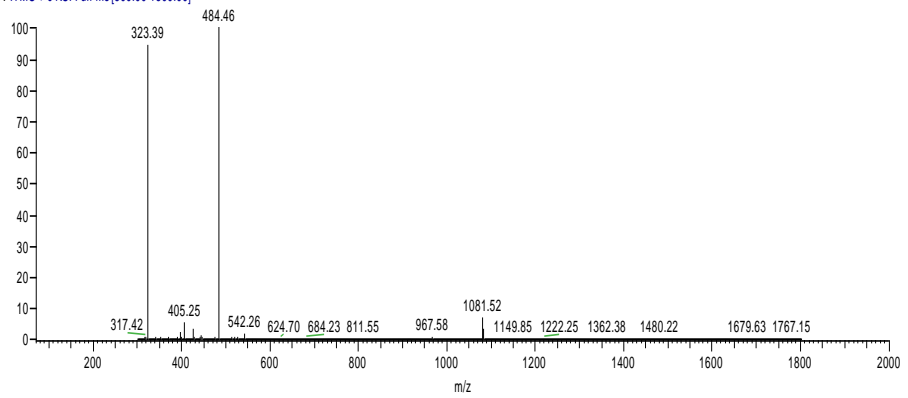


Figure C7: HPLC-MS data for IO7 peptide (R G L V H S S G R-NH<sub>2</sub>)

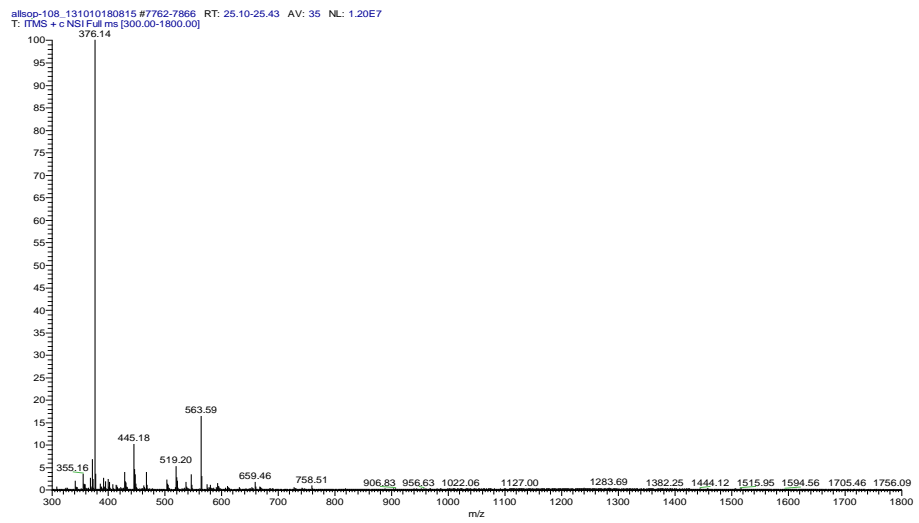
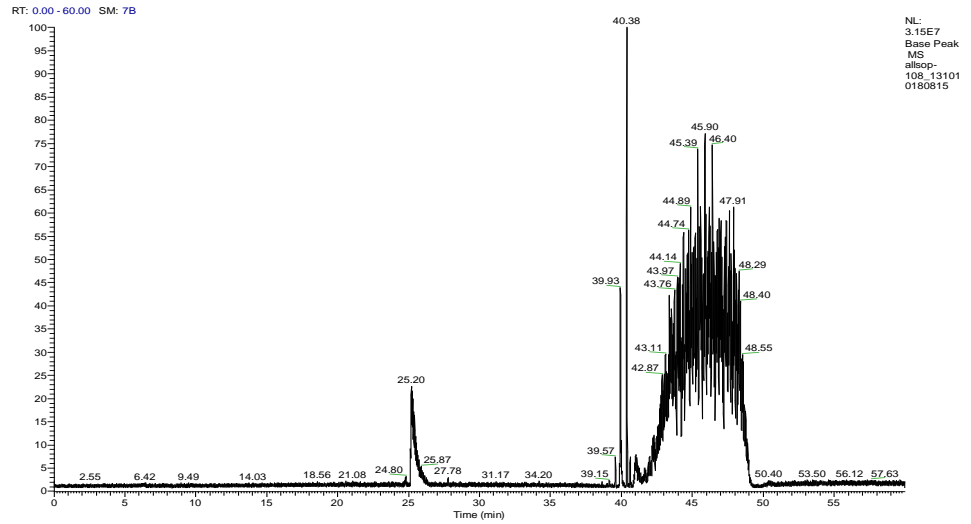


Figure C8: HPLC-MS data for IO8 peptide (RGANFLVHGR-NH<sub>2</sub>)

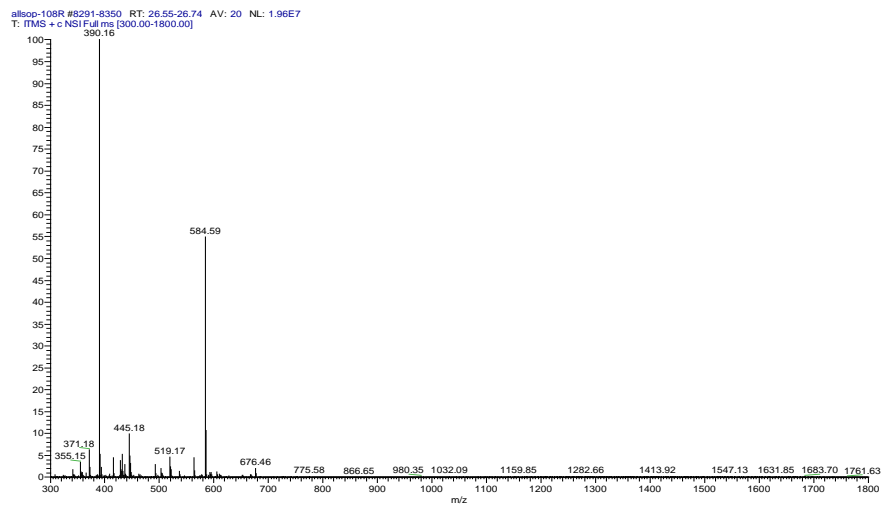
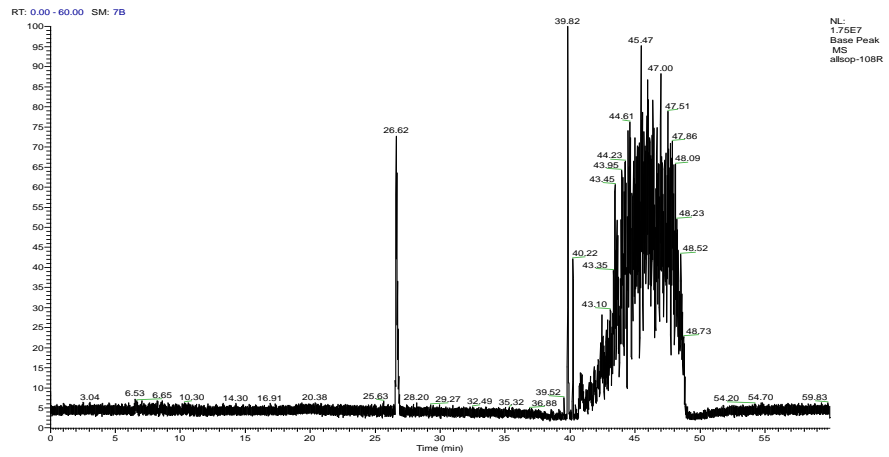


Figure C9: HPLC-MS data for RI-IO8 peptide (Ac-rGhvlfnaGr-NH<sub>2</sub>)

## APPENDIX D

### Th-T data of peptides alone in the absence of amylin

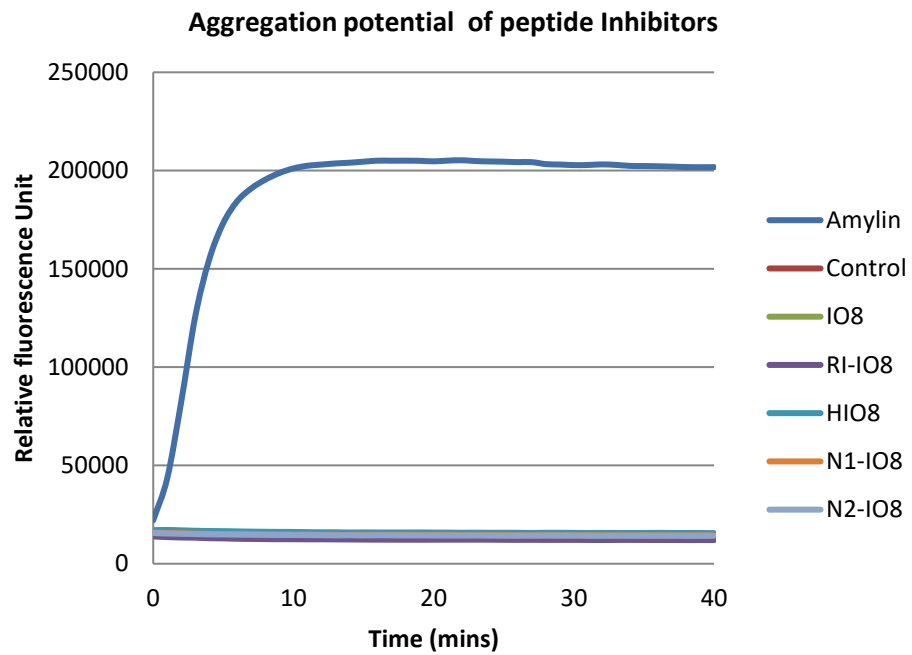


Figure D1: Examples of ThT fluorescence curves for time-dependent aggregation of human amylin alone and peptide inhibitors alone. Amylin alone at 25  $\mu\text{M}$  displayed a characteristic increase in ThT fluorescence corresponding to the lag, sigmoidal and plateau phases of fibril formation, while the inhibitors alone, at 100  $\mu\text{M}$ , showed no characteristic of fibril formation and were comparable to buffer control. Buffer control contained neither amylin nor inhibitors.

## APPENDIX E

### List of publications

- A. **Obasse I, Taylor M, Fullwood NJ, Allsop D. (2017). Development of proteolytically stable N-methylated peptide inhibitors of aggregation of the amylin peptide implicated in type 2 diabetes. *Interface Focus*. 7: 20160127**

## Research



**Cite this article:** Obasse I, Taylor M, Fullwood NJ, Allsop D. 2017 Development of proteolytically stable N-methylated peptide inhibitors of aggregation of the amylin peptide implicated in type 2 diabetes. *Interface Focus* 7: 20160127. <http://dx.doi.org/10.1098/rsfs.2016.0127>

One contribution of 12 to a theme issue 'Self-assembled peptides: from nanostructures to bioactivity'.

**Subject Areas:**  
biochemistry

**Keywords:**  
diabetes, amylin, islet amyloid polypeptide, IAPP, N-methylated peptide, amyloid

**Author for correspondence:**  
David Allsop  
e-mail: [d.allsop@lancaster.ac.uk](mailto:d.allsop@lancaster.ac.uk)

Electronic supplementary material is available online at <https://dx.doi.org/10.6084/m9.figshare.c.3876073>.

# Development of proteolytically stable N-methylated peptide inhibitors of aggregation of the amylin peptide implicated in type 2 diabetes

Idira Obasse, Mark Taylor, Nigel J. Fullwood and David Allsop

Division of Biomedical and Life Sciences, Faculty of Health and Medicine, University of Lancaster, Lancaster LA1 4YQ, UK

DA, 0000-0002-0513-5575

Islet amyloid polypeptide, also known as amylin, is the main component of the amyloid deposits present in approximately 90% of people with type 2 diabetes mellitus (T2DM). In this disease, amylin aggregates into multimeric  $\beta$ -pleated sheet structures which cause damage to pancreatic islet  $\beta$ -cells. Inhibitors of early-stage amylin aggregation could therefore provide a disease-modifying treatment for T2DM. In this study, overlapping peptides were designed to target the 'binding' region (RLANFLVHSS, residues 11–20) of human amylin, and their effects on amyloid fibril formation were determined by thioflavin-T assay. The first generation peptides showed less than 50% inhibition of aggregation, but a second generation peptide (H<sub>2</sub>N-RGANFLVHGR-CONH<sub>2</sub>) showed strong inhibitory effects on amylin aggregation, and this was confirmed by negative stain electron microscopy. Cytotoxicity studies revealed that this peptide protected human pancreatic 1.4E7 (ECACC 10070102) insulin-secreting cells from the toxic effects of human amylin. Unlike the retro-inverso version of this peptide, which stimulated aggregation, two N-methylated peptides (H<sub>2</sub>N-RGAmNFmLVmHGR-CONH<sub>2</sub> and H<sub>2</sub>N-RGANmFLmVHmR-CONH<sub>2</sub>) gave very clear dose-dependent inhibition of fibril formation. These two peptides were also stable against a range of different proteolytic enzymes, and in human plasma. These N-methylated peptides could provide a novel treatment for slowing progression of T2DM.

## 1. Introduction

Amyloid is a generic term for pathological protein deposits that accumulate in many different organs and tissues when protein molecules in a predominantly  $\beta$ -pleated sheet conformation self-associate, mainly by hydrogen bonds, to form long and unbranching 8–10 nm diameter fibrils [1,2]. More than 30 different proteins are known to form these fibrils in a wide variety of diseases in humans, including various forms of systemic and inherited amyloidosis [3–5], Alzheimer's disease (AD) [6] and other neurodegenerative diseases [7], and type 2 diabetes mellitus (T2DM) [8–10]. One of the most prevalent of these diseases (along with AD) is T2DM, where the amyloid deposits are found in the islets of Langerhans of the pancreas, and are composed of islet amyloid polypeptide (IAPP), also known as amylin [10]. Amylin is a 37 amino acid peptide belonging to the calcitonin family, members of which have a disulfide bridge between Cys residues 2 and 7, as well as an amidated carboxyl terminus [10,11]. Amyloid deposits have been reported in around 90% of cases of T2DM [12,13] and amylin aggregation has been strongly linked with the development of islet  $\beta$ -cell failure in this disease [13,14]. Early studies demonstrated the toxicity of human amylin to cultured islet cells, through induction of membrane damage, Ca<sup>2+</sup> ion influx, and apoptosis, and suggested that this toxicity resides in the amyloid fibrils themselves [15–18]. However, as is the case with other amyloids, more recent studies have indicated that smaller 'soluble oligomers' could be the most toxic form of this molecule [19–21].

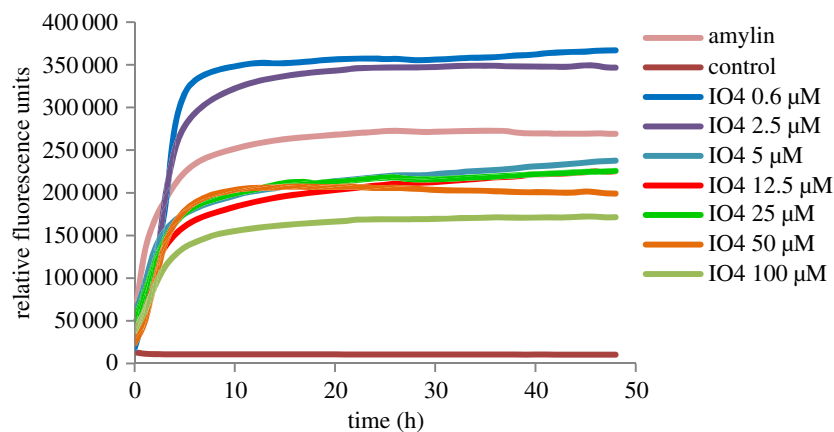


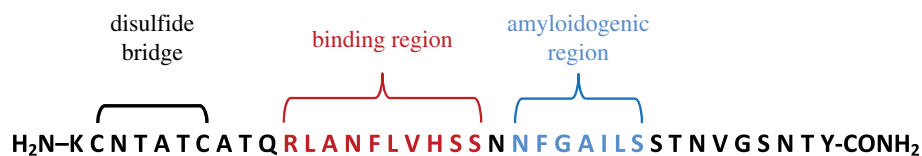
**Figure 1.** Example of ThT fluorescence curves for human amylin in the presence of different concentrations of an inhibitor (IO4). Data are means for a single experiment carried out in triplicate, with readings taken every 10 min. Amylin alone (at 25  $\mu\text{M}$ ) displays a characteristic increase in fluorescence corresponding to the 'sigmoidal' and 'plateau' phases of amyloid fibril formation, while the addition of the inhibitor, at varying concentrations, has a dose-dependent effect on fibril formation. The buffer control ('control') contained neither amylin nor inhibitor.

Currently, approximately 425 million people globally have diabetes and this figure is expected to rise to 642 million by the year 2040 [22]. Moreover, total deaths from diabetes have been predicted to increase by 50% in the next 10 years [23]. Diabetes leads to a number of secondary complications including blindness, heart disease, kidney failure and stroke. A healthy diet, weight control, and exercise, are all necessary for management of T2DM [24,25]. In addition to these lifestyle changes, a number of drug treatment options are available, including insulin therapy. However, these drugs do not provide a cure for diabetes, or prevent secondary complications. There is, therefore, a great need for more research to develop new and potentially more effective treatment options for diabetes.

Compounds that inhibit the self-assembly of amylin are a potential therapeutic target for limiting damage to pancreatic islet cells in T2DM, and this would be expected to slow progression of this disease (i.e. have a disease-modifying effect). The objective of this study was to develop novel peptide-based inhibitors of amylin aggregation that impede the spontaneous assembly of amylin into oligomers and fibrils *in vitro*. In general, it has been challenging to find suitable drug-like therapeutic agents that inhibit the aggregation of amyloid proteins. However, small organic molecules, peptides, peptidomimetics and nanoparticles have all been developed for this purpose. In the case of AD, where this type of therapy is most advanced, a number of inhibitors of aggregation of the A $\beta$  peptide found in senile plaques, including small molecules and peptides, have been developed over the years, but none of these compounds have been successful yet in human clinical trials [26,27]. This is partly due to the fact that inhibition of amyloid aggregation involves blocking the interactions between protein monomers, and protein-protein interactions are recognized as difficult therapeutic targets [28,29]. Generally, regions for protein-protein interactions are 1500–3000 Å in size [30,31], while the region for protein-small molecule interactions is only 300–1000 Å [32,33]. Therefore, small molecules are not able to build adequate steric interruptions to inhibit protein aggregation [34]. These challenges make it difficult to develop potent and selective small molecule inhibitors of amyloid aggregation.

An alternative strategy for inhibition of amyloid aggregation is the use of peptide-based inhibitors. Peptide-based

inhibitors directed against specific amyloid sub-regions represent the first generation of amyloid-based therapeutics, which can then be developed further into more drug-like molecules, and this could be a promising avenue for development of a new disease-modifying therapy for T2DM. In the case of amylin, previous studies along these lines have focused almost exclusively on the primary 'amyloidogenic' region of the peptide (amino acid residues 22–28, with sequence NFGAILS), which is the main region involved in protein misfolding into the toxic  $\beta$ -sheet conformational structure [35,36]. These peptide inhibitors are designed to act as ' $\beta$ -sheet breakers' and are typically compounds that consist of this amyloidogenic motif in combination with a  $\beta$ -sheet breaker element. The latter can be comprised, for example, of methylated amino acids, or prolines [37,38]. However, these ' $\beta$ -breaker' peptides do not completely inhibit fibril formation and their inhibitory effects are often seen only at high concentrations, when the peptides are present in molar excess compared to amylin [39–41]. In contrast, the peptide inhibitors described in this report are designed to interact with amylin at the 11–20 'binding' region (RLANFLVHSS), peptide derivatives from which show maximum binding to full-length human amylin [42]. Many peptides face the challenge of insolubility in aqueous solution and/or susceptibility to proteolytic degradation. To improve the solubility of the peptides described here, and to limit their self-aggregation, arginine-glycine residues (RG...GR) were placed at both N- and C-termini (figure 1). This approach differs from the ' $\beta$ -sheet blockers' presented in other studies [43–45] and this rationale follows previous successful research where a peptide inhibitor (OR2) with the sequence H<sub>2</sub>N-RGKLVFFGR-CONH<sub>2</sub> was found to inhibit A $\beta$  oligomer and fibril formation [46]. A proteolytically stable retro-inverso version of this peptide (RI-OR2), with sequence reversal and substitution of L-amino acids with D-amino acids, was then developed [47]. The next step was to attach a 'TAT' transit sequence (trans-activator of transcription from HIV) to RI-OR2 to allow it to penetrate into cells, and cross the blood-brain barrier [48]. In a final iteration, RI-OR2-TAT was covalently bound to the surface of nanoliposomes to produce a highly potent multivalent inhibitor [49,50]. Here, the first steps of a similar strategy are described for inhibition of aggregation of the amylin peptide in T2DM.

**Table 1.** Design of peptide inhibitors employed for this study. (Online version in colour.)

peptide inhibitor ID	sequence	purity %
IO1	$\text{H}_2\text{N-R G RLANFLVHSS G R-CONH}_2$	95%
IO2	$\text{H}_2\text{N-R G RLANF G R-CONH}_2$	95%
IO3	$\text{H}_2\text{N-R G LANFL G R-CONH}_2$	93%
IO4	$\text{H}_2\text{N-R G ANFLV G R-CONH}_2$	95%
IO5	$\text{H}_2\text{N-R G NFLVH G R-CONH}_2$	95%
IO6	$\text{H}_2\text{N-R G FLVHS G R-CONH}_2$	96%
IO7	$\text{H}_2\text{N-R G LVHSS G R-CONH}_2$	95%
IO8	$\text{H}_2\text{N-R G ANFLVH G R-CONH}_2$	95%
RI-IO8	Ac-r G <i>h</i> v <i>l</i> f <i>n</i> a G r-CONH <sub>2</sub>	96%
N1-IO8	$\text{H}_2\text{N-R G Am N Fm LVm H G R-CONH}_2$	86%
N2-IO8	$\text{H}_2\text{N-R G ANm FLm V Hm G R-CONH}_2$	96%
NFGAILS	$\text{H}_2\text{N-R G NFGAILS G R-CONH}_2$	98%

The amino acid sequence of human amylin, showing the binding region for amylin self-association [42] and the main amyloidogenic region [35]. All of the short peptide inhibitors are designed to interact with the binding region of full-length amylin, except for the last peptide. The arginine–glycine flanking residues (RG. .GR) impede peptide self-aggregation. In the retro-inverted peptide (RI-IO8), *D* amino acids are in lower case. N-methylated peptide residues are indicated by lower case ‘m’.

## 2. Material and methods

### 2.1. Peptides

Full length human amylin (1–37 amide) was purchased from American Peptide Company, California, USA. Structures of the new peptides designed for this study are presented in table 1. Seven peptide inhibitors (IO1–IO7) derived from the 11–20 binding region of amylin (RLANFLVHSS), together with IO8 (the combined amino acid sequences of IO4 and IO5), and NFGAILS ( $\text{H}_2\text{N-RGNFGAILSGR-CONH}_2$ , from the primary amyloidogenic region), were purchased from ChinaPeptide Company, Shanghai, China. RI-IO8 (retro-inverso IO8), and two N-methylated peptides (N1-IO8, N2-IO8), were synthesized by Cambridge Peptides, Birmingham, UK. The effects of two previously published inhibitors were also assessed. The first of these is the hexapeptide  $\text{H}_2\text{N-NF(N-Me)GA(N-Me)IL-COOH}$  (abbreviated here to NMeG24 NMeI26) which is a modification of the amylin 22–27 fragment (NFGAIL), with an N-methylation of the amide bonds at G24 and I26 [51], and was purchased from Anaspec EGT Group, California, USA. The second of these peptides, with amino acid sequence  $\text{H}_2\text{N-ANFLVH-COOH}$  [52], was synthesized by ChinaPeptide Company. All peptides were analysed for purity (table 1) and had their mass confirmed by high

performance liquid chromatography (HPLC)-mass spectrometry (MS) (electronic supplementary material, figure S1).

### 2.2. Determination of peptide aggregation by thioflavin-T assay

Amylin was ‘deseeded’ in trifluoroacetic acid (TFA), followed by 1,1,1,3,3,3-hexafluoro-2-propanol (HFIP), to remove any pre-formed aggregates prior to these experiments. ThT assays were carried out in 384-well clear-bottomed microtitre plates (NUNC) by incubating the amylin peptide (25  $\mu\text{M}$ ) in the presence of ThT (15  $\mu\text{M}$ ) in 10 mM phosphate-buffered saline (PBS), pH 7.4, at 30°C. The inhibitors, when present, were at varying molar ratios relative to amylin, with the total volume of solution in each well set at 60  $\mu\text{l}$ . The plates were shaken every 10 min, and the fluorescence was then read ( $\lambda_{\text{ex}} = 442 \text{ nm}$ , and  $\lambda_{\text{em}} = 483 \text{ nm}$ ) in a BioTek Synergy 2 plate reader. Triplicate readings were taken for each condition, with each experiment being repeated three times.

### 2.3. Cell toxicity experiments

Human pancreatic 1.4E7 (ECACC 10070102) insulin-secreting cells were obtained from Public Health England Culture Collection.

1.4E7 is a hybrid cell line formed by the electrofusion of a primary culture of human pancreatic islets with PANC-1, a human pancreatic ductal carcinoma cell line (ECACC 87092802). These cells were routinely grown in RPMI-1640 medium with L-glutamine (Gibco Life Technologies), supplemented with 10% fetal calf serum and 1% penicillin/streptomycin. Monolayers of cells were grown in 75 cm<sup>3</sup> flasks with incubation at 37°C, 5% CO<sub>2</sub>. Cell viability was assessed using the Promega CellTiter 96 aqueous one solution cell proliferation (MTS) assay. A confluent layer of cells was detached using trypsin, washed, and then suspended and replated, at 250 000 cells/ml, in culture medium. After 24 h, the medium was replaced with fresh medium containing amylin (10 or 20 µM), with the required concentration of peptide inhibitor, with replicates of six wells. After incubation for 24 h, 20 µl of CellTiter 96 aqueous one solution reagent was added to each well and the plate was incubated for a further 3 h. Absorbance at 490 nm was determined using a Wallac Victor<sup>2</sup> 1420 multilabel counter (PerkinElmer). Each experiment was repeated three times.

## 2.4. Determination of peptide stability

Reverse-phase (RP) HPLC was used to determine the stability of the peptide inhibitors in plasma, and in the presence of the stated proteolytic enzymes. A C18 column (Phenomenex, 250 × 4 mm) was used for these experiments, with elution by a gradient of acetonitrile, containing 0.01% trifluoro acetic acid (TFA). A sample of human plasma was obtained, with ethical approval (Oldham Ethics Committee), from Prof. David Mann (University of Manchester). Each peptide (5 µl of 100 µM peptide) was added to 95 µl of 50% plasma. To assess the stability of peptides in the presence of proteolytic enzymes, 2 µl of enzyme (1 mg ml<sup>-1</sup>) was added to 98 µl of peptide (100 µM) in PBS. After incubation, the samples were injected onto the RP-HPLC column and eluted with a linear gradient of 0–60% acetonitrile, with continuous monitoring of absorbance ( $\lambda = 220$  nm).

## 2.5. Transmission electron microscopy

Solutions of amylin (25 µM), and amylin in the presence of inhibitors at varying concentrations, were incubated in PBS at room temperature for 48 h, with continuous orbital shaking, and a 5 µl sample was applied to a carbon-coated formvar grid. After 3 min, the liquid was adsorbed by filter paper, then 5 µl of 2% aqueous phosphotungstic acid (PTA) (adjusted to pH 7.3 using 1N NaOH) was applied, and left for 1 min. Excess liquid was removed, and the grid was allowed to dry overnight before observation under a Jeol JEM-1010 electron microscope. Five fields were photographed at random for each sample, after first examining the grids for uniformity.

## 2.6. Statistical analysis

Data for ThT and cell toxicity assays are expressed as mean  $\pm$  standard error of mean (s.e.m.), for one representative experiment. Statistical analysis was performed using a two-tailed Student's *t* test. ANOVA and confidence interval (CI) analysis ( $p < 0.05 + 95\%$  CI) was used to compare mean values.

## 3. Results

The aggregation of human amylin at 25 µM in the presence of varying concentrations of peptides IO1–IO7 was monitored by ThT assay. Figure 1 shows typical examples of ThT aggregation curves, demonstrating the effects of one of these peptides (IO4) on fibril formation. Figure 2 presents data for percentage aggregation of amylin when incubated in the presence of different concentrations of each peptide,

as determined by ThT fluorescence after 48 h incubation (corresponding to the level of the final plateau phase of fibril formation). Surprisingly, IO1 (H<sub>2</sub>N-RGRLANFLVHSSGR-CONH<sub>2</sub>), which spans the entire binding region of amylin, gave no significant inhibition. Lower concentrations (0.6 and 2 µM) of all of the peptides IO1–IO7 appeared to stimulate fibril formation, and no peptide inhibited aggregation to less than 50% of the non-treated control. The most convincing inhibition of amylin aggregation was obtained with IO4 and IO5, and particularly with IO5 (H<sub>2</sub>N-RGNFLVHGR-CONH<sub>2</sub>) which inhibited at all concentrations  $\geq 12.5$  µM, and so another inhibitor, IO8 (H<sub>2</sub>N-RGANFLVHGR-CONH<sub>2</sub>), was designed by combining the sequences of these two peptides. In order to protect IO8 from proteolysis, a retro-inverso version (RI-IO8, Ac-rGhvlfnaGr-CONH<sub>2</sub>) was also made, by reversing the peptide sequence and replacing the L-amino acids with D-amino acids. IO8 displayed pronounced inhibitory effects on amylin aggregation at all concentrations  $\geq 1$  µM (i.e. down to 1:25 molar ratio of inhibitor to amylin), with 100 µM IO8 decreasing ThT fluorescence to levels comparable with a buffer only control (figure 3*a*). In contrast, RI-IO8 showed no inhibitory effects on amylin aggregation, but appeared to enhance fibril formation at all concentrations  $\leq 50$  µM (figure 3*a*). In addition to retro-inversion, another method to improve the physicochemical properties of IO8 is through N-methylation, and so the next step was to carry out ThT assays with two different N-methylated peptides, N1-IO8 and N2-IO8. Both of these peptides displayed a clear and almost identical dose-dependent inhibition of amylin aggregation (figure 3*b*). Results for IO8 and related peptides from three independent experiments, each carried out in triplicate, are presented in electronic supplementary material, figure S2. Inhibitor IO8 was then compared with peptide 'NFGAILS' (H<sub>2</sub>N-RGNFGAILSGR-CONH<sub>2</sub>) which was derived from the amyloidogenic region of human amylin. NFGAILS enhanced amylin aggregation at all concentrations  $\geq 25$  µM. The effects of NMeG24 NMeI26 [51] and ANFLVH [52], which are inhibitors reported in the literature to reduce amylin fibril formation, were also assessed. ANFLVH did not dissolve in aqueous solution, and NMeG24 NMeI26 showed no inhibitory effects (figure 3*d*).

Figure 4 focusses on the early stages of amylin (25 µM) aggregation in the presence of varying concentrations (0.1–100 µM) of N1-IO8 (figure 4*a*) and N2-IO8 (figure 4*b*). It can be seen that increasing concentrations of these inhibitors were found to progressively reduce the steepness of the curve during the fibril growth phase, indicating a reduction in the rate of fibril growth. There was also a progressive decrease in the level of the final plateau phase, indicating a reduction in the amount of fibrils formed (it has been demonstrated previously that ThT fluorescence correlates linearly with amyloid fibril concentration [53]). The ThT curves, both in the absence and presence of inhibitors, showed virtually no 'lag' phase, and so any effects of the inhibitors on the initial nucleation steps are not clearly defined.

TEM was used to monitor the effects of IO8, RI-IO8, N1-IO8 and N2-IO8 peptides on amylin aggregation, with samples being negatively stained by 2% phosphotungstic acid (PTA). Amylin (at 25 µM) was incubated with 100, 50, 25, 5 and 0 µM (non-inhibited control) of each of these peptides. Figure 5*a* shows the typical dense meshwork of amyloid fibrils that was observed after 48 h incubation of amylin alone. With addition of 100, 50 or 25 µM of IO8

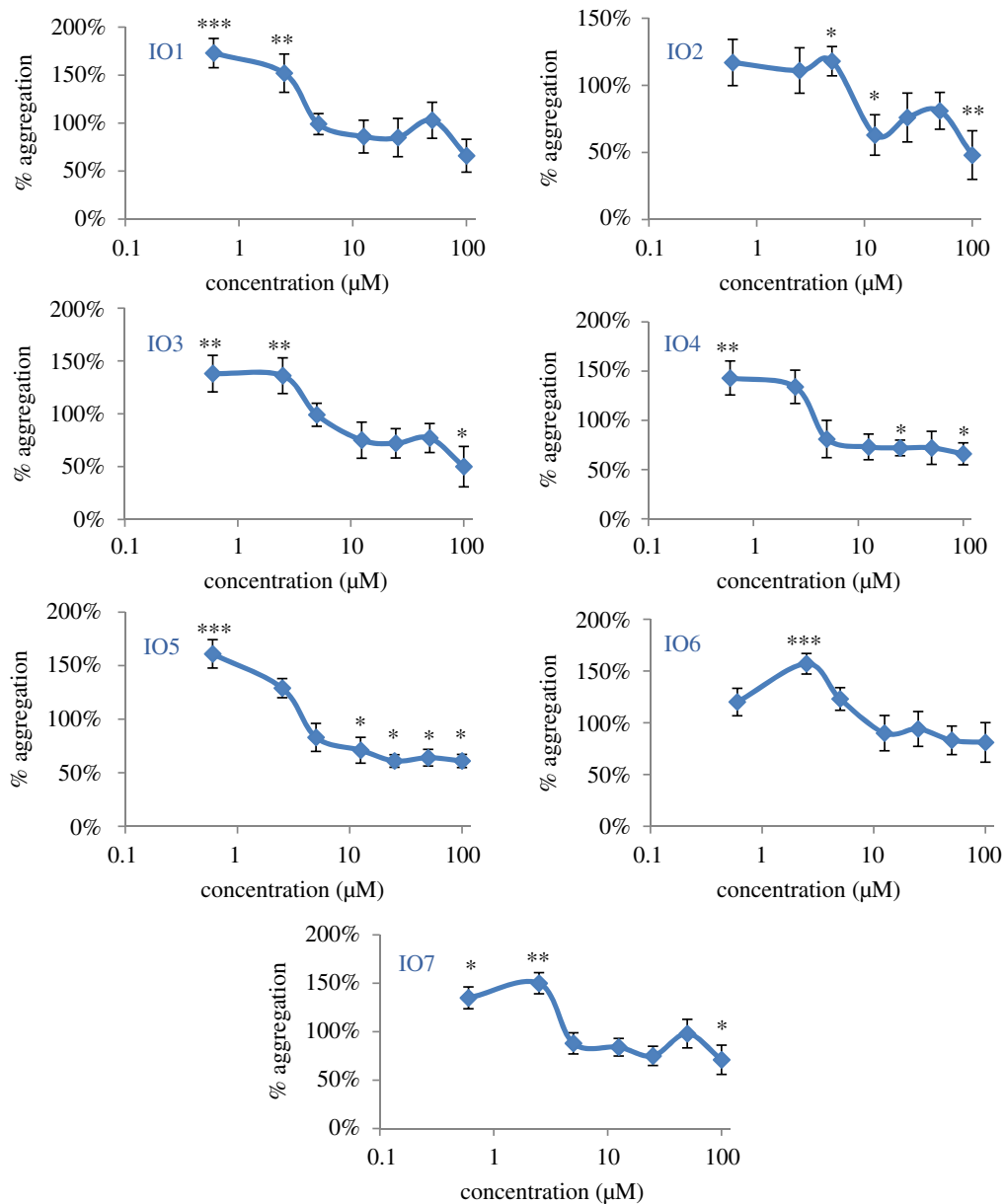


**Figure 2.** ThT data showing effects of IO1, IO2, IO3, IO4, IO5, IO6 and IO7 peptides on amylin aggregation, after 48 h incubation. All peptides were assayed at 0.6, 2.5, 5, 12.5, 25, 50 and 100  $\mu\text{M}$  concentrations in the presence of 25  $\mu\text{M}$  amylin. Results are means  $\pm$  s.e.m.,  $n = 3$ , for a single experiment. Student's  $t$ -test was used to establish significance at  $*p < 0.05$ ,  $**p < 0.01$ , or  $***p < 0.001$ , compared to 100% control (amylin alone). (Online version in colour.)

(i.e. 4 : 1, 2 : 1 and 1 : 1 molar ratios of IO8 to amylin), no fibrils were observed (illustrated for 25  $\mu\text{M}$  IO8 in figure 5*b*). At 5  $\mu\text{M}$  IO8 (1 : 5 molar ratio of IO8 to amylin) some fibrils were observed, but at a lower density than that seen in the amylin control. On addition of 100, 50, 25 or 5  $\mu\text{M}$  RI-IO8 to 25  $\mu\text{M}$  amylin, very dense fibrillar aggregates of amylin were observed (illustrated for 25  $\mu\text{M}$  RI-IO8 in figure 5*c*). In the presence of 100, 50 or 25  $\mu\text{M}$  of either N1-IO8 or N2-IO8, no fibrils were seen after 48 h incubation (illustrated for 25  $\mu\text{M}$  N1-IO8 and N2-IO8 in figure 5*d,e*). At 5  $\mu\text{M}$  of N1-IO8, a few fibrils were observed, but no fibrils were seen with 5  $\mu\text{M}$  of N2-IO8. None of the peptides tested showed any tendency to form oligomers or fibrils when incubated alone (figure 5*f-i*). These TEM results support the ThT data and confirm that IO8, N1-IO8 and N2-IO8 are effective inhibitors of amylin aggregation, whereas RI-IO8 has no inhibitory effect, and may even stimulate fibril formation.

The stability of the most promising inhibitory peptides (IO8, N1-IO8 and N2-IO8) towards individual proteolytic enzymes (see electronic supplementary material, figure S3), and in

human plasma, was assessed by RP-HPLC. The data are summarized in table 2, with examples of RP-HPLC traces of peptides in plasma presented in figure 6. IO8 was highly susceptible to the effects of trypsin and chymotrypsin, which rapidly degraded this peptide, but it was also degraded by cathepsin G, elastase, thrombin, kallikrein, plasmin, and factor X. Not surprisingly, therefore, IO8 was very unstable in human plasma (figure 6*A*). In contrast, both N1-IO8 and N2-IO8 were stable for up to 24 h incubation in plasma (figure 6*B,C*), and, unlike IO8, remained intact after 3 h incubation with each of the individual proteolytic enzymes, although some degradation was noted after 24 h incubation (table 2).

The toxic effect of human amylin (20 and 10  $\mu\text{M}$ ) on human pancreatic 1.4E7 cells was determined by MTS assay, in the presence and absence of 1 : 1 and 1 : 4 molar ratios (inhibitor:amylin) of the IO8, N1-IO8 and N2-IO8 peptides (for results see figure 7). Amylin at 20  $\mu\text{M}$  was cytotoxic to PANC-1 cells and consistently reduced cell viability to approximately 40% of untreated control cells, whereas at 10  $\mu\text{M}$  amylin the results were more variable and cell

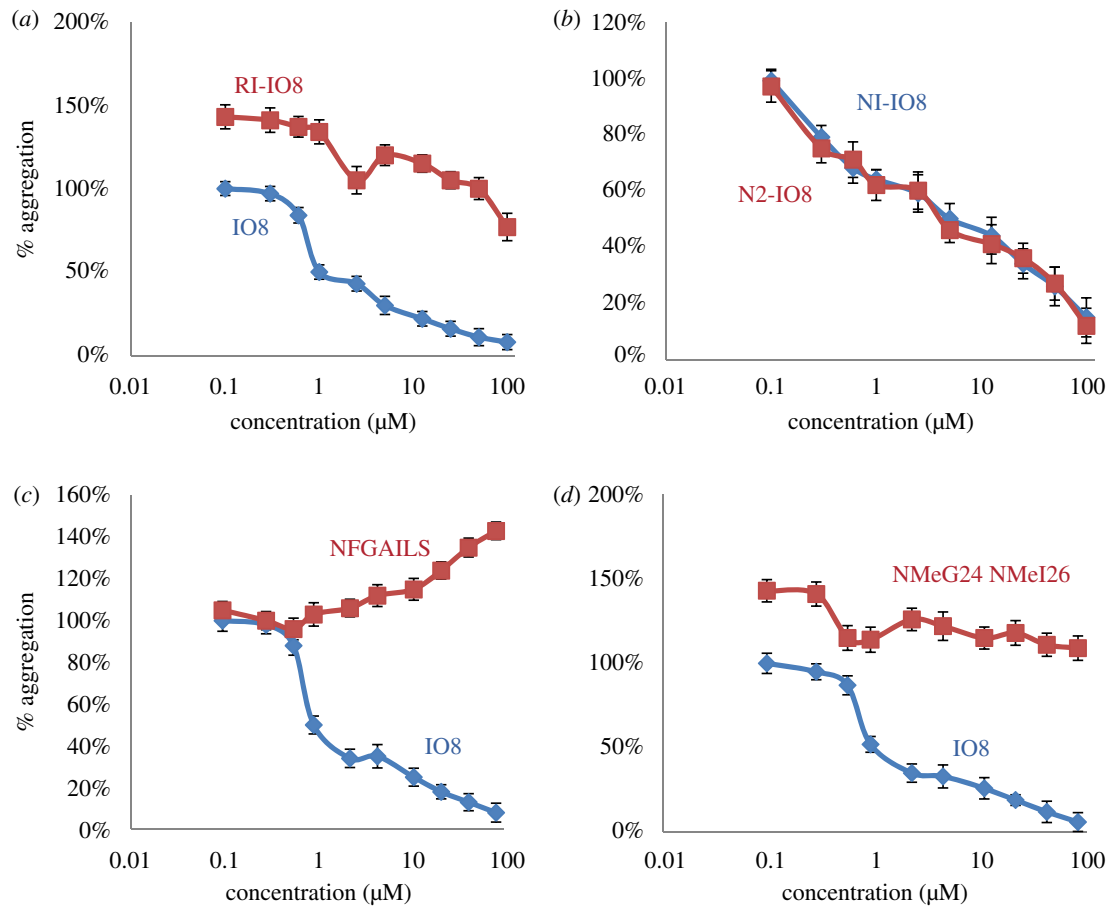


**Figure 3.** ThT data showing the effects of IO8 and related peptides, as well NFGAILS and NMeG24 NMeI26, on amylin aggregation, after 48 h incubation. (a) IO8 and RI-IO8. (b) N1-IO8 and N2-IO8. (c) NFGAILS ( $H_2N-RGNFGAILSGR-CONH_2$ ). (d) NMeG24 NMeI26. All peptides were assayed at 0.6, 2.5, 5, 12.5, 25, 50 and 100  $\mu\text{M}$  in the presence of 25  $\mu\text{M}$  amylin. Results show means  $\pm$  s.e.m.,  $n = 3$ , for a single experiment. See electronic supplementary material, figure S2 for the data from three independent experiments. Note the clear dose-dependent effects of the two N-methylated peptides (N1-IO8 and N2-IO8). (Online version in colour.)

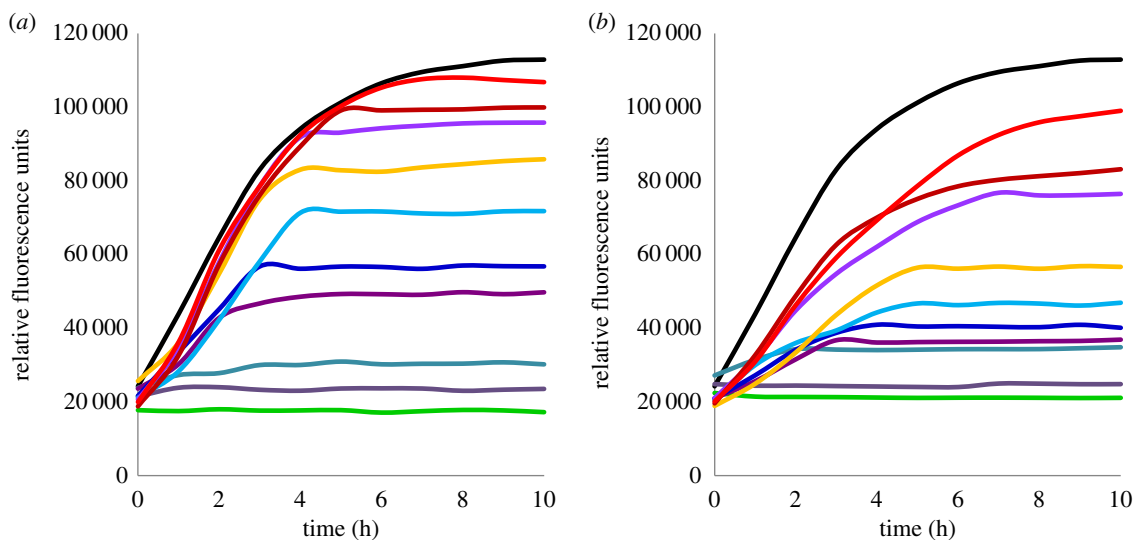


**Figure 4.** ThT fluorescence curves for the first 10 h of incubation of amylin in the presence of different concentrations of (a) N1-IO8 and (b) N2-IO8. Data are means for a single experiment carried out in triplicate, with readings taken every 10 min. Amylin alone (at 25  $\mu\text{M}$ ) displays a characteristic increase in fluorescence corresponding to the 'sigmoidal' and 'plateau' phases of amyloid fibril formation (top curve in both cases). In both (a) and (b), the stepwise decrease in the final level of ThT fluorescence in the 10 curves underneath is due to addition of the inhibitors at concentrations of 0.1, 0.3, 0.6, 1, 2.5, 5, 12.5, 25, 50 and 100  $\mu\text{M}$ .

viability was reduced to 60–90%. All of these inhibitor peptides, at both molar ratios, rescued the cells from the toxic effect of 20  $\mu\text{M}$  amylin and 10  $\mu\text{M}$  amylin. None of the inhibitors alone, at concentrations of up to 20  $\mu\text{M}$ , had any

effect on cell viability. Cell toxicity results for IO8 and related peptides from three independent experiments, each carried out with  $n = 6$  replicates, are presented in electronic supplementary material, figure S4.

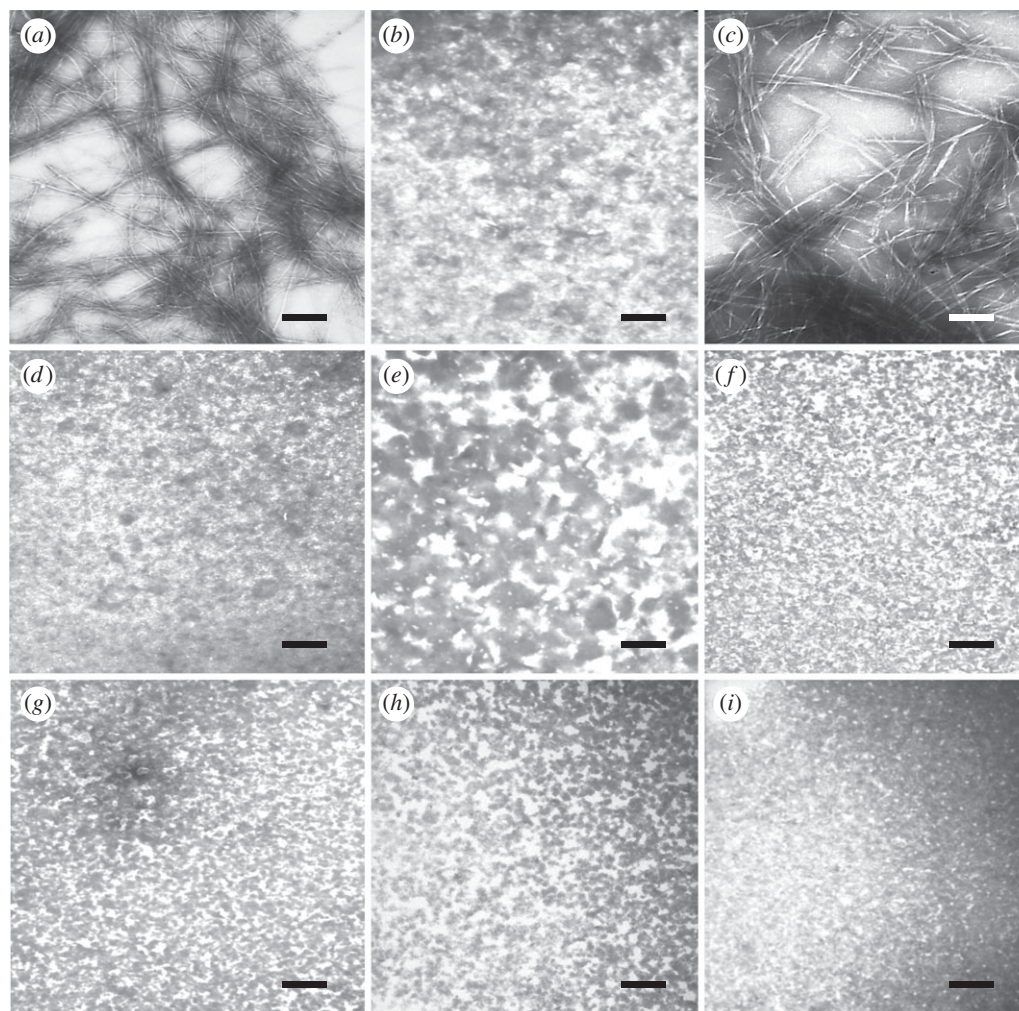


**Figure 5.** Negative stain EM images of amylin incubated in the presence and absence of inhibitors. (a) Sample of amylin (25  $\mu\text{M}$ ) incubated for 48 h in PBS at room temperature and stained with phosphotungstic acid (2% w/v). (b) Amylin (25  $\mu\text{M}$ ) + I08 (25  $\mu\text{M}$ ); (c) amylin (25  $\mu\text{M}$ ) + RI-I08 (25  $\mu\text{M}$ ); (d) amylin (25  $\mu\text{M}$ ) + N1-I08 (25  $\mu\text{M}$ ); (e) amylin (25  $\mu\text{M}$ ) + N2-I08 (25  $\mu\text{M}$ ); (f) I08 alone (100  $\mu\text{M}$ ); (g) RI-I08 alone (100  $\mu\text{M}$ ); (h) N1-I08 alone (100  $\mu\text{M}$ ); and (i) N2-I08 alone (100  $\mu\text{M}$ ). Scale bar, 100 nm.

**Table 2.** Stability of peptide-inhibitors to proteolysis.  $\checkmark$ , stable;  $\times$ , degraded, after 3 h incubation with the enzyme.

	I08	RI-I08	N1-I08	N2-I08
blood plasma	$\times$	$\checkmark$	$\checkmark$	$\checkmark$
trypsin	$\times$	$\checkmark$	$\checkmark^a$	$\checkmark^a$
chymotrypsin	$\times$	$\checkmark$	$\checkmark$	$\checkmark$
cathepsin G	$\times$	$\checkmark$	$\checkmark$	$\checkmark$
elastase	$\times$	$\checkmark$	$\checkmark$	$\checkmark$
thrombin	$\times$	$\checkmark$	$\checkmark^a$	$\checkmark$
kallikrein	$\times$	$\checkmark$	$\checkmark^a$	$\checkmark^a$
plasmin	$\times$	$\checkmark$	$\checkmark$	$\checkmark$
factor X	$\times$	$\checkmark$	$\checkmark$	$\checkmark$

<sup>a</sup>Some degradation seen after 24 h incubation. HPLC traces for I08, N1-I08 and N2-I08 are given in electronic supplementary material, figure S3.

## 4. Discussion

T2DM is the most widespread endocrine disorder [54], and is characterized by a reduction in  $\beta$ -cell mass, insulin resistance, and the presence of amyloid deposits in the pancreatic islets, the main component being amylin [55]. The 22–28

(NFGAILS) segment of amylin is regarded as the most highly amyloidogenic region of this peptide, and will itself assemble into amyloid fibrils [39,56]. However, residues 8–20 [57], 14–20 [58], and 30–37 [59] have also been reported to form  $\beta$ -sheet fibrils. Although several amyloidogenic regions of human amylin have been proposed, this study was concerned with developing peptide inhibitors from the ‘binding’ region of human amylin, corresponding to amino acid residues 11–20 (RLANFLVHSS), and on studying their impact on the fibrillogenesis of full-length human amylin. This region is thought to be involved in the initial interactions between two misfolded amylin molecules, after which they begin to aggregate [42]. Thus, preventing this interaction should impede aggregation. This strategy, to target the binding region, has been successfully applied to the development of inhibitors of A $\beta$  aggregation as a potential disease-modifying treatment for AD [47–50].

Seven potential inhibitor peptides were derived from this binding region, and investigated for their ability to influence amylin fibril formation, based on the ThT fluorescence assay [60]. Peptides IO2, IO3, IO4, IO5 and IO7 (table 1) showed some inhibitory effects, but IO4 and IO5 gave the most promising results, and were considered for further investigation. These two amino acid sequences were combined to give I08 (amino acid sequence: H<sub>2</sub>N-RGANFLVHGR-CONH<sub>2</sub>). Retro-inverso peptides often retain bioactivity and are stable to proteolysis [47,61], and so the retro-inverso version of I08 (RI-

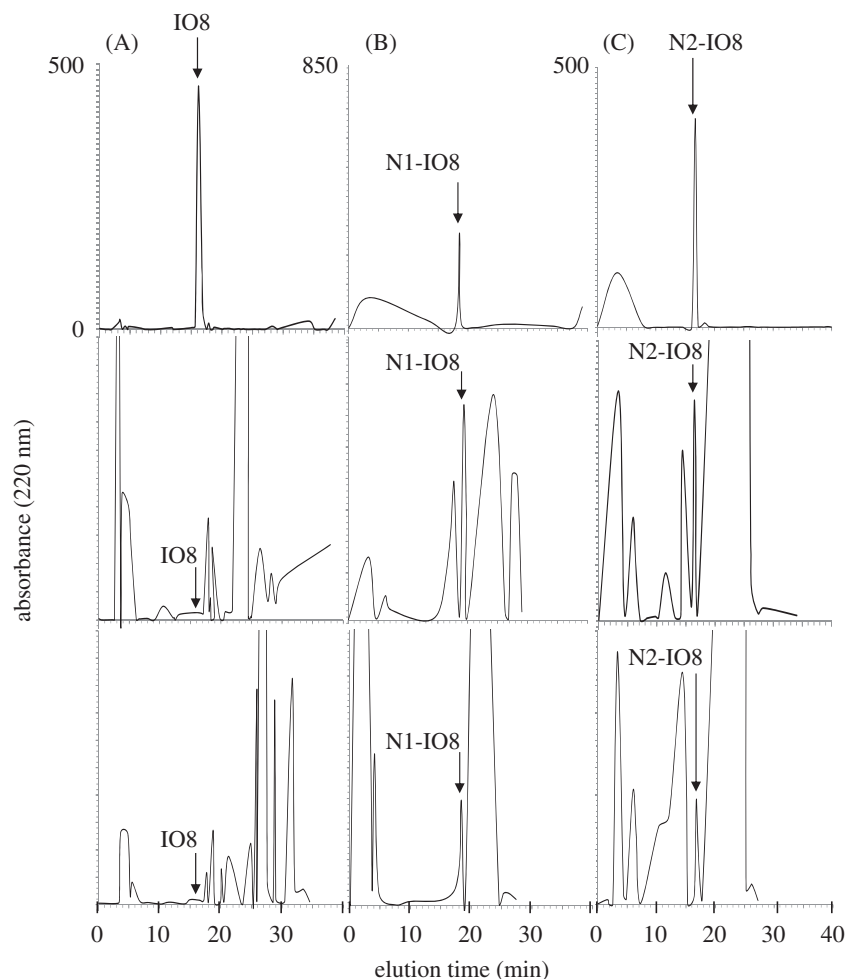


**Figure 6.** Reverse-phase HPLC traces showing stability of peptide inhibitors in human plasma. Column (A) IO8; column (B) N1-IO8; column (C) N2-IO8. For each column, the top trace shows elution of the peptide standard without plasma; the middle trace is for 0 h incubation in plasma; and the lower trace is after 48 h incubation in plasma. Note that IO8 is degraded, whereas N1-IO8 and N2-IO8 are more stable.

IO8: Ac-rGhvlfnGr-CONH<sub>2</sub>) was derived by sequence reversal and D-amino acid substitution. The IO8 peptide showed a strong inhibitory effect on amylin aggregation, and, unlike peptides IO1-IO7, did not stimulate amylin aggregation at low concentrations. However, RI-IO8 had no inhibitory effect on amylin aggregation, except at a 4:1 molar ratio RI-IO8 to amylin, where the peptide reduced amylin aggregation to only 77% of a non-inhibited control (figure 3). At lower concentrations, RI-IO8 actually stimulated amylin aggregation. This finding was unexpected and suggests that RI-IO8 does not interact in the same way as IO8 to full-length human amylin. Congo red binding experiments have also confirmed the inhibitory effect of IO8, and the stimulatory effect of RI-IO8, on amylin aggregation (data not shown). This finding was further supported by TEM studies, where IO8 abolished and RI-IO8 increased amylin fibril formation (figure 5). This result with RI-IO8 is contrary to a previous study, where the retro-inverso peptide RI-OR2, developed against  $\beta$ -amyloid (A $\beta$ ) aggregation, was shown to inhibit amyloid fibril formation, and also rescue cells from the toxic effects of A $\beta$ , as well as being highly resistant to proteolysis [47].

Since RI-IO8 did not inhibit amylin aggregation, N-methylation was considered as an alternative means to improve its stability and pharmacokinetic properties. It is not surprising that IO8 was rapidly degraded in plasma, and in the presence of proteolytic enzymes, because L-peptides are quickly metabolized in this way [62]. IO8 would be cleaved after amino acid 5 (Phe) by high specificity chymotrypsin, and after amino

acids 5, 6 and 8 (Phe, Leu, His) by low specificity chymotrypsin, while trypsin will cleave after position 1 (Arg). N-methylation has been shown to improve the pharmacokinetic properties of peptides, by protecting them from proteolysis [63]. Also, N-methylation of alternate amino acid residues gives one face of the peptide molecule that is not available for H-bonding, which impedes amyloid fibril formation [64]. N-methylated derivatives of A $\beta$ (25–35) have been reported to impede the aggregation of fibrils and prevent A $\beta$  cytotoxicity, and N-methylated analogues of amylin do not form fibrils [18,65]. Here, IO8 was stabilized against proteolytic degradation through N-methylation of alternate amino acid residues, to give N1-IO8 (H<sub>2</sub>N-R-G-Am-N-Fm-L-Vm-H-G-R-CONH<sub>2</sub>) and N2-IO8 (H<sub>2</sub>N-R-G-A-Nm-F-Lm-V-Hm-G-R-CONH<sub>2</sub>). ThT and TEM data showed that both NI-IO8 and N2-IO8 are excellent and highly convincing inhibitors of amylin aggregation (figures 3–5) and are relatively stable against proteolytic degradation (figure 6).

New inhibitors of amylin aggregation are desired, as many of the reported inhibitors only work when present in molar excess over amylin [65–67]. For example, a study on peptide fragments corresponding to human amylin residues 20–25 (SNNFGA) and 24–29 (GAILSS) showed an inhibitory effect on  $\beta$ -sheet transition and amyloid aggregation at 10:1 and 20:1 molar ratios of peptide to amylin, and the GAILSS peptide had no significant effect on amylin-induced cytotoxicity [41]. The inadequacy of some previously published inhibitors is also highlighted by the comparison of the effects of IO8, ANFLVH [52] and NMeG24 NMeI26 [51] on amylin

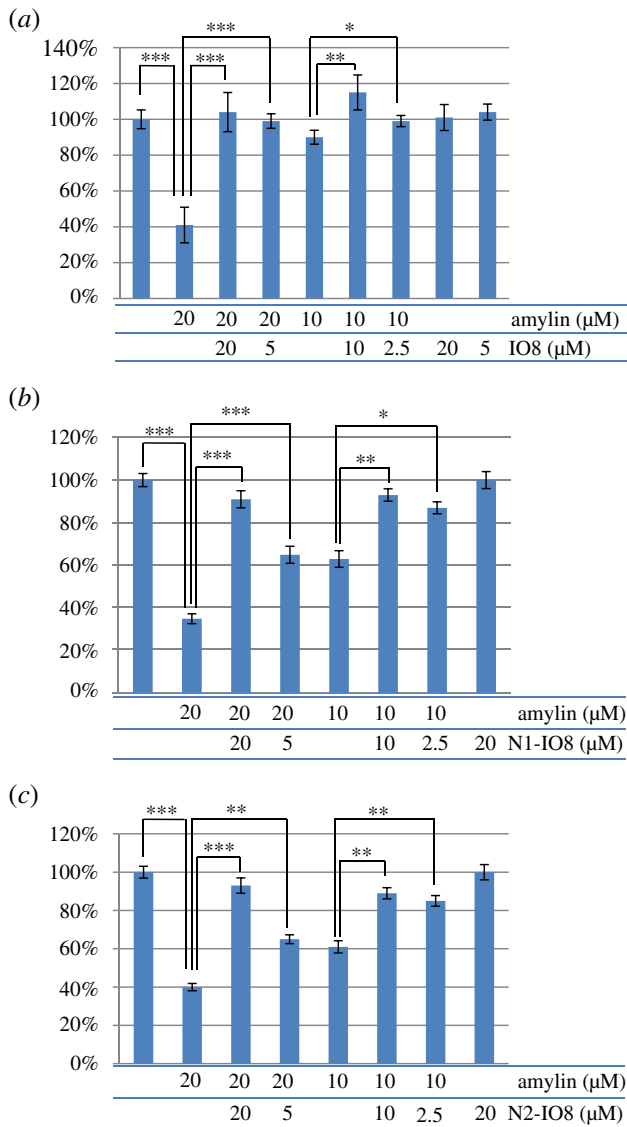


**Figure 7.** Cytotoxic effect of amylin on human pancreatic 1.4E7 insulin-secreting cells in the presence or absence of inhibitor peptides. (a) Cells were incubated for 24 h with 20 μM or 10 μM human amylin in RPMI-1640 medium, with or without IO8 inhibitor, and viability was measured using the MTS assay. (b) Results for N1-IO8. (c) Results for N2-IO8. In all cases, results show mean ± s.e.m.,  $n = 6$ . ANOVA followed by Student's  $t$ -test established significance at \* $p < 0.05$ , \*\* $p < 0.01$ , \*\*\* $p < 0.001$ . (Online version in colour.)

aggregation in this report. ANFLVH has the same amino acid sequence as IO8, but without the flanking cationic arginine residues together with their glycine spacers. Although ANFLVH was reported to inhibit amylin fibril formation *in vitro* and to protect against amylin cytotoxicity, the latter effect was only observed at 10-fold and 20-fold molar excess concentrations of the peptide [52]. In contrast, the IO8 peptide inhibits amylin aggregation at much lower concentrations than this, and, given the inability to dissolve ANFLVH in aqueous solution, is clearly much more soluble. Moreover, IO8, N1-IO8 and N2-IO8 were seen to rescue human pancreatic 1.4E7 cells

from the toxic effects of amylin at a 1 : 4 molar ratio of these peptides to amylin. In contrast to a previous report [51], no evidence of inhibition of aggregation was observed upon addition of NMeG24 NMeI26, at reasonable concentrations, to amylin. In fact, NMeG24 NMeI26 was seen to promote fibril formation (figure 3). This discrepancy could be due to the fact that NMeG24 NMeI26 was reported to inhibit IAPP aggregation when added before nucleation [68] but the aggregation system reported here lacks any lag-phase (figure 4), and so nucleation may be too rapid for this inhibitor to be effective. Two human amylin-derived peptides, with sequences NFGAIL and SNNFGAILSS, were unable to inhibit fibrillation of human amylin [69]. Another study has indicated that NFGAIL causes an immediate shift of amylin to the  $\beta$ -sheet conformation, suggesting that this peptide promotes fibril formation [41]. These results, together with the lack of effect of the H<sub>2</sub>N-RGNFGAILSGR-CONH<sub>2</sub> peptide in this study (figure 3), justify the decision to focus on the RLANFLVHSS (residues 11–20) amylin binding region.

As noted above, modified full-length amylin with N-methylation at positions 24 and 26 has been shown to impede amylin aggregation and its associated cytotoxicity [65]. In addition, a human amylin derived peptide marketed as pramlintide, with proline substitutions at positions 25, 28 and 29, has undergone clinical trials [70–73] where it was administered, alongside insulin, for management of T2DM. This combination of drugs was able to maintain near-normal glycaemic levels, but pramlintide peptide does not appear to have been assessed as an inhibitor of human amylin aggregation. The short peptides described in this report would be much easier and less expensive to synthesize than these full-length human amylin analogues, and would, potentially, be less immunogenic. N1-IO8 and N2-IO8 in particular appear to be potent and stable aggregation inhibitors that are suitable for further development and testing in human amylin transgenic rodent models as potential disease-modifying agents for T2DM. However, the effects of these inhibitors on oligomer formation are not clear from the data presented here, and will need to be examined in further studies. Also, it is emerging that a significant component of amylin toxicity is mediated by inflammation [74], and so the ability of these inhibitors to attenuate amylin-mediated macrophage activation and associated  $\beta$ -cell dysfunction will also need to be determined.

**Data accessibility.** This article has no additional data.

**Authors' contributions.** D.A. conceived of the study and wrote the manuscript. I.O. carried out all of the experiments, data collection and statistical analyses. M.T. designed some of the peptides and N.J.F. was responsible for the electron microscopy. All authors contributed to design of the study and gave final approval for publication.

**Competing interests.** We declare we have no competing interests.

**Funding.** This work was partially supported by a scholarship to I.O. from the Faculty of Health and Medicine, Lancaster University.

**Acknowledgements.** D.A. wishes to thank Professor Ian Hamley and the other conference organizers for his invitation to this very interesting and stimulating meeting. The authors also thank the editor and anonymous reviewers for their helpful comments and suggestions, and Dr Fuyuki Kametani (Tokyo, Japan) for peptide HPLC-MS analysis.

## References

1. Dobson CM. 1999 Protein misfolding, evolution and disease. *Trends Biochem. Sci.* **24**, 329–332. (doi:10.1016/S0968-0004(99)01445-0)
2. Rochet JC, Lansbury PT. 2000 Amyloid fibrillogenesis: themes and variations. *Curr. Opin. Struct. Biol.* **10**, 60–68. (doi:10.1016/S0959-440X(99)00049-4)
3. Westermark P *et al.* 2007 A primer of amyloid nomenclature. *Amyloid* **14**, 179–183. (doi:10.1080/13506120701460923)

4. Westermark P. 2005 Aspects on human amyloid forms and their fibril polypeptides. *FEBS Lett.* **272**, 5942–5949. (doi:10.1111/j.1742-4658.2005.05024.x)
5. Pepys MB. 2006 Amyloidosis. *Annu. Rev. Med.* **57**, 223–241. (doi:10.1146/annurev.med.57.121304.131243)
6. Allsop D, Mayes J. 2014 Amyloid- $\beta$  protein and Alzheimer's disease. *Essays Biochem.* **56**, 99–110. (doi:10.1042/bse0560099)
7. Soto C, Estrada LD. 2008 Protein misfolding and neurodegeneration. *Arch. Neurol.* **65**, 184–189. (doi:10.1001/archneurol.2007.56)
8. Ahmad E, Ahmad A, Singh S, Arshad M, Khan AH, Khan RH. 2011 A mechanistic approach for islet amyloid polypeptide aggregation to develop anti-amyloidogenic agents for type-2 diabetes. *Biochimie* **93**, 793–805. (doi:10.1016/j.biochi.2010.12.012)
9. Kapurniotu A. 2001 Amyloidogenicity and cytotoxicity of islet amyloid polypeptide. *Biopolymers* **60**, 438–459. (doi:10.1002/1097-0282(2001)60:6<438::AID-BIP10182>3.0.CO;2-A)
10. Westermark P. 2011 Amyloid in the islets of Langerhans: thoughts and some historical aspects. *Upsala J. Med. Sci.* **116**, 81–89. (doi:10.3109/03009734.2011.573884)
11. Wimalawansa SJ. 1997 Amylin, calcitonin gene-related peptide, calcitonin, and adrenomedullin: a peptide superfamily. *Crit. Rev. Neurobiol.* **11**, 167–239. (doi:10.1615/CritRevNeurobiol.v11.i2-3.40)
12. Kahn SE. 2003 The relative contributions of insulin resistance and  $\beta$ -cell dysfunction to the pathophysiology of type 2 diabetes. *Diabetologia* **46**, 3–19. (doi:10.1007/s00125-002-1009-0)
13. Zraika S *et al.* 2010 Toxic oligomers and islet  $\beta$  cell death: guilty by association or convicted by circumstantial evidence? *Diabetologia* **53**, 1046–1056. (doi:10.1007/s00125-010-1671-6)
14. Hull RL, Westermark GT, Westermark P, Kahn SE. 2004 Islet amyloid: a critical entity in the pathogenesis of type 2 diabetes. *J. Clin. Endocrinol. Metab.* **89**, 3629–3643. (doi:10.1210/jc.2004-0405)
15. Hiddinga HJ, Eberhardt NL. 1999 Intracellular amyloidogenesis by human islet amyloid polypeptide induces apoptosis in COS-1 cells. *Am. J. Pathol.* **154**, 1077–1088. (doi:10.1016/S0002-9440(10)65360-6)
16. Kapurniotu A, Bernhagen J, Greenfield N, Al-Abed Y, Teichberg S, Frank RW, Voelter W, Bucala R. 1998 Contribution of advanced glycosylation to the amyloidogenicity of islet and amyloid polypeptide. *Eur. J. Biochem.* **251**, 208–216. (doi:10.1046/j.1432-1327.1998.2510208.x)
17. Lorenzo A, Yankner BA. 1996 Amyloid fibril toxicity in Alzheimer's disease and diabetes. *Ann. NY Acad. Sci.* **777**, 89–95. (doi:10.1111/j.1749-6632.1996.tb34406.x)
18. Yan LM, Velkova A, Tarek-Nossol M, Andreetto E, Kapurniotu A. 2007 Amylin mimic blocks A $\beta$  cytotoxic self-assembly: cross-suppression of amyloid toxicity of A $\beta$  and amylin suggests a molecular link between Alzheimer's disease and type II diabetes. *Angew. Chem. Int. Ed.* **46**, 1246–1252. (doi:10.1002/anie.200604056)
19. Kodali R, Wetzel R. 2007 Polymorphism in the intermediates and products of amyloid assembly. *Curr. Opin. Struct. Biol.* **17**, 48–57. (doi:10.1016/j.sbi.2007.01.007)
20. Aitken JF *et al.* 2010 Tetracycline treatment retards the onset and slows the progression of diabetes in human amylin/islet amyloid polypeptide transgenic mice. *Diabetes* **59**, 161–171. (doi:10.2337/db09-0548)
21. Ritzel RA, Meier JJ, Lin C-Y, Veldhuis JD, Butler PC. 2007 Human islet amyloid polypeptide oligomers disrupt cell coupling, induce apoptosis, and impair insulin secretion in isolated human islets. *Diabetes* **56**, 65–71. (doi:10.2337/db06-0734)
22. Diabetes UK. 2015 *Key statistics on diabetes*. <http://www.diabetes.org.uk> (accessed 17 August 2015).
23. WHO. 2016 World Health Organisation. *Diabetes*. <http://www.who.int/diabetes/en/> (accessed 12 January 2016).
24. Colhoun HM *et al.* 2004 Primary prevention of cardiovascular disease with atorvastatin in type 2 diabetes in the collaborative atorvastatin diabetes study (CARDS): multicentre randomised placebo-controlled trial. *Lancet* **364**, 685–696. (doi:10.1016/S0140-6736(04)16895-5)
25. Morrish NJ, Wang SL, Stevens LK, Fuller JH, Keen H. 2001 Mortality and causes of death in the WHO multinational study of vascular disease in diabetes. *Diabetologia* **44**, S14–S21. (doi:10.1007/PL00002934)
26. Castello MA, Jeppson JD, Soriano S. 2014 Moving beyond anti-amyloid therapy for the prevention and treatment of Alzheimer's disease. *BMC Neurol.* **14**, 311. (doi:10.1186/s12883-014-0169-0)
27. Rosenblum WL. 2014 Why Alzheimer trials fail: removing soluble oligomeric  $\beta$  amyloid is essential, inconsistent, and difficult. *Neurobiol. Ageing* **35**, 969–974. (doi:10.1016/j.neurobiolaging.2013.10.085)
28. Whitty A, Kumaravel G. 2006 Between a rock and a hard place. *Nat. Chem. Biol.* **2**, 112–118. (doi:10.1038/nchembio0306-112)
29. Hajduk PJ, Burns DJ. 2002 Integration of NMR and high-throughput screening. *Comb. Chem. High Throughput Screen.* **5**, 613–621. (doi:10.2174/1386207023329996)
30. Keskin O, Gursoy A, Ma B, Nussinov R. 2008 Principles of protein–protein interactions: what are the preferred ways for proteins to interact? *Chem. Rev.* **108**, 1225–1244. (doi:10.1021/cr040409x)
31. Teichmann SA. 2002 Principles of protein–protein interactions. *Bioinformatics* **18**, S249. (doi:10.1093/bioinformatics/18.suppl\_2.S249)
32. Smith RD, Hu L, Falkner JA, Benson ML, Nerothn JP, Carlson HA. 2006 Exploring protein–ligand recognition with Binding MOAD. *J. Mol. Graph. Model.* **24**, 414–425. (doi:10.1016/j.jmkgm.2005.08.002)
33. Cheng AC, Coleman RG, Smyth KT, Cao Q, Soulard P, Caffrey DR, Salzberg AC, Huang ES. 2007 Structure-based maximal affinity model predicts small-molecule druggability. *Nat. Biotechnol.* **25**, 71–75. (doi:10.1038/nbt1273)
34. Wells JA, McClendon CL. 2007 Reaching for high-hanging fruit in drug discovery at protein–protein interfaces. *Nature* **450**, 1001–1009. (doi:10.1038/nature06526)
35. Goldsbury C, Goldie K, Pellaud J, Seelig J, Frey P, Müller SA, Kistler J, Cooper GJS, Aebi U. 2000 Amyloid fibril formation from full-length and fragments of amylin. *J. Struct. Biol.* **130**, 352–362. (doi:10.1006/jsbi.2000.4268)
36. Tenidis K *et al.* 2000 Identification of a penta- and hexapeptide of islet amyloid polypeptide (amylin) and with amyloidogenic and cytotoxic properties. *J. Mol. Biol.* **295**, 1055–1071. (doi:10.1006/jmbi.1999.3422)
37. Elgersma RC, Meijneke T, Posthuma G, Rijkers DTS, Liskamp RMJ. 2006 Self-assembly of amylin (20–29) amide-bond derivatives into helical ribbons and peptide nanotubes rather than fibrils. *Chemistry* **12**, 3714–3725. (doi:10.1002/chem.200501374)
38. Soto C, Kindy MS, Baumann M, Frangione B. 1996 Inhibition of Alzheimer's amyloidosis by peptides that prevent  $\beta$ -sheet conformation. *Biochem. Biophys. Res. Commun.* **226**, 672–680. (doi:10.1006/bbrc.1996.1413)
39. Westermark P, Engstrom U, Johnson KH, Westermark GT, Betsholtz C. 1990 Islet amyloid polypeptide—pinpointing amino-acid residues linked to amyloid fibril formation. *Proc. Natl Acad. Sci. USA* **87**, 5036–5040. (doi:10.1073/pnas.87.13.5036)
40. Abedini A, Meng FL, Raleigh, DP. 2007 A single-point mutation converts the highly amyloidogenic human islet amyloid polypeptide into a potent fibrillization inhibitor. *J. Am. Chem. Soc.* **129**, 11 300–11 301. (doi:10.1021/ja072157y)
41. Scrocchi LA, Chen Y, Waschuk S, Wang F, Cheung S, Darabie AA, McLaurin J, Fraser PE. 2002 Design of peptide-based Inhibitors of human islet amyloid polypeptide fibrillogenesis. *J. Mol. Biol.* **318**, 697–706. (doi:10.1016/S0022-2836(02)00164-X)
42. Mazor Y, Gilead S, Benhar I, Gazit E. 2002 Identification and characterization of a novel molecular-recognition and self-assembly domain within the islet amyloid polypeptide. *J. Mol. Biol.* **322**, 1013–1024. (doi:10.1016/S0022-2836(02)00887-2)
43. Nie Q, Du X, Geng M. 2011 Small molecule inhibitors of amyloid  $\beta$  peptide aggregation as a potential therapeutic strategy for Alzheimer's disease. *Acta Pharmacol. Sin.* **32**, 545–551. (doi:10.1038/aps.2011.14)
44. Aitken JF, Loomes KM, Konarkowska B, Cooper GJ. 2003. Suppression by polycyclic compounds of the conversion of human amylin into insoluble amyloid. *Biochem. J.* **374**, 779–784. (doi:10.1042/bj20030422)
45. Ono K, Yoshiike Y, Takashima A, Hasegawa K, Naiki H, Yamada M. 2003 Potent anti-amyloidogenic and fibril-destabilizing effects of polyphenols *in vitro*:

- implications for the prevention and therapeutics of Alzheimer's disease. *J. Neurochem.* **87**, 172–181. (doi:10.1046/j.1471-4159.2003.01976.x)
46. Austen BM, Paleologou KE, Ali SAE, Qureshi MM, Allsop D, El-Agnaf OMA. 2008 Designing peptide inhibitors for oligomerization and toxicity of Alzheimer's  $\beta$ -amyloid peptide. *Biochemistry* **47**, 1984–1992. (doi:10.1021/bi701415b)
  47. Taylor M, Moore S, Mayes J, Parkin E, Beeg M, Canovi M, Gobbi M, Mann DMA, Allsop D. 2010 Development of a proteolytically stable retro-inverso peptide inhibitor of  $\beta$ -amyloid oligomerization as a potential novel treatment for Alzheimer's disease. *Biochemistry* **49**, 3261–3272. (doi:10.1021/bi100144m)
  48. Parthasarathy V *et al.* 2013 A novel retro-inverso peptide inhibitor reduces amyloid deposition, oxidation and inflammation and stimulates neurogenesis in the APPSWE/PS1 $\Delta$ E9 mouse model of Alzheimer's disease. *PLoS ONE* **8**, e54769. (doi:10.1371/journal.pone.0054769)
  49. Gregori M *et al.* 2016 Retro-inverso peptide inhibitor nanoparticles as potent inhibitors of aggregation of the Alzheimer's A $\beta$  peptide. *Nanomedicine* **13**, 723–732. (doi:10.1016/j.nano.2016.10.006)
  50. Sherer M, Fullwood NJ, Taylor M, Allsop D. 2015 A preliminary electron microscopic investigation into the interaction between A $\beta$ 1–42 peptide and a novel nanoliposome-coupled retro-inverso peptide inhibitor, developed as a potential treatment for Alzheimer's disease. *J. Phys. Conf. Ser.* **644**, 012040. (doi:10.1088/1742-6596/644/1/012040)
  51. Sellin D, Yan L, Kapurniotu A, Winter R. 2010 Suppression of amylin fibrillation at anionic lipid membranes via amylin-derived amyloid inhibitors and insulin. *Biophys. Chem.* **150**, 73–79. (doi:10.1016/j.bpc.2010.01.006)
  52. Potter KJ, Scrocchi LA, Warnock GL, Ao Z, Younker MA, Rosenberg L, Lipsett M, Verchere CB, Fraser PE. 2009 Amyloid inhibitors enhance survival of cultured human islets. *Biochim. Biophys. Acta* **1790**, 566–574. (doi:10.1016/j.bbagen.2009.02.013)
  53. Xue C, Lin TY, Chang D, Guo Z. 2017 Thioflavin T as an amyloid dye: fibril quantification, optimal concentration and effect on aggregation. *R. Soc. open sci.* **4**, 160696. (doi:10.1098/rsos.160696)
  54. Hossain P, Kavar B, Nahas ME. 2007 Obesity and diabetes in the developing world—a growing challenge. *N. Engl. J. Med.* **356**, 213–235. (doi:10.1056/NEJMp068177)
  55. Westermark P, Wernstedt C, Wilander E, Hayden DW, O'Brien TD, Johnson KH. 1987 Amyloid fibrils in human insulinoma and islets of Langerhans of the diabetic cat are derived from a neuropeptide-like protein also present in normal islet cells. *Proc. Natl Acad. Sci. USA* **84**, 3881–3885. (doi:10.1073/pnas.84.11.3881)
  56. Moriarty DF, Raleigh DP. 1999 Effects of sequential proline substitutions on amyloid formation by human amylin 20–29. *Biochemistry* **38**, 1811–1818. (doi:10.1021/bi981658g)
  57. Jaikaran ET, Higham CE, Serpell LC, Zurdo J, Gross M, Clark A, Fraser PE. 2001 Identification of a novel human islet amyloid polypeptide  $\beta$ -sheet domain and factors influencing fibrillogenesis. *J. Mol. Biol.* **308**, 515–525. (doi:10.1006/jmbi.2001.4593)
  58. Sawaya MR *et al.* 2007 Atomic structures of amyloid cross- $\beta$  spines reveal varied steric zippers. *Nature* **447**, 453–457. (doi:10.1038/nature05695)
  59. Nilsson MR, Raleigh DP. 1999 Analysis of amylin cleavage products provides new insights into the amyloidogenic region of human amylin. *J. Mol. Biol.* **294**, 1375–1385. (doi:10.1006/jmbi.1999.3286)
  60. Biancalana M, Koide S. 2010 Molecular mechanism of thioflavin-T binding to amyloid fibrils. *Biochem. Biophys. Acta* **1804**, 1405–1412. (doi:10.1016/j.bbapap.2010.04.001)
  61. Chen X, Fan Z, Chen Y, Fang X, Sha X, Barchi JJ. 2013 Retro-inverso carbohydrate mimetic peptides with annexin1-binding selectivity, are stable *in vivo*, and target tumor vasculature. *PLoS ONE* **8**, e80390. (doi:10.1371/journal.pone.0080390)
  62. Kellock J, Hopping G, Caughet B, Daggetti V. 2016 Peptides composed of alternating L- and D-amino acids inhibit amyloidogenesis in three distinct amyloid systems independent of sequence. *J. Mol. Biol.* **428**, 2317–2328. (doi:10.1016/j.jmb.2016.03.013)
  63. Chatterjee J, Rechenmacher F, Kessler H. 2013 N-methylation of peptides and proteins: an important element for modulating biological functions. *Angew. Chem. Int. Ed.* **52**, 254–269. (doi:10.1002/anie.201205674)
  64. Hughes E, Burke RM, Doig AJ. 2000 Inhibition of toxicity in the  $\beta$ -amyloid peptide fragment  $\beta$ -(25–35) using N-methylated derivatives: a general strategy to prevent amyloid formation. *J. Biol. Chem.* **275**, 25 109–25 115. (doi:10.1074/jbc.M003554200)
  65. Yan L, Tarek-Nossol M, Velkova A, Kazantzis A, Kapurniotu A. 2006 Design of a mimic of nonamyloidogenic and bioactive human islet amyloid polypeptide (amylin) as nanomolar affinity inhibitor of amylin cytotoxic fibrillogenesis. *Proc. Natl Acad. Sci. USA* **103**, 2046–2051. (doi:10.1073/pnas.0507471103)
  66. Meng F, Abedini A, Plesner A, Middleton CT, Potter KJ, Zanni MT, Verchere CB, Raleigh DP. 2010 The sulfated triphenyl methane derivative acid fuchsin is a potent inhibitor of amyloid formation by human islet amyloid polypeptide and protects against the toxic effects of amyloid formation. *J. Mol. Biol.* **400**, 555–566. (doi:10.1016/j.jmb.2010.05.001)
  67. Saraogi I, Hebda JA, Becerril J, Estroff LA, Miranker AD, Hamilton AD. 2010 Synthetic  $\alpha$ -helix mimetics as agonists and antagonists of islet amyloid polypeptide aggregation. *Angew. Chem. Int. Ed.* **49**, 736–739. (doi:10.1002/anie.200901694)
  68. Tarek-Nossol M, Yan L-M, Schmauder A, Tenidis K, Westermark G, Kapurniotu A. 2005 Inhibition of hIAPP amyloid-fibril formation and apoptotic cell death by a designed hIAPP amyloid-core-containing hexapeptide. *Chem. Biol.* **12**, 797–809. (doi:10.1016/j.chembiol.2005.05.010)
  69. Andreasen M *et al.* 2012 Modulation of fibrillation of amylin core fragments by chemical modification of the peptide backbone. *Biochim. Biophys. Acta* **1824**, 274–285. (doi:10.1016/j.bbapap.2011.10.014)
  70. Pullman J, Darsow T, Frias JP. 2006 Pramlintide in the management of insulin-using patients with type 2 and type 1 diabetes. *Vasc. Health Risk Manag.* **2**, 203–212. (doi:10.2147/vhrm.2006.2.3.203)
  71. Kong MF *et al.* 1998 The effect of single doses of pramlintide on gastric emptying of two meals in men with IDDM. *Diabetologia* **41**, 577–583. (doi:10.1007/s001250050949)
  72. Maggs DG *et al.* 2004 Pramlintide reduces postprandial glucose excursions when added to insulin lispro in subjects with type 2 diabetes: a dose-timing study. *Diabetes Metab. Res. Rev.* **20**, 55–60. (doi:10.1002/dmrr.419)
  73. Thompson RG, Pearson L, Schoenfeld SL, Kolterman OG. 1998 Pramlintide, a synthetic analog of human amylin, improves the metabolic profile of patients with type 2 diabetes using insulin. The Pramlintide in type 2 Diabetes Group. *Diabetes Care* **21**, 987–993. (doi:10.2337/diacare.21.6.987)
  74. Westwell-Roper CY, Ehses JA, Verchere CB. 2014 Resident macrophages mediate islet amyloid polypeptide-induced islet IL-1 $\beta$  production and  $\beta$ -cell dysfunction. *Diabetes* **63**, 1698–1711. (doi:10.2337/db13-0863)

## APPENDIX F

### List of trainings/courses attended with dates

<b>Course/Training/Seminar</b>	<b>Date</b>
Seminar-Using cellular electron tomography and serial block-face scanning electron microscopy to reconstruct 3-dimensional cellular architecture	6/2/2013
Writing grant proposals & getting funding	4/3/2013
Maximising the impact of your work	11/3/2013
Seminar-Personalizing biomedicine-from care to capital	12/3/2013
International students writing group 6	13/3/2013
Seminar- Multiple roles for the pattern recognition receptor NOD 2 in the gut and skin	20/3/2013
Faculty of Health & Medicine poster presentation	26/3/2013
Manchester Life Science PhD Conference	10/05/2013
Designing early phase clinical trials	10/6/2013 11/6/2013
Career in medical communications by Knowledge Point 360 group	18/6/2013
Ageing Research Conference	27/9/2013
Support learning programme (SLP) -intensive route	30/9/2013 1/10/2013 3/10/2013
Support learning programme (SLP) - HEA course	10/2013- 01/2014
Talk on moodle	21/10/2013
Endnote workshop	23/10/2013
Seminar- Advancing Schizophrenia drug discovery: optimizing preclinical models to bridge the translational gap	30/10/2013
SLP intensive tutorial	13/11/2013
Introduction to Statistics (SPSS1)	14/11/2013 15/11/2013

Postgraduate Research Conference	22/03/2014
Research Council UK EPQ training	02/04/2016 08/04/2016
Introduction to intellectual property	30/09/14
Training for demonstrators	30/09/14
Seminar- Shedding new light on the cellular response to ultraviolet radiation	15/10/14
PG board training	28/10/14
Introductory Workshop: Inspiring the Next Generation of Researchers	10/11/14
Writing scientific papers	10/11/14
Ethics Seminar	18/11/14
Excel workshop	19/11/14
Seminar: Compartmentalised MAPK signalling in mammalian cells	25/2/2015
Seminar: Peptide-inhibitor nanoparticles (PINPs) as a new treatment for progression of Alzheimer's disease	11/03/2015
PhD Seminars	27/05/2015 03/06/2015 10/06/2015 17/06/2015 24/06/2015
Seminar: Peptide conjugates: From self-assembly towards applications in biomedicine	4/11/15

Transmission Electron Microscopy training	04/2016- 07/2016
Biochemistry Summer School tutor	05/07/2016- 07/07/2016
Demonstrating for BLS	02/2013- 06/2016